

**Dissertation zur Erlangung des Doktorgrades
der Fakultät für Chemie und Pharmazie
der Ludwig-Maximilian-Universität München**

**The role of PIP aquaporins in response to various
environmental scenarios in *Arabidopsis thaliana***

Ming Jin

aus

Huhehaote, Inner Mongolia, China

2015

Erklärung

Diese Dissertation wurde im Sinne von § 7 der Promotionsordnung vom 28. November 2011 von PD Dr. Anton R. Schäffner betreut.

Eidesstattliche Versicherung

Diese Dissertation wurde eigenständig und ohne unerlaubte Hilfe erarbeitet.

München,

.....
(Ming Jin)

Dissertation eingereicht am

1. Gutachter: PD Dr. Anton R. Schäffner

2. Gutachter: Prof. Dr. Jörg Durner

Mündliche Prüfung am 15.04.2015

ABSTRACT

Plants like all other organisms depend on the uptake of water and the homeostasis of water relations, which, however, are frequently challenged by environmental cues like drought or heat. Plasma membrane intrinsic proteins (PIPs) are aquaporins, which facilitate gradient-driven water permeation across the plasma membrane and are therefore considered to impact plant water relations. *PIP2;1* and *PIP2;2* represent two major PIPs in *Arabidopsis thaliana* and are highly expressed mainly in the vascular tissues of roots and leaves. They have been shown to affect cell water permeability as well as hydraulic conductance in roots and rosette leaves. To further study their roles in plant physiology, the loss-of-function *pip2;1 pip2;2* double mutant was examined for altered physiological and molecular responses in comparison to wild-type plants under well-watered growth condition and under single and combined drought and heat scenarios. Heat stress was exerted in two different ways, either with a parallel increase of the vapor pressure deficit (lowered relative air humidity) due to the increase of temperature (regular heat stress) or with keeping the vapor pressure deficit constant by supplementing water vapor (high relative air humidity) in order to eliminate the heat-associated water deficit effects. Loss of *PIP2;1* and *PIP2;2* marginally impacts the plant water relations or transcriptional responses under well-watered condition and water stresses. The transpiration rate and stomatal conductance of water vapor are slightly reduced in *pip2;1 pip2;2* double mutant compared to the wild type under well-watered condition and this tendency is getting more obvious when the relative air humidity is declined and the root water transport is restricted by loss of the root-specific *PIP2;4*. These data suggest that the impacts of *PIP2;1* and *PIP2;2* in water relations are dependent on leaf water demand and root water supply. In addition, *PIP2;1* and *PIP2;2* are downregulated under drought stress, but irrespective of transpirational water loss. Loss of *PIP2;1* and *PIP2;2* alleviates the drought responses at the transcriptional level. In addition, high relative air humidity aggravates the heat stress responses at the transcriptional level by preventing transpiration cooling as compared to heat stress with low relative air humidity. *PIP2;1* and

PIP2;2 are upregulated under heat stress, irrespective of differences in relative air humidity. Surprisingly, loss of *PIP2;1* and *PIP2;2* marginally impacts the heat stress responses either with high relative air humidity or low relative air humidity. These data suggest that the role of the upregulated *PIPs* under heat stress is not associated to the transpiration-cooling process. *PIP2;1* and *PIP2;2* are downregulated under combined drought and heat stress with low relative air humidity (DH LrH) when drought stress is predominantly contributing to combined stress responses. Although *PIP2;1* and *PIP2;2* are not changed under combined stress with high relative air humidity (DH HrH), they are relatively upregulated under DH HrH in comparison to DH LrH. These data indicate that high relative air humidity shifts the combined stress responses towards a predominant heat effect. Loss of *PIP2;1* and *PIP2;2* alleviates the stress responses under DH LrH, which is similar to the impact in response to drought stress. Then transcriptional responses are not changed in *pip2;1 pip2;2* compared to wild type under DH HrH. The differentially expressed genes in *pip2;1 pip2;2* as compared to the wild type under water stresses indicate that regulation of osmotic potential and cell wall modification may compensate the loss of functions of *PIP2;1* and *PIP2;2*, although this compensation is considered to be weak, especially for heat stress responses. In summary, although previous studies have shown that *PIP2;1* and *PIP2;2* contributed to the cell water permeability and hydraulic conductivity in *Arabidopsis thaliana*, loss of *PIP2;1* and *PIP2;2* do not dramatically impair the water relations and growth under well-watered condition as well as water stress responses. However, the regulation of water homeostasis mediated by aquaporins may be critical in the transition after changing the environmental conditions. Therefore, such dynamic changes in response to water stresses will be a focus of future research.

CONTENTS

ABSTRACT	I
CONTENTS	III
ABBREVIATIONS	VII
1 INTRODUCTION	1
1.1 Water relations in plants.....	1
1.1.1 The role of water in plants.....	1
1.1.2 Water uptake and transport in plants	1
1.2 Water stress responses in plants	2
1.2.1 Drought stress responses in plants.....	2
1.2.2 Heat stress responses in plants	3
1.2.3 Combined drought and heat stress responses in plants	4
1.3 Aquaporins in plants	5
1.3.1 Molecular structure of aquaporins	5
1.3.2 Classification of aquaporins in <i>Arabidopsis thaliana</i>	6
1.3.3 Substrate selectivity of aquaporins of <i>Arabidopsis thaliana</i>	7
1.3.4 Gating of aquaporins in <i>Arabidopsis thaliana</i>	7
1.3.5 Expression profiles and co-regulation of <i>PIPs</i> in <i>Arabidopsis thaliana</i>	7
1.3.6 Aquaporin-dependent water transport in <i>Arabidopsis thaliana</i>	9
1.3.7 Regulation of <i>PIPs</i> in response to abiotic stresses in <i>Arabidopsis thaliana</i>	10
1.4 Aims of this project	12
2 RESULTS.....	14
2.1 Global variation in transcriptome analysis after drought and heat stress and different VPD.....	15

2.2 Impact of relative air humidity on water stress responses	16
2.2.1 Transcriptional responses to heat stress and combined drought and heat stress .	18
2.2.2 Impact of high relative air humidity on heat stress responses	21
2.2.3 Impact of high relative air humidity on combined drought and heat stress.....	32
2.2.4 Impact on expression of aquaporins under water-deficit stresses	42
2.3 Involvement of <i>PIP2;1</i> , <i>PIP2;2</i> and <i>PIP2;4</i> in responses to variable environmental scenarios	45
2.3.1 Phenotypic and physiological characteristics of <i>pip2;1 pip2;2</i> and <i>pip2;1 pip2;2 pip2;4</i>	45
2.3.2 Variation of aquaporin expression in <i>pip</i> mutants under variable environmental scenarios	49
2.3.3 Changes of <i>pip</i> mutants in response to variable environmental scenarios	52
2.3.3.1 Transcriptome profiling of <i>pip</i> mutants under well-watered condition	52
2.3.3.2 Metabolite profiling of <i>pip2;1 pip2;2</i> under well-watered condition.....	59
2.3.3.3 Integration of transcriptome and metabolome changes in <i>pip2;1 pip2;2</i> under well-watered condition.....	61
2.3.4 Transcriptome profiling of <i>pip</i> mutants in response to water stresses	62
3 DISCUSSION.....	87
3.1 Effect of high relative air humidity on the responses to heat stress and combined drought and heat stress.....	87
3.1.1 High relative air humidity aggravates heat stress responses and induces specific transcriptional changes in response to heat stress.....	87
3.1.2 High relative air humidity shifts the combined stress responses from a predominant drought effect to a heat effect and induces specific transcriptional changes in response to combined drought and heat stresses.....	91
3.2 The role of major <i>PIP2s</i> in leaves under well-watered condition and water stresses ...	92

3.2.1 Marginal impact of the loss of major <i>PIP2s</i> in leaves under well-watered condition	93
3.2.2 Marginal impact of loss of major <i>PIPs</i> in leaves in response to water stresses at molecular level.....	96
4 MATERIALS AND METHODS	101
4.1 Materials	101
4.1.1 Plant materials	101
4.1.2 Chemicals, buffers and media.....	101
4.2 Methods.....	102
4.2.1 Methods of physiological characterization.....	102
4.2.1.1 Plant growth condition	102
4.2.1.2 Growth measurements.....	102
4.2.1.3 Gas exchange measurements.....	103
4.2.1.4 Carbon isotope composition measurements	103
4.2.1.5 Relative water loss measurements	104
4.2.2 Methods of transcriptome analysis	104
4.2.2.1 Plant growth conditions and water-deficit stress applications.....	104
4.2.2.2 The arrangement of the replicates and harvest.....	105
4.2.2.3 Isolation of the total RNA	106
4.2.2.4 RNA quality and quantity control	107
4.2.2.4.1 RNA 6000 Nano assay	107
4.2.2.4.2 Nanodrop ND-1000 spectrophotometer	108
4.2.2.5 Agilent microarray analysis.....	108
4.2.2.5.1 One-color Spike Mix preparation.....	109

CONTENTS

4.2.2.5.2 Labeling reaction preparation	110
4.2.2.5.3 Labeled and amplified RNA purification.....	111
4.2.2.5.4 cRNA quantification	111
4.2.2.5.5 Hybridization.....	111
4.2.2.5.6 Microarray wash	112
4.2.2.5.7 Slide scan and figure extraction	113
4.2.3 GC-MS measurements	113
4.2.4 Statistical analysis	113
4.2.4.1 Gene expression analysis	113
4.2.4.2 Metabolomic analysis.....	114
4.2.4.3 Integrative analysis.....	114
4.2.5 Data mining from public expression data.....	114
4.2.6 Co-expression analysis	115
SUPPLEMENTARY MATERIALS	116
REFERENCE.....	167
CURRICULUM VITAE.....	177
ACKNOWLEDGEMENT	178

ABBREVIATIONS

ABA	abscisic acid
adj. <i>P</i>	adjusted <i>P</i> -value
cDNA	complementary DNA
C _i	intercellular CO ₂ concentration
D	drought stress
DH HrH	combined drought and heat stress with high relative air humidity
DH LrH	combined drought and heat stress with low relative air humidity
DM	<i>pip2;1 pip2;2</i>
DNA	deoxyribonucleic acid
E	transpiration rate
FC	fold change
GC-MS	gas chromatography-mass spectrometry
GO	gene ontology
g _s	stomata conductance of water vapor
H HrH	heat stress with high relative air humidity/regular heat stress
H LrH	heat stress with low relative air humidity
HSF	heat shock factor
HSP	heat shock protein
LIMMA	linear models for microarray data
MIP	major intrinsic protein

ABBREVIATIONS

MS	Murashige and Skoog
NIP	Nodulin-26-like intrinsic protein
PC	principle component
PCA	principal component analysis
PIP	plasma membrane intrinsic protein
rH	relative air humidity
RIN	RNA integrity number
RNA	ribonucleic acid
SIP	small basic intrinsic protein
TIP	tonoplast intrinsic protein
TM	<i>pip2;1 pip2;2 pip2;4</i>
VPD	vapor pressure deficit
WT	wild type

1 INTRODUCTION

1.1 Water relations in plants

1.1.1 The role of water in plants

Water is the major component contributing 80% – 90% of the mass of plant tissues. It plays essential roles in plant growth and development including maintaining cell turgidity for structure and cell expansion, transporting nutrients and organic compounds throughout the plant as a solvent, serving as an electron donor for photosynthesis, regulating plant temperature through transpiration against environment temperature fluctuations and regulating stomatal aperture for gas exchange (Taiz and Zeiger, 2006).

1.1.2 Water uptake and transport in plants

In plants, most of the water is taken up by the root system, although water exchange and uptake may also occur on other surfaces. More than 95% of the water taken up from roots is lost to the atmosphere through transpiration, and only less than 5% is retained for cellular physiological functions (Taiz and Zeiger, 2006). Thus, maintaining a balance of water uptake and water loss represents an important challenge for plants.

Soil water first enters the root system through root hairs or fine roots. Water can move across the cortex to the endodermis and then freely enters into xylem cells for long-distance transport in roots. Water in the xylem is driven up by transpiration pull and is then distributed into mesophyll and epidermal cells or transpired through stomata in leaves. The water movement through living plant tissues follows three pathways: the apoplastic pathway, a continuous extracellular system within the cell wall; the symplastic pathway, a cytoplasmic network of intercellular connections *via* plasmodesmata, and the transmembrane pathway from cell to cell across the plasma membrane. Water transport efficiency *via* the transmembrane pathway and the initial entry into the symplastic pathway can be facilitated by aquaporins, which are water-conducting channels integrated into the

plasma membrane (Steudle, 2001). These three pathways coexist and their contribution to water transport varies depending on the composite structures of the tissues and the environmental conditions. For instance, the transmembrane pathway and the symplastic pathway are predominant in water transport in the endodermis when the apoplastic pathway is blocked by the water-impermeable Casparian band. However, the contribution of the transmembrane pathway and the symplastic pathway is alleviated under high transpiration conditions (Steudle, 1994; Steudle and Peterson, 1998).

1.2 Water stress responses in plants

Plants are sessile organisms that cannot escape from environmental constraints. Therefore, they have evolved numerous adaptive responses to cope with environmental stresses. Drought stress and heat stress are two of the most important water stresses and occur in the field simultaneously (Mittler, 2006; Bates *et al.*, 2008). These stress conditions disturb the water homeostasis and in turn induce physiological, molecular and biochemical changes which eventually adversely impact plant growth and development.

1.2.1 Drought stress responses in plants

Drought stress due to water deficit of the soil adversely impacts plant growth. Under drought stress, water lost through transpiration cannot be fully supplemented due to the low water content of the soil and in turn causes a decrease of cell turgor. In addition, the relative water content and the water potential are also reduced (Morgan, 1984; Bray, 1997). As a defense against the water loss, drought stress triggers the production of abscisic acid (ABA) and subsequently results in stomata closure, leading to the reduction of transpiration and photosynthesis (Zhang and Davies, 1990; Chaves *et al.*, 2002; Parent *et al.*, 2009; Shatil-Cohen *et al.*, 2011; Osakabe *et al.*, 2014). On the other hand, drought stress induces the expression of drought-responsive genes encoding functional proteins (transporters, enzymes and protection factors) as well as regulatory proteins (transcription factors and protein kinases) (Seki *et al.*, 2001; Seki *et al.*, 2002; Shinozaki and Yamaguchi-Shinozaki, 2007; Aprile

et al., 2009; Le *et al.*, 2012; Prasch and Sonnewald, 2013). These drought-responsive genes are regulated through both ABA-dependent pathways and ABA-independent pathways (Stockinger *et al.*, 1997; Shinozaki *et al.*, 2003; Sakuma *et al.*, 2006; Nakashima *et al.*, 2009). In addition, drought stress also induces the accumulation of soluble sugars (raffinose and trehalose), amino acids (proline) as well as amines (glycine betaine and polyamines) as osmoprotectants to regulate water potential or as antioxidants to prevent oxidative damage (Seki *et al.*, 2007; Krasensky and Jonak, 2012).

1.2.2 Heat stress responses in plants

Heat stress due to elevated temperatures of ambient air is accompanied by an enhanced vapor pressure deficit (VPD) without additional water supplement in air. Thus, transpiration is increased to prevent heat damage, known as the transpiration-cooling process, and in turn causes a reduction of leaf water potential (Tsukaguchi *et al.*, 2003; Crawford *et al.*, 2012; Will *et al.*, 2013). In addition, heat stress adversely affects photosynthesis as well as respiration and increases the fluidity of membranes (Salvucci and Crafts-Brandner, 2004; Howarth, 2005; Sharkey, 2005; Wahid *et al.*, 2007; Allakhverdiev *et al.*, 2008). Furthermore, a number of transcriptome studies have revealed that the genes encoding proteins are associated with primary and secondary metabolism, protein degradation and modification, signal transduction as well as transcription regulation are differentially regulated (Lim *et al.*, 2006; Larkindale and Vierling, 2008; Matsuura *et al.*, 2010; Mittler *et al.*, 2012; Yángüez *et al.*, 2013). In particular, heat stress induces the expression of specific transcription factors, heat shock factors (HSFs), and subsequently mediates accumulation of heat shock proteins (HSPs), which act as molecular chaperones to prevent protein misfolding and aggregation (Baniwal *et al.*, 2004; Kotak *et al.*, 2007; von Koskull-Döring *et al.*, 2007; Mittler *et al.*, 2012; Qu *et al.*, 2013). In addition, heat stress also modulates the accumulation of compatible osmolytes and antioxidants, such as sugars, amino acids and polyamines (Kaplan *et al.*, 2004; Rizhsky *et al.*, 2004; Bokszczanin and Fragkostefanakis, 2013). On the other hand, heat stress with low VPD

by supplementing the additional water vapor in air restricts transpiration cooling and in turn increases leaf temperatures which may aggravate heat damage (Taiz and Zeiger, 2006).

1.2.3 Combined drought and heat stress responses in plants

Although drought and heat stresses have been extensively studied independently, relatively little is known about their combined effects on plants. Drought stress induces stomata closure and reduces water loss by transpiration, which in turn restricts transpiration cooling and potentially enhances heat susceptibility. On the other hand, heat stress increases water loss through transpiration, but reduces root growth, thus causes the drought susceptibility (Taiz and Zeiger, 2006). Stomata are closed under combined drought and heat stress. Then photosynthesis is in turn restricted by downregulation of the photosynthetic genes and consequently reduce the plant growth under combined stress (Rizhsky *et al.*, 2004; Prasch and Sonnewald, 2013). Vile *et al.* (2012) found that the effects of combined drought and heat stress on plant growth traits are globally additive. For example, plant growth is restricted under both drought stress and heat stress and this restriction is getting more severe under combined drought and heat stress. In addition, all of the growth traits, which are varied under combined drought and heat stress, are also changed in response to at least one of them. Thus, there are no growth traits which are specifically affected by combined drought and heat stress (Vile *et al.*, 2012). However, transcriptome studies show a unique response under combined drought and heat stress involving specific changed transcripts that are not altered under individual drought or heat stress (Rizhsky *et al.*, 2004; Prasch and Sonnewald, 2013). In addition, a larger amount of altered genes are overlapping between drought and combined stress as compared to heat and combined stress, which suggests the drought effect predominantly contributes to combined drought and heat stress responses (Rizhsky *et al.*, 2002; Rizhsky *et al.*, 2004; Mittler, 2006). Moreover, the accumulation of metabolites is highly specific and sucrose replaces proline as the major osmolyte under combined drought and heat stress (Rizhsky *et al.*, 2004; Prasch and Sonnewald, 2013).

1.3 Aquaporins in plants

1.3.1 Molecular structure of aquaporins

Aquaporins belong to the major intrinsic proteins (MIPs) with molecular masses of 23-31 kDa and have conserved structures across kingdoms of organisms (Fujiyoshi *et al.*, 2002; Wallace and Roberts, 2004; Bansal and Sankararamakrishnan, 2007). They assemble as tetramers and each of the monomers defines an individual pore. These monomers comprise six transmembrane α -helices (1 to 6) tilted along the plane of the membrane and linked by five loops (A to E). Loops B and D as well as the N- and C-terminals protrude to the cytosol, whereas loops A, C and E face to extracellular or intraorganellar side. Loops B and E contain the highly conserved NPA (Asn-Pro-Ala) motifs and form two half-helices that insert into the membrane from opposite sides. This is one of the two major constrictions in the channel (Figure 1). The second major constriction known as aromatic/arginine (ar/R) region is formed by two residues from TM2 and TM5 as well as two residues from loop E and it is localized on the extra-cytoplasmic mouth of the pore. These two constrictions determine the substrate specificity.

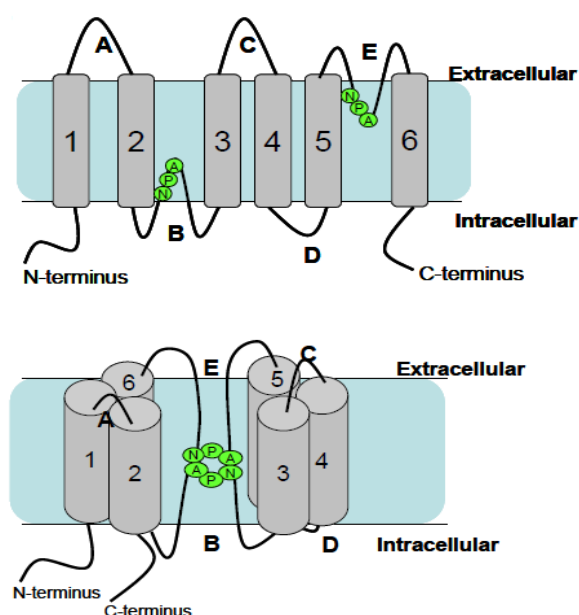


Figure 1. Schematic presentation of an aquaporin monomer. Six transmembrane α -helices (1 to 6) are linked by five loops (A to E). Two conserved NPA motifs located at the loop B and E, respectively, fold into the lipid bilayer to form a single aqueous pathway.

1.3.2 Classification of aquaporins in *Arabidopsis thaliana*

Arabidopsis thaliana contains 35 aquaporins that belong to four subfamilies (PIPs, TIPs, SIPs and NIPs) based on sequence homologies and subcellular localization (Johanson *et al.*, 2001; Quigley *et al.*, 2002). The plasma membrane intrinsic proteins (PIPs) and the tonoplast intrinsic proteins (TIPs) represent the most abundant aquaporins of plasma membrane and tonoplast, respectively. PIPs can be subdivided into PIP1s including five isoforms and PIP2s including eight isoforms. Nodulin-26-like intrinsic proteins (NIPs) are homologous to nodulin-26 in soybean (Rivers *et al.*, 1997). NIPs comprise nine isoforms and are localized in the plasma membrane and the endoplasmic reticulum (ER) (Wallace *et al.*, 2006). In addition, small basic intrinsic proteins (SIPs) have three isoforms and are integrated in ER membranes (Ishikawa *et al.*, 2005) (Figure 2).

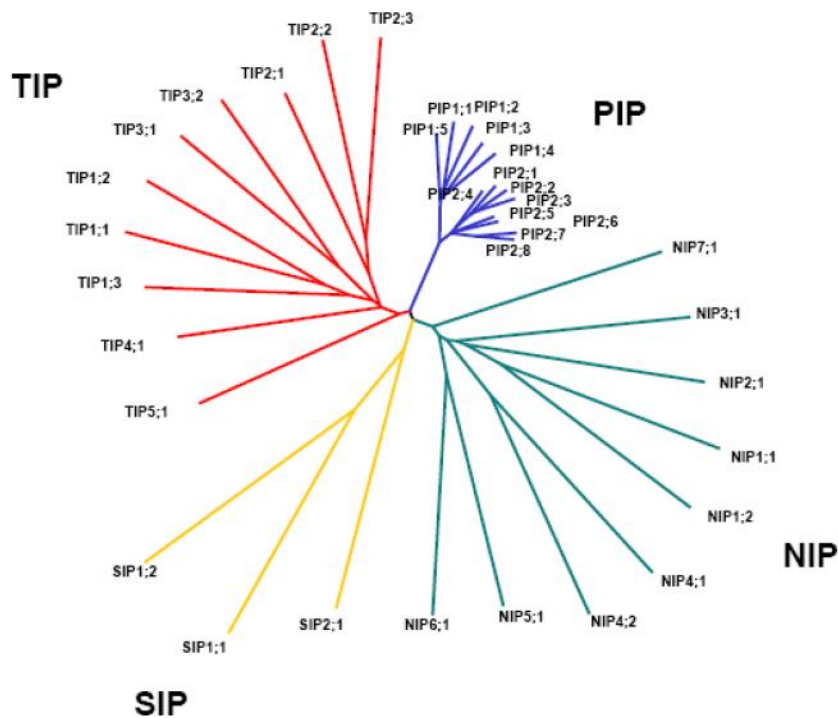


Figure 2. Phylogenetic tree of the 35 aquaporins grouped into four subfamilies in *Arabidopsis thaliana*

1.3.3 Substrate selectivity of aquaporins in *Arabidopsis thaliana*

Aquaporins in *Arabidopsis thaliana* mainly mediate water movement across biomembranes, but also transport small solutes including urea (Klebl *et al.*, 2003; Liu *et al.*, 2003), boric acid (Takano *et al.*, 2006), hydrogen peroxide (Bienert *et al.*, 2007; Dynowski *et al.*, 2008; Hooijmaijers *et al.*, 2012), ammonia (Holm *et al.*, 2005) and carbon dioxide (Heckwolf *et al.*, 2011; Uehlein *et al.*, 2012). Several TIPs including TIP1;1 (Maurel *et al.*, 1993) and TIP3;1 (Daniels *et al.*, 1996) as well as PIPs involving PIP1;1, PIP1;2, PIP1;3, PIP2;1, PIP2;2, PIP2;3 and PIP2;7 have been verified to possess water transport activities (Daniels *et al.*, 1994; Hachez *et al.*, 2014; Kammerloher *et al.*, 1994).

1.3.4 Gating of aquaporins in *Arabidopsis thaliana*

The gating of aquaporins (opening and closing of the pore) can be regulated by phosphorylation, pH and Ca^{2+} (Chaumont *et al.*, 2005a). Mass spectrometry (MS) analysis has shown the presence of phosphorylated forms of both the AtPIP1s (PIP1;1 and PIP1;2) and AtPIP2s (PIP2;1 and PIP2;2) subgroups (Santoni *et al.*, 2003). A role of phosphorylation due to sucrose-induced receptor kinase SIRK1 in activating the AtPIP1s and AtPIP2s has been verified by protoplast swelling assays (Wu *et al.*, 2013). However, the water permeability of plasma membrane vesicles equilibrated with Ca^{2+} was reduced and H^+ has been shown to reversibly reduce water channel activity (Gerbeau *et al.*, 2002). The inhibition of aquaporin activity by Ca^{2+} and H^+ has further been confirmed by expression of *PIP2;1* in proteoliposomes (Verdoucq *et al.*, 2008).

1.3.5 Expression profiles and co-regulation of PIPs in *Arabidopsis thaliana*

Aquaporin expression profiles across different organs in *Arabidopsis* provide fundamental information about the possible functions of aquaporins. Semiquantitative slot-blot analysis showed that the PIPs are mainly expressed in roots and leaves (Weig *et al.*, 1997).

Furthermore, cDNA microarray and proteomics profiling of *Arabidopsis* aquaporins has revealed highly transcriptional and translational (79% of the total PIPs protein) levels of PIP1;1, PIP1;2, PIP2;1 and PIP2;2 in roots (Santoni *et al.*, 2003; Alexandersson *et al.*, 2005; Monneuse *et al.*, 2011). In addition, PIP1;2 and PIP2;1 are the major isoforms, whereas PIP1;1 and PIP2;2 are the less abundant ones in leaves. These four isoforms represent 80% of the overall PIPs at the protein level of leaves. PIP2;7 is also ubiquitously expressed in roots and leaves, but still less abundant than PIP1;2 and PIP2;1. Although *PIP2;6* exhibits highly transcriptional level in leaves, its protein level is considerably lower than that of PIP1;2 and PIP2;1 (Alexandersson *et al.*, 2005; Monneuse *et al.*, 2011; Prado *et al.*, 2013).

The in situ localization of the β -glucuronidase reporter gene governed by PIP promoters (*proPIP::GUS*) provides additional information regarding the cellular expression of aquaporins. The observations confirm the major expressions of *PIP1;2*, *PIP2;1* and *PIP2;2* in roots and leaves as well as the specific expression of *PIP2;4* in roots (Da Ines, 2008; Postaire *et al.*, 2010). The cross-sections of GUS-stained roots reveal that *PIP1;2*, *PIP2;1* and *PIP2;2* are mainly expressed in the stele. In addition, both *PIP1;1* and *PIP2;2* are expressed in cortical cells, and *PIP1;2* is also expressed in the endodermis (Javot *et al.*, 2003; Postaire *et al.*, 2010; Zhao, 2013). Furthermore, the cross-sections of leaves show that *PIP1;2* is expressed in all leaf tissues, *PIP2;1* is also expressed in vascular tissue and bundle sheath cells as well as that *PIP2;2* is expressed in cells surrounding the veins (Da Ines *et al.*, 2010; Postaire *et al.*, 2010).

The similar expression patterns of *PIPs* at the cellular level suggest potential interactions and co-regulation between them. Co-expression analysis of aquaporins in *Arabidopsis thaliana* predicts that *PIP1;1*, *PIP1;2*, *PIP2;1* and *PIP2;2/2;3* are most strongly correlated with each other (Alexandersson *et al.*, 2010). Interestingly, the repression of PIP1;1 and PIP1;2 in the *pip2;1 pip2;2* mutant was observed at the protein level (Chen Liu's work), suggesting the important role of the mainly expressed *PIPs*, *PIP2;1* and *PIP2;2*, in regulation of other aquaporins and in turn impacting the water relations of *Arabidopsis thaliana*.

1.3.6 Aquaporin-dependent water transport in *Arabidopsis thaliana*

PIPs are thought to represent the major components for transcellular water transport due to their abundance and localization. Mercury is a general aquaporin inhibitor that can reversibly block the water channel activities when *PIPs* are heterologously expressed in *Xenopus* oocytes. Therefore, the overall contribution of aquaporins to hydraulic conductivity in roots and leaves has been initially examined by employing HgCl_2 in *Arabidopsis thaliana*. The mercury treatments lead to reduced root hydraulic conductivity by 50% (Sutka *et al.*, 2011) and decreased leaf hydraulic conductivity by 26% (Postaire *et al.*, 2010), indicating the important role of aquaporins in plant water relations. However, the general toxicity of mercury may induce side effects on other physiological processes and the specific functions of aquaporins cannot be exactly defined (Zhang and Tyerman, 1999). Thus, reverse genetic approaches are employed to explore the functions of the individual aquaporins with respect to water relations. Antisense inhibition of *PIP1s* and *PIP2s* reduces osmotic hydraulic conductivity of protoplasts isolated from roots and leaves, but only root hydraulic conductivity is decreased by threefold (Martre *et al.*, 2002). Two independent *pip2;2* knockout mutants reduce the hydraulic conductivity in root cortex cells by 25% - 30% and the osmotic hydraulic conductivity of entire roots is reduced by 14% in mutants (Javot *et al.*, 2003). Two allelic *pip2;1* T-DNA insertion lines show a reduction of 14% in root hydraulic conductivity and a further decrease in the *pip2;1 pip2;2* mutant (Péret *et al.*, 2012), suggesting the important role of *PIP2s* in root water transport. In rosettes, *AtPIP1;2*, *AtPIP2;1* and *AtPIP2;6* contribute to rosette water transport and *AtPIP2;1* can fully account for rosette hydraulic conductivity under dark condition (Prado *et al.*, 2013), pointing to a predominant contribution to leaf water relations. In addition, relative water flux from root to shoot is evaluated by employing deuterium tracer to assess the water relocation in *Arabidopsis thaliana*. Both *pip2;1* and *pip2;2* single mutants show the reduction of water flux by 20% (Da Ines *et al.*, 2010).

1.3.7 Regulation of *PIPs* in response to abiotic stresses in *Arabidopsis thaliana*

Water status in plants is challenged by variable abiotic stresses, such as drought, salinity, extreme temperature and anoxia. Therefore, regulation of *PIPs* is considered to be essential for water homeostasis in response to these abiotic stresses.

Salt stress results in a marked decrease in root hydraulic conductivity in *Arabidopsis thaliana* (Martínez-Ballesta *et al.*, 2003; Boursiac *et al.*, 2005; Sutka *et al.*, 2011). This reduction is considered to be associated with transcriptional, translational and post-translational regulations of *PIPs*. All *PIP* transcripts and protein abundances including *PIP1;1*, *PIP1;2*, *PIP2;1* and *PIP2;2* are strongly decreased after exposure to salt stress (Boursiac *et al.*, 2005; di Pietro *et al.*, 2013). The reduction of phosphorylation of *PIP1s* (*PIP1;1* and *PIP1;2*) as well as of *PIP2s* (*PIP2;1*, *PIP2;2*, *PIP2;3*, *PIP2;4* and *PIP2;7*) also contribute to the decreased root hydraulic conductivity under salt stress by inactivating the aquaporins and inducing rapid internalization (Boursiac *et al.*, 2008; Prak *et al.*, 2008; Li *et al.*, 2011; di Pietro *et al.*, 2013). Similarly, the reduction of root hydraulic conductivity under cold stress is due to the repression of *PIP* expression and the dephosphorylation (Jang *et al.*, 2004; Lee *et al.*, 2012). In addition, the downregulation of *PIP* transcripts and closure of the water channels due to cytosol acidosis result in the reduced root hydraulic conductivity under anoxia stress (Tournaire-Roux *et al.*, 2003; Liu *et al.*, 2005).

Similar to other water stresses, drought stress reduces the hydraulic conductivity by regulation of *PIPs* at transcriptional and post-transcriptional levels. *PIPs* transcription are generally downregulated under drought stress, apart from *PIP1;4* and *PIP2;5* which are upregulated, as well as *PIP2;6* which is unresponsive to drought. The alterations of *PIPs* transcription can be restored after rehydration (Alexandersson *et al.*, 2005; Alexandersson *et al.*, 2010). In addition, the reduction of leaf hydraulic conductivity is also determined by ABA-dependent inactivation of *PIPs* in bundle-sheath cells (Shatil-Cohen *et al.*, 2011). *PIP2;1* and

PIP2;2, which are dephosphorylated by ABA treatment, may be involved in this process (Kline *et al.*, 2010). Moreover, the trafficking of *PIP2;1* from ER to plasma membrane is inhibited and the protein level of *PIP2;1* is reduced due to degradation of ER-retained *PIP2;1* under drought stress (Lee *et al.*, 2009). The important role of PIPs in recovery from drought stress in *Arabidopsis thaliana* was verified in antisense of *PIP1s* and *PIP2s* mutants. After rewatering, the recovery of hydraulic conductance is slower in the *pip* mutants than in the wild-type plants (Martre *et al.*, 2002). In addition, regulation of *PIPs* expression under heat stress is dependent on the plant growth conditions, plant age, temperature and duration used in heat stress. Only *PIP2;2* is generally upregulated under heat (Figure 3). Interestingly, high relative air humidity also reduces the hydraulic conductivity by repression of aquaporins (Levin *et al.*, 2007).

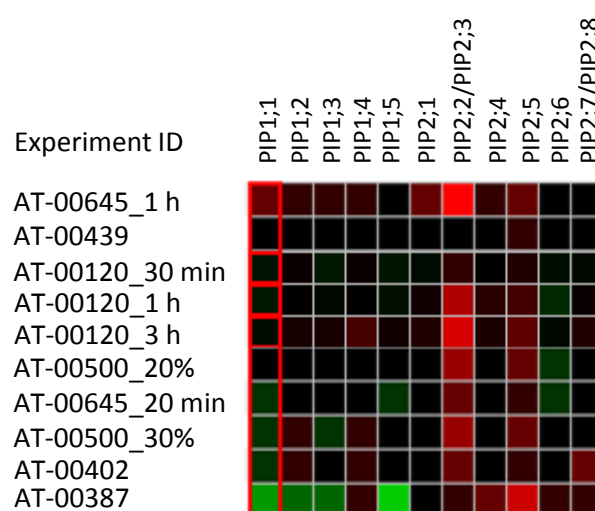


Figure 3. Regulation of *PIPs* expression under heat stress in Genevestigator.

*Experiment ID: AT-00645. 11-day-old plants were subjected to 40°C for 20 min and 1 h.

*Experiment ID: AT-00500. Plants were grown at 22°C and then the temperature was gradually increased until photosynthesis was inhibited by 20% and 30%.

*Experiment ID: AT-00120. 16-day-old plants were treated at 38°C for 0.5 h, 1 h and 3 h.

*Experiment ID: AT-00402. 8-week-old plants were treated at 37°C for 2 h.

*Experiment ID: AT-00387. 3-week-old plants were exposed to 37°C for 30 h.

*Experiment ID: AT-00439. 7-day-old plants grown on ½ MS plates were subjected to 37°C for 1 h.

Taken together, aquaporins play an important role in regulating water homeostasis through modulation of their transcription, translation and modification under abiotic stresses. However, little is known about *PIPs*-dependent changes at transcriptional and metabolism level in response to environmental scenarios.

1.4 Aims of this project

The first aim of this project was to understand the impact of high relative air humidity on heat stress responses and on combined drought and heat stress responses. Regular heat stress results in reduced relative air humidity/enhanced vapor pressure deficit that involves additional air water deficiency. To address the effect on stress responses after eliminating the additional water-deficit stress in the ambient air, heat stress and combined drought and heat stress were employed with supplementing additional ambient humidity to keep the VPD constant at high temperature and without adjusting the air humidity that leads to strongly enhanced VPD at high temperature. The specific transcriptional changes in response to heat stress as well as combined drought and heat stress with high relative air humidity in comparison to the corresponding stresses with low air humidity and their potential functions should be identified.

The second aim of this project was to assess the effects of loss of major *PIPs* (*PIP2;1*, *PIP2;2* and *PIP2;4*) in leaves under well-watered condition and under water stresses including drought stress, heat stress with high/low relative air humidity and combined drought and heat stress with high/low relative air humidity outlined above. Combining physiological characterizations, transcriptomic and metabolic analysis, the differential responses induced by the loss of *PIP2;1* and *PIP2;2* under well-watered condition should be identified. The transcriptional changes induced by the loss of *PIP2;1*, *PIP2;2* and *PIP2;4* under various water stresses should be also explored.

2 RESULTS

Different environmental scenarios exerting water stresses on plants were applied to characterize stress responses at the transcriptome level in *Arabidopsis thaliana*. Although there had been previous studies on similar topics (see 1.2), here two specific aspects and questions were emphasized.

First of all, regular heat stress is accompanied by an increased vapor pressure deficit (VPD)/decreased relative air humidity (rH). This aggravates the water demand in air and induces additional water deficit in the ambient air. To explore the real heat effect on stress responses after eliminating the impact of heat-dependent VPD increase leading to a VPD (LrH) of 3.168 kPa (37%) at 33°C, the regular heat scenarios were compared with environmental conditions eliminating the impact of VPD by keeping it constant at 33°C during heating. This was achieved by supplementing the ambient air with additional humidity, thereby raising the relative air humidity from 70% with a VPD of 0.793 kPa at 22°C to 84% with a VPD of 0.793 kPa at 33°C. Thus, the following scenarios were applied to wild-type plants: drought stress (D; 22°C, drought initiated in soil by stopping watering for seven days), regular heat stress (H LrH, 33°C for 6 h) and their combination (DH LrH; developing drought for seven days and then 6 h at 33°C), heat stress and combined drought and heat stress with additional air humidity supplementation (H HrH & DH HrH) (Figure 4). Then they were analyzed at the transcriptional level (see 4.2.2).

Secondly, since we were interested in the contribution of major *PIPs* to plant water relations and eventually plant growth under well-watered condition and water stresses, two loss of function mutants *pip2;1 pip2;2* and *pip2;1 pip2;2 pip2;4* were also subjected to the same stress conditions in parallel and analyzed at the transcriptional and physiological level (see 4.2.1 and 4.2.2).

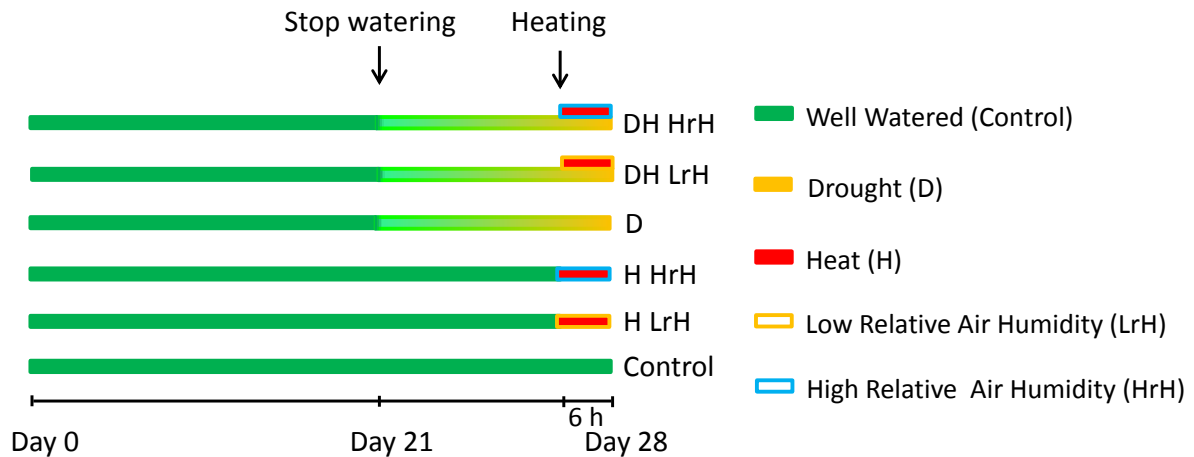


Figure 4. Experiment design for applying the drought stress (D), heat stress (H HrH/H LrH) and a combined drought and heat stress (DH HrH/DH LrH). The black line represents the plant growth and treatment durations. The dark green bars represent well-watered condition. The bars with gradient color from light green to orange represent drought stress. The red bars represent heat stress. The orange frames represent low relative air humidity. The blue frames represent high relative air humidity.

2.1 Global variation in transcriptome analysis after drought and heat stress and different VPD

Three-week-old wild-type plants, *pip2;1 pip2;2* and *pip2;1 pip2;2 pip2;4* mutant plants of *Arabidopsis thaliana* were raised and treated with the different stress scenarios D, H LrH, DH LrH, H HrH and DH HrH and control condition (22°C, well-watered) (See 4.2.2.1). Total RNA was isolated from rosettes and labeled cDNA was then used for hybridization of Agilent microarrays for *Arabidopsis thaliana* (See 4.2.2). Two independent experiments for D, H LrH and DH LrH or three independent experiments for H HrH and DH HrH with three biological replicates each of *pip* mutants and wild type were conducted. Expression data were extracted using Agilent Feature Extraction (FE) software and the data evaluation was based on LIMMA (linear models for microarray data) (done by Dr. Elisabeth Georgii from the Institute of Biochemical Plant Pathology, Helmholtz Zentrum München) (See 4.2.4).

To evaluate the effects of treatments and genotypes on transcriptional variations, principal component analysis (PCA) was conducted on all datasets (See 4.2.4.1). The first two principle components (PCs) could cumulatively explain more than 70% of the variations of the datasets (Figure 5A and 5B). PC1 and PC2 showed a separation according to the treatments. PC1 mainly separated DH HrH and DH LrH from the other treatments and PC2 can separate the high relative air humidity effect from the other treatment effect (Figure 5C). Furthermore, PC3 and PC6 clearly showed a separation of the *pip* mutants from wild type (Figure 5D). These data indicate that treatments exert major effects on transcriptional variations whereas genotypes have only a minor impact.

2.2 Impact of relative air humidity on water stress responses

The need to balance water availability in the soil on the one hand and water demand in the atmosphere on the other hand critically affects water relations and eventually plant growth and development. Drought stress, regular heat stress and their combination as the major water stresses have therefore been well studied with regard to physiological, transcriptional and metabolic aspects (see 1.2). To better understand the responses of wild-type plants to heat stress and combined drought and heat stress, the additional water deficit in ambient air was eliminated by employing heat stress and combined drought and heat stress while maintaining a constant VPD by enhancing air humidity (H HrH & DH HrH). For comparison, regular heat stress (H LrH) and combined drought and regular heat stress (DH LrH) were applied to the wild-type plants (See 4.2.2.1). Transcriptional datasets were derived from Agilent microarrays and transcripts having an absolute Log_2 fold change ($|\text{Log}_2\text{FC}| \geq 1$) with an adjusted P -value ($\text{adj.}P \leq 0.05$) under water stresses compared to the well-watered condition (control) were considered to be significantly changed gene expressions to be further analyzed.

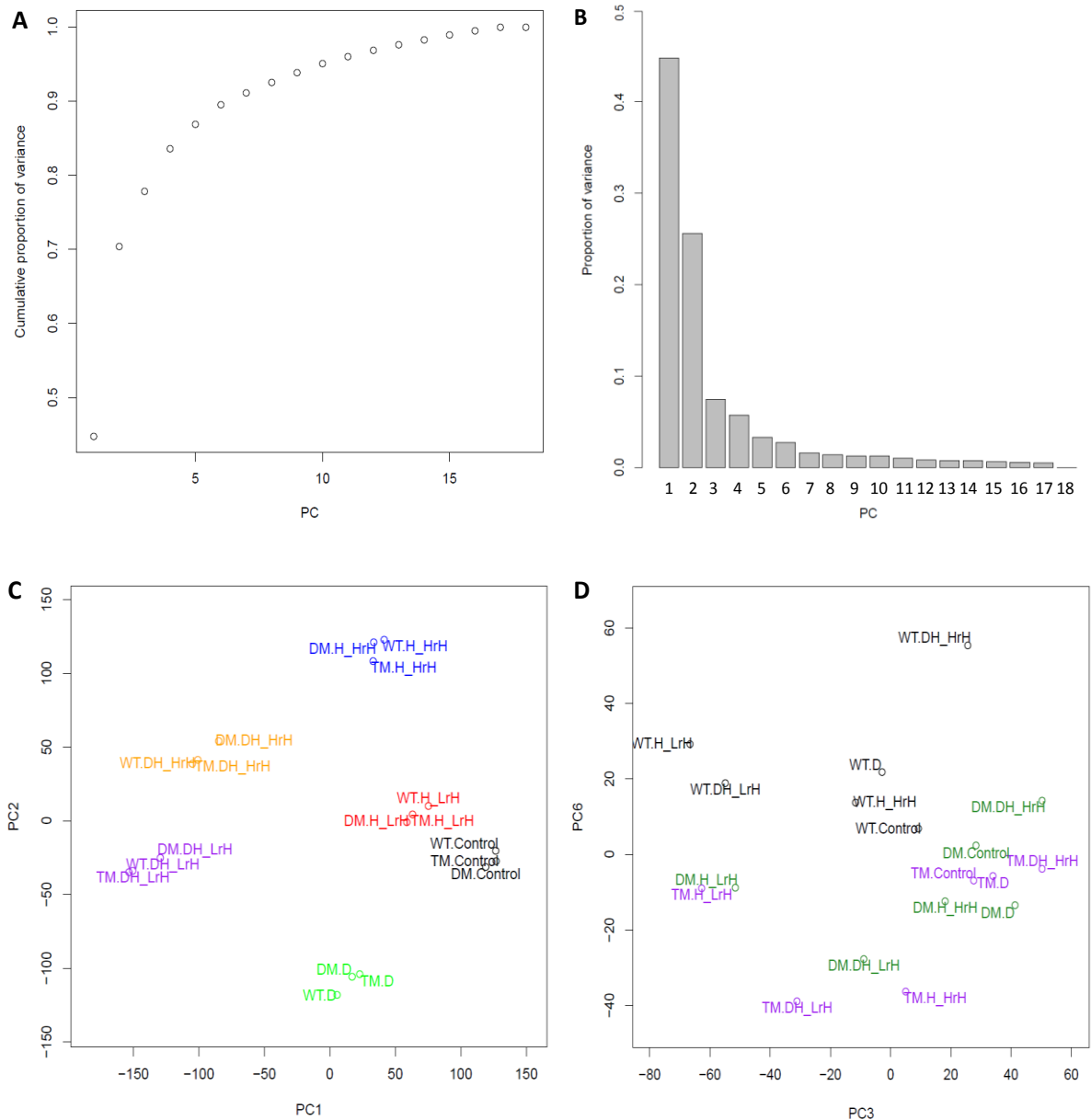


Figure 5. Principle component analysis (PCA) of the transcriptome of *pip* mutants and wild type under variable environmental scenarios. (A) Cumulatively explained variance of the principle component. (B) Variance explained by all the components of 18 observations. Each bar represents the individual variance explained by the principle component. (C) Projection of observations onto the first two principle components. (D) Projection of observations onto the third and sixth principle components.

2.2.1 Transcriptional responses to heat stress and combined drought and heat stress

In total, 361 genes were differentially expressed under H LrH, involving 197 upregulated genes and 164 downregulated genes. Under H HrH, on the other hand, 1318 genes were changed including 524 elevated and 794 reduced genes. In addition, drought stress resulted in 1830 altered genes, 1011 of which were enhanced and 819 were reduced. Under DH LrH, a total of 4561 genes were altered with 2051 upregulated genes and 2510 downregulated genes. Under DH HrH, a total of 3349 genes were differentially expressed including 1499 enhanced genes and 1850 reduced genes (Figure 6). These data suggest that high relative air humidity increases the number of altered gene expressions under heat stress, but alleviates the transcriptional changes under combined drought and heat stress.

Intersections supply an overview for distribution of stress-specific and commonly regulated genes and allow to identify the genes which are important for different stress responses. Our transcriptome data revealed that 43 downregulated genes and 36 upregulated genes were shared under all the water stresses we used (Figure 7; Table 1 and Table 2). Interestingly, 15 genes out of 36 upregulated genes were heat shock transcription factors (*HSFs*) and heat shock proteins (*HSPs*) (Table 2). This suggests that protein misfolding occurs under all of the water stresses we used and the *HSFs*-activated *HSPs* are critical for maintenance or restoration of protein homeostasis as the molecular chaperones (Scharf *et al.*, 2011).

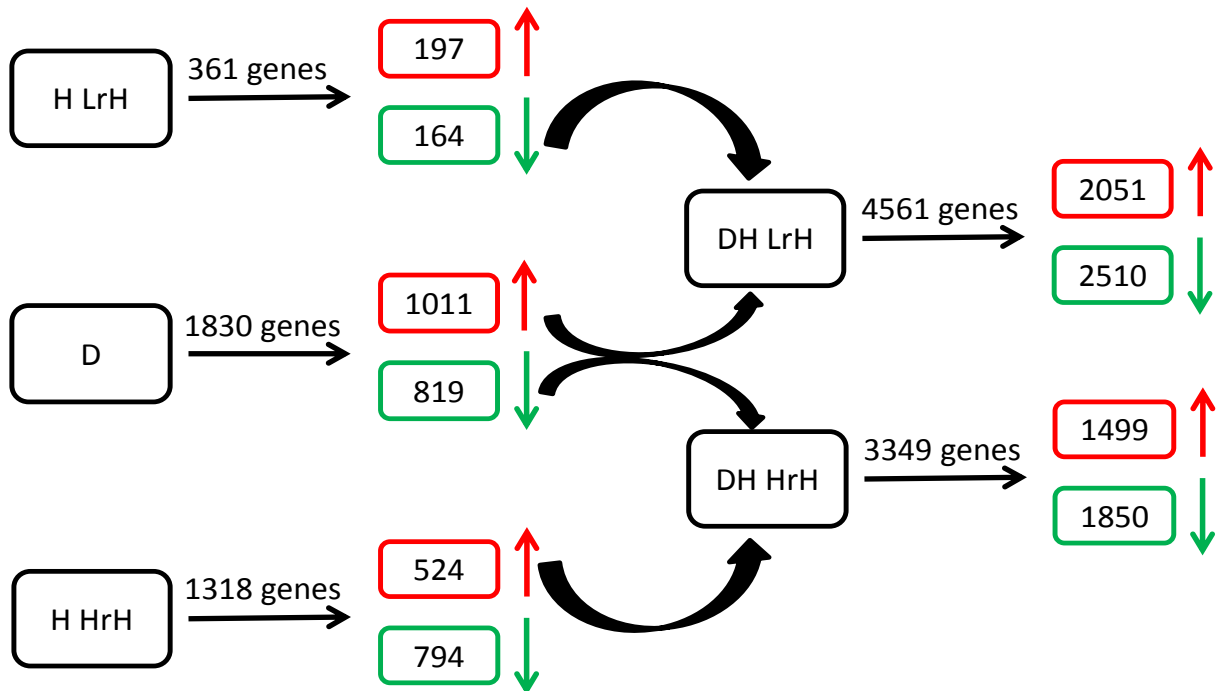


Figure 6. Number of differentially expressed genes in wild type under water stresses compared to control condition. Red and green marks represent upregulated and downregulated genes, respectively. Only transcripts with changes in steady-state level of $|\text{Log}_2\text{FC}| \geq 1$ and $\text{adj. } P \leq 0.05$ are included.

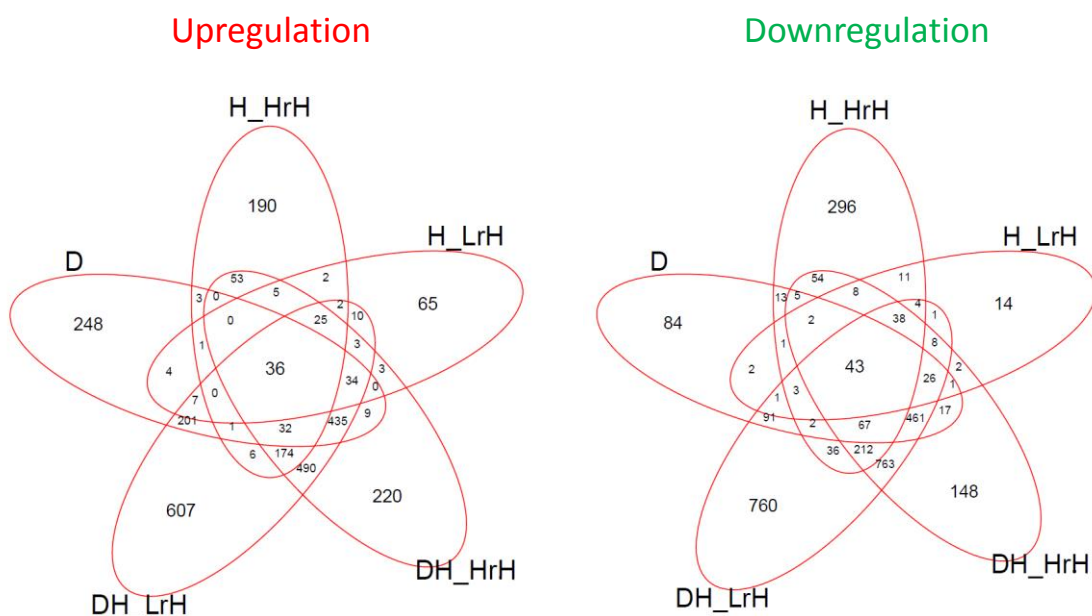


Figure 7. Intersections of differentially expressed genes in wild type under water stresses compared to control condition. Only genes with changes in steady-state level of $|\text{Log}_2\text{FC}| \geq 1$ and $\text{adj. } P \leq 0.05$ are included.

Table 1. Commonly downregulated genes under all of the water stress conditions

AGI	Gene Name
AT4G29740	<i>CKX4</i>
AT5G61160	<i>AACT1</i>
AT5G07100	<i>WRKY26</i>
AT3G57240	<i>BG3</i>
AT2G26560	<i>PLP2</i>
AT3G09940	<i>MDAR3</i>
AT1G75040	<i>PR5</i>
AT2G26400	<i>ARD3</i>
AT2G04450	<i>NUDX6</i>
AT2G21650	<i>RSM1</i>
AT1G35230	<i>AGP5</i>
AT5G44420	<i>PDF1.2</i>
AT2G14610	<i>PR1</i>
AT1G67810	<i>SUFE2</i>
AT3G44990	<i>XTH31</i>
AT5G62920	<i>ARR6</i>
AT1G15520	<i>ABCG40</i>
AT3G04570	<i>AHL19</i>
AT2G30770	<i>CYP71A13</i>
AT4G23210	<i>CRK13</i>
AT5G62310	<i>IRE</i>
AT4G10820	<i>F-box family protein</i>
AT3G15356	<i>Legume lectin family protein</i>
AT1G06830	<i>Glutaredoxin family protein</i>
AT4G11290	<i>Peroxidase superfamily protein</i>
AT1G31690	<i>Copper amine oxidase family protein</i>
AT5G24200	<i>alpha/beta-Hydrolases superfamily protein</i>
AT4G15660	<i>Thioredoxin superfamily protein</i>
AT4G15670	<i>Thioredoxin superfamily protein</i>
AT4G12490	<i>Bifunctional inhibitor/lipid-transfer protein</i>
AT4G12500	<i>Bifunctional inhibitor/lipid-transfer protein</i>
AT3G28510	<i>P-loop containing nucleoside triphosphate hydrolases</i>
AT4G29610	<i>Cytidine/deoxycytidylate deaminase family protein</i>
AT5G54020	<i>Cysteine/Histidine-rich C1 domain family protein</i>
AT5G43520	<i>Cysteine/Histidine-rich C1 domain family protein</i>
AT4G33390	<i>unknown protein</i>
AT1G23640	<i>unknown protein</i>
AT5G22520	<i>unknown protein</i>
AT3G55646	<i>unknown protein</i>
AT1G67670	<i>unknown protein</i>
AT1G78922	<i>unknown protein</i>
AT5G44568	<i>unknown protein</i>

 AT5G57760 *unknown protein*

Table 2. Commonly upregulated genes under all of the water stress conditions

AGI	Gene Name
AT3G12580	<i>HSP70</i>
AT3G24500	<i>MBF1C</i>
AT1G71000	Chaperone DnaJ-domain superfamily protein
AT5G62020	<i>HSFB2A</i>
AT2G20560	DNAJ heat shock family protein
AT4G21320	<i>HSA32</i>
AT2G29500	HSP20-like chaperones superfamily protein
AT5G52640	<i>HSP90.1</i>
AT3G46230	<i>HSP17.4</i>
AT4G12400	<i>HOP3</i>
AT1G07400	HSP20-like chaperones superfamily protein
AT1G53540	HSP20-like chaperones superfamily protein
AT5G12030	<i>HSP17.6A</i>
AT5G51440	HSP20-like chaperones superfamily protein
AT2G26150	<i>HSFA2</i>
AT3G53230	<i>ATCDC48B</i>
AT2G47180	<i>GOLS1</i>
AT5G59310	<i>LTP4</i>
AT4G21650	<i>SBT3.13</i>
AT5G66110	<i>HIPP27</i>
AT1G62510	<i>Bifunctional inhibitor/lipid-transfer protein</i>
AT4G30540	<i>Class I glutamine amidotransferase-like superfamily protein</i>
AT5G25450	<i>Cytochrome bd ubiquinol oxidase</i>
AT4G20820	<i>FAD-binding Berberine family protein</i>
AT2G37900	<i>Major facilitator superfamily protein</i>
AT1G73040	<i>Mannose-binding lectin superfamily protein</i>
AT2G29300	<i>NAD(P)-binding Rossmann-fold superfamily protein</i>
AT4G33420	<i>Peroxidase superfamily protein</i>
AT1G72660	<i>P-loop containing nucleoside triphosphate hydrolases</i>
AT1G30190	<i>unknown protein</i>
AT4G31354	<i>unknown protein</i>
AT4G31351	<i>unknown protein</i>
AT5G54165	<i>unknown protein</i>
AT4G14819	<i>unknown protein</i>
AT4G23493	<i>unknown protein</i>
AT5G10946	<i>unknown protein</i>

2.2.2 Impact of high relative air humidity on heat stress responses

To identify the alteration of heat stress responses with different relative air humidity in wild type, gene ontology (GO) terms of upregulated and downregulated genes were performed using MapMan 3.5.1R2 and the function categories without the group of *not assigned genes* were shown in Figure 8 and Figure 9. Either upregulated or downregulated genes were mainly associated with *miscellaneous enzyme families, stress responses, RNA related process* and *protein modification or degradation* under both H HrH and H LrH (Figure 8 and Figure 9). For example, upregulated genes were overrepresented in protein folding process and downregulated genes were overrepresented in flavonoid biosynthesis and response to abiotic stimulus under H HrH, which were also detected under H LrH. This indicates that no specific biological processes are influenced under H HrH. On the other hand, to identify how high relative air humidity generally changes the heat stress responses, the differentially expressed genes sorted according to the adjusted *P*-value under H HrH and the top listed genes showed stronger changes as compared to under H LrH (Table 3). In particular, the heat marker genes including heat shock factors (*HSFs*) and heat shock proteins (*HSPs*) also showed stronger changes under H HrH in comparison to under H LrH (Figure 10). These results suggest that high relative air humidity induces the stronger heat stress responses as compared to low relative air humidity.

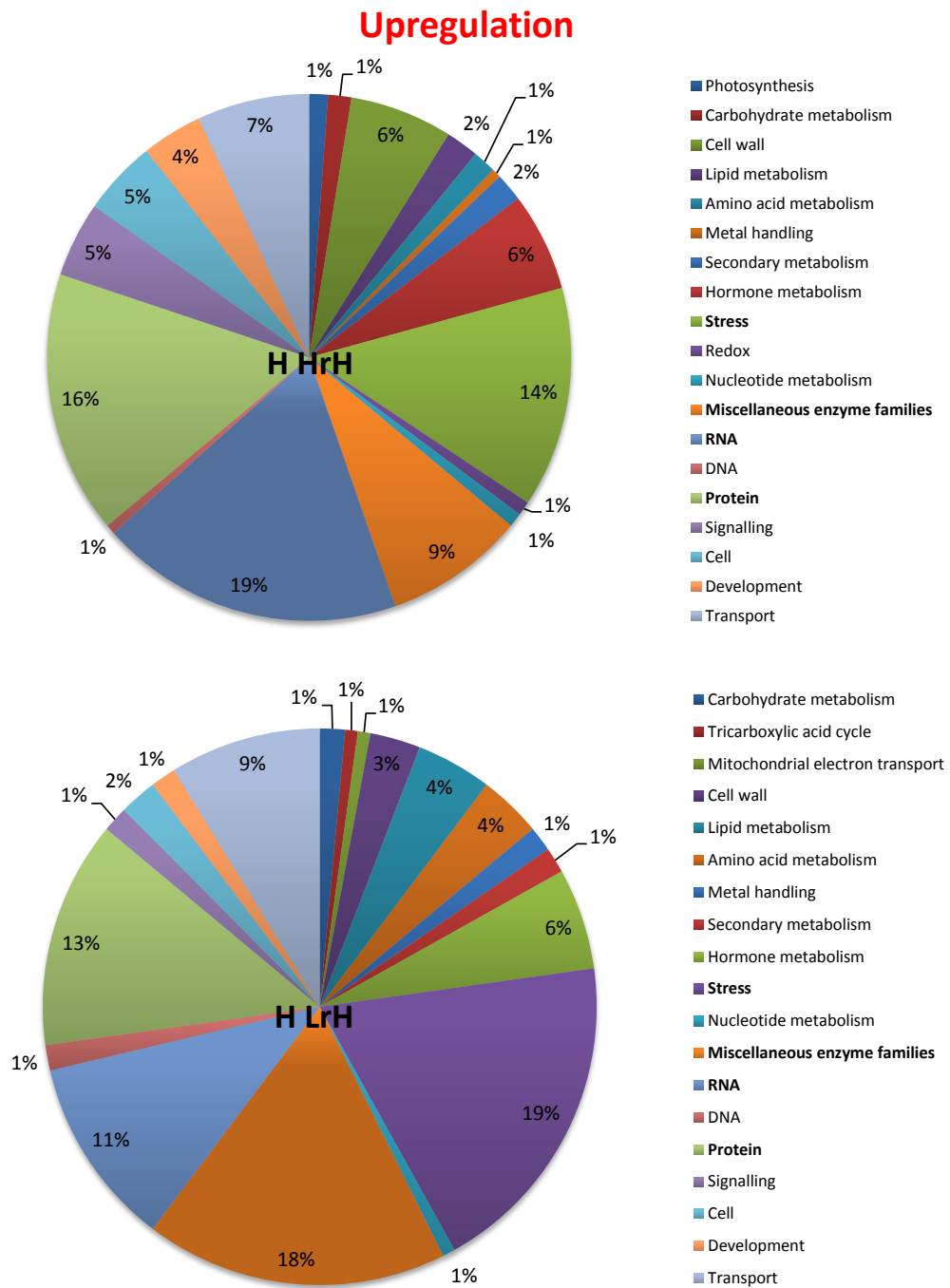


Figure 8. Gene ontology (GO) categories of upregulated genes in wild type under H HrH and H LrH as compared to control condition. MapMan 3.5.1R2 was applied to differentially expressed genes (See 4.2.4.1). The portion of different groups is given in percent.

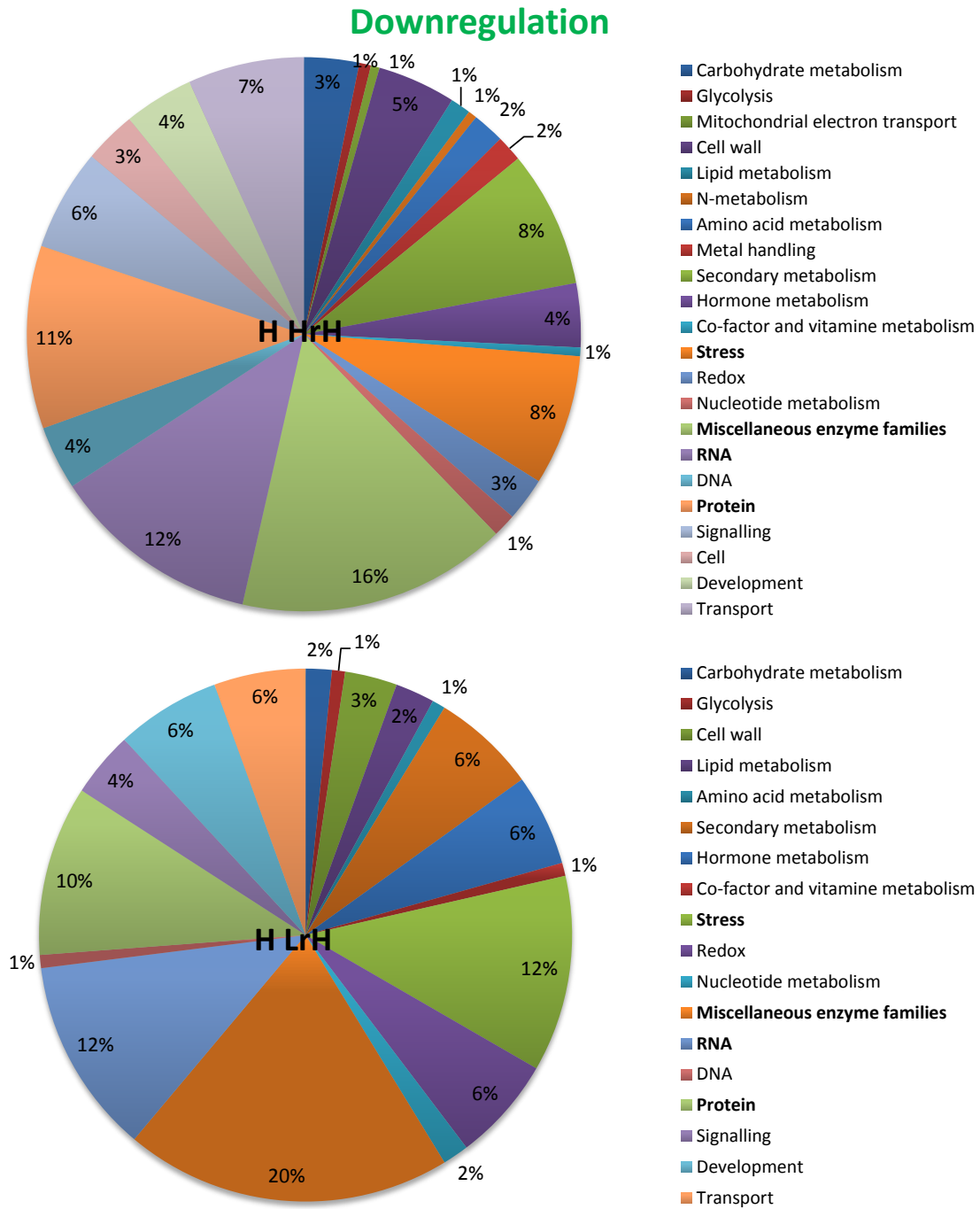


Figure 9. Gene ontology (GO) categories of downregulated genes in wild type under H HrH and H LrH as compared to control condition. MapMan 3.5.1R2 was applied to differentially expressed genes. The portion of different groups is given in percent.

Table 3. The top listed differentially expressed genes in wild type under H HrH as compared to control condition. The genes were selected according to adj.*P*. The expression ratios of these genes under H LrH were added along with the expression under H HrH.

AGI	Log ₂ FC		AGI	Log ₂ FC		AGI	Log ₂ FC	
	H HrH	H LrH		H HrH	H LrH		H HrH	H LrH
AT3G50970	-4.6	-1.7	AT3G54460	1.0	0.4	AT1G08300	1.5	0.6
AT1G09350	-3.8	-2.0	AT2G29260	1.0	0.2	AT2G30480	1.5	0.4
AT5G52310	-3.5	-1.0	AT3G10030	1.0	0.5	AT1G65040	1.5	0.5
AT2G42540	-3.4	-0.8	AT2G01100	1.0	0.5	AT5G47830	1.5	0.5
AT5G08640	-3.0	-1.9	AT4G02210	1.0	0.5	AT3G45420	1.5	0.5
AT4G16740	-2.8	-0.7	AT1G48970	1.0	0.3	AT4G30570	1.5	0.6
AT4G30650	-2.6	-1.1	AT5G06340	1.0	0.3	AT4G15780	1.6	0.6
AT5G48880	-2.5	-1.0	AT1G54250	1.0	0.4	AT1G76065	1.6	0.6
AT5G59670	-2.5	-0.5	AT3G53630	1.0	0.2	AT1G72645	1.6	0.7
AT1G25422	-2.5	-0.8	AT2G24830	1.0	0.4	AT4G25980	1.6	0.7
AT5G45280	-2.3	-0.9	AT2G31890	1.0	0.3	AT1G10960	1.7	1.0
AT1G76790	-2.3	-0.7	AT3G43210	1.0	0.6	AT1G09140	1.7	1.0
AT1G06000	-2.2	-1.0	AT1G20920	1.0	0.5	AT1G27590	1.7	0.7
AT4G31870	-2.2	-0.9	AT3G60910	1.0	0.5	AT2G36950	1.7	0.8
AT1G51090	-2.1	-0.4	AT5G16110	1.1	0.5	AT3G59750	1.7	0.9
AT4G27570	-2.1	-0.7	AT1G10240	1.1	0.6	AT2G17036	1.8	0.8
AT4G21400	-2.0	-0.5	AT2G29400	1.1	0.5	AT1G27420	1.8	1.2
AT1G06690	-2.0	-0.8	AT5G56380	1.1	0.5	AT2G17900	1.8	0.6
AT5G55570	-2.0	-0.8	AT1G71260	1.1	0.3	AT2G32340	1.8	0.8
AT4G27560	-1.9	-0.5	AT5G66090	1.1	0.4	AT1G77880	1.8	0.7
AT1G09780	-1.8	-1.1	AT3G17740	1.1	0.5	AT1G14360	1.8	0.8
AT4G34950	-1.8	-0.9	AT5G44660	1.1	0.6	AT4G38700	1.8	0.7
AT5G46230	-1.8	-0.6	AT3G19508	1.1	0.4	AT2G42330	1.9	0.8
AT1G76020	-1.8	-0.8	AT3G26180	1.1	0.7	AT2G21640	1.9	0.7
AT5G05580	-1.7	-0.9	AT3G05790	1.1	0.3	AT4G31351	1.9	1.1
AT4G23020	-1.7	-0.6	AT1G56200	1.1	0.4	AT4G31354	1.9	1.2
AT1G52770	-1.7	-0.4	AT2G46610	1.2	0.9	AT1G03470	1.9	0.7
AT1G29720	-1.7	-0.6	AT2G37340	1.2	0.6	AT3G24100	2.1	0.9
AT3G23810	-1.7	-0.7	AT5G66240	1.2	0.5	AT5G03720	2.1	0.8
AT1G18265	-1.6	-0.5	AT5G59440	1.2	0.6	AT1G64720	2.1	1.0
AT5G17780	-1.6	-0.8	AT2G23348	1.2	0.4	AT1G29465	2.2	1.0
AT1G79460	-1.6	-0.6	AT2G47420	1.2	0.2	AT2G19310	2.2	1.1
AT4G21215	-1.5	-1.0	AT1G13790	1.2	0.4	AT5G46490	2.3	1.3
AT2G31390	-1.5	-0.6	AT1G23860	1.2	0.9	AT2G07671	2.3	0.5
AT3G09540	-1.5	-0.7	AT2G32920	1.2	0.3	AT4G29770	2.3	0.8
AT2G36500	-1.5	-0.6	AT1G58150	1.2	0.5	AT3G29810	2.4	1.2
AT5G59130	-1.4	-0.4	AT1G24095	1.2	0.5	AT1G07350	2.4	1.5
AT1G14580	-1.4	-0.9	AT1G26580	1.3	0.7	AT5G25280	2.4	0.9
AT2G36880	-1.4	-0.7	AT3G58930	1.3	0.5	AT4G23493	2.9	1.1

RESULTS

AT1G31190	-1.3	-0.6	AT3G13224	1.3	0.8	AT2G32120	3.6	0.9
AT1G78570	-1.3	-0.7	AT2G33250	1.3	0.4	AT5G64510	3.8	1.7
AT4G15450	-1.2	-0.2	AT1G76080	1.3	0.8	AT3G24500	4.1	2.6
AT1G18360	-1.2	-0.6	AT3G60300	1.3	0.6	AT4G19430	4.5	2.4
AT2G38740	-1.2	-0.3	AT1G78750	1.3	0.5	AT5G25450	5.0	2.0
AT5G15760	-1.2	-0.8	AT3G17460	1.4	0.6	AT5G52640	5.1	2.6
AT5G14570	-1.2	-0.5	AT3G04160	1.4	0.6	AT3G12580	5.4	3.1
AT1G64890	-1.2	-0.4	AT4G27370	1.4	0.4	AT5G59720	5.5	0.4
AT5G15650	-1.1	-0.4	AT3G62600	1.4	0.3	AT1G07400	6.1	3.1
AT5G06060	-1.1	-0.4	AT5G03830	1.4	0.7	AT1G72660	6.2	1.9
AT3G03350	-1.1	-0.5	AT2G45920	1.4	1.0	AT5G51440	6.4	2.8
AT3G13060	-1.1	-0.4	AT1G03410	1.4	1.2	AT4G12400	6.5	3.1
AT4G28550	-1.0	-0.5	AT2G20585	1.4	0.4	AT2G29500	6.7	1.6
AT1G79080	-1.0	-0.4	AT3G01770	1.5	0.6	AT5G12030	7.1	2.4
AT1G13930	-1.0	-0.2	AT1G61970	1.5	0.7	AT3G46230	7.3	2.3
AT2G33740	1.0	0.5	AT5G58590	1.5	0.7	AT1G53540	7.8	2.0
AT4G02980	1.0	0.2	AT5G24155	1.5	0.7			

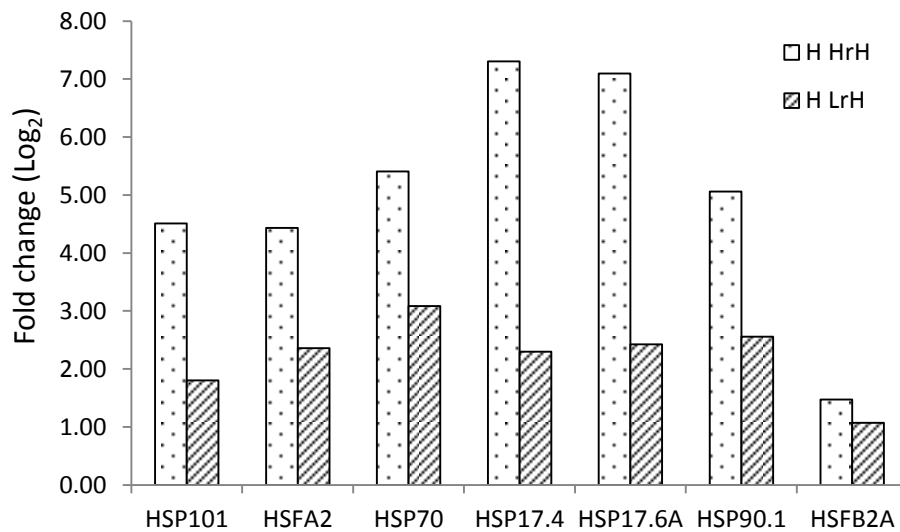


Figure 10. Relative expression levels of heat marker genes including heat shock factors (*HSFs*) and heat shock proteins (*HSPs*) in wild type under H HrH and H LrH as compared to control condition. The values were extracted from Agilent microarray analysis.

A Venn diagram depicted that out of 524 upregulated and 794 downregulated genes under H HrH, 453 enhanced genes and 685 decreased genes were specific to heat stress with high relative air humidity, whereas 71 elevated genes and 109 reduced genes were differentially expressed under both H HrH and H LrH (Figure 11). To better elucidate the specific changes associated with H HrH treatment, exclusively differentially expressed genes under H HrH were compiled excluding genes displaying a tendency of change at the transcriptional level under H LrH ($0.5 \leq |\text{Log}_2\text{FC}| < 1$ and $\text{adj.}P \leq 0.05$). Furthermore, these genes were analyzed whether they had been detected in eight other regular heat stress experiments listed in the Genevestigator database (<https://www.genevestigator.com/gv/plant.jsp>; May 2014). According to these criteria, 129 upregulated genes and 215 downregulated genes were specific to the H HrH condition (Figure 12). These specifically regulated genes were associated with photosynthesis, carbohydrate metabolism, cell wall, lipid metabolism and other functional classifications (Table 4 and Table S1). Several interesting aspects will be described in the following.

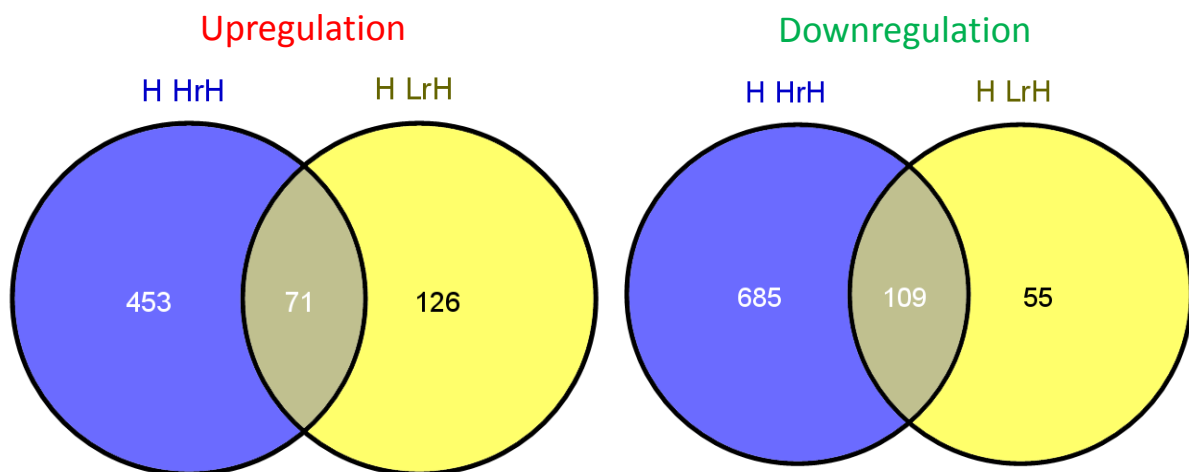


Figure 11. Venn diagram of differentially expressed genes in wild type under H HrH and H LrH in comparison to control condition. Only genes with changes in steady-state level of $|\text{Log}_2\text{FC}| \geq 1$ and $\text{adj.}P \leq 0.05$ are included.

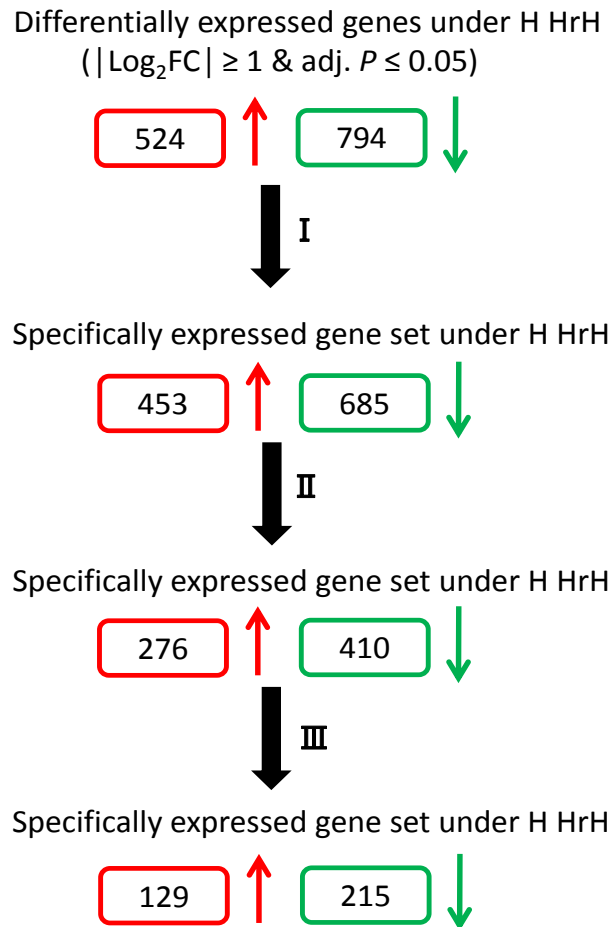


Figure 12. Scheme of specifically regulated genes in wild type under H HrH as compared to control condition selected according to the following criteria: I . Exclude the genes that were significantly changed under H LrH ($|\text{Log}_2\text{FC}| \geq 1$ & $\text{adj. } P \leq 0.05$); II . Exclude the genes that had a tendency to change under H LrH ($0.5 \leq |\text{Log}_2\text{FC}| < 1$ & $\text{adj. } P \leq 0.05$); III . Exclude the genes that significantly changed and had a tendency to change as compared to eight other regular heat stress treatments (*) in Genevestigator databases ($|\text{Log}_2\text{FC}| \geq 0.5$ & $\text{adj. } P \leq 0.05$).

*Experiment ID: AT-00645. 11-day-old plants were subjected to 40°C for 20 min and 1 h.

*Experiment ID: AT-00500. Plants were grown at 22°C and then the temperature was gradually increased until photosynthesis was inhibited by 20% and 30%.

*Experiment ID: AT-00120. 16-day-old plants were treated at 38°C for 0.5 h, 1 h and 3 h.

*Experiment ID: AT-00402. 8-week-old plants were treated at 37°C for 2 h.

*Experiment ID: AT-00387. 3-week-old plants were exposed to 37°C for 30 h.

*Experiment ID: AT-00439. 7-day-old plants grown on ½ MS plates (i.e. also high air humidity) were subjected to 37°C for 1 h.

2.2.2.1 Photosynthesis

In our study, the photosynthesis associated gene *LIGHT HARVESTING COMPLEX PHOTOSYSTEM II (LHCB4.2)* was specifically elevated under H HrH (Table 4). As one component of the light-harvesting complex Lhcb4, *LHCB4.2* plays a role in photoprotection and the enhanced *LHCB4.2* may function in repairing the photooxidative damage induced by H HrH (de Bianchi *et al.*, 2011).

2.2.2.2 Carbohydrate metabolism

Carbohydrate metabolism was balanced by both upregulated and downregulated genes under H HrH (Figure 8 and Figure 9). Two suppressed genes *STARCH EXCESS 4 (SEX4)* and *BETA-AMYLASE 5 (BAM5)* may operate to degrade starch in a coordinated manner (Kötting *et al.*, 2009; Hejazi *et al.*, 2010). In addition, *MYO-INOSITOL OXYGENASE 1 (MIOX1)* was downregulated, suggesting the accumulation of *myo*-inositol as a substrate of raffinose biosynthesis and raffinose biosynthesis genes *GALACTINOL SYNTHASE 4 (GOLS4)* and *RAFFINOSE SYNTHASE 6 (RS6)* were elevated under H HrH (Table 4). These results suggest their specific roles in regulation of starch degradation as well as raffinose biosynthesis under H HrH.

2.2.2.3 Cell wall

Cell wall-related processes include biosynthesis of cell wall components, cell wall degradation and modification. A bi-directional regulation of cell wall processes was found under H HrH (Figure 8 and Figure 9). Among these genes, *MYO-INOSITOL OXYGENASE 1 (MIOX1)* involved in the biosynthesis of a pectin and hemicellulose precursor was downregulated, but *FRA8 HOMOLOG (F8H)* associated with hemicellulose biosynthesis was upregulated. Another two genes encoding cellulose synthase-like proteins, *CSLA14* and *CSLG1*, were elevated and reduced, respectively. In addition, cell wall degradation-associated genes *BETA-XYLOSIDASE 1 (BXL1)* and *AT5G39910* encoding pectin lyase-like proteins were both upregulated, whereas another pectin lyase-like protein encoding gene *AT1G02460* was

downregulated. Cell wall extensibility are dependent on xyloglucan endotransglucosylase/hydrolases (*XTHs*) and expansins (*EXPs*). Interestingly, all specifically regulated *XTHs* and *EXPs* were increased under H HrH (Table 4). Altogether, these data indicate that cell wall biosynthesis and degradation were specifically disturbed under H HrH and cell wall extensibility may be improved mainly by upregulation of *XTHs* and *EXPs*.

2.2.2.4 Lipid metabolism

Genes associated with lipid metabolism were either upregulated or downregulated under H HrH (Figure 8 and Figure 9). 3-Ketoacyl CoA Synthase *KCS12* and carboxyl-CoA ligase *AAE12* may be involved in fatty acid and lipid biosynthetic pathways, but these two genes were oppositely regulated. Another lipid transfer protein encoding gene *A7* was specifically elevated under H HrH, but the function was not clear yet (Table 4). These specific changes in lipid metabolism under H HrH may impact cutin, wax and phospholipid biosynthesis and in turn alter the membrane integrity and plant morphology to deal with the heat stress.

2.2.2.5 Secondary metabolism

Secondary metabolism was mainly restricted under H HrH (Figure 8 and Figure 9). These genes were associated with biosynthesis of isoprenoids, phenylpropanoids and glucosinolates. Genes encoding terpene synthases *TPS10* were reduced, but *1-DEOXY-D-XYLULOSE-5-PHOSPHATE SYNTHASE 1 (DXS1)* involved in monoterpene biosynthesis was elevated. In addition, *FLAVIN-MONOOXYGENASE GLUCOSINOLATE S-OXYGENASE 4 (FMO GS-OX4)* and *IQ-DOMAIN (IQD1)* were related to glucosinolate accumulation and they were both repressed under H HrH (Table 4). Altogether, the specific changes of genes associated to secondary metabolism may play a role in restriction of terpene biosynthesis, lignin biosynthesis and glucosinolate accumulation under H HrH.

2.2.2.6 Hormone metabolism

The specific changed genes classified into hormone metabolism were associated with auxin responses under H HrH. *NITRILASE 2 (NIT2)* that catalyzes the hydrolysis of indole-3-acetonitrile (IAN) to indole-3-acetic acid (IAA) was reduced, but the small auxin upregulated RNAs (*SAURs*) that are involved in early auxin-responsive processes were enhanced. In addition, cytokinin and gibberellin associated genes were also differentially regulated under H HrH by elevating the expression of *CYTOKININ OXIDASE 2 (CKX2)* and *GA-STIMULATED ARABIDOPSIS 1 (GASA1)* (Table 4). This implies their specific roles in regulation of hormone metabolism under H HrH.

2.2.2.7 Transport

Specific genes relevant to transport processes were mainly deregulated under H HrH. Among these genes, sucrose transporter *GLUCOSE-6-PHOSPHATE/PHOSPHATE TRANSLOCATOR 2 (GPT2)* and cation transporter *CATION/H⁺ EXCHANGER 7 (CHX7)* were repressed. In addition, *TONOPLAST INTRINSIC PROTEIN 2;1 (TIP2;1)* was specifically increased under H HrH (Table 4). The differential regulation of transporters and channels may impact the membrane properties and contribute to osmotic regulation in H HrH treatment.

Last but not least, a large number of the functionally uncharacterized genes were associated with *stress responses, signalling transduction, development* and other functional classifications. These genes, either upregulated or highly expressed (down- or upregulated) in rosettes (Table 4) or lowly expressed and downregulated in rosettes (Table S1), were compiled into a resource for further studies of stress responses (Table 4 and Table S1). Altogether, the specific responses to H HrH involved genes related to modifying the cell wall and cell membrane properties, regulating the carbohydrate and secondary metabolism as well as adjusting the osmosis and hormone metabolism.

Table 4. Specifically altered genes that are upregulated or highly expressed (down- or upregulated) in rosettes of wild type under H HrH (red and green values represent fold change of significantly increased and decreased genes, respectively). See also Table S1.

AGI	Gene Name	Log ₂ FC	adj.P
Photosynthesis			
AT3G08940	<i>LHCB4.2</i>	1.02	9.71E-13
Carbohydrate metabolism			
AT1G14520	<i>MIOX1</i>	-1.07	2.45E-05
AT4G15210	<i>BAM5</i>	-1.96	1.26E-07
AT3G52180	<i>SEX4</i>	-1.04	4.11E-09
AT5G20250	<i>RS6</i>	1.86	1.08E-21
AT1G60470	<i>GoIS4</i>	2.07	0.02
Cell wall			
AT4G24010	<i>CSLG1</i>	-1.53	2.13E-16
AT3G56000	<i>CSLA14</i>	1.40	2.74E-12
AT5G22940	<i>F8H</i>	1.04	1.24E-08
AT5G49360	<i>BXL1</i>	2.13	2.56E-14
AT1G02460	<i>Pectin lyase-like superfamily protein</i>	-1.23	3.15E-11
AT5G39910	<i>Pectin lyase-like superfamily protein</i>	2.25	8.18E-04
AT5G57560	<i>XTH22</i>	1.04	0.02
AT1G10550	<i>XTH33</i>	1.07	6.93E-07
AT1G32170	<i>XTH30</i>	1.21	9.99E-13
AT4G37800	<i>XTH7</i>	1.54	2.38E-08
AT3G25050	<i>XTH3</i>	1.77	0.01
AT3G45960	<i>EXPL3</i>	1.39	3.07E-11
AT2G40610	<i>EXP8</i>	1.56	2.10E-07
Lipid metabolism			
AT1G65890	<i>AAE12</i>	-1.41	1.86E-08
AT2G28630	<i>KCS12</i>	1.43	6.55E-16
AT4G28395	<i>ATA7</i>	6.16	3.76E-04
Secondary metabolism			
AT4G15560	<i>DXS1</i>	1.04	1.26E-25
AT2G24210	<i>TPS10</i>	-3.32	3.64E-10
AT4G23600	<i>COR13</i>	-1.67	6.70E-10
AT4G37990	<i>CAD8</i>	-2.36	4.22E-09
AT1G62570	<i>FMO GS-OX4</i>	-1.64	5.86E-13
AT3G09710	<i>IQD1</i>	-1.09	9.13E-18
AT3G50280	<i>HXXXD-type acyl-transferase family protein</i>	-1.22	3.53E-07
AT4G28420	<i>Tyrosine transaminase family protein</i>	1.16	5.99E-04
AT2G38240	<i>ZOG-Fe(II) oxygenase superfamily protein</i>	-2.28	5.25E-05
Hormone metabolism			
AT3G44300	<i>NIT2</i>	-1.14	6.11E-04
AT3G25880	<i>NAD(P)-binding Rossmann-fold superfamily protein</i>	1.15	0.01
AT4G34770	<i>SAUR1</i>	1.20	1.25E-05

AT1G29490	<i>SAUR68</i>	1.31	2.43E-11
AT4G38825	<i>SAUR13</i>	1.46	1.05E-10
AT2G19500	<i>CKX2</i>	1.46	1.39E-03
AT1G74670	<i>GASA6</i>	1.87	2.60E-13
AT3G10185	<i>Gibberellin-regulated GASA/GAST/Snakin family protein</i>	-1.67	5.16E-13
Transport			
AT1G74810	<i>BOR5</i>	-1.42	1.51E-07
AT1G61800	<i>GPT2</i>	-1.31	1.85E-03
AT5G61810	<i>APC1</i>	-1.05	4.14E-21
AT1G57990	<i>PUP18</i>	1.02	4.36E-04
AT3G16240	<i>TIP2;1</i>	1.06	9.44E-07
AT4G27420	<i>ABCG9</i>	1.12	0.05
RNA			
AT1G21910	<i>DREB26</i>	1.19	3.16E-06
AT1G36060	<i>DREB subfamily A-6 of ERF/AP2 transcription factor family</i>	1.75	4.80E-12
AT1G51120	<i>AP2/B3 transcription factor family protein</i>	1.54	0.03
AT3G46770	<i>AP2/B3-like transcriptional factor family protein</i>	1.08	9.53E-12
AT1G68840	<i>RAP2.8</i>	1.16	9.82E-06
AT5G22570	<i>WRKY38</i>	-1.95	2.69E-10
AT2G25230	<i>MYB100</i>	2.67	0.05
AT1G66370	<i>MYB113</i>	-1.63	4.22E-09
AT1G48000	<i>MYB112</i>	-1.01	3.59E-04
AT5G24110	<i>WRKY30</i>	1.17	1.55E-04
AT2G40740	<i>WRKY55</i>	1.26	1.57E-03
AT4G09820	<i>TT8</i>	-1.81	6.01E-07
AT4G20970	<i>bHLH DNA-binding superfamily protein</i>	-1.48	2.35E-26
AT4G05170	<i>bHLH DNA-binding superfamily protein</i>	1.65	0.02
AT2G47890	<i>B-box type zinc finger protein with CCT domain</i>	-1.07	3.76E-16
AT5G25390	<i>SHN2</i>	-1.07	1.50E-06
AT5G28770	<i>BZIP63</i>	1.20	6.90E-12
AT5G15830	<i>bZIP3</i>	1.51	7.30E-08
AT2G37060	<i>NF-YB8</i>	1.54	1.95E-23
AT1G28450	<i>AGL58</i>	2.54	0.02
AT2G06020	<i>Homeodomain-like superfamily protein</i>	2.65	4.33E-03
AT3G27860	<i>Tudor/PWWP/MBT superfamily protein</i>	1.00	1.41E-14
AT5G66270	<i>Zinc finger C-x8-C-x5-C-x3-H type family protein</i>	1.01	2.09E-16
Fermentation			
AT1G77120	<i>ADH1</i>	-1.10	8.40E-07
AT1G23800	<i>ALDH2B7</i>	-1.00	9.34E-12
Pentose phosphate pathway			
AT1G13700	<i>PGL1</i>	1.28	2.35E-06
Amino acid metabolism			
AT3G16150	<i>ASPG1</i>	1.13	0.01
Metal handling			
AT1G51090	<i>Heavy metal transport/detoxification superfamily protein</i>	-2.12	3.59E-28

RESULTS

AT3G09390	<i>MT2A</i>	-1.07	6.88E-11
AT5G01600	<i>FER1</i>	-1.05	1.80E-04
AT4G39700	<i>Heavy metal transport/detoxification superfamily protein</i>	1.05	4.24E-11
Stress			
AT1G73325	<i>Kunitz family trypsin and protease inhibitor protein</i>	-1.47	2.61E-05
AT1G58602	<i>Disease resistance protein</i>	-1.34	2.07E-12
AT4G38410	<i>Dehydrin family protein</i>	-1.18	2.32E-11
AT2G21620	<i>RD2</i>	-1.11	5.58E-19
AT4G16880	<i>Leucine-rich repeat family protein</i>	-1.05	5.69E-12
AT4G36010	<i>Pathogenesis-related thaumatin superfamily protein</i>	-1.01	9.30E-11
AT1G11000	<i>MLO4</i>	1.03	1.03E-16
AT1G71400	<i>RLP12</i>	1.11	7.98E-10
AT1G50060	<i>CAP superfamily protein</i>	2.25	0.02
Nucleotide metabolism			
AT1G14240	<i>Nucleoside phosphatase family protein</i>	-1.60	3.77E-11
AT1G73540	<i>NUDT21</i>	1.02	3.58E-03
Miscellaneous enzyme families			
AT2G39030	<i>NATA1</i>	-2.14	2.93E-09
AT1G45191	<i>BGLU1</i>	-2.02	3.03E-16
AT2G29460	<i>GST22</i>	-1.58	1.42E-07
AT4G39500	<i>CYP96A11</i>	1.39	0.03
AT4G15490	<i>UGT84A3</i>	-1.04	1.51E-15
AT5G61290	<i>Flavin-binding monooxygenase family protein</i>	-1.42	2.38E-13
AT4G22517	<i>Protease inhibitor/LTP family protein</i>	-1.29	1.12E-03
AT4G22513	<i>Protease inhibitor/LTP family protein</i>	-1.63	5.80E-05
AT4G22485	<i>Protease inhibitor/LTP family protein</i>	-1.10	3.60E-03
AT3G16410	<i>NSP4</i>	-1.28	1.35E-07
AT4G09750	<i>Oxidoreductase superfamily protein</i>	-1.27	6.52E-16
AT1G68470	<i>Exostosin family protein</i>	-1.12	7.98E-13
AT2G48130	<i>Bifunctional inhibitor/lipid-transfer protein</i>	1.02	0.04
AT2G45180	<i>Bifunctional inhibitor/lipid-transfer protein</i>	1.07	4.83E-08
AT4G22505	<i>Bifunctional inhibitor/lipid-transfer protein</i>	-1.08	3.89E-03
AT4G28405	<i>Bifunctional inhibitor/lipid-transfer protein</i>	1.13	0.01
AT1G33811	<i>GDSL-like Lipase/Acylhydrolase superfamily protein</i>	1.10	1.78E-06
AT4G18970	<i>GDSL-like Lipase/Acylhydrolase superfamily protein</i>	1.34	3.65E-09
Protein			
AT5G25110	<i>SnRK3.25</i>	-1.73	1.74E-10
AT4G17470	<i>Alpha/beta-Hydrolases superfamily protein</i>	-1.48	2.85E-04
AT3G50720	<i>Protein kinase superfamily protein</i>	2.18	0.04

2.2.3 Impact of high relative air humidity on combined drought and heat stress

To identify the alteration of responses to combined drought and heat stresses with different relative air humidity in wild type, GO assignment was performed by MapMan 3.5.1R2 and the functional categories excluding the group of *not assigned* genes are shown in Figure 13 and Figure 14. Either upregulated or downregulated genes were mainly associated with *miscellaneous enzyme families, stress responses, RNA related process and protein modification or degradation* under both DH HrH and DH LrH (Figure 13 and Figure 14). In addition, to evaluate the drought effect and heat effect in response to combined drought and heat stress, Venn diagram was applied with the differentially expressed genes under drought stress, heat stress and combined drought and heat stress as compared to control condition (Figure 15). The results showed that out of 1499 upregulated and 1850 downregulated genes under DH HrH, 478 enhanced and 505 reduced genes were changed due to the drought effect as well as 251 increased and 312 decreased genes were changed due to the heat effect. Another 68 upregulated and 117 downregulated genes were regulated by both drought effect and heat effect (Figure 15A). In addition, out of 2051 upregulated and 2510 downregulated genes under DH LrH, 669 enhanced and 621 reduced genes were changed due to the drought effect as well as 40 increased and 50 decreased genes were changed due to the heat effect. Another 77 enhanced and 73 repressed genes were differentially regulated by both drought effect and heat effect (Figure 15B). These results suggest that less drought responsive genes, but more heat responsive genes were differentially regulated under DH HrH than under DH LrH. In particular, the drought marker genes including *ABSCISIC ACID RESPONSIVE ELEMENTS-BINDING FACTOR 2 (ABF2)*, *NINE-CIS-EPOXYCAROTENOID DIOXYGENASE 3 (NCED3)*, *ABSCISIC ACID RESPONSIVE ELEMENTS-BINDING FACTOR 3 (ABF3)*, *DEHYDRATION-RESPONSIVE ELEMENT BINDING PROTEIN 2 (DREB2A)* and *RESPONSIVE TO DESSICATION 29B (RD29B)* were generally less upregulated under DH HrH than under DH LrH (Figure 16A) and the heat marker genes involved in heat

shock factors (*HSFs*) and heat shock proteins (*HSPs*) were generally stronger upregulated except *HSFB2A* under DH HrH than under DH LrH (Figure 16B). Altogether, these results indicate that drought effect is alleviated, but heat effect is aggravated under DH HrH as compared to DH LrH.

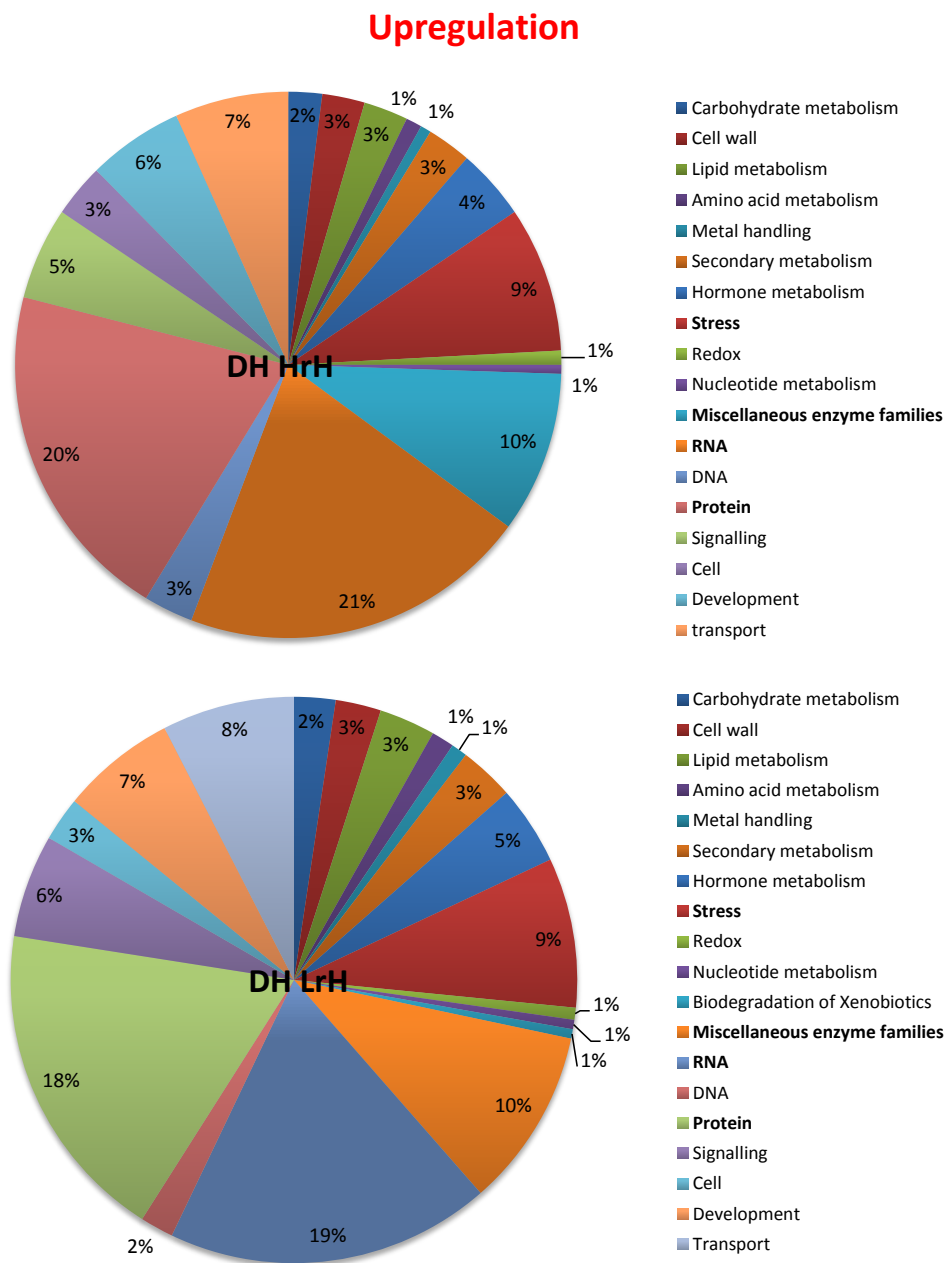


Figure 13. Gene ontology (GO) categories of upregulated genes in wild type under DH HrH and DH LrH in comparison to control condition. MapMan 3.5.1R2 was applied using differentially expressed genes (See 4.2.4.1). The portion of different groups is given in percent.

Downregulation

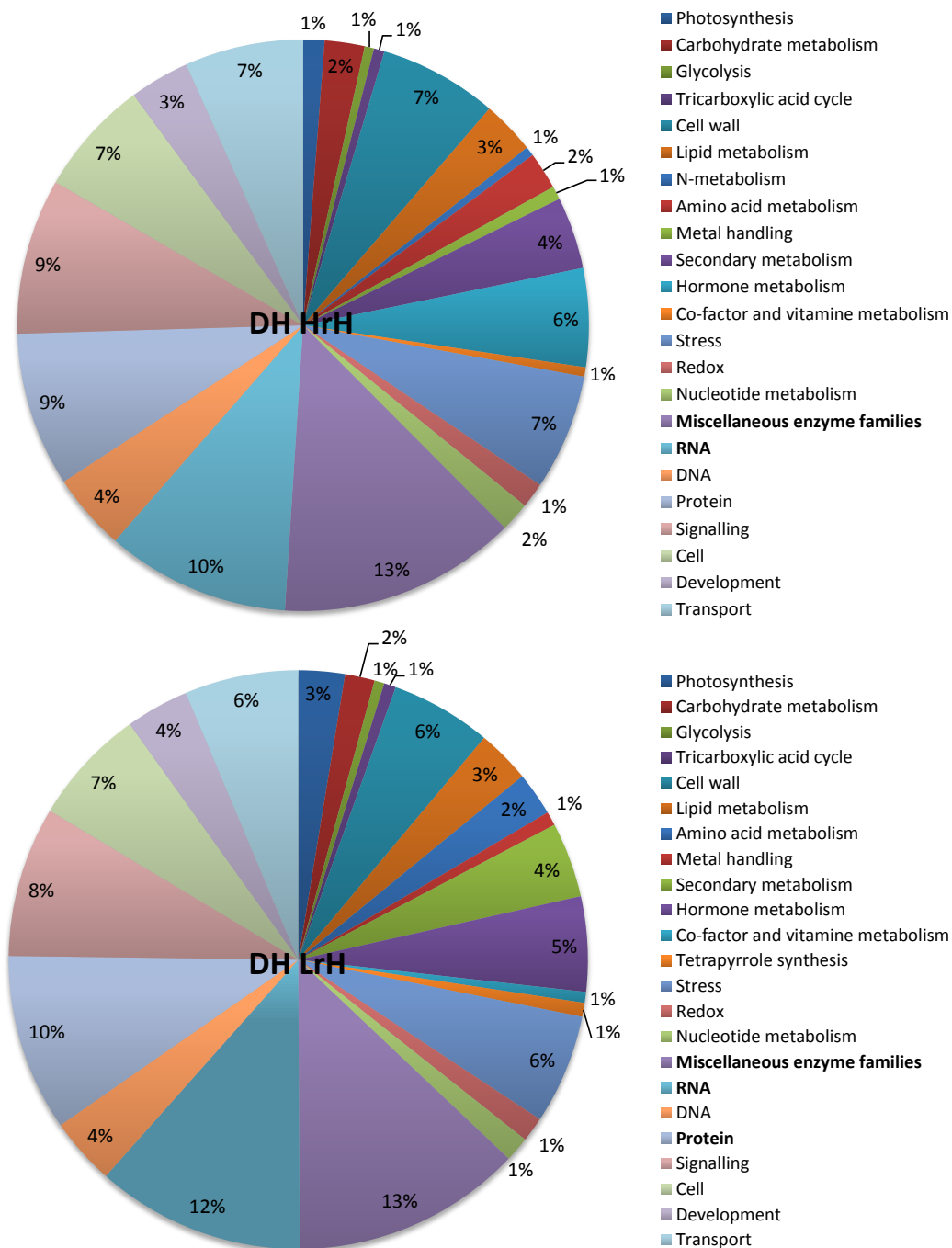


Figure 14. Gene ontology (GO) categories of downregulated genes of wild type under DH HrH and DH LrH as compared to control condition. MapMan 3.5.1R2 was applied to differential expressed genes (See 4.2.4.1). The portion of different groups is given in percent.

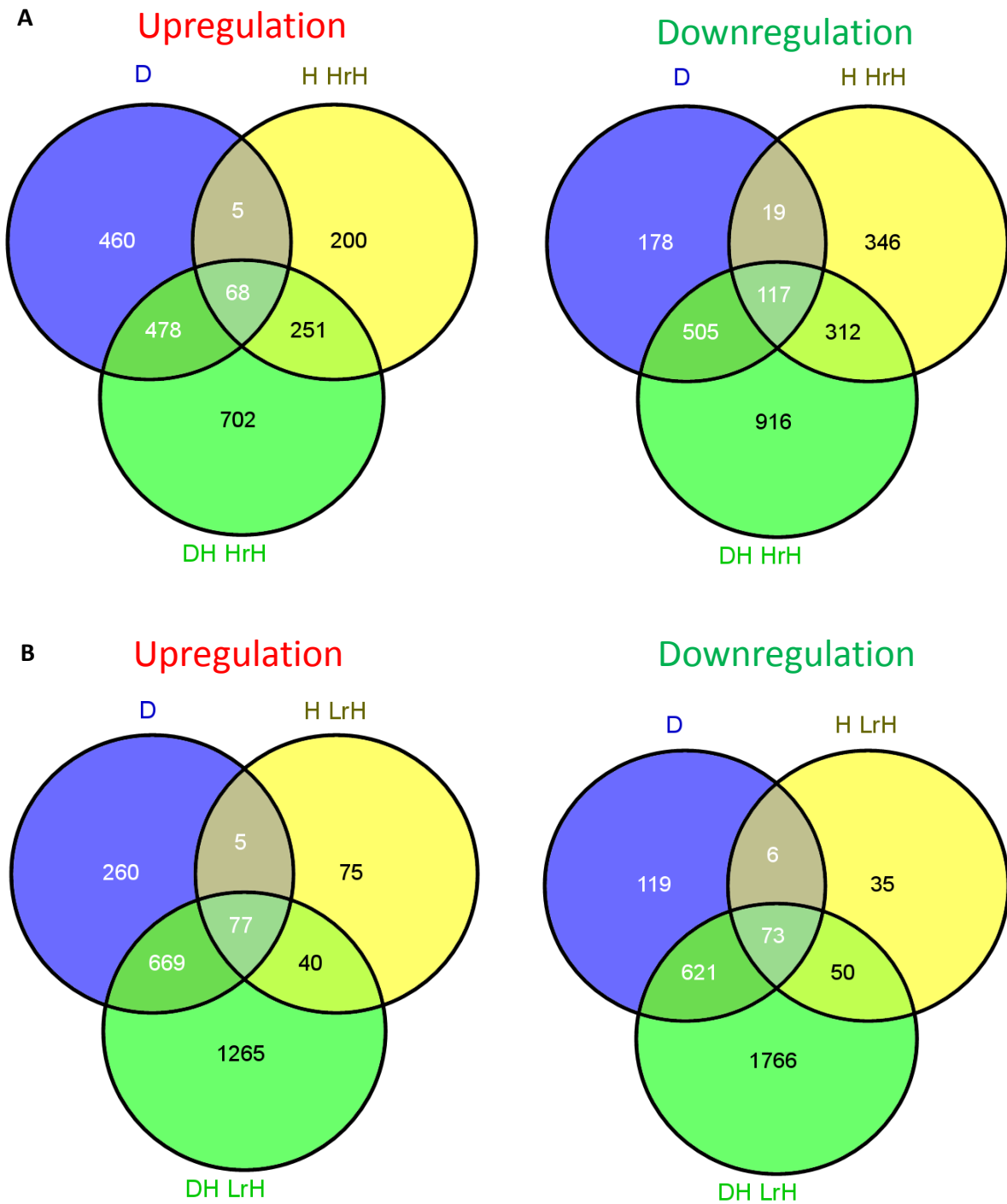


Figure 15. Venn diagram of differentially expressed genes in wild type under (A) drought stress, H HrH and DH HrH; (B) drought stress, H LrH and DH LrH in comparison to control condition. Only genes with changes in steady-state level of $|\text{Log}_2\text{FC}| \geq 1$ and $\text{adj. } P \leq 0.05$ are included.

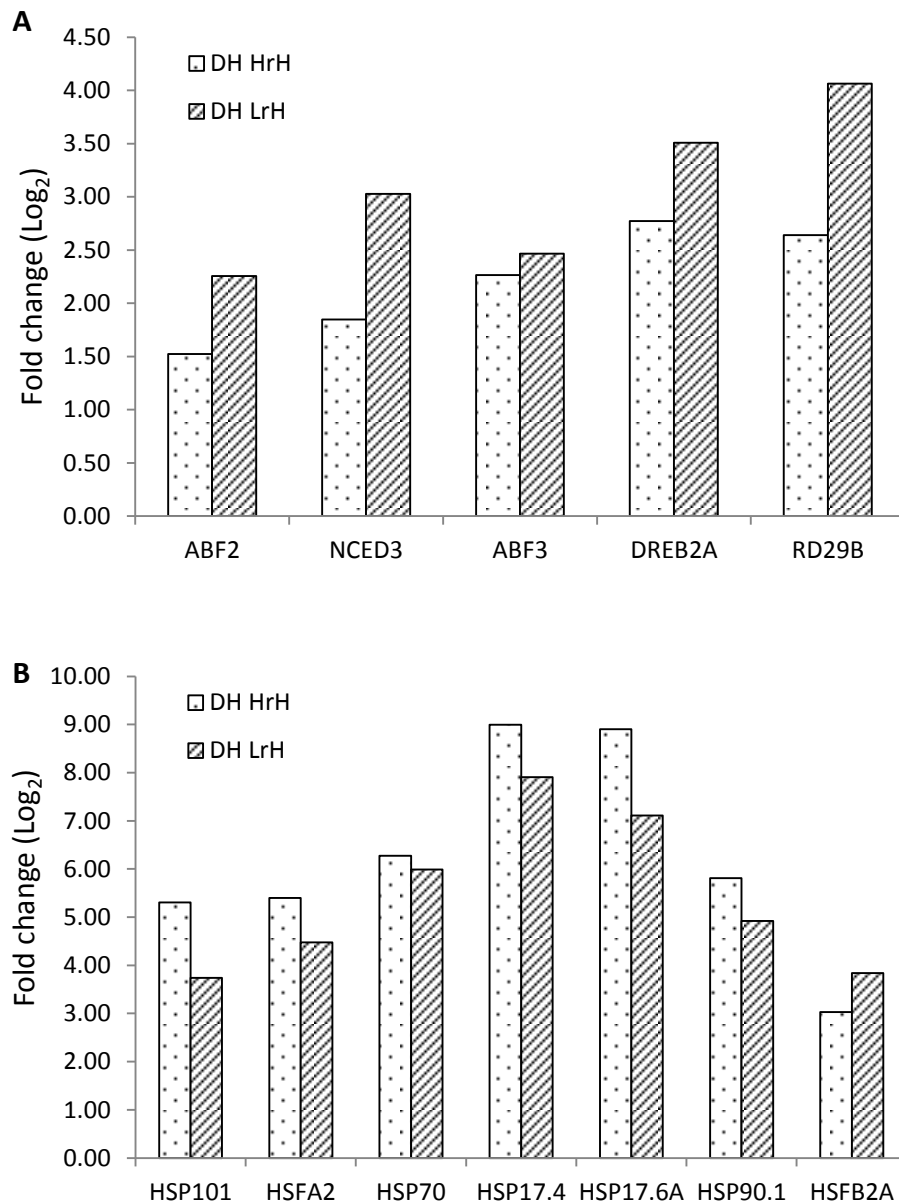


Figure 16. Relative expression levels of (A) drought marker genes and (B) heat marker genes in wild type under DH HrH and DH LrH as compared to control condition. The values were extracted from Agilent microarray analysis.

A Venn diagram depicted that out of 1499 upregulated and 1850 downregulated genes under DH HrH, 282 enhanced genes and 237 decreased genes were specifically regulated under combined stress with high air humidity, whereas additional 1217 elevated genes and 1613 reduced genes were differentially regulated under both DH HrH and DH LrH (Figure 17).

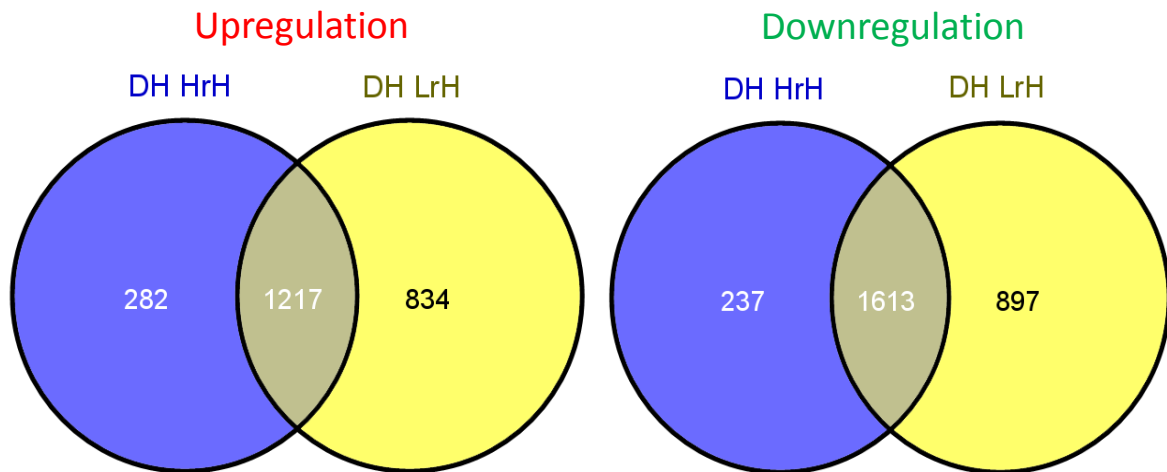


Figure 17. Venn diagram of differentially expressed genes in wild type under DH HrH and DH LrH as compared to control condition. Only genes with changes in steady-state level of $|\text{Log}_2\text{FC}| \geq 1$ and $\text{adj. } P \leq 0.05$ are included.

To better elucidate the specific changes in response to DH HrH treatment, exclusively altered genes under DH HrH were compiled excluding the genes even with a tendency to change at the transcriptional level under DH LrH ($0.5 \leq |\text{Log}_2\text{FC}| < 1$ and $\text{adj. } P \leq 0.05$) as well as the genes which were significantly changed or tended to be changed ($|\text{Log}_2\text{FC}| \geq 0.5$ and $\text{adj. } P \leq 0.05$) in another combined drought and regular heat stress (Prasch and Sonnewald, 2013; Figure 18). Then 80 upregulated genes and 62 downregulated genes were specific to the DH HrH treatment (Figure 18). These specifically regulated genes under DH HrH were associated with *carbohydrate metabolism*, *cell wall*, *lipid metabolism* and other aspects (Table 5 and Table S2). Among these genes, *KCS19* was repressed which may play a role in reducing the wax biosynthesis. The genes associated with hormone metabolism were bi-directionally regulated. The auxin-responsive gene *SAUR69* was upregulated, but *GRETCHEN HAGEN 3.12* (*GH3.12*) was downregulated. The gene encoding *CKX3*, which catalyzes the degradation of cytokinins, was elevated. This suggests that the hormone metabolism was specific modified under DH HrH. In addition, a large number of functionally uncharacterized genes specifically under DH HrH were detected and could be compiled as a genetic resource for further studies on stress responses in plants.

Although a strong alteration of transcription was elucidated under DH HrH, most of the genes were commonly regulated in comparison to DH LrH and only a small number of genes were specifically regulated during DH HrH responses. Therefore, in contrast to the findings for heat stress, high relative air humidity has only a slight impact in response to combined drought and heat stress.

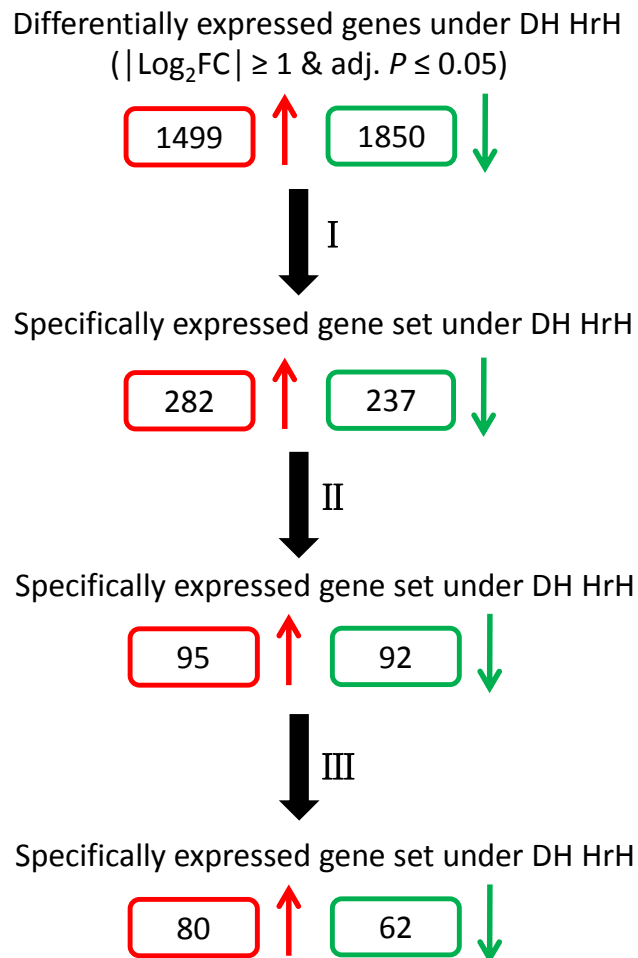


Figure 18. Scheme of specifically regulated genes in wild type under DH HrH as compared to control condition selected according to the following criteria: **I** . Exclude the genes that were significantly changed under DH LrH ($|\text{Log}_2\text{FC}| \geq 1$ & $\text{adj. } P \leq 0.05$); **II** . Exclude the genes that had a tendency to change under DH LrH ($0.5 \leq |\text{Log}_2\text{FC}| < 1$ & $\text{adj. } P \leq 0.05$); **III** . Exclude the genes that significantly changed and had a tendency to change as compared to published data ($|\text{Log}_2\text{FC}| \geq 0.5$ & $\text{adj. } P \leq 0.05$) (Prasch and Sonnewald, 2013).

RESULTS

Table 5. Specifically altered genes that are upregulated or highly expressed (down- or upregulated) in rosettes of wild type under DH HrH (red and green values represent fold change of significantly increased and decreased genes, respectively). See also Table S2.

AGI	Gene Name	Log ₂ FC	adj. <i>P</i>
Cell wall			
AT1G54970	<i>PRP1</i>	3.51	0.01
AT4G33840	<i>Glycosyl hydrolase family 10 protein</i>	2.58	4.68E-04
AT5G48140	<i>Pectin lyase-like superfamily protein</i>	1.37	0.02
Lipid metabolism			
AT4G04930	<i>DES-1-LIKE</i>	1.47	0.03
AT5G04530	<i>KCS19</i>	-1.02	2.33E-07
Secondary metabolism			
AT1G32910	NA	1.33	0.02
AT5G54060	<i>UF3GT</i>	1.11	0.03
Hormone metabolism			
AT5G10990	<i>SAUR69</i>	2.09	1.87E-10
AT5G13320	<i>GH3.12</i>	-1.23	3.08E-18
AT5G24140	<i>SQP2</i>	2.63	6.83E-06
AT5G56970	<i>CKX3</i>	1.23	7.95E-04
Transport			
AT4G00350	<i>MATE efflux family protein</i>	3.02	0.02
Pentose phosphate pathway			
AT5G24410	<i>PGL4</i>	1.02	0.03
Amino acid metabolism			
AT4G28410	NA	1.67	6.07E-07
Stress			
AT1G33900	NA	2.64	0.01
AT4G22115	<i>SCRL14</i>	1.57	0.01
AT4G23515	NA	1.88	9.40E-04
AT5G66890	NA	3.21	2.51E-04
Miscellaneous enzyme families			
AT1G33220	NA	1.71	1.64E-03
AT1G48700	NA	1.16	1.28E-03
AT1G67110	<i>CYP735A2</i>	1.39	0.02
AT1G73560	NA	2.01	1.12E-03
AT3G50990	NA	1.04	1.07E-03
AT3G55780	NA	1.34	0.04
AT5G24540	<i>BGLU31</i>	2.20	4.76E-04
AT5G42260	<i>BGLU12</i>	1.99	8.55E-04
AT5G46990	NA	1.49	0.04
RNA			
AT1G18790	<i>RKD1</i>	3.04	1.61E-03
AT1G49130	NA	1.16	6.27E-07
AT2G30380	NA	4.52	3.44E-03

			RESULTS	
AT3G53600	NA		1.93	0.01
AT4G10680	NA		2.46	0.01
AT5G27090	AGL54		1.55	0.01
DNA				
AT4G04402	NA		4.83	0.01
AT4G04957	NA		2.19	0.02
Protein				
AT1G14315	NA		1.66	0.01
AT2G03000	NA		1.96	0.03
AT2G16450	NA		1.24	0.03
AT2G27650	NA		1.82	8.44E-04
AT3G09790	UBQ8		3.37	0.02
AT3G19890	NA		3.83	0.04
AT5G12090	NA		1.67	0.03
AT5G17730	NA		1.18	3.86E-03
AT5G41440	NA		1.87	9.65E-04
AT5G67120	NA		1.37	3.13E-03
Signalling				
AT1G18210	NA		-1.21	2.95E-17
AT2G04300	NA		1.70	0.02
AT2G20660	RALFL14		3.64	7.12E-04
AT3G29780	RALFL27		2.25	0.01
AT3G46760	NA		2.15	0.01
AT5G41300	NA		1.15	0.04
AT5G48130	NA		1.70	0.04
Cell				
AT3G11820	SYP121		-1.08	1.48E-11
Development				
AT3G20400	EMB2743		1.83	0.01

2.2.4 Impact on expression of aquaporins under water-deficit stresses

Aquaporins are highly diverse in *Arabidopsis thaliana* (Johanson *et al.*, 2001) and the differential regulation of *PIPs* is considered to be essential for water homeostasis in response to drought stress (Alexandersson *et al.*, 2005). To test the transcriptional alteration of aquaporins in wild-type rosettes under water stresses, expression of all the *PIPs* and *TIPs* were extracted from Agilent microarray data described in the beginning of this chapter. The results showed that *PIPs* were generally repressed under drought stress except that *PIP1;4* and *PIP2;5* tended to be increased, which is in agreement with a previous study (Alexandersson *et al.*, 2005). Interestingly, *PIP2;1* and *PIP2;2*, two major *PIP* isoforms

expressed in leaves, were upregulated under both H HrH and H LrH. This upregulation was irrelevant to the different relative air humidity. Then *PIP2;3*, *PIP2;7* and *PIP1;5* were also induced by heat, at least in one heat scenario (H LrH and/or H HrH). In addition, the regulation of aquaporins under combined drought and heat stress was different from either heat stress or drought stress. *PIP2;8* was apparently repressed, whereas *PIP1;4*, *PIP2;3* and *PIP2;5* were induced under combined drought and heat stress (Figure 19). Altogether, differential regulation of aquaporin expressions was exhibited in response to variable water stresses. This implies different roles of aquaporin isoforms in adjusting the water homeostasis during water stress responses.

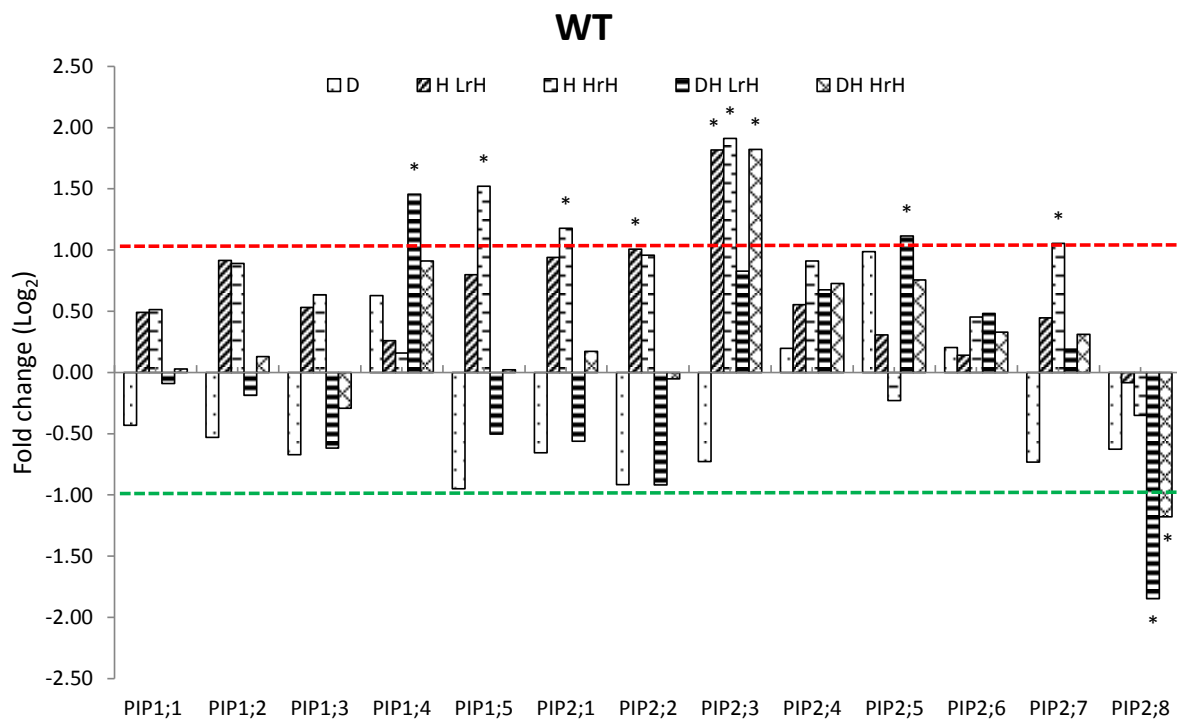


Figure 19. Relative expression levels of *PIPs* in wild type under water stresses as compared to control condition. Values present the integration of microarray data from at least two independent experiments. Significant differences from control condition followed by an asterisk (*) are based on ANOVA analysis.

2.3 Involvement of *PIP2;1*, *PIP2;2* and *PIP2;4* in responses to variable environmental scenarios

2.3.1 Phenotypic and physiological characteristics of *pip2;1 pip2;2* and *pip2;1 pip2;2 pip2;4*

Plant aquaporins facilitate transport of water and small neutral solutes such as CO₂. Therefore, loss of the functions of aquaporins may affect various physiological processes and eventually plant growth. To elucidate the impact of major *PIPs*, *PIP2;1* and *PIP2;2* as well as an additional root-specifically expressed *PIP* gene, *PIP2;4*, on plant phenotypic characteristics, the growth of *pip2;1 pip2;2*, *pip2;1 pip2;2 pip2;4* and wild type was examined using two-week-old seedlings grown on ½ MS agar medium or four-week-old plants grown on well-watered soil. The results showed that there were no visible differences in vegetative growth among *pip* mutants and wild type (Figure 20A and Figure 21A). Also, fresh weight of the rosettes and roots (Figure 20B and Figure 21C) as well as the leaf area (Figure 21B) were not changed in *pip* mutants as compared to the wild type.

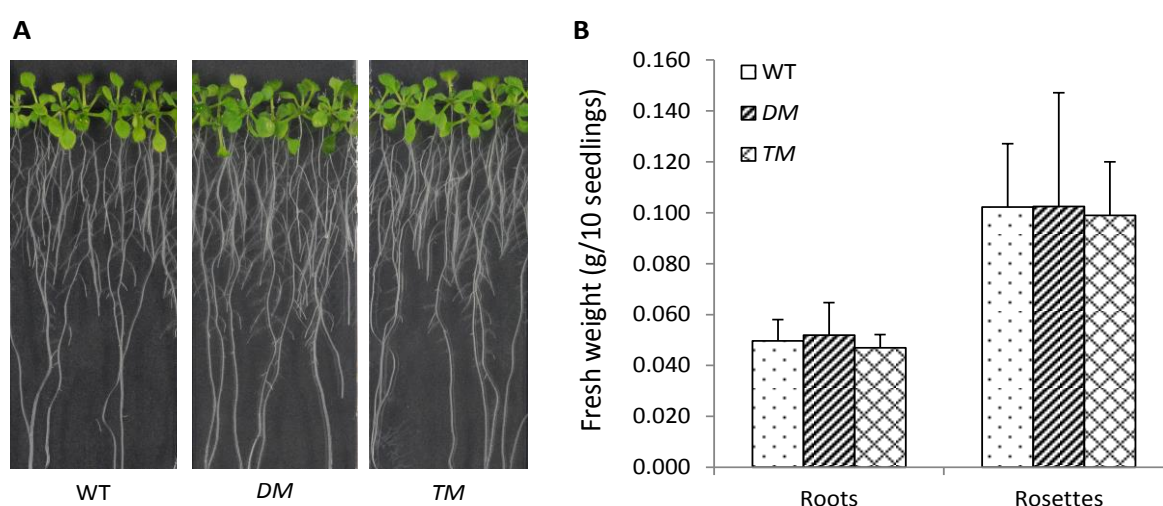
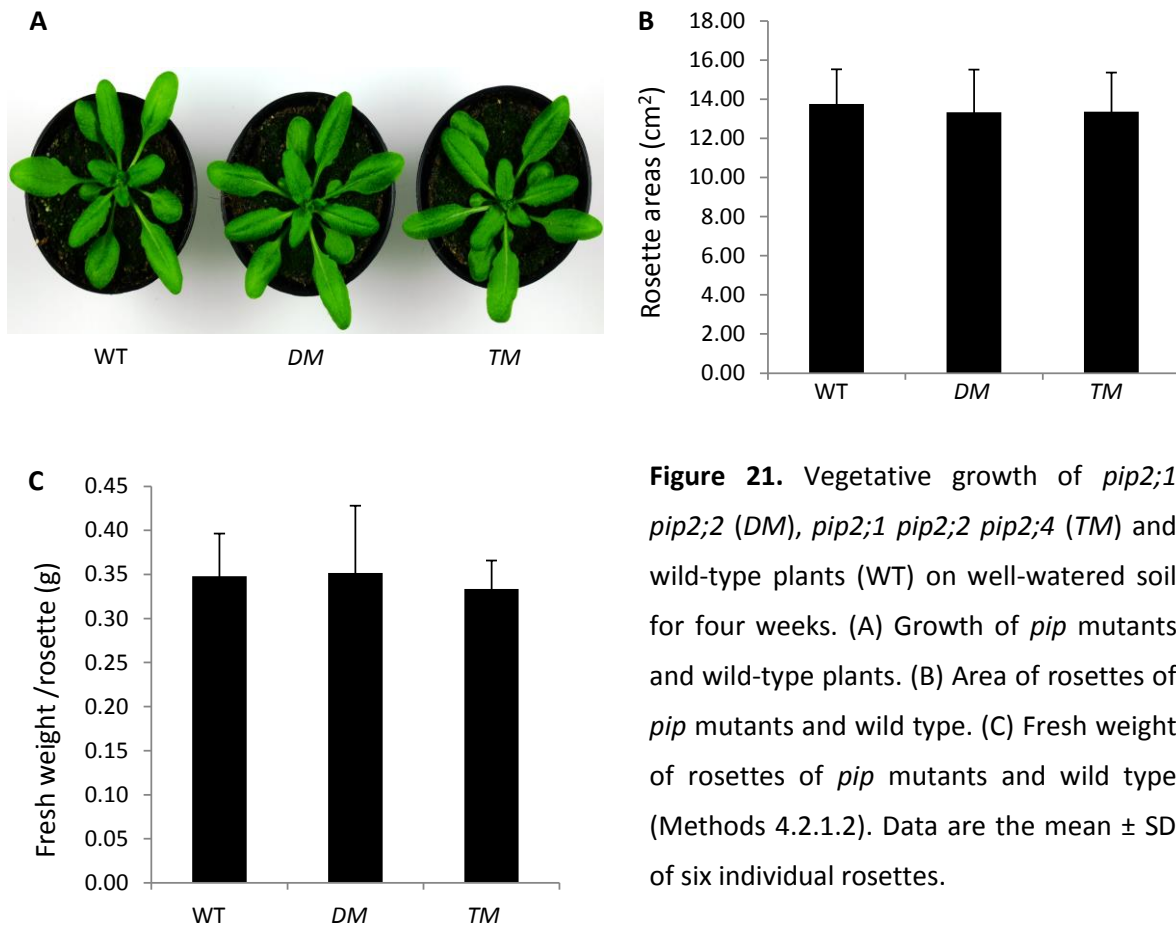


Figure 20. Vegetative growth of *pip2;1 pip2;2* (*DM*), *pip2;1 pip2;2 pip2;4* (*TM*) and wild type (*WT*) grown on ½ MS medium for two weeks. (A) Growth of *Arabidopsis* seedlings. (B) Fresh weights of the roots and rosettes in *pip* mutants and wild type. Data are the mean ± SD of six biological replicates, each containing five to seven individual seedlings.



The alteration of rH/VPD at a given temperature has effects on plant water homeostasis through water-loss modulation. This adaptation may involve the functions of aquaporins (See 1.2). Thus, to explore the effects of loss of *PIP2;1* and *PIP2;2* as well as *PIP2;4* on water relations under variable relative air humidity in intact plants, gas exchange and photosynthesis were assessed at gradually increased rH (20%, 40%, 60% and 75%) in *pip* mutants and wild type (See 4.2.1.3). Overall, the transpiration rate (E) and the stomata conductance of water vapor (g_s) of all genotypes were progressively increased with the reduction of rH, whereas the net photosynthesis (A) and intercellular CO_2 concentration (C_i) were not changed (Figure 22). These results are in agreement with a previous study (Ottosen *et al.*, 2002). In particular, no differences were observed with a measurement of gas exchange in *pip2;1 pip2;2* at high relative air humidity, but a slightly reduction was detected in *pip2;1 pip2;2* as compared to the wild type at low rH condition. In addition, transpiration rate, stomatal conductance of water vapor and intracellular CO_2 concentration were slightly

inhibited in *pip2;1 pip2;2 pip2;4* in comparison to the wild type at 20%, 40% or 60% rH (Figure 22A-D).

Water use efficiency (WUE) was calculated as a ratio of net photosynthesis and transpiration rate. The results showed that water use efficiency was enhanced with increasing rH in all genotypes which can be explained by the reduction of the transpiration rate. However, water use efficiency was marginally increased in *pip2;1 pip2;2 pip2;4* as compared to the wild type at each rH condition, still there were no changes in *pip2;1 pip2;2* (Figure 22E). On the other hand, the discrimination against $^{13}\text{CO}_2$ vs. $^{12}\text{CO}_2$ by ribulose-bisphosphate carboxylase/ oxygenase (Rubisco) is associated with the relative magnitudes of net photosynthesis and stomatal conductance. Carbon isotope composition ($\delta^{13}\text{C}$), which indicates the relative abundance of ^{13}C and ^{12}C , will be increased when gas exchange and stomatal conductance are reduced. Thus, this is a useful index for assessing water use efficiency (Seibt *et al.*, 2008). The isotopic ratio was measured using four-week-old rosettes grown on well-watered soil by mass spectrometry (See 4.2.1.4). There were no apparent changes of $\delta^{13}\text{C}$ in *pip2;1 pip2;2* and *pip2;1 pip2;2 pip2;4* as compared to the wild type (Figure 23A). Thus, the slight changes in WUE could not be confirmed by this assessment.

In parallel, the relative water loss of the detached leaves, which is determined by leaf properties such as stomatal aperture, hydraulic conductance and leaf morphology, was examined by measurement of water retention in *pip* mutants and wild type. Interestingly, a decreased water loss was observed in *pip2;1 pip2;2* as compared to the wild type, but not in *pip2;1 pip2;2 pip2;4* (Figure 23B).

Taken together, these data showed that loss of *PIP2;1* and *PIP2;2* reduced the relative water loss of detached leaves, but loss of additional *PIP2;4* eliminated this reduction of relative water loss. In addition, loss of *PIP2;1* and *PIP2;2* tended to reduce the transpiration rate and the stomata conductance of water vapor and this impact was getting more obvious under low relative air humidity or in *pip2;1 pip2;2 pip2;4*. This implies that the impacts of *PIP2;1*

and *PIP2;2* as well as of *PIP2;4* on leaf physiological characteristics are dependent on the water demand in air and the water transport in root.

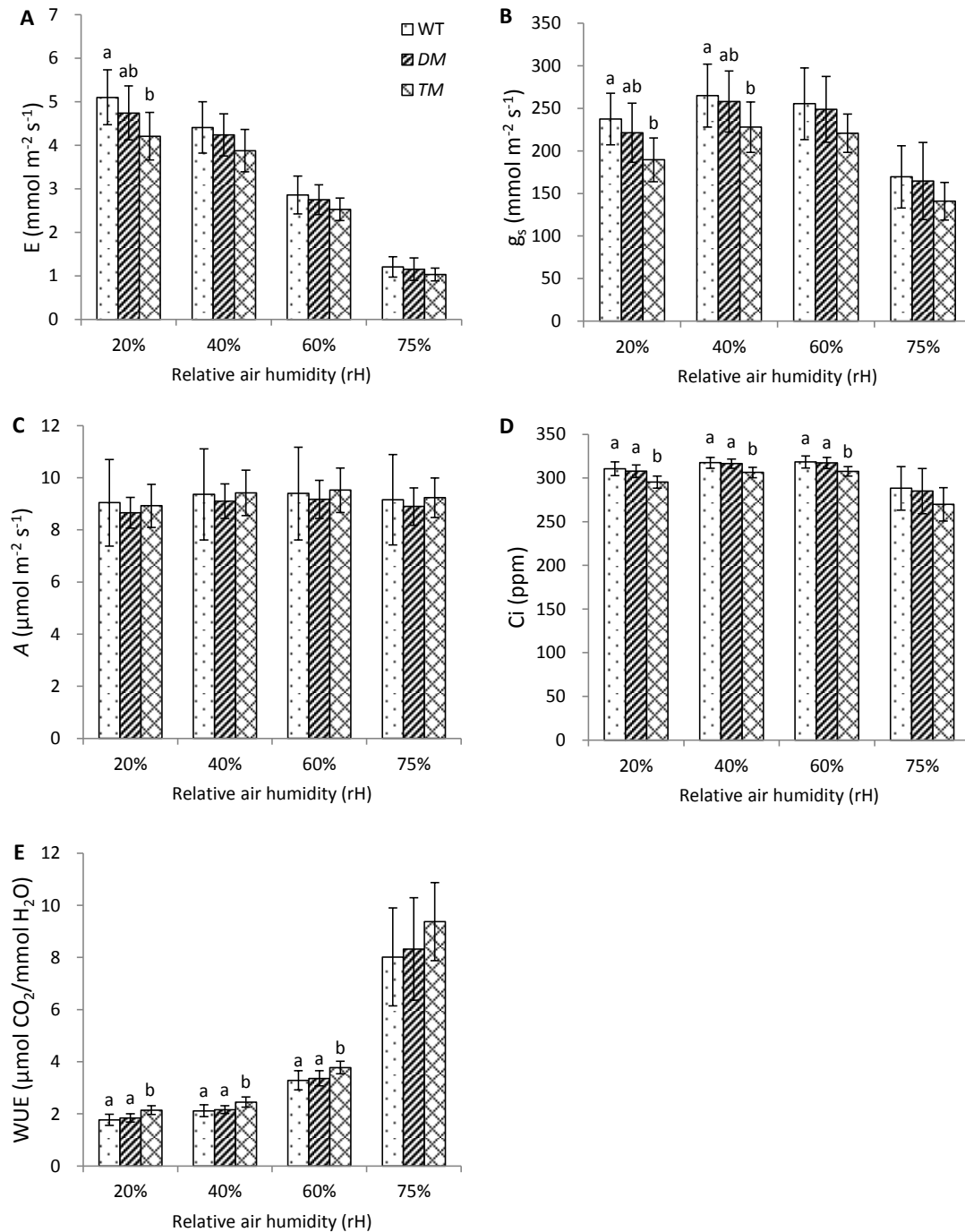


Figure 22. Gas exchange characteristics in leaves of four-week-old *pip* mutants and wild type at different relative air humidity conditions. (A) Transpiration rate. (B) Stomatal conductance of water vapor. (C) Net photosynthesis. (D) Intercellular CO_2 concentration. (E) Water use efficiency (ratio of net photosynthesis and transpiration rate). Data are mean \pm SD ($n=8$). Different letters correspond to significant differences ($P < 0.05$) between genotypes based on the Student's *t* test.

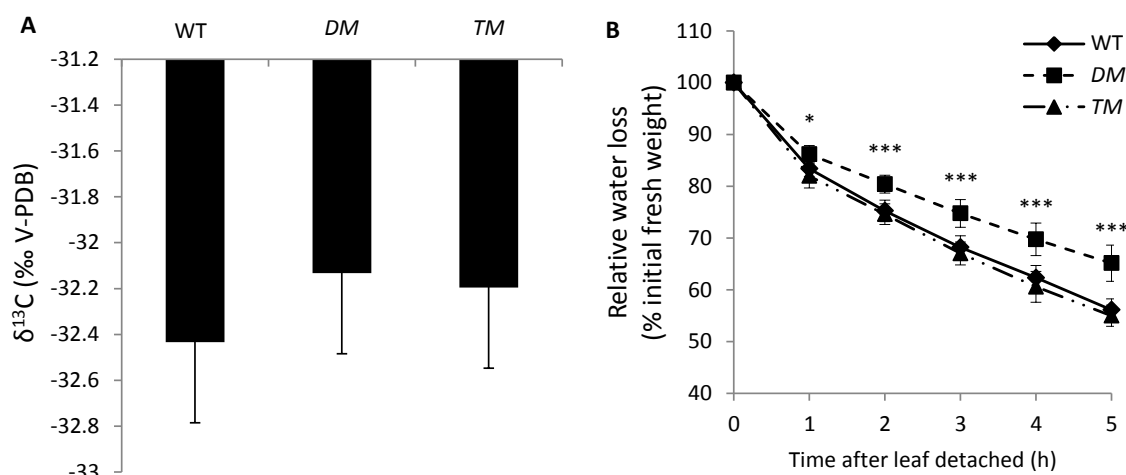


Figure 23. Physiological properties of four-week-old *pip* mutants and wild type under well watered condition. (A) Carbon isotope composition ($\delta^{13}\text{C}$) of leaves. (B) Relative water loss of detached rosettes assessed *via* percentage of initial fresh weight. Values are displayed as mean \pm SD of three biological replicates, each including three to four rosettes. Significant differences of *pip* mutants as compared to the wild type according to Student's *t* test are marked by asterisks (** $P < 0.01$ and *** $P < 0.001$).

2.3.2 Variation of aquaporin expression in *pip* mutants under variable environmental scenarios

The expression of all the other *PIPs* was assessed in *pip* mutants under variable conditions using Agilent microarrays in order to address the effects of the loss of *PIP2;1*, *PIP2;2* and the additional knockout of *PIP2;4* on the transcription of other aquaporins. The significantly changed genes in *pip* mutants were defined as the ones having $|\text{Log}_2\text{FC}| \geq 1$ and $\text{adj.}P \leq 0.05$ as compared to the wild type (See 4.2.4.1). Under well-watered condition, none of the aquaporin genes was apparently changed and only *PIP2;3* showed a slight reduced in both *pip* mutants (Figure 24). The slight reduction of *PIP2;3* was exhibited in *pip2;1 pip2;2* also under D, H LrH and DH LrH stresses (Figure 25A) as well as in *pip2;1 pip2;2 pip2;4* under DH LrH stress (Figure 25B). However, the loci of *PIP2;2* and *PIP2;3* are within 3 kb of the genomic DNA and it cannot therefore be excluded that the T-DNA insertion also effects the expression of *PIP2;3*. Therefore, there were no substantial changes in major *PIPs* expression

levels associated with the loss of the isoforms *PIP2;1*, *PIP2;2* and *PIP2;4*. Importantly, there were no compensating upregulation of other *PIP* isoforms.

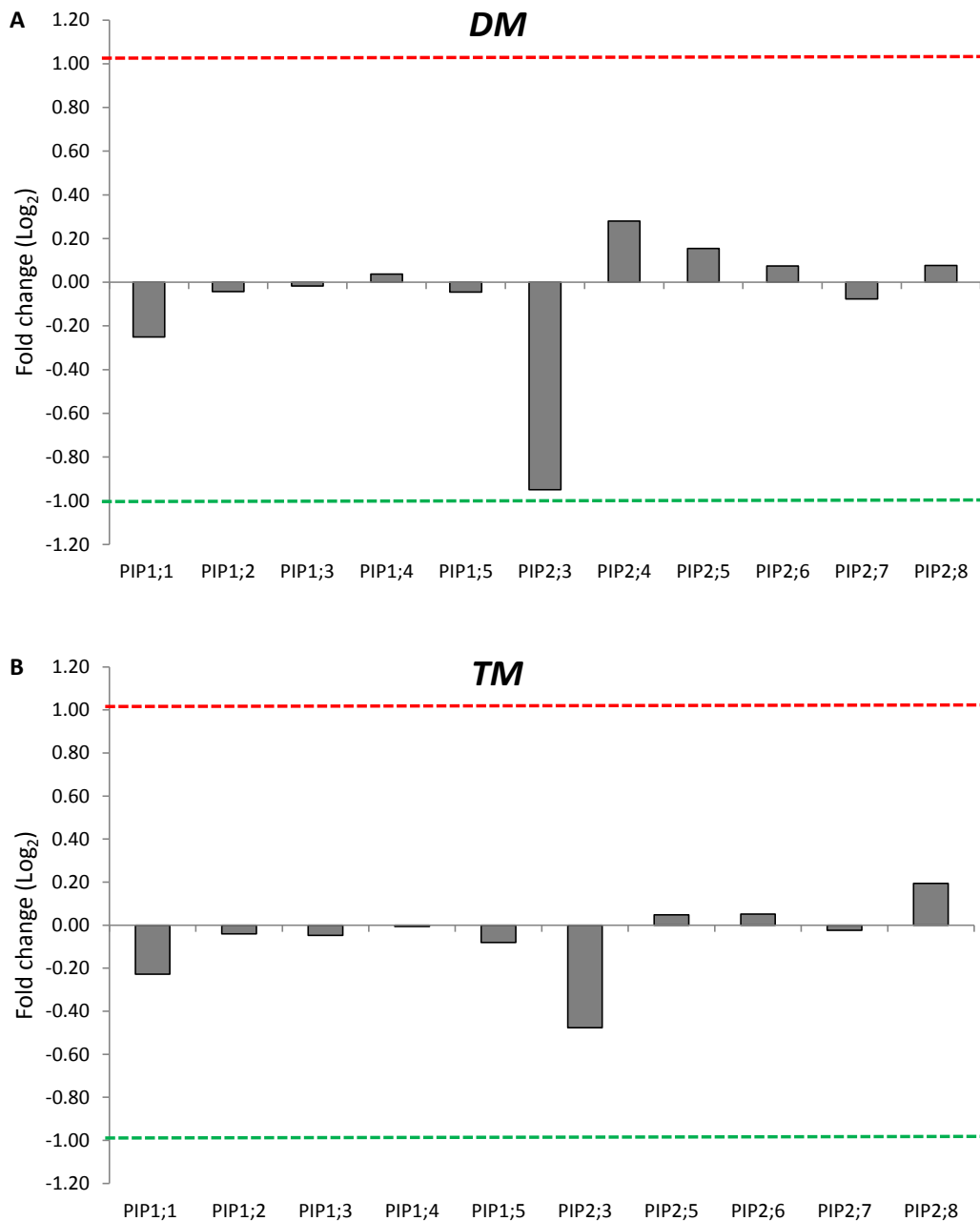


Figure 24. Relative expression levels of *PIPs* in (A) *pip2;1 pip2;2* (*DM*) and (B) *pip2;1 pip2;2 pip2;4* (*TM*) as compared to the wild type under well-watered condition. Expression values were obtained from three independent microarray experiments with three biological replicates each and integrated by the limma R package (Smyth *et al.*, 2005). The red and green lines show the selection thresholds for upregulated and downregulated genes, respectively. Significant changes (if any) are marked by an asterisk.

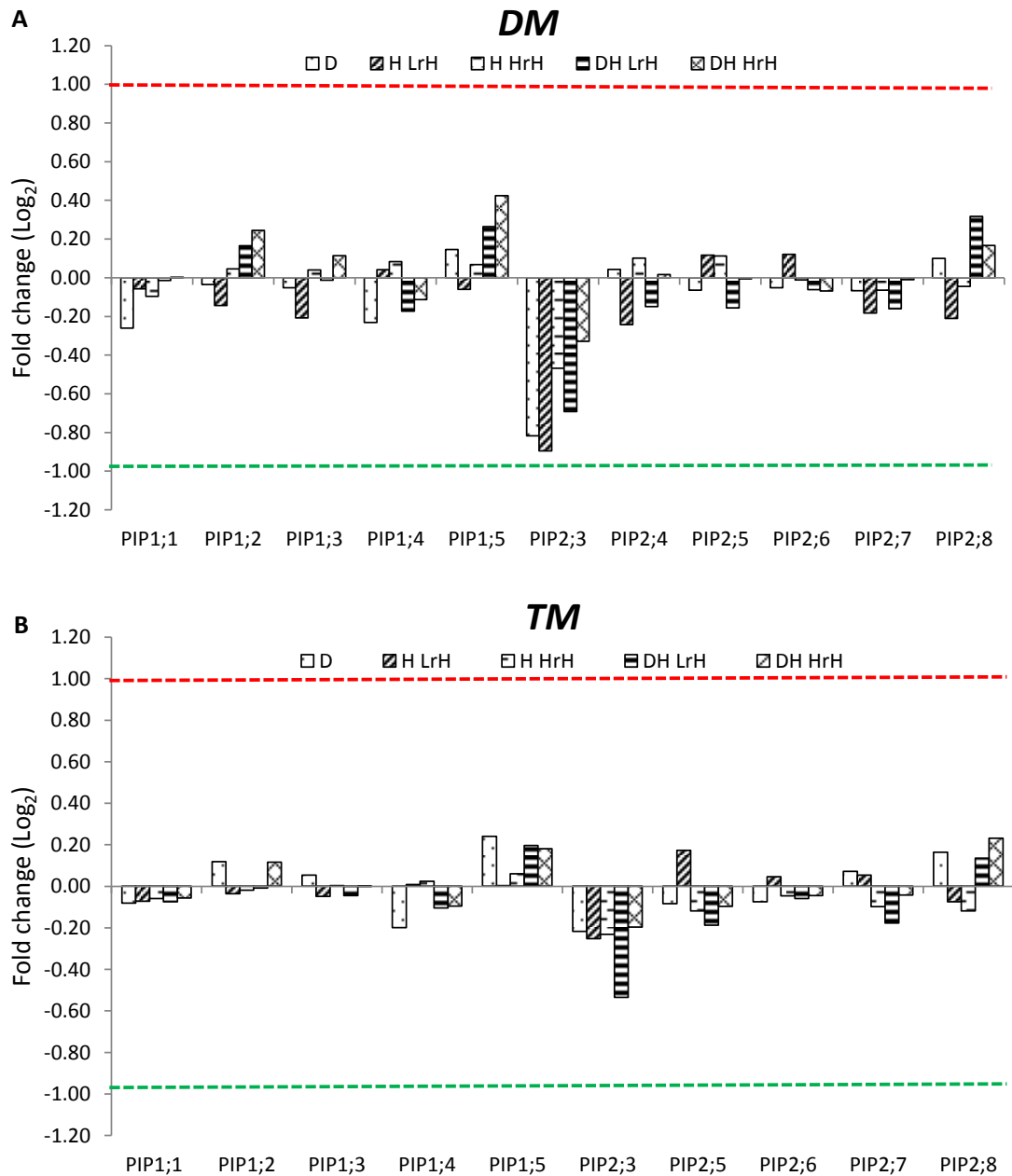


Figure 25. Relative expression levels of *PIPs* in (A) *pip2;1 pip2;2* (*DM*) and (B) *pip2;1 pip2;2 pip2;4* (*TM*) as compared to the wild type under water stresses. Expression values were obtained from two (D, H LrH and DH LrH) or three (H HrH and DH HrH) independent microarray experiments with three biological replicates each and integrated by the limma R package (Smyth *et al.*, 2005). The red and green lines show the selection thresholds for upregulated and downregulated genes, respectively. Significant changes (if any) are marked by an asterisk.

2.3.3 Changes of *pip* mutants in response to variable environmental scenarios

2.3.3.1 Transcriptome profiling of *pip* mutants under well-watered condition

To test the transcriptional changes in rosettes induced by loss of the major *PIPs* and additional root specific *PIP* expression under normal growth condition, Agilent microarrays were employed for transcriptome analysis in *pip2;1 pip2;2* and *pip2;1 pip2;2 pip2;4* grown on well-watered soil for four weeks (See 4.2.2.1). Transcripts having $|\text{Log}_2\text{FC}| \geq 1$ and $\text{adj.}P \leq 0.05$ in *pip* mutants as compared to the wild type were selected as differentially expressed genes and used for further analysis (See 4.2.4.1).

In total, 65 genes were differentially regulated in *pip2;1 pip2;2*. Among these genes, 17 were induced and 48 were repressed. In *pip2;1 pip2;2 pip2;4*, only 18 genes were differentially expressed including six upregulated genes and 12 downregulated genes (Figure 26A; Table 6). Two upregulated genes and 11 downregulated genes were overlapping between the two mutants. Consequently, 15 induced genes and 37 repressed genes were unique to *pip2;1 pip2;2*, but only four upregulated and one downregulated genes were unique to *pip2;1 pip2;2 pip2;4* (Figure 26B; Table 6). These data indicate that greater transcriptional changes as a response to the loss of *PIP2;1* and *PIP2;2* in the presence of *PIP2;4*.

To better understand the functional classification of the differentially expressed genes in *pip* mutants, gene ontology (GO) analysis was employed using MapMan 3.5.1R2. The differentially regulated genes were involved in *major carbohydrates metabolism, cell wall, lipid metabolism, secondary metabolism, RNA transcripts, protein modification and degradation* in both *pip* mutants. In addition, the differential regulations in *signalling, transport, development, miscellaneous enzyme families* as well as *biotic and abiotic stress*

responses were specifically displayed in *pip2;1 pip2;2*. Moreover, a large number of functionally uncharacterized genes were detected in both *pip* mutants (Figure 27; Table 6).

Among the differentially expressed genes of both *pip2;1 pip2;2* and *pip2;1 pip2;2 pip2;4* under well-watered condition, *QUA-QUINE STARCH (QQS)*, which is a negative regulator of starch accumulation, and *DESULFO-GLUCOSINOLATE SULFOTRANSFERASE 18 (SOT18)*, which is involved in the final step of glucosinolate core structure biosynthesis, were enhanced. Among the transcripts that were specifically decreased in *pip2;1 pip2;2*, two genes encoding cell wall surface modification, *AGP5* and *PME17*, as well as the transporter *CATION EXCHANGER 3 (CAX3)* was detected. In addition, the protein kinase *CYSTEINE-RICH RECEPTOR-LIKE PROTEIN KINASE 7 (CRK7)* was repressed. For specifically regulated genes in *pip2;1 pip2;2 pip2;4*, no clear cellular function could be assigned (Table 6).

To extend the functional interpretation of the unknown genes, co-expressed gene networks of identified differentially expressed genes in *pip* mutants were retrieved from ATTED-II (<http://atted.jp>) (Figure 28; Table 6). Interestingly, the function unknown genes *AT2G44240*, *AT3G13950*, *AT4G10500* as well as *AT1G26380* were strongly co-expressed with *AGP5*, *CAX3*, two protein kinases *CRK7* and *RLP7* as well as three stress responding genes *SAG13*, *PR1* and *YLS9* (Figure 28A). In addition, the function unknown gene *AT1G30700* was positively co-expressed with *PME17*, *CHX17* and defense responding gene *KUNITZ trypsin inhibitor 1 (KT11)* (Figure 28B). The extended genes included in the co-expression network also displayed a slight reduction in our data (Table 7). The coexpression networks suggest that these functionally unknown genes may be involved in cell wall modification, ion homeostasis or defense responses. In contrast to *pip2;1 pip2;2*, the transcripts altered in *pip2;1 pip2;2 pip2;4* were not part of specific co-expression networks which could give additional information on their functional implication.

Taken together, the transcriptome data showed that loss of the functional *PIP2;1* and *PIP2;2* induced the alterations associated to *cell wall modification*, *cell membrane compartments*, *modulation of membrane transporters* and *starch metabolism* under well-watered condition.

The alterations at the transcriptional levels were more pronounced in *pip2;1 pip2;2* than in *pip2;1 pip2;2 pip2;4*.

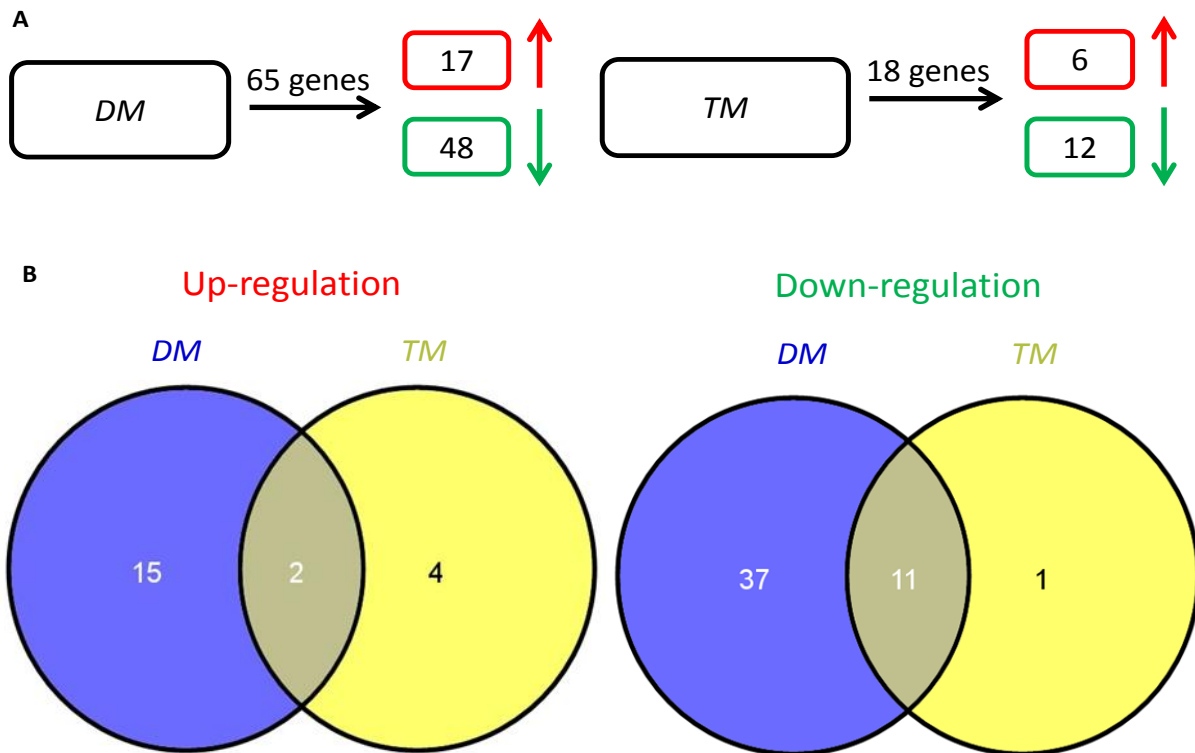


Figure 26. Global differentially expressed genes in *pip* mutants as compared to the wild type under well-watered condition. (A) Number of differentially expressed genes in *pip2;1 pip2;2* (*DM*) and *pip2;1 pip2;2 pip2;4* (*TM*). Red and green marks represent upregulated and downregulated genes, respectively. (B) Venn diagrams showing the differentially expressed genes unique or common to *pip2;1 pip2;2* and *pip2;1 pip2;2 pip2;4*. Only transcripts with steady-state fold change $|\text{Log}_2\text{FC}| \geq 1$ and $\text{adj.}P \leq 0.05$ are included.

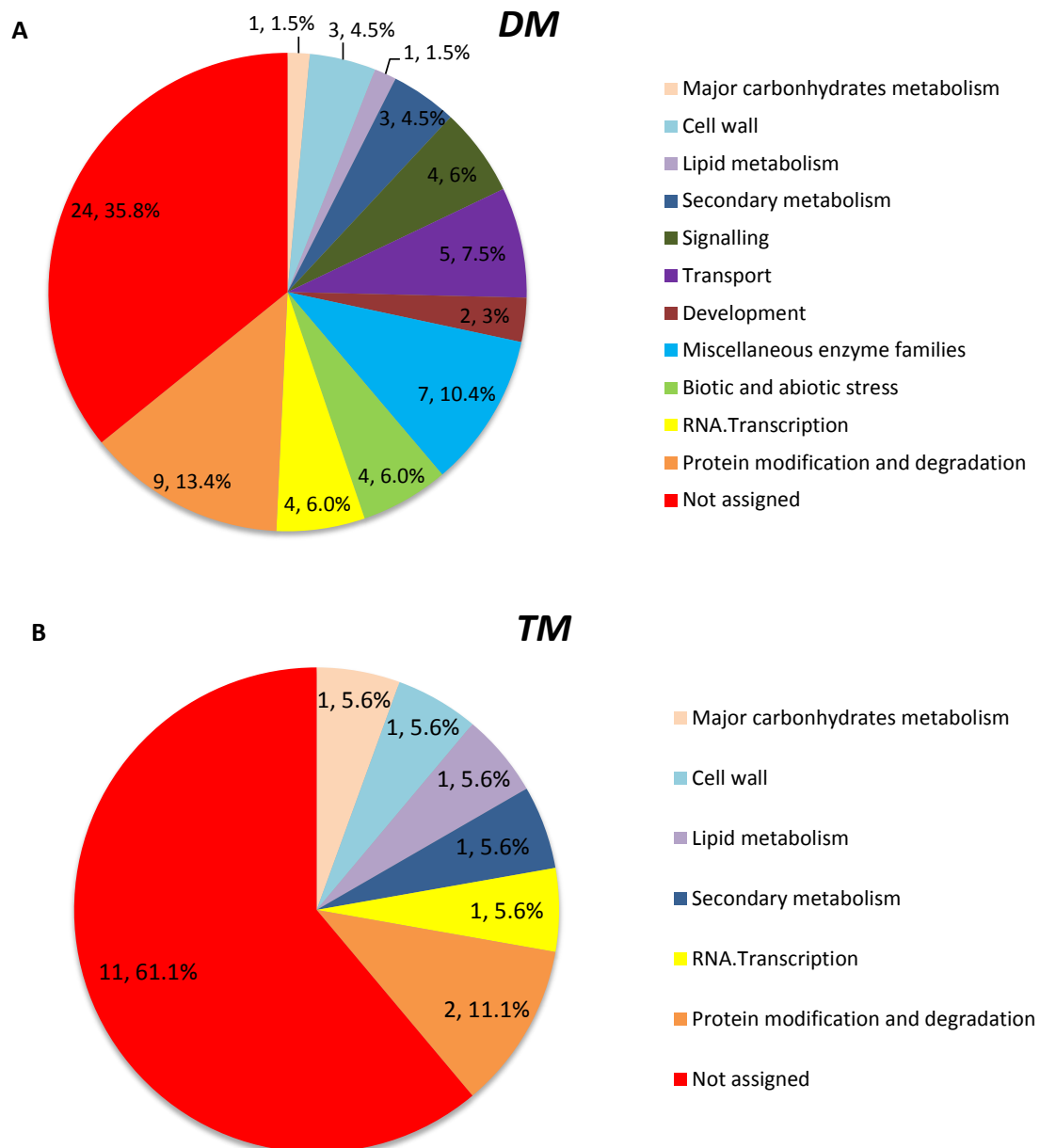


Figure 27. Gene ontology categories of differentially expressed genes in (A) *pip2;1 pip2;2* (*DM*) and (B) *pip2;1 pip2;2 pip2;4* (*TM*), respectively, under well-watered condition. The total number of differentially expressed genes assigned to each category and the percentage among all differentially expressed genes are given. The categorization was done by MapMan 3.5.1R2.

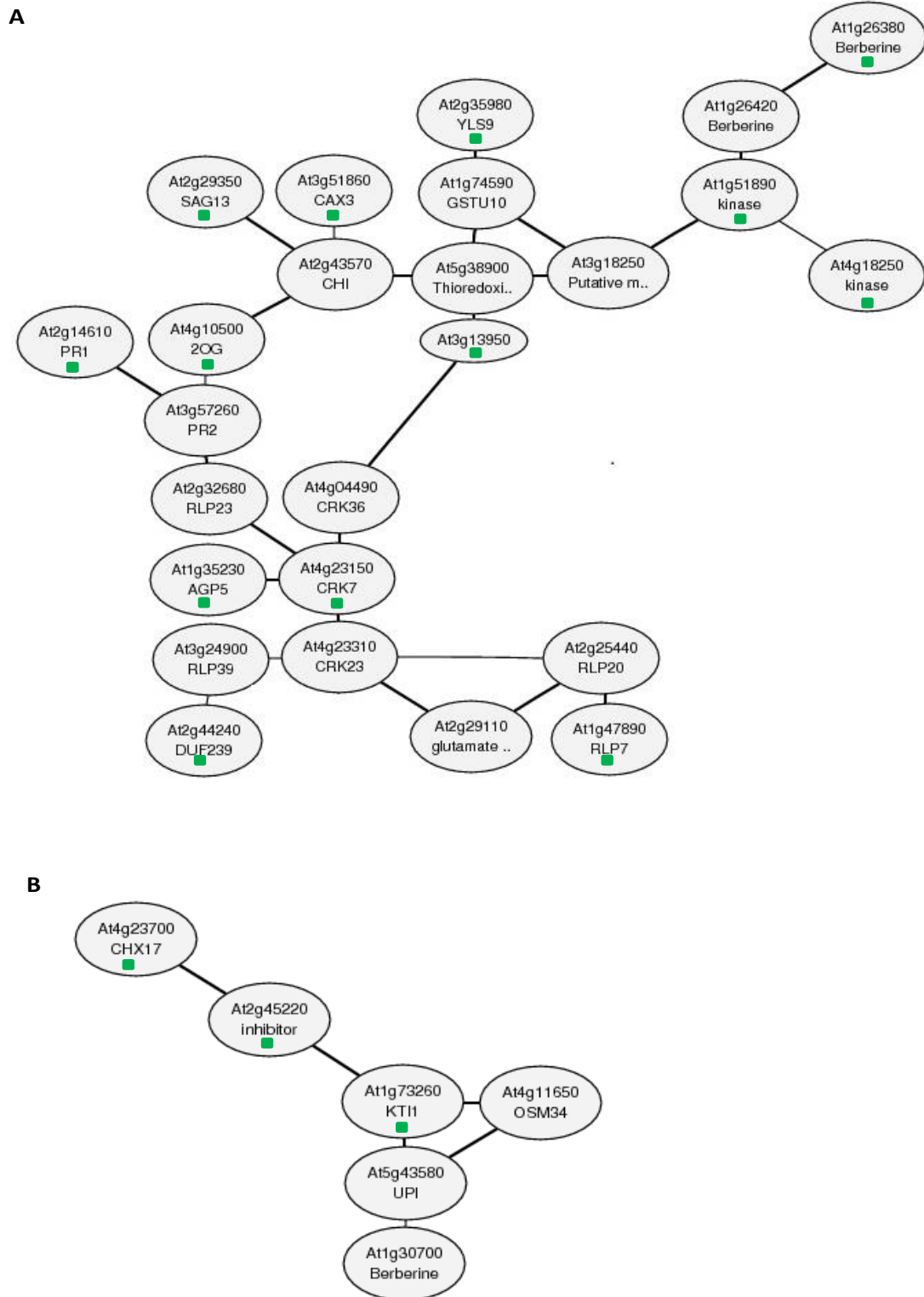


Figure 28. Co-expression networks obtained from ATTED-II (<http://atted.jp>) by querying with specifically repressed genes (marked by green squares) in *pip2;1 pip2;2* as compared to wild type under well-watered condition.

Table 6. Differentially expressed genes either in *pip2;1 pip2;2* (DM) or *pip2;1 pip2;2 pip2;4* (TM) as compared to the wild type under well-watered condition (red and green values represent fold change of significantly increased and decreased genes, respectively; black values represent non-significant fold changes with $\text{adj.}P \geq 0.05$; Black dashes “–” represent the low expressed genes that cannot be detected; NA, Not Assigned; The genes in bold are highly expressed in leaves).

AGI Code	Log ₂ FC		Name	Annotation
	DM	TM		
Major carbohydrates metabolism				
AT3G30720	1.60	2.61	QQS	Starch metabolism
Cell wall				
AT1G35230	-1.11	-0.62	<i>AGP5</i>	Arabinogalactan-protein
AT2G45220	-1.07	-0.63	<i>PME17</i>	Pectin methylesterase 17
AT5G39280	-3.90	-3.10	<i>EXPA23</i>	Expansin 23
Lipid metabolism				
AT3G55180	-1.80	-2.13	NA	Alpha/beta-Hydrolases superfamily protein
Secondary metabolism				
AT3G44300	-1.12	-0.45	<i>NIT2</i>	Nitrilase 2 that catalyzes the hydrolysis of IAN to IAA
AT3G19160	3.46	-	<i>PGA22</i>	ATP/ADP isopentenyl transferases
AT1G74090	1.29	1.31	<i>SOT18</i>	Desulfoglucosinolate sulfotransferase
Signalling				
AT4G23150	-1.09	-0.34	<i>CRK7</i>	Cysteine-rich receptor-like protein kinase
AT1G47890	-1.11	-0.56	<i>RLP7</i>	Receptor like protein 7
AT4G18250	-1.01	-0.51	NA	Transmembrane receptor serine/threonine kinase
AT1G51890	-1.28	-0.68	NA	Leucine-rich repeat protein kinase family protein
Transport				
AT3G51860	-1.00	-0.51	<i>CAX3</i>	Ca ²⁺ /H ⁺ antiporter
AT4G23700	-1.11	-0.44	<i>CHX17</i>	Member of K ⁺ /H ⁺ antiporter family
AT1G14870	-1.01	-0.45	<i>PCR2</i>	Membrane protein involved in zinc transport
AT3G23550	-1.39	-1.09	NA	MATE efflux family protein
AT4G08570	1.48	0.96	NA	Heavy metal transport/detoxification superfamily protein
Development				
AT2G35980	-1.07	-0.86	<i>YLS9</i>	Similar to tobacco hairpin-induced gene (HIN1)
AT5G07930	-1.46	-	<i>MCT2</i>	Member of mei2-like gene family
Miscellaneous enzyme families				
AT1G26380	-1.05	-0.74	NA	FAD-binding Berberine family protein
AT1G30700	-1.15	-0.68	NA	FAD-binding Berberine family protein
AT5G35920	4.89	0.00	<i>CYP79A4P</i>	Cytochrome P450 pseudogene
AT3G30290	1.64	0.05	<i>CYP702A8</i>	Member of cytochrome P450 gene family
AT3G48270	2.81	-	<i>CYP71A26</i>	Putative cytochrome P450
AT5G37940	1.04	0.90	NA	Zinc-binding dehydrogenase family protein
AT1G73610	2.01	0.01	NA	GDSL-like Lipase/Acylhydrolase superfamily protein
Biotic and abiotic stress				
AT2G29350	-1.00	-0.42	<i>SAG13</i>	Senescence-associated gene 13
AT2G14610	-2.10	-0.75	<i>PR1</i>	Pathogenesis-related gene 1

RESULTS

AT1G73260	-1.64	-0.52	<i>KT11</i>	Kunitz trypsin inhibitor 1
AT1G09260	-3.27	-3.37	NA	Chaperone DnaJ-domain superfamily protein
RNA.Transcription				
AT3G28470	-2.59	-	<i>MYB35</i>	Member of the R2R3 factor gene family.
AT3G04570	-1.57	-1.41	<i>AHL19</i>	AT-hook motif nuclear-localized protein 19
AT1G53490	-1.67	-1.72	<i>HEI10</i>	A RING finger-containing protein
AT4G21010	7.10	0.73	NA	Transcription initiation factor TFIIE, beta subunit
Protein modification and degradation				
AT2G03160	-2.21	-	<i>SK19</i>	SKP1-like 19
AT4G21830	-1.00	-0.63	<i>MSRB7</i>	Methionine sulfoxide reductase B7
AT4G21840	-1.53	-0.70	<i>MSRB8</i>	Methionine sulfoxide reductase B8
AT3G28510	-1.64	-0.73	NA	P-loop containing nucleoside triphosphate hydrolases
AT4G10820	-2.14	-2.03	NA	F-box family protein
AT1G17545	-4.19	-4.98	NA	Protein phosphatase 2C family protein
AT5G39560	-3.33	-3.07	NA	Galactose oxidase/kelch repeat superfamily protein
AT2G02660	5.90	-	NA	F-box associated ubiquitination effector family protein
AT5G04010	4.20	-	NA	F-box family protein
AT1G33910	2.33	-	NA	P-loop containing nucleoside triphosphate hydrolases
AT1G07430	1.11	0.78	<i>HAI2</i>	AKT1 interacting protein phosphatase
Not assigned				
AT1G67270	-1.00	-1.00	NA	Zinc-finger domain of monoamine-oxidase A repressor
AT4G00700	-1.23	-0.37	NA	C2 calcium/lipid-binding plant phosphoribosyltransferase
AT4G08097	-4.05	-3.27	NA	Best protein match is myosin heavy chain-related
AT4G10500	-1.33	-0.27	NA	2-oxoglutarate (2OG) and Fe(II)-dependent oxygenase
AT1G67670	-1.91	-	NA	Unknown protein
AT2G44240	-1.55	-0.63	NA	Unknown protein
AT3G13950	-1.01	-0.42	NA	Unknown protein
AT3G28320	-1.56	-1.27	NA	Unknown protein
AT3G63020	-3.29	-	NA	Unknown protein
AT4G33390	-1.59	-1.54	NA	Unknown protein
AT4G35837	-2.52	-	NA	Unknown protein
AT4G33905	1.10	0.69	NA	Peroxisomal membrane 22 kDa family protein
AT5G05430	1.12	-0.07	NA	Unknown protein
AT3G09110	3.41	0.67	NA	Unknown protein
AT1G53480	-5.46	-5.31	<i>MRD1</i>	<i>mto 1</i> responding down
AT5G03090	-2.52	-2.49	NA	Best Arabidopsis thaliana protein match is MRD1
AT1G68680	-1.41	-1.40	NA	Unknown protein
AT1G75870	-2.28	-2.32	NA	Unknown protein
AT1G78922	-1.46	-1.47	NA	Unknown protein
AT5G26290	-2.78	-2.36	NA	TRAF-like family protein
AT5G54020	-1.75	-1.69	NA	Cysteine/Histidine-rich C1 domain family protein
AT1G29180	0.15	1.39	NA	Cysteine/Histidine-rich C1 domain family protein
AT5G15690	-0.62	2.80	NA	zinc ion binding
AT4G18500	0.03	1.60	NA	Unknown protein
AT5G60650	0.10	1.73	NA	Unknown protein

Table 7. Co-expression partners of downregulated genes in *pip2;1 pip2;2* from ATTED- II networks.

AGI Code	Log ₂ FC	adj.P	Name	Annotation
AT1G26420	-0.94	0.01	<i>NN</i>	FAD-binding Berberine family protein
AT1G74590	-0.98	0.00	<i>GSTU10</i>	Glutathione transferase
AT2G25440	-0.70	0.14	<i>RLP20</i>	Receptor like protein 20
AT2G29110	-0.96	0.02	<i>GLR2.8</i>	Member of Putative ligand-gated ion channel family
AT2G32680	-0.94	0.08	<i>RLP23</i>	Receptor like protein 23
AT2G43570	-1.00	0.06	<i>CHI</i>	Putative chitinase
AT3G18250	-0.96	0.00	<i>NN</i>	Putative membrane lipoprotein
AT3G24900	-0.72	0.13	<i>RLP39</i>	Receptor like protein 39
AT3G57260	-0.70	0.45	<i>PR2</i>	Beta 1,3-glucanase
AT4G04490	-0.62	0.10	<i>CRK36</i>	Cysteine-rich receptor-like protein kinase
AT4G11650	-0.73	0.08	<i>OSM34</i>	Osmotin-like protein
AT4G23310	-0.90	0.07	<i>CRK23</i>	Cysteine-rich receptor-like protein kinase
AT5G43580	-0.42	0.59	<i>UPI</i>	Unusual serine protease inhibitor
AT2G26560	-0.85	0.00	<i>PLP2</i>	Lipid acyl hydrolase

2.3.3.2 Metabolite profiling of *pip2;1 pip2;2* under well-watered condition

To determine the accumulation of genotype-associated metabolites in rosettes under well-watered condition, gas chromatography-mass spectrometry (GC-MS) measurements were performed using both the *regular mode* for normal or highly accumulated metabolites and the *upconcentrated mode* for lowly accumulated metabolites in *pip2;1 pip2;2* and wild type (See 4.2.3). In total, 138 unknown compounds and 65 annotated metabolites including 11 amino acids, 23 sugars, 27 organic acids and four other organic chemical compounds were detected with the *regular mode*. The metabolites with $|\text{Log}_2\text{FC}| \geq 0.5$ and P value ≤ 0.1 were considered as being altered in their abundance. The results showed that one amino acid (proline) was decreased, whereas three sugars (maltitol, maltose and raffinose) and one other organic chemical compound (similar to glycerolaldopyranosid) were increased in *pip2;1 pip2;2* as compared to wild-type extracts (Table 8).

Furthermore, additional 51 unknown compounds and 70 annotated metabolites involving 15 amino acids, 16 sugars, 25 organic acids and 14 other chemical metabolites were detected with the *upconcentrated mode*. Out of these 70 metabolites, two amino acids (N-

RESULTS

Carboxyglycine and lysine) and two sugars (erythrose and arabitol) were reduced, whereas the amino acid leucine, the organic acid malonic acid and one other chemical compound, succinic semialdehyde, were enhanced in *pip2;1 pip2;2* as compared to the wild type (Table 8).

Altogether, marginal changes of metabolite accumulation in *pip2;1 pip2;2* collectively suggest a subtle impact of the loss of these two major *PIPs* on plant metabolism.

Table 8. Changed metabolites *via* the *regular mode* or *upconcentrated mode* in *pip2;1 pip2;2* under well-watered condition (¹ Metabolites measured using the *regular mode*; ² Metabolites measured using the *upconcentrated mode*)

Metabolites	Log ₂ FC	P Value
Amino acids		
Proline ¹	-2.08	0.03
N-Carboxyglycine ²	-0.92	0.00
Lysine ²	-0.52	0.08
Leucine ²	0.59	0.06
Sugars		
Maltitol ¹	0.72	0.04
Maltose ¹	0.51	0.09
Raffinose ¹	1.21	0.02
Erythrose ²	-0.68	0.00
Arabitol ²	-0.51	0.04
Other compounds		
similar to Glycerolaldopyranosid ¹	0.53	0.03
Malonic acid ²	0.60	0.03
Succinic semialdehyde ²	0.61	0.01
Unknown compounds		
UNKNOWN 35 ¹	1.41	0.02
UNKNOWN 70 ¹	1.01	0.09
UNKNOWN 71 ¹	1.08	0.06
UNKNOWN ANALYTE LIBRARY 42 ¹	0.78	0.04
UNKNOWN ANALYTE LIBRARY 44 ¹	0.67	0.07
UNKNOWN ANALYTE LIBRARY 48 ¹	0.76	0.02

2.3.3.3 Integration of transcriptome and metabolome changes in *pip2;1 pip2;2* under well-watered condition

To identify co-regulatory relationships between transcripts and metabolites derived in the *normal mode*, a correlation analysis of the two datasets was performed and the networks were displayed from a gene-centered perspective (See 4.2.4.3). The results showed that overaccumulation of maltitol and raffinose was highly correlated to the upregulation of *QQS*, which could be in line with the gene function in negative regulation of the starch accumulation. In addition, this network also included another six increased unknown metabolites, which suggests that these compounds could be involved in the altered carbohydrates metabolism (Figure 29).

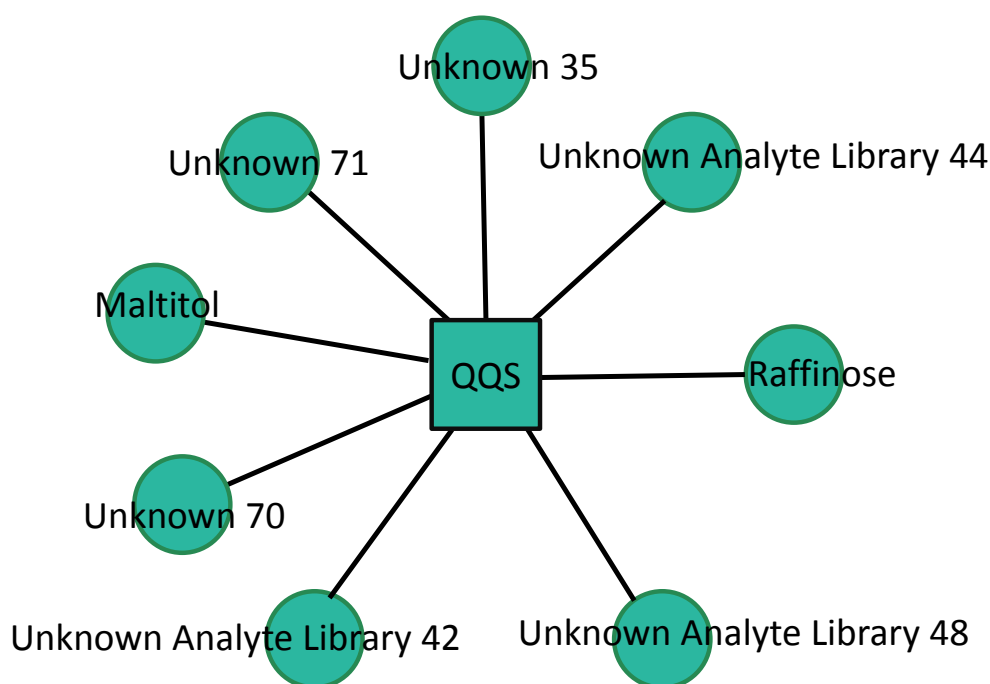


Figure 29. Changed metabolites exhibiting correlated changes with the upregulated *QQS* in *pip2;1 pip2;2* as compared to the wild type under well-watered condition. The network visualization was done by Cytoscape 3.1.1.

2.3.4 Transcriptome profiling of *pip* mutants in response to water stresses

To examine how *Arabidopsis thaliana* that lost *PIP2;1* and *PIP2;2* as well as *PIP2;4* responses to water stresses at the transcriptional level, RNA samples isolated from rosettes subjected to D, H LrH, H HrH, DH LrH and DH HrH were analyzed using Agilent microarrays. To address how loss of PIPs generally impacts the water stress responses, the water-stress responsive genes in wild type, which were defined as the genes with $|\text{Log}_2\text{FC}| \geq 1$ and $\text{adj.}P \leq 0.05$ under stress conditions in comparison to control condition, were sorted according to $\text{adj.}P$ and the changes of the top listed differentially expressed genes were representatively assessed in *pip* mutants under water stresses as compared to control condition. More importantly, to investigate the specifically responses to water stress after loss of *PIPs*, genes that were differentially expressed in *pip* mutants in comparison to wild type under a certain stress condition were identified as the transcripts with $|\text{Log}_2\text{FC}| \geq 1$ and $\text{adj.}P \leq 0.05$.

The results showed that the drought-responsive genes and the DH LrH stress-responsive genes in wild type were generally less deregulated in *pip2;1 pip2;2* and in *pip2;1 pip2;2 pip2;4* (Table 9 and Table 13). However, the heat-responsive genes and the DH HrH stress-responsive genes in wild type were similarly regulated in both *pip2;1 pip2;2* and *pip2;1 pip2;2 pip2;4* (Table 10, Table 11 and Table 12).

Table 9. The top listed differentially expressed genes in wild type under drought stress as compared to control condition. The genes were selected according to adj.*P*. The expression ratios of these genes in wild type were added along with the expression in *pip2;1 pip2;2 (DM)* and *pip2;1 pip2;2 pip2;4 (TM)*.

AGI	Log ₂ FC			AGI	Log ₂ FC			AGI	Log ₂ FC		
	WT	DM	TM		WT	DM	TM		WT	DM	TM
AT3G16530	-4.4	-4.5	-4.5	AT3G15780	1.4	1.2	1.4	AT1G68500	2.6	2.1	2.2
AT5G44020	-3.5	-2.7	-2.8	AT5G22860	1.5	1.2	1.1	AT3G11410	2.6	1.9	2.1
AT1G74670	-3	-2.6	-2.8	AT1G01580	1.5	1.2	1.3	AT1G67856	2.6	1.7	1.9
AT1G16390	-2.9	-2.2	-2.2	AT4G17550	1.5	1.2	1.2	AT1G16515	2.6	2	2.3
AT2G27402	-2.8	-2.6	-2.5	AT4G22820	1.6	1.2	1.2	AT3G61890	2.7	2	2.2
AT4G29740	-2.8	-2.2	-2.3	AT1G73390	1.6	1.2	1.2	AT3G22560	2.7	2.2	2.1
AT1G75750	-2.7	-2.1	-2.2	AT3G20300	1.6	1.3	1.5	AT3G14440	2.7	1.8	2.1
AT3G50560	-2.6	-1.9	-2.1	AT1G20160	1.6	1.3	1.4	AT3G29575	2.7	2	2
AT2G06850	-2.6	-1.9	-2	AT3G25870	1.6	1.1	1.3	AT5G37300	2.7	2	2.1
AT4G30610	-2.5	-2	-2	AT5G07920	1.6	1.2	1.3	AT3G28270	2.7	1.9	2
AT4G11290	-2.3	-2.1	-2.1	AT1G15310	1.6	1.3	1.2	AT1G77450	2.8	1.9	2.2
AT4G16980	-2.1	-1.9	-1.7	AT4G23450	1.7	1.4	1.5	AT1G07500	2.8	2	2.2
AT4G38850	-2	-1.8	-1.6	AT2G04240	1.7	1.2	1.3	AT3G24520	2.8	2	2.3
AT1G14430	-1.9	-1.4	-1.4	AT1G45249	1.7	1.4	1.4	AT3G03170	2.8	2.3	2.3
AT3G22210	-1.8	-1.3	-1.4	AT4G21570	1.7	1.3	1.2	AT4G30460	2.9	2.1	2.4
AT3G30180	-1.5	-1.1	-1.2	AT1G20440	1.7	1.1	1.2	AT1G62570	2.9	2	2.2
AT3G14310	-1.5	-1.1	-1.2	AT3G55940	1.7	1.2	1.3	AT1G49450	2.9	1.9	2.1
AT5G38430	-1.4	-1.2	-1.1	AT3G23920	1.8	1.3	1.5	AT5G53870	2.9	2.5	2.5
AT1G31200	-1.4	-0.8	-1	AT1G01470	1.8	1.3	1.3	AT3G48240	3	2.7	3
AT4G30190	-1.2	-1	-1.1	AT1G27200	1.8	1.3	1.4	AT1G30190	3	2.2	2.3
AT5G21930	-1.2	-0.9	-0.8	AT4G18280	1.8	1.2	1.2	AT2G47780	3	2.4	2.4
AT4G33360	-1.1	-0.9	-1	AT4G24960	1.8	1.4	1.5	AT1G79900	3	2.2	2.4
AT3G26490	-1.1	-0.7	-0.9	AT4G34230	1.8	1.4	1.4	AT2G46270	3	2.5	2.5
AT2G21080	-1	-0.8	-0.6	AT1G73040	1.8	1.6	1.6	AT3G48510	3	2.5	2.6
AT3G04240	1	0.7	0.8	AT2G39050	1.8	1.2	1.2	AT1G69260	3	2.6	2.5
AT4G00440	1	0.8	0.8	AT4G04020	1.8	1.5	1.6	AT3G28007	3	2.1	2.3
AT5G57040	1	0.8	0.9	AT3G19620	1.9	1.5	1.5	AT1G24600	3.1	2.1	2.2
AT4G13010	1	0.8	0.9	AT3G15280	1.9	1.1	1.5	AT4G02360	3.1	2.2	2
AT5G12840	1	0.8	0.9	AT5G37550	1.9	1.5	1.6	AT4G25433	3.1	2	2.2
AT1G04830	1.1	0.8	0.7	AT1G79270	1.9	1.3	1.5	AT3G13672	3.3	2.8	3
AT1G75400	1.1	0.7	0.8	AT5G02640	1.9	1.5	1.4	AT1G24580	3.3	3.1	3.2
AT4G29070	1.1	0.8	0.8	AT4G34000	2	1.5	1.5	AT1G30220	3.3	2.5	3
AT5G12140	1.1	0.9	0.8	AT1G79520	2	1.5	1.6	AT5G15500	3.3	2.5	2.8
AT4G23630	1.1	0.9	0.9	AT1G20450	2	1.4	1.5	AT2G35070	3.3	2.5	2.6
AT1G52920	1.2	0.9	1.1	AT4G11350	2	1.8	1.6	AT4G02280	3.4	2.6	2.8
AT5G09620	1.2	0.9	0.9	AT4G40010	2	1.6	1.6	AT5G63350	3.4	2.3	2.7
AT5G65830	1.2	0.7	0.8	AT5G23750	2.1	1.6	1.8	AT3G12580	3.4	2.7	3

RESULTS

AT5G66052	1.2	1	1	AT1G62620	2.1	1.6	1.5	AT5G28080	3.4	2.5	2.7
AT4G31351	1.2	1	1.1	AT2G16990	2.1	1.5	1.6	AT3G50970	3.4	2.5	2.5
AT1G69295	1.2	0.9	0.9	AT5G03190	2.1	1.5	1.7	AT5G03210	3.5	2.4	2.9
AT4G31354	1.2	1	1.1	AT1G64660	2.1	1.9	2	AT4G17030	3.5	2.9	3.1
AT1G20030	1.2	0.9	1	AT3G62090	2.1	1.6	1.5	AT1G60190	3.6	2.5	2.9
AT1G67850	1.2	1	1.1	AT2G12400	2.2	1.6	1.7	AT2G46680	3.7	2.9	2.9
AT1G06430	1.2	1.1	1.2	AT5G01520	2.2	1.4	1.7	AT5G40790	3.7	2.9	3.1
AT5G17460	1.3	0.9	0.9	AT3G14560	2.2	1.6	1.8	AT1G16850	3.8	2.9	3
AT3G26290	1.3	1	1	AT2G28500	2.2	1.6	1.6	AT5G66400	3.8	3.1	3.3
AT3G14595	1.3	1	0.9	AT5G57050	2.2	1.7	1.9	AT5G53710	4	3.4	3.5
AT5G04760	1.3	0.9	1	AT5G61820	2.2	1.5	1.6	AT1G07430	4	2.9	3.4
AT5G53120	1.3	1.1	1	AT1G54100	2.2	1.8	1.9	AT4G33905	4.2	3	3.3
AT4G22270	1.3	1	1	AT1G01250	2.3	1.7	1.9	AT5G15190	4.4	3.2	3.7
AT1G32860	1.3	0.9	1	AT5G19875	2.3	1.8	2.1	AT2G41190	4.5	3.4	3.4
AT2G04350	1.3	0.9	0.9	AT1G04220	2.3	1.8	1.7	AT4G33550	4.7	4	4.2
AT3G01350	1.3	1.1	1.2	AT4G05100	2.3	2.1	2	AT5G59330	4.7	3.8	3.9
AT5G17210	1.3	1	1	AT5G16600	2.3	1.7	1.8	AT5G62040	4.9	4	4.1
AT5G57790	1.3	1.1	1.2	AT1G17940	2.3	1.8	1.7	AT5G59320	5.1	4	4.1
AT3G11420	1.3	1	1.1	AT5G66460	2.3	1.9	1.9	AT1G22990	5.2	4.2	4.2
AT4G36900	1.4	1	1.2	AT1G21400	2.4	1.9	2	AT3G53980	5.3	4.4	4.7
AT5G56160	1.4	1	1.1	AT1G02390	2.4	1.8	2.1	AT5G13170	5.6	5.2	5.3
AT5G50240	1.4	0.9	1.2	AT3G15534	2.5	2	2.1	AT4G01985	5.6	4.7	4.8
AT4G23670	1.4	1.1	1	AT1G72770	2.5	1.8	2	AT5G50360	5.6	4.5	4.8
AT4G22240	1.4	1.1	1.1	AT4G30830	2.5	2	2.3	AT2G47770	5.7	4.6	4.7
AT4G26080	1.4	1	1	AT3G14590	2.5	1.9	2.1	AT5G59310	5.7	4.2	4.4
AT5G42570	1.4	1	1	AT1G04570	2.5	2	2.2	AT5G59220	6	4.6	4.8
AT1G71360	1.4	1.3	1.4	AT2G34850	2.5	2	2.2	AT4G08570	6.2	4.7	5.2
AT5G13820	1.4	1.2	1.1								

Table 10. The top listed differentially expressed genes in wild type under H HrH as compared to control condition. The genes were selected according to adj.*P*. The expression ratios of these genes in wild type were added along with the expression in *pip2;1 pip2;2 (DM)* and *pip2;1 pip2;2 pip2;4 (TM)*.

AGI	Log ₂ FC			AGI	Log ₂ FC			AGI	Log ₂ FC		
	WT	DM	TM		WT	DM	TM		WT	DM	TM
AT3G50970	-4.6	-4.9	-5	AT3G54460	1	1	1	AT1G08300	1.5	1.5	1.4
AT1G09350	-3.8	-4	-3.9	AT2G29260	1	1	0.9	AT2G30480	1.5	1.5	1.5
AT5G52310	-3.5	-3.6	-3.4	AT3G10030	1	1	0.9	AT1G65040	1.5	1.6	1.5
AT2G42540	-3.4	-3.5	-3.4	AT2G01100	1	1	0.9	AT5G47830	1.5	1.5	1.4
AT5G08640	-3	-3.2	-3	AT4G02210	1	1	1	AT3G45420	1.5	1.5	1.2
AT4G16740	-2.8	-2.6	-2.3	AT1G48970	1	1	1	AT4G30570	1.5	1.5	1.3
AT4G30650	-2.6	-2.7	-2.7	AT5G06340	1	1.1	1	AT4G15780	1.6	1.5	1.4
AT5G48880	-2.5	-2.7	-2.5	AT1G54250	1	1.1	1	AT1G76065	1.6	1.5	1.6
AT5G59670	-2.5	-2.5	-2.3	AT3G53630	1	1	1	AT1G72645	1.6	1.5	1.5
AT1G25422	-2.5	-2.7	-2.7	AT2G24830	1	1	1	AT4G25980	1.6	1.4	1.3
AT5G45280	-2.3	-2.4	-2.4	AT2G31890	1	1	1.1	AT1G10960	1.7	1.7	1.6
AT1G76790	-2.3	-2.6	-2.3	AT3G43210	1	1	0.9	AT1G09140	1.7	1.6	1.6
AT1G06000	-2.2	-2.6	-2.2	AT1G20920	1	0.9	1.1	AT1G27590	1.7	1.7	1.8
AT4G31870	-2.2	-2.2	-2	AT3G60910	1	1.1	1.1	AT2G36950	1.7	1.8	1.9
AT1G51090	-2.1	-2.3	-1.9	AT5G16110	1.1	1	1	AT3G59750	1.7	1.6	1.6
AT4G27570	-2.1	-2.2	-1.9	AT1G10240	1.1	1.1	1.1	AT2G17036	1.8	1.7	1.6
AT4G21400	-2	-2.1	-2	AT2G29400	1.1	1.1	1.1	AT1G27420	1.8	1.7	1.5
AT1G06690	-2	-2.1	-1.8	AT5G56380	1.1	1.1	1.1	AT2G17900	1.8	1.8	1.7
AT5G55570	-2	-2.1	-1.9	AT1G71260	1.1	1.1	1.1	AT2G32340	1.8	1.8	1.9
AT4G27560	-1.9	-2.1	-1.9	AT5G66090	1.1	1.1	1.1	AT1G77880	1.8	1.8	1.7
AT1G09780	-1.8	-1.9	-1.9	AT3G17740	1.1	1.2	1.2	AT1G14360	1.8	1.9	1.7
AT4G34950	-1.8	-1.9	-1.7	AT5G44660	1.1	1.1	1	AT4G38700	1.8	1.8	1.8
AT5G46230	-1.8	-1.8	-1.6	AT3G19508	1.1	1	1.1	AT2G42330	1.9	1.7	1.8
AT1G76020	-1.8	-1.8	-1.7	AT3G26180	1.1	1.2	1.1	AT2G21640	1.9	1.8	1.6
AT5G05580	-1.7	-1.7	-1.7	AT3G05790	1.1	1.2	1.1	AT4G31351	1.9	1.9	1.9
AT4G23020	-1.7	-1.7	-1.7	AT1G56200	1.1	1	1	AT4G31354	1.9	1.9	1.9
AT1G52770	-1.7	-1.8	-1.8	AT2G46610	1.2	1.1	1.1	AT1G03470	1.9	1.9	1.9
AT1G29720	-1.7	-1.6	-1.6	AT2G37340	1.2	1.2	1.2	AT3G24100	2.1	1.7	1.7
AT3G23810	-1.7	-1.8	-1.8	AT5G66240	1.2	1.2	1.2	AT5G03720	2.1	1.9	2.1
AT1G18265	-1.6	-1.7	-1.5	AT5G59440	1.2	1.1	1.1	AT1G64720	2.1	2.1	2.2
AT5G17780	-1.6	-1.5	-1.6	AT2G23348	1.2	1.2	1.1	AT1G29465	2.2	2.3	2.2
AT1G79460	-1.6	-1.7	-1.8	AT2G47420	1.2	1.2	1.1	AT2G19310	2.2	2.1	2.1
AT4G21215	-1.5	-1.6	-1.5	AT1G13790	1.2	1.2	1.1	AT5G46490	2.3	2.2	2.4
AT2G31390	-1.5	-1.5	-1.5	AT1G23860	1.2	1.1	1.1	AT2G07671	2.3	2.1	2.3
AT3G09540	-1.5	-1.5	-1.4	AT2G32920	1.2	1.1	1.1	AT4G29770	2.3	2.2	2.1
AT2G36500	-1.5	-1.3	-1.4	AT1G58150	1.2	1.2	1.2	AT3G29810	2.4	2.4	2.4
AT5G59130	-1.4	-1.2	-1.2	AT1G24095	1.2	1	0.9	AT1G07350	2.4	2.6	2.1
AT1G14580	-1.4	-1.3	-1.3	AT1G26580	1.3	1.3	1.2	AT5G25280	2.4	2.3	2.5
AT2G36880	-1.4	-1.5	-1.4	AT3G58930	1.3	1.2	1.1	AT4G23493	2.9	2.8	2.4

RESULTS

AT1G31190	-1.3	-1.4	-1.3	AT3G13224	1.3	1.2	1.1	AT2G32120	3.6	3.5	3.4
AT1G78570	-1.3	-1.4	-1.3	AT2G33250	1.3	1.1	1.2	AT5G64510	3.8	4.1	3.7
AT4G15450	-1.2	-1.2	-1.1	AT1G76080	1.3	1.2	1.4	AT3G24500	4.1	4	3.7
AT1G18360	-1.2	-1.3	-1.4	AT3G60300	1.3	1.2	1.2	AT4G19430	4.5	4.6	4.3
AT2G38740	-1.2	-1.2	-1.1	AT1G78750	1.3	1.2	1.3	AT5G25450	5	5.1	4.9
AT5G15760	-1.2	-1.2	-1.2	AT3G17460	1.4	1.3	1.3	AT5G52640	5.1	4.9	4.9
AT5G14570	-1.2	-1.4	-1.1	AT3G04160	1.4	1.3	1.3	AT3G12580	5.4	5.1	5.2
AT1G64890	-1.2	-1.3	-1.2	AT4G27370	1.4	1.3	1.1	AT5G59720	5.5	5	5.2
AT5G15650	-1.1	-1.3	-1.2	AT3G62600	1.4	1.4	1.3	AT1G07400	6.1	5.8	5.7
AT5G06060	-1.1	-1.1	-1.2	AT5G03830	1.4	1.3	1.1	AT1G72660	6.2	6	6.1
AT3G03350	-1.1	-1.1	-1	AT2G45920	1.4	1.3	1.2	AT5G51440	6.4	6.1	5.7
AT3G13060	-1.1	-1	-1	AT1G03410	1.4	1.4	1.4	AT4G12400	6.5	6.4	6.4
AT4G28550	-1	-1.1	-1.2	AT2G20585	1.4	1.5	1.4	AT2G29500	6.7	6.7	6.7
AT1G79080	-1	-1.1	-1	AT3G01770	1.5	1.4	1.4	AT5G12030	7.1	5.9	6.7
AT1G13930	-1	-1.1	-1	AT1G61970	1.5	1.4	1.3	AT3G46230	7.3	7.3	7.5
AT2G33740	1	0.9	0.9	AT5G58590	1.5	1.5	1.4	AT1G53540	7.8	7.4	7.9

Table 11. The top listed differentially expressed genes in wild type under H LrH as compared to control condition. The genes were selected according to adj.*P*. The expression ratios of these genes in wild type were added along with the expression in *pip2;1 pip2;2 (DM)* and *pip2;1 pip2;2 pip2;4 (TM)*.

AGI	Log ₂ FC			AGI	Log ₂ FC			AGI	Log ₂ FC		
	WT	DM	TM		WT	DM	TM		WT	DM	TM
AT5G61160	-3.3	-3.3	-3.2	AT2G18890	-1	-1	-0.9	AT1G52720	1.2	1.1	1.2
AT3G15356	-3	-2.4	-3.2	AT4G21215	-1	-1	-1	AT3G45680	1.3	1.1	1.2
AT4G14690	-2.5	-2.8	-2.5	AT1G08840	-1	-1	-1.1	AT5G25140	1.3	1.4	1.4
AT4G16260	-2.2	-1.9	-2	AT1G29465	1	0.9	0.9	AT5G46490	1.3	1.4	1.5
AT5G57220	-2.2	-1.5	-1.9	AT1G10960	1	1.1	1.1	AT1G73040	1.5	1.2	1.2
AT1G09350	-2	-2.3	-2.4	AT1G51440	1	0.7	0.9	AT1G07350	1.5	1.5	1.5
AT3G44990	-2	-1.8	-1.8	AT1G64720	1	1.1	1.2	AT1G65490	1.5	1.9	1.7
AT5G08640	-1.9	-2	-2	AT1G09140	1	1	0.9	AT4G21930	1.6	1.2	1.1
AT1G78410	-1.8	-1.2	-1.4	AT2G45920	1	1	1	AT5G57785	1.6	1.6	1.2
AT3G21460	-1.8	-1.3	-1.3	AT3G47360	1	0.9	0.9	AT2G29500	1.6	2.2	2.3
AT3G59480	-1.6	-1.4	-1.7	AT4G11960	1	1.1	1.2	AT2G46270	1.7	1.6	1.4
AT3G19350	-1.5	-1.8	-1.5	AT1G15960	1	0.9	0.9	AT2G37900	1.7	1.1	1.3
AT4G11290	-1.3	-1.3	-1.4	AT4G23670	1.1	1.1	0.9	AT2G37180	1.8	1.9	2
AT1G24530	-1.3	-1.1	-1	AT5G10946	1.1	1.2	1.2	AT1G72660	1.9	2	2.2
AT5G02260	-1.3	-1	-1	AT4G31351	1.1	1.2	1.4	AT5G25450	2	2.2	2.2
AT5G18290	-1.1	-0.8	-0.8	AT2G19310	1.1	1.3	1.3	AT5G52640	2.6	2.7	3
AT5G46600	-1.1	-1.1	-1.3	AT1G27420	1.2	1	1	AT3G24500	2.6	2.7	2.7
AT4G30650	-1.1	-1.1	-1.4	AT3G29810	1.2	1.1	1.3	AT5G51440	2.8	2.7	3
AT5G52940	-1.1	-1	-1.2	AT1G13080	1.2	1.3	1.3	AT1G07400	3.1	3.1	3.2
AT1G09780	-1.1	-1.2	-1.1	AT4G31354	1.2	1.1	1.4	AT3G12580	3.1	2.9	3.3
AT5G48880	-1	-1.1	-1.2	AT1G03410	1.2	1.3	1.3	AT4G12400	3.1	3.3	3.6

Table 12. The top listed differentially expressed genes in wild type under DH HrH as compared to control condition. The genes were selected according to adj.*P*. The expression ratios of these genes in wild type were added along with the expression in *pip2;1 pip2;2 (DM)* and *pip2;1 pip2;2 pip2;4 (TM)*.

AGI	Log ₂ FC			AGI	Log ₂ FC			AGI	Log ₂ FC		
	WT	DM	TM		WT	DM	TM		WT	DM	TM
AT5G59870	-4.2	-4	-4.2	AT5G62575	1.2	1.1	1.1	AT2G11891	2	1.7	2
AT2G26560	-3.9	-3.2	-3.6	AT2G41440	1.2	1.1	1.1	AT2G17036	2	2	1.8
AT3G46320	-3.7	-3.4	-3.8	AT3G03330	1.2	1.2	1.3	AT2G30480	2	2	2.2
AT5G12910	-3.6	-3.5	-3.7	AT4G02980	1.2	1.1	1.2	AT5G05400	2.1	2	2
AT5G10390	-3.4	-3.3	-3.5	AT4G28370	1.3	1.1	1.1	AT4G11220	2.1	1.8	1.9
AT4G19410	-3	-2.6	-3	AT3G43210	1.3	1.1	1.2	AT1G74860	2.1	1.9	2.1
AT1G19940	-2.9	-2.9	-2.8	AT5G58470	1.3	1.2	1.3	AT3G45420	2.1	2	1.9
AT2G35970	-2.9	-2.5	-2.6	AT5G59440	1.3	1.2	1.3	AT1G27590	2.1	2.1	2.2
AT5G05580	-2.7	-2.3	-2.4	AT5G66240	1.3	1.3	1.3	AT2G32340	2.2	2.2	2.2
AT1G63220	-2.6	-2.3	-2.4	AT4G15090	1.3	1.2	1.2	AT5G24155	2.2	2	2.1
AT5G39320	-2.5	-2.4	-2.5	AT4G12560	1.3	1.3	1.4	AT2G45920	2.2	1.9	2
AT5G19250	-2.4	-2.2	-2.5	AT2G33740	1.3	1.2	1.2	AT5G47830	2.2	1.9	2.1
AT5G44110	-2.3	-2.3	-2.3	AT3G46920	1.3	1.2	1.3	AT5G57790	2.2	1.8	2
AT3G53730	-2.2	-2.1	-2.1	AT1G06110	1.3	1.1	1.3	AT4G16280	2.2	1.9	2
AT3G23810	-2.2	-2.2	-2.2	AT3G43520	1.3	1.1	1.2	AT5G49990	2.2	1.9	2.1
AT5G07110	-2.1	-1.9	-2	AT5G16110	1.3	1.3	1.3	AT1G44414	2.4	2	2.2
AT5G46230	-2.1	-2.1	-2.1	AT1G10240	1.3	1.3	1.4	AT2G17900	2.4	2	2
AT5G07720	-2	-1.9	-2	AT5G62090	1.4	1.1	1.3	AT1G27420	2.4	2.3	2.3
AT5G24850	-2	-1.7	-1.8	AT4G02210	1.4	1.4	1.4	AT1G71330	2.4	2.2	2.1
AT1G29720	-2	-1.9	-1.9	AT5G56600	1.4	1.2	1.3	AT2G42330	2.4	2.3	2.5
AT2G36470	-2	-2	-2	AT1G19980	1.4	1.2	1.5	AT1G09140	2.4	2.2	2.4
AT4G33360	-1.9	-1.7	-1.9	AT5G08230	1.4	1.3	1.3	AT3G24100	2.5	2.1	2.2
AT2G36880	-1.8	-1.9	-1.8	AT4G36910	1.4	1.4	1.4	AT5G10946	2.5	2.4	2.5
AT3G45980	-1.7	-1.6	-1.7	AT1G72650	1.4	1.4	1.5	AT4G18280	2.5	1.8	2.2
AT3G59970	-1.7	-1.5	-1.6	AT3G17740	1.4	1.5	1.5	AT4G31354	2.6	2.4	2.5
AT1G53040	-1.6	-1.5	-1.6	AT5G63830	1.4	1.4	1.5	AT4G31351	2.6	2.5	2.6
AT5G62630	-1.6	-1.3	-1.4	AT1G26580	1.5	1.5	1.5	AT1G49405	2.6	2.2	2.4
AT4G13930	-1.6	-1.6	-1.6	AT1G20920	1.5	1.5	1.5	AT1G64561	2.7	2.7	2.7
AT3G51160	-1.6	-1.6	-1.7	AT1G72090	1.5	1.4	1.4	AT2G19310	2.7	2.6	2.7
AT1G34010	-1.5	-1.3	-1.4	AT5G56380	1.5	1.5	1.5	AT1G34042	2.8	2.6	2.8
AT3G61440	-1.5	-1.3	-1.4	AT1G17460	1.5	1.4	1.6	AT2G07671	2.9	2.7	3
AT1G31190	-1.4	-1.4	-1.4	AT3G60300	1.5	1.3	1.4	AT1G56170	2.9	2.6	2.7
AT5G05820	-1.4	-1.2	-1.4	AT3G53630	1.5	1.5	1.5	AT3G14560	2.9	2.3	2.6
AT1G79080	-1.4	-1.3	-1.4	AT1G01710	1.6	1.4	1.4	AT1G67265	3.1	2.7	2.8
AT3G11800	-1.4	-1.4	-1.4	AT1G71260	1.6	1.6	1.6	AT1G07350	3.1	2.8	3
AT5G64290	-1.3	-1.2	-1.1	AT4G17440	1.6	1.5	1.6	AT3G07150	3.2	3	3.2
AT3G46030	-1.3	-1.2	-1.3	AT5G03830	1.6	1.4	1.3	AT3G48830	3.3	3.4	3.4
AT3G03350	-1.3	-1.2	-1.2	AT5G62200	1.6	1.4	1.6	AT4G29770	3.3	3	3.2
AT2G36320	-1.3	-1.2	-1.3	AT3G01770	1.6	1.5	1.6	AT5G25280	3.5	3.2	3.6

RESULTS

AT3G13060	-1.2	-1.1	-1.1	AT1G24095	1.6	1.3	1.4	AT5G19875	3.6	3.1	3.4
AT5G03040	-1.2	-1.1	-1.1	AT2G46610	1.7	1.4	1.5	AT2G46270	3.6	3	3.3
AT4G27720	-1.2	-1.1	-1.2	AT4G38020	1.7	1.7	1.8	AT4G14819	3.7	2.8	3.2
AT5G26667	-1.2	-1.2	-1.2	AT1G29465	1.7	1.9	1.8	AT5G47610	3.7	3.2	3.6
AT5G46800	-1.1	-1.1	-1.1	AT4G15780	1.7	1.6	1.6	AT1G03070	3.7	3.1	3.4
AT4G26910	-1.1	-1	-1.1	AT2G37340	1.7	1.6	1.7	AT4G23493	4.2	3.6	3.7
AT3G07170	-1.1	-1.1	-1.2	AT3G04160	1.7	1.5	1.6	AT1G30190	4.6	3.9	4.4
AT5G63060	-1.1	-1.2	-1.1	AT2G26860	1.7	1.5	1.6	AT4G33550	4.7	3.9	4.4
AT5G36890	-1	-1	-1	AT2G20585	1.7	1.7	1.6	AT3G24500	5.1	4.6	4.8
AT4G31430	1	0.9	0.9	AT2G46800	1.7	1.5	1.8	AT2G32120	5.1	4.6	4.9
AT5G51730	1	0.9	1	AT3G17460	1.7	1.6	1.6	AT1G07500	5.1	4.5	4.8
AT4G21860	1	1	1.1	AT4G32450	1.7	1.6	1.7	AT4G21320	5.5	4.9	5.1
AT3G60910	1	1.1	1.1	AT5G51170	1.7	1.6	1.6	AT5G25450	5.7	5.4	5.6
AT1G48970	1	1	1.1	AT5G66090	1.7	1.6	1.8	AT5G52640	5.8	5.5	5.8
AT2G48100	1.1	1	1	AT4G11960	1.8	1.5	1.7	AT5G59320	5.9	4.4	5.1
AT3G12300	1.1	1	1	AT3G54000	1.8	1.7	1.7	AT3G12580	6.3	5.7	6.1
AT1G01160	1.1	1.1	1.1	AT5G03560	1.8	1.6	1.8	AT5G51440	6.4	5.8	6
AT3G62560	1.1	1	1.1	AT3G13224	1.8	1.6	1.7	AT4G12400	6.8	6.5	6.7
AT3G62330	1.2	1.1	1.2	AT4G36900	1.8	1.4	1.6	AT1G72660	7	6.7	7.2
AT1G05970	1.2	1.1	1	AT3G62770	1.9	1.9	1.9	AT1G07400	7.2	6.5	6.9
AT1G45976	1.2	0.9	1.1	AT1G23860	2	1.7	1.8	AT2G29500	7.8	7.6	7.7
AT3G21740	1.2	1.1	1.2	AT5G58590	2	1.8	1.9	AT5G59720	8.1	7.6	7.8
AT5G42820	1.2	1	1.1	AT4G30570	2	1.9	2	AT3G46230	9	8.8	9.2
AT1G20890	1.2	1	1.1	AT1G76065	2	1.8	2.1	AT1G53540	9.6	9	9.8
AT3G10030	1.2	1.1	1.2								

Table 13. The top listed differentially expressed genes in wild type under DH LrH as compared to control condition. The genes were selected according to adj.*P*. The expression ratios of these genes in wild type were added along with the expression in *pip2;1 pip2;2 (DM)* and *pip2;1 pip2;2 pip2;4 (TM)*.

AGI	Log ₂ FC			AGI	Log ₂ FC			AGI	Log ₂ FC		
	WT	DM	TM		WT	DM	TM		WT	DM	TM
AT1G29660	-3.9	-3.4	-3.5	AT5G37720	1.1	0.9	0.9	AT5G04250	2.5	1.7	2.1
AT5G12910	-3.8	-3.5	-3.6	AT1G17680	1.1	1.1	1	AT5G49990	2.5	2.3	2.4
AT2G26560	-3.7	-3.5	-3.8	AT4G34370	1.2	0.9	1.1	AT1G71330	2.6	2.1	2.2
AT3G44450	-3.7	-3.3	-3.5	AT3G12300	1.2	1	1	AT1G09140	2.6	2.2	2.4
AT3G46320	-3.7	-3.3	-3.7	AT3G10030	1.2	1.1	1.2	AT1G15960	2.6	2.3	2.1
AT5G10390	-3.6	-3.2	-3.5	AT5G58470	1.2	1.1	1.2	AT5G60580	2.6	2.2	2.4
AT3G22142	-3.3	-3.3	-3.3	AT1G10240	1.3	1.1	1.3	AT4G18280	2.6	2.2	2.2
AT2G35970	-3.3	-2.9	-3	AT2G41440	1.3	1.2	1.1	AT5G11090	2.7	2.4	2.6
AT4G19410	-3.2	-2.8	-3.1	AT1G72090	1.3	1.3	1.4	AT2G07671	2.8	2.5	2.9
AT3G21950	-3.2	-2.7	-3	AT4G15780	1.3	1.3	1.3	AT5G10946	2.8	2.5	2.5
AT5G05580	-3	-2.6	-2.8	AT1G29465	1.3	1.4	1.5	AT4G31354	2.8	2.5	2.9
AT1G19940	-2.8	-2.7	-3.1	AT3G62330	1.4	1.3	1.4	AT4G30470	2.8	2.4	2.8
AT2G28740	-2.7	-2.4	-2.7	AT3G01770	1.4	1.2	1.3	AT4G31351	2.8	2.6	3
AT1G63220	-2.7	-2.3	-2.5	AT5G59440	1.4	1.3	1.3	AT4G34230	2.8	2.3	2.5
AT5G39320	-2.6	-2.5	-2.7	AT2G34730	1.4	1.2	1.4	AT4G30490	2.8	2.5	2.7
AT5G19250	-2.5	-2.3	-2.6	AT3G43520	1.4	1.3	1.3	AT1G07350	2.9	2.8	2.7
AT5G49215	-2.5	-2	-2.3	AT4G03230	1.4	1	1.4	AT3G23920	2.9	2.3	2.8
AT5G11420	-2.4	-2.1	-2.3	AT1G72650	1.4	1.3	1.4	AT1G17940	2.9	2.4	2.5
AT5G44340	-2.4	-2.2	-2.2	AT1G45976	1.4	1.2	1.3	AT1G04220	3.1	2.7	2.8
AT3G14310	-2.4	-1.9	-2.1	AT1G26580	1.4	1.3	1.4	AT3G48830	3.2	3.1	3.2
AT3G28180	-2.3	-2.1	-2.2	AT1G06110	1.4	1.4	1.3	AT3G11410	3.2	2.5	2.8
AT5G07110	-2.3	-2.1	-2.2	AT5G16110	1.4	1.4	1.5	AT4G23493	3.2	2.8	2.8
AT4G33360	-2.3	-2.1	-2.4	AT3G17740	1.5	1.3	1.5	AT4G40010	3.4	2.8	3.1
AT5G44110	-2.3	-2.2	-2.2	AT3G17460	1.5	1.3	1.4	AT3G63060	3.4	2.4	2.8
AT2G04780	-2.3	-1.9	-2.2	AT3G46920	1.5	1.2	1.5	AT1G80320	3.5	3	3.3
AT5G04160	-2.2	-2.1	-2.2	AT1G04970	1.5	1.3	1.3	AT1G70300	3.5	3.2	3.4
AT2G03350	-2.2	-1.7	-2	AT3G04240	1.5	1.3	1.5	AT3G14560	3.5	3.1	3.3
AT1G52290	-2.2	-1.6	-2.1	AT3G04160	1.5	1.4	1.4	AT4G14819	3.7	2.9	3
AT2G36470	-2.2	-2.1	-2.2	AT3G43210	1.6	1.3	1.4	AT1G03070	3.7	3	3.3
AT1G01790	-2.2	-2	-2.1	AT5G62200	1.6	1.4	1.4	AT4G05100	3.8	3	3.3
AT5G26670	-2.1	-1.8	-1.9	AT1G58470	1.6	1.4	1.5	AT5G62150	3.9	3.6	3.8
AT1G62790	-2.1	-1.8	-2	AT4G28370	1.6	1.3	1.5	AT5G25280	4	3.7	4
AT5G41140	-2	-1.8	-1.7	AT5G62090	1.6	1.4	1.5	AT3G02140	4.3	3.3	4
AT3G45980	-2	-1.7	-1.9	AT1G01710	1.7	1.4	1.4	AT1G67920	4.3	4.2	4.4
AT2G36880	-2	-1.9	-2	AT5G25560	1.7	1.6	1.6	AT1G49450	4.3	2.9	3.5
AT1G29720	-2	-1.8	-2	AT2G37340	1.7	1.7	1.8	AT3G03170	4.3	3.7	3.8
AT5G07590	-1.9	-1.5	-1.8	AT2G46610	1.7	1.5	1.6	AT2G46270	4.3	3.9	4
AT5G48830	-1.9	-1.6	-1.8	AT3G13224	1.8	1.6	1.6	AT5G47550	4.4	3.9	3.9
AT3G59970	-1.8	-1.7	-1.9	AT5G51170	1.8	1.6	1.7	AT5G02020	4.5	3.9	4.3

RESULTS

AT3G10050	-1.8	-1.5	-1.7	AT2G46800	1.8	1.7	1.8	AT3G48240	4.7	3.9	4.3
AT5G65810	-1.8	-1.6	-1.8	AT1G76065	1.8	1.8	1.8	AT3G24500	4.7	4.5	4.6
AT2G43360	-1.8	-1.5	-1.8	AT1G27590	1.8	1.8	1.7	AT5G63350	4.8	3.9	4.6
AT1G06960	-1.8	-1.6	-1.9	AT1G25211	1.8	1.6	1.9	AT5G25450	4.9	4.7	4.9
AT5G40610	-1.8	-1.5	-1.8	AT2G17036	1.9	1.8	1.7	AT1G30190	5	4.6	4.7
AT1G53040	-1.8	-1.6	-1.8	AT1G78610	1.9	1.7	1.9	AT1G60190	5.1	3.9	4.4
AT1G04430	-1.7	-1.4	-1.5	AT5G35560	1.9	1.7	1.9	AT1G24600	5.2	3.8	4.4
AT5G62630	-1.7	-1.3	-1.6	AT1G23860	2	1.8	1.9	AT1G07500	5.3	4.7	5.4
AT4G13930	-1.7	-1.5	-1.7	AT3G62770	2	1.7	2	AT4G33550	5.4	4.9	4.8
AT2G19680	-1.7	-1.5	-1.7	AT3G03310	2	1.6	1.8	AT5G54165	5.6	4.9	5.3
AT1G09630	-1.6	-1.4	-1.6	AT4G36900	2	1.7	2	AT2G29500	5.7	5.3	5.5
AT1G34010	-1.5	-1.3	-1.6	AT4G30570	2.1	1.9	1.8	AT4G12400	5.7	5.4	5.6
AT1G31190	-1.5	-1.4	-1.6	AT5G04760	2.1	1.8	2	AT5G53710	5.8	5.1	5.3
AT3G10840	-1.5	-1.3	-1.4	AT4G14270	2.1	1.7	1.7	AT3G12580	6	5.4	5.8
AT4G27720	-1.5	-1.2	-1.3	AT3G47600	2.2	2	2.2	AT5G59320	6.1	4.8	5.2
AT5G05820	-1.4	-1.3	-1.5	AT5G57790	2.2	1.9	2.1	AT1G07400	6.3	5.3	5.9
AT5G03300	-1.4	-1.2	-1.3	AT1G49405	2.2	1.8	2	AT4G01985	6.3	5.1	5.6
AT3G26780	-1.4	-1.2	-1.3	AT2G37150	2.2	1.7	1.9	AT5G62040	6.3	5.4	5.3
AT3G46030	-1.4	-1.2	-1.5	AT4G26080	2.3	1.8	1.9	AT1G72660	6.4	5.7	6.1
AT4G24620	-1.4	-1.3	-1.4	AT1G74860	2.3	2	2.2	AT5G50360	6.9	5.5	5.9
AT5G46800	-1.4	-1.3	-1.3	AT5G13820	2.3	2	2.2	AT1G22990	7.3	6.2	6.3
AT3G07170	-1.1	-1.1	-1.1	AT1G27420	2.3	2.1	2.2	AT1G05340	7.6	7.2	7.4
AT5G36890	-1.1	-1.1	-1.2	AT5G22860	2.3	2	2	AT1G53540	7.8	6.7	8
AT5G26667	-1	-1.1	-1.2	AT5G57565	2.4	2	2.2	AT3G46230	7.9	7.4	7.9
AT4G31430	1	0.9	1	AT2G11891	2.4	1.9	2.4	AT5G59220	8	6.6	7
AT3G03330	1.1	1.2	1.1	AT4G11220	2.4	2	2.2	AT2G47770	8.1	7.1	7.5
AT1G20890	1.1	1	1.1	AT2G45920	2.4	2.2	2.2				

On the other hand, a larger number of genes were significantly changed in *pip2;1 pip2;2* than in *pip2;1 pip2;2 pip2;4* under each treatment, but only a small portion of these genes overlapped between the two mutants (Figure 30). Among these genes, only four genes, *QQS*, *MRD1*, *AT5G03090* and *HEI10*, were differentially regulated in both *pip* mutants under all the treatments (Figure 31). Genes specifically altered due to a certain stress in *pip2;1 pip2;2* or in *pip2;1 pip2;2 pip2;4* were examined to understand the exclusive responses to water stresses in *pip* mutants. Interestingly, there was almost no overlap between the different stresses for each *pip* mutant (Figure 32). On the other hand, GO assignment by MapMan 3.5.1R2 showed that a large amount of the differentially expressed genes were *not assigned* in both *pip* mutants under water stresses. The rest of the genes were associated to *carbohydrate metabolism, cell wall, secondary metabolism, biotic and abiotic stresses, protein modification and degradation* as well as other functional classifications under water stresses (Figure 33 and Table 14-18), suggesting at least partly common responses in terms of the affected biological processes.

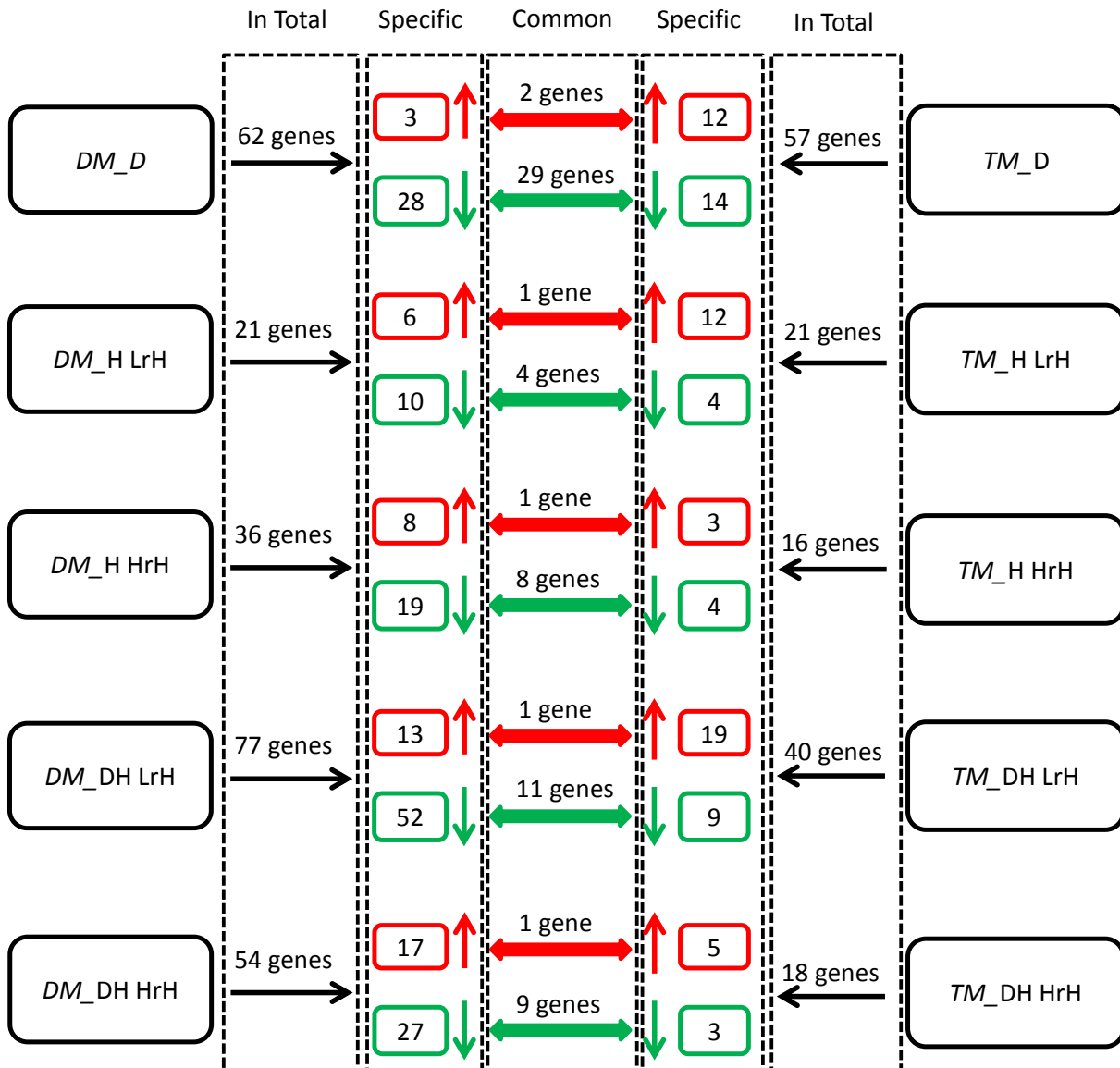


Figure 30. Number of differentially expressed genes in *pip* mutants as compared to the wild type under water stresses. The total number (In total), number of specifically changed genes (Specific) in either *pip2;1 pip2;2* (*DM*) and *pip2;1 pip2;2 pip2;4* (*TM*) under each stress condition and the number of common elements in both mutants (Common) are shown ($|\text{Log}_2\text{FC}| \geq 1$ & $\text{adj. } P \leq 0.05$).

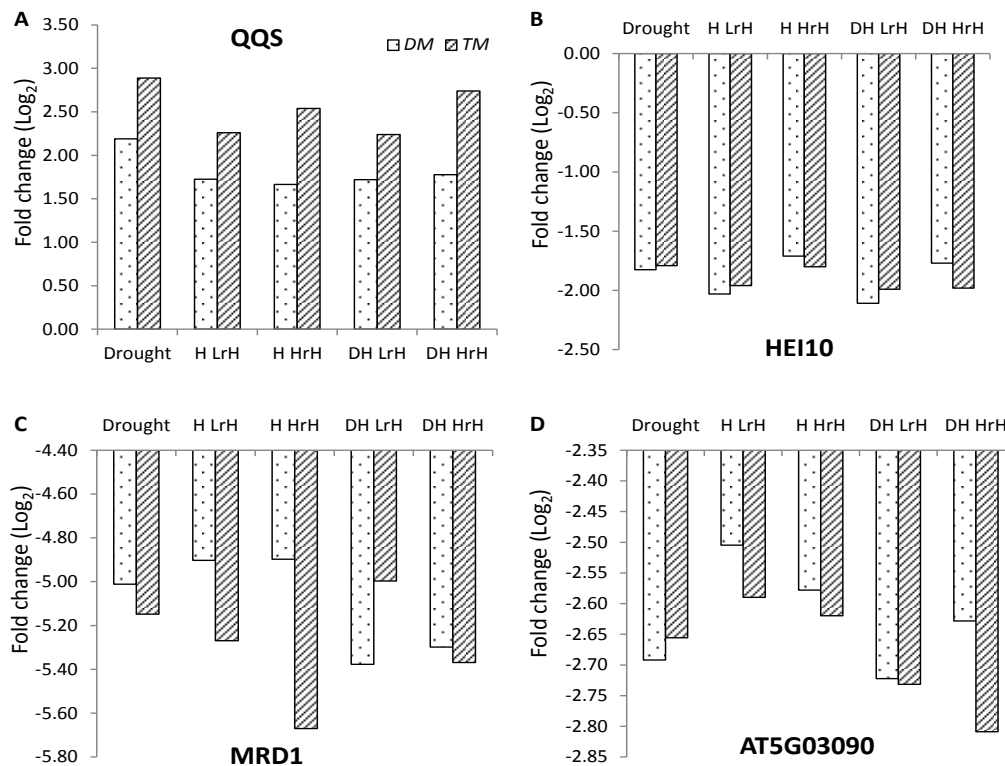


Figure 31. Relative expression levels of four differentially expressed genes in common between *pip2;1 pip2;2* (DM) and *pip2;1 pip2;2 pip2;4* (TM) as compared to wild type under all the water stresses D, H LrH, H HrH, DH LrH and DH HrH. The values were extracted from Agilent microarray analysis.

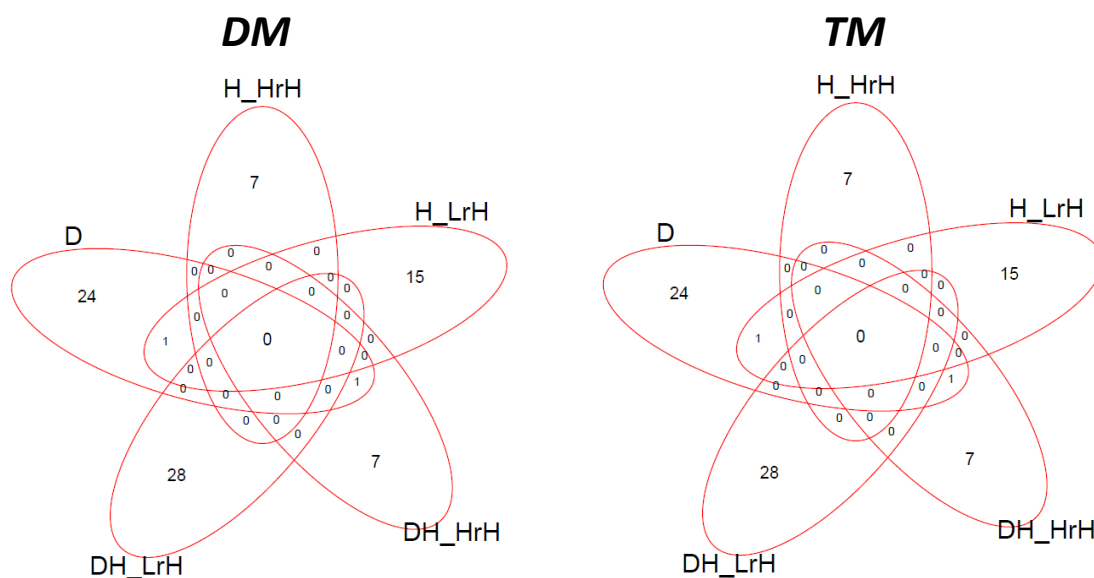


Figure 32. Venn diagram of specifically altered genes in *pip2;1 pip2;2* (DM) or *pip2;1 pip2;2 pip2;4* (TM) as compared to wild type under water stresses ($|\text{Log}_2\text{FC}| \geq 1$ & $\text{adj. } P \leq 0.05$)

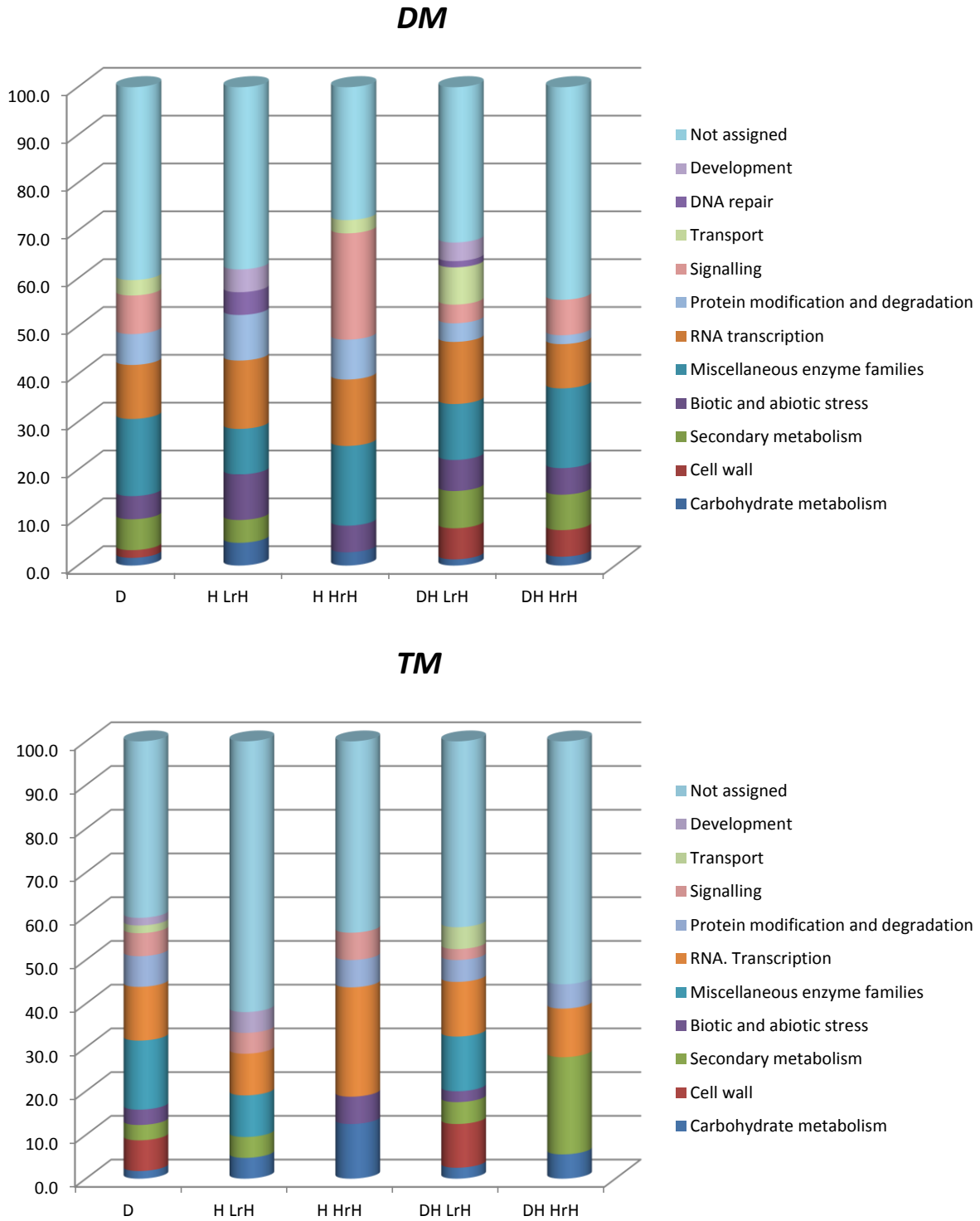


Figure 33. Gene ontology categories of differentially expressed genes in *pip2;1 pip2;2* (DM) and *pip2;1 pip2;2 pip2;4* (TM) as compared to the wild type under water stresses. The categorization was done by MapMan 3.2.1R2 and the percentages among all differentially expressed genes are given.

Several specifically altered genes associated to cell wall in *pip* mutants in response to water stresses were particularly interesting in the context of plant water relations. Under drought stress, *FUCOSYLTRANSFERASE 4 (FUT4)*, which functions in fucosylation of arabinogalactan proteins (Tryfona *et al.*, 2014), was downregulated in both *pip* mutants, whereas one pectin lyase-like protein, *POLYGALACTURONASE 4 (PGA4)* was specifically upregulated in *pip2;1 pip2;2 pip2;4* (Table 14). Under DH HrH, one transcript encoding a pectate lyase protein was specifically enhanced in *pip2;1 pip2;2* (Table 17). Under DH LrH, *LEUCINE-RICH REPEAT/EXTENSIN 1 (LRX1)* and *CELLULOSE SYNTHASE-LIKE A1 (CSLA01)* were enhanced in *pip2;1 pip2;2*, whereas one plant invertase/pectin methylesterase inhibitor superfamily protein encoding gene, *AT2G47050*, and one pectin lyase-like superfamily protein gene, *AT2G43870*, were specifically upregulated in *pip2;1 pip2;2 pip2;4* (Table 18). But no cell wall related genes were changed under H HrH and H LrH (Table 15 and Table 16). In addition, more than 30% of the differentially expressed genes under Drought, H LrH, DH LrH and DH HrH and 15% of the differentially expressed genes under H HrH in both *pip* mutants were functional uncharacterized genes (Table 14-18). To better understand the functions of uncharacterized genes in *pip* mutants under water stresses, co-expression analysis was applied via ATTED-II (<http://atted.jp>). However, no co-expressed networks between these differentially expressed genes were detected.

Taken together, loss of *PIP2;1*, *PIP2;2* and loss of additional *PIP2;4* marginally impacted the water stress responses at transcriptional level. The differentially expressed genes in *pip2;1 pip2;2* and *pip2;1 pip2;2 pip2;4* under water stresses shared the same regulatory pathways, although the individual genes were mostly not regulated in common and were highly dependent on the treatments.

Table 14. Differentially expressed genes either in *pip2;1 pip2;2* (*DM*) or *pip2;1 pip2;2 pip2;4* (*TM*) as compared to the wild type under drought stress (red and green values represent fold change of significantly increased and decreased genes, respectively; black values represent non-significant fold changes with $\text{adj.}P \geq 0.05$; Black dashes “-” represent the low expressed genes that cannot be detected; NA, Not Assigned; The genes in bold are highly expressed in leaves).

AGI Code	Log ₂ FC		Name	Annotation
	<i>DM</i>	<i>TM</i>		
Major carbohydrate metabolism				
AT3G30720	2.19	2.89	QQS	Starch metabolism
Cell wall				
AT2G15390	-1.03	-1.03	<i>FUT4</i>	Predicted fucosyltransferase
AT1G02790	-	2.35	<i>PGA4</i>	Exopolygalacturonase
AT3G07850	-	2.13	NA	Pectin lyase-like superfamily protein
AT3G59850	-	-1.18	NA	Pectin lyase-like superfamily protein
Secondary metabolism				
AT1G74090	1.01	1.09	<i>SOT18</i>	Desulfoglucosinolate sulfotransferase
AT5G24140	-2.13	-	<i>SQP2</i>	Similarity to squalene monooxygenases
AT3G55970	-1.31	-1.36	<i>JRG21</i>	Jasmonate-regulated gene 21
AT1G23320	3.38	-	<i>TAR1</i>	Similarity to the TAA1 tryptophan aminotransferase
Biotic stress				
AT1G33910	-3.33	-	NA	P-loop containing nucleoside triphosphate hydrolase
AT2G35980	-1.15	-	<i>YLS9</i>	Similar to tobacco hairpin-induced gene (HIN1)
AT4G30430	-1.06	-	<i>TET9</i>	Tetraspanin
AT3G52400	-	-1.01	<i>SYP122</i>	Syntaxin protein
AT3G51560	-	2.72	NA	Disease resistance protein (TIR-NBS-LRR class) family
Miscellaneous enzyme families				
AT5G56470	-4.43	-	<i>GULLO7</i>	FAD-dependent oxidoreductase family protein
AT1G26420	-1.06	-	NA	FAD-binding Berberine family protein
AT1G69240	-2.54	-2.51	<i>MES15</i>	Act as a carboxylesterase
AT2G29350	-1.37	-	<i>SAG13</i>	Senescence-associated gene
AT2G29460	-1.55	-1.27	<i>GSTU4</i>	Glutathione transferase
AT3G26830	-1.67	-1.38	<i>PAD3</i>	Conversion of dihydrocamalexin acid to camalexin
AT2G18980	-1.42	-1.20	NA	Peroxidase superfamily protein
AT5G06730	-1.75	-1.72	NA	Peroxidase superfamily protein
AT5G35950	-1.53	-1.42	NA	Mannose-binding lectin superfamily protein
AT1G64235	-1.35	-	NA	lipid-transfer protein
AT3G13390	-	2.23	<i>SKS11</i>	SKU5 similar 11
AT3G13400	-	2.30	<i>SKS13</i>	SKU5 similar 13
AT3G53070	-	3.59	NA	Putative membrane lipoprotein
RNA.Transcription				
AT5G67060	-1.81	-1.54	<i>HEC1</i>	DNA binding transcription factor activity
AT4G21080	-2.34	-	<i>DOF4.5</i>	Dof-type zinc finger domain-containing protein
AT3G01030	-1.51	-	NA	C2H2 and C2HC zinc fingers superfamily protein
AT5G17320	-1.38	-1.40	<i>HDG9</i>	Homeobox-leucine zipper family protein

AT1G53490	-1.82	-1.79	<i>HEI10</i>	A RING finger-containing protein
AT3G10815	-1.07	-	NA	RING/U-box superfamily protein
AT5G22380	-1.37	-	<i>NAC090</i>	NAC domain containing protein 90
AT2G33710	-	-2.18	NA	ERF subfamily B-4 of ERF/AP2 transcription factor
AT2G15660	-	3.50	<i>AGL95</i>	AGAMOUS-like 95
AT1G66550	-	2.85	<i>WRKY67</i>	WRKY Transcription Factor
AT1G28300	-	1.19	<i>LEC2</i>	Transcription factor that contains a B3 domain
DNA.Repair				
AT3G32330	-	-1.60	NA	DNA repair protein-related
Protein modification and degradation				
AT2G33010	-3.74	-	NA	Ubiquitin-associated (UBA) protein F-box and associated interaction domains-containing protein
AT4G19940	-1.64	-	NA	NA
AT5G55150	-1.37	-	NA	NA
AT1G56030	-1.08	-	NA	RING/U-box superfamily protein
AT3G46240	-	2.75	NA	Best protein match is: receptor protein kinase-related
AT4G05250	-	2.05	NA	Ubiquitin-like superfamily protein F-box and associated interaction domains-containing protein
AT1G58090	-	-1.09	NA	protein
AT3G59230	-	-1.99	NA	RNI-like superfamily protein
Signalling				
AT2G29110	-1.27	-1.31	<i>GLR2.8</i>	Putative ligand-gated ion channel subunit
AT1G79680	-1.26	-1.14	<i>WAKL10</i>	Twin-domain, kinase-GC signaling molecule
AT3G15050	-1.27	-1.28	<i>IQD10</i>	IQD10 and functions in calmodulin binding
AT5G26920	-1.00	-	<i>CBP60G</i>	Calmodulin-binding protein CBP60G
AT4G03156	-2.08	-	NA	Small GTPase-related
Cell.Vesicle transport				
AT5G13990	-	-3.02	<i>EXO70C2</i>	Putative exocyst subunits
Development				
AT3G43660	-3.13	-2.94	NA	Putative nodulin-like21 protein
Transport				
AT3G48850	-1.03	-	<i>PHT3;2</i>	Mitochondrial phosphate transporter
AT1G17810	-2.06	-2.07	<i>TIP3;2</i>	Beta-tonoplast intrinsic protein (beta-TIP)
Not assigned				
AT1G53480	-5.01	-5.15	<i>MRD1</i>	<i>mto 1</i> responding down
AT1G54095	-3.80	-	NA	NA
AT1G59590	-1.06	-	<i>ZCF37</i>	ZCF37 mRNA, complete cds
AT1G68680	-1.20	-1.25	NA	NA
AT2G07215	-2.07	-	NA	NA
AT2G18690	-1.33	-1.26	NA	NA
AT3G01290	-1.20	-	<i>HIR2</i>	Membrane-associated protein
AT3G11405	-2.26	-1.64	NA	NA
AT3G13950	-1.23	-	NA	NA
AT3G15518	-1.16	-1.14	NA	NA
AT3G16432	-2.19	-2.17	NA	NA
AT3G26855	-1.85	-2.03	NA	Reverse transcriptase-related family protein

RESULTS

AT3G29033	-1.99	-2.02	NA	NA
AT3G42990	-2.29	-1.97	NA	NA
AT4G17505	3.00	-	NA	NA
AT4G19095	-2.50	-2.49	NA	NA
AT4G29103	-1.06	-1.15	NA	NA
AT4G29250	-2.23	-	NA	HXXXD-type acyl-transferase family protein
AT5G03090	-2.69	-2.66	NA	Best protein match is: mto 1 responding down 1
AT5G05300	-1.09	-	NA	NA
AT5G08240	-1.01	-	NA	NA
AT5G35050	-1.06	-1.09	NA	NA
AT5G36100	-1.96	-	NA	NA
AT4G03480	2.13	-	NA	Ankyrin repeat family protein
AT1G52810	-	-1.72	NA	2OG and Fe(II)-dependent oxygenase superfamily protein
AT1G25400	-	-1.06	NA	NA
AT1G27610	-	-1.79	NA	NA
AT1G34400	-	-1.22	NA	NA
AT2G41640	-	-1.03	NA	Glycosyltransferase family 61 protein
AT3G50130	-	-1.49	NA	NA
AT4G33320	-	-2.38	NA	NA
AT5G60650	-	1.23	NA	NA

Table 15. Differentially expressed genes either in *pip2;1 pip2;2* (DM) or *pip2;1 pip2;2 pip2;4* (TM) as compared to the wild type under H HrH (red and green values represent fold change of significantly increased and decreased genes, respectively; black values represent non-significant fold changes with $\text{adj.}P \geq 0.05$; Black dashes “-” represent the low expressed genes that cannot be detected; NA, Not Assigned; The genes in bold are highly expressed in leaves).

AGI Code	Log ₂ FC		Name	Annotation
	DM	TM		
Major carbohydrate metabolism				
AT3G30720	1.67	2.54	<i>QQS</i>	Starch metabolism
Secondary metabolism				
AT4G27550	-	-2.72	<i>TPS4</i>	Putative enzyme involved in trehalose biosynthesis
Biotic and abiotic stress				
AT2G32680	-1.22	-	<i>RLP23</i>	Receptor like protein 23
AT1G11040	3.04	-	NA	HSP40/DnaJ peptide-binding protein
AT2G42885	-	2.08	NA	Defensin-like (DEFL) family protein
Miscellaneous enzyme families				
AT4G16260	-1.22	-	NA	Putative beta-1,3-endoglucanase
AT1G26380	-1.21	-	NA	FAD-binding Berberine family protein
AT1G02920	-1.02	-	<i>GST11</i>	Glutathione transferase
AT3G11980	4.30	-	<i>FAR2</i>	Similar to fatty acid reductases
AT4G29580	3.42	-	NA	Cytidine/deoxycytidylate deaminase family protein
AT5G09290	-1.07	-	NA	Inositol monophosphatase family protein
RNA.Transcription				
AT1G30455	-1.72	-4.50	NA	Transcription regulators
AT1G53490	-1.71	-1.80	<i>HEI10</i>	A RING finger-containing protein
AT5G52170	2.53	-	<i>HDG7</i>	Homeobox-leucine zipper family protein
AT2G40740	-1.36	-	<i>WRKY55</i>	Member of WRKY Transcription Factor
AT5G10760	-1.15	-	NA	Eukaryotic aspartyl protease family protein
AT1G18710	-	1.03	<i>MYB47</i>	Member of the R2R3 factor gene family.
AT3G28470	-	-6.01	<i>MYB35</i>	Member of the R2R3 factor gene family.
Protein modification and degradation				
AT4G25110	-1.30	-	<i>MC2</i>	Type I metacaspase 2
AT2G18080	3.48	-	<i>EDA2</i>	Embryo sac development arrest 2
AT3G28580	-1.55	-	NA	P-loop containing nucleoside triphosphate hydrolase
AT5G39440	-	3.51	<i>SnRK1.3</i>	SNF1-related protein kinase 1.3
Signalling				
AT2G29110	-1.01	-	<i>GLR2.8</i>	Putative ligand-gated ion channel
AT4G11460	-1.02	-	<i>CRK30</i>	Cysteine-rich receptor-like protein kinase ABA- and osmotic-stress-inducible receptor-like cytosolic
AT4G11890	-1.11	-	<i>ARCK1</i>	kinase
AT4G23150	-1.21	-	<i>CRK7</i>	Cysteine-rich receptor-like protein kinase
AT1G51890	-1.00	-	NA	Leucine-rich repeat protein kinase family protein
AT3G21945	1.39	-	NA	Receptor-like protein kinase-related family protein

RESULTS

AT2G41100	-1.04	-	<i>TCH3</i>	Calmodulin-like protein
AT5G39670	-1.03	-	NA	Calcium-binding EF-hand family protein
AT4G03156	-	-2.90	NA	small GTPase-related
Transport				
AT4G18790	-2.72	-	<i>NRAMP5</i>	Member of Nramp2 family
Not assigned				
AT1G53480	-4.90	-5.67	<i>MRD1</i>	<i>mto 1</i> responding down
AT1G68680	-1.09	-1.12	NA	NA
AT2G18690	-1.03	-	NA	NA
AT2G44195	-1.73	-1.52	NA	CBF1-interacting co-repressor CIR
AT3G01290	-1.16	-	<i>HIR2</i>	Hypersensitive induced reaction 2
AT3G15578	-1.69	-1.90	NA	NA
AT3G30350	-2.77	-2.28	<i>RGF4</i>	Root meristem growth factor
AT4G26920	3.47	-	NA	StAR-related lipid-transfer lipid-binding domain
AT5G03090	-2.58	-2.62	NA	Best protein match is <i>mto 1</i> responding down 1
AT5G27370	1.15	-	NA	NA
AT4G28405	-	-1.57	NA	NA

Table 16. Differentially expressed genes either in *pip2;1 pip2;2* (DM) or *pip2;1 pip2;2 pip2;4* (TM) as compared to the wild type under H LrH (red and green values represent fold change of significantly increased and decreased genes, respectively; black values represent non-significant fold changes with $\text{adj.}P \geq 0.05$; Black dashes “-” represent the low expressed genes that cannot be detected; NA, Not Assigned; The genes in bold are highly expressed in leaves).

AGI Code	Log ₂ FC		Name	Annotation
	DM	TM		
Major carbohydrate metabolism				
AT3G30720	1.73	2.26	QQS	Starch metabolism
Secondary metabolism				
AT5G51420	-2.48	-	NA	Long-chain-alcohol O-fatty-acyltransferase
AT5G60510	-	1.82	CPT9	<i>cis</i> -prenyltransferase 9
Biotic and abiotic stress				
AT1G52660	1.98	-	NA	P-loop containing nucleoside triphosphate hydrolase
AT5G37760	-1.53	-	NA	Chaperone DnaJ-domain superfamily protein
Miscellaneous enzyme families				
AT3G01620	-1.66	-	NA	Beta-1,4-N-acetylglucosaminyltransferase
AT1G27140	1.37	-	GSTU14	Glutathione transferase
AT2G16730	-	4.60	BGAL13	Putative beta-galactosidase
AT4G02250	-	-13.32	NA	Plant invertase/pectin methylesterase
Signalling				
AT2G22290	-	2.29	RABH1d	RAB GTPase homolog 6
RNA.Transcription				
AT4G10240	-3.43	-	BBX23	B-box zinc finger family protein
AT5G07100	-1.05	-	WRKY26	WRKY DNA-binding protein 26
AT1G53490	-2.03	-1.96	HEI10	A RING finger-containing protein
AT5G46660	-	1.33	NA	Protein kinase C-like zinc finger protein
DNA.Synthesis/chromatin structure				
AT5G16850	-2.03	-	TERT	Catalytic subunit of telomerase reverse transcriptase
Protein targeting and degradation				
AT3G05720	-2.65	-	IMPA-7	Putative importin alpha isoform
AT2G38900	1.49	-	NA	PR (pathogenesis-related) peptide
Development				
AT3G20400	4.66	-	EMB2743	Embryo defective 2743
AT3G18518	-	-1.76	RTFL20	ROTUNDIFOLIA like 20
Not assigned				
AT1G53480	-4.90	-5.27	MRD1	<i>mto 1</i> responding down
AT1G27260	-4.29	-	NA	Paired amphipathic helix superfamily protein
AT5G03090	-2.50	-2.59	NA	Best protein match is <i>mto 1</i> responding down 1
AT5G44920	-1.13	-	NA	Toll-Interleukin-Resistance (TIR) domain family protein
AT5G33898	-1.99	-	NA	NA
AT1G68680	-1.30	-1.40	NA	NA
AT1G48740	2.25	-	NA	2-oxoglutarate (2OG) and Fe(II)-dependent oxygenase

RESULTS

AT1G16025	1.24	-	NA	NA
AT2G26865	-	-1.49	NA	A Plant thionin family protein
AT4G27890	-	1.89	NA	HSP20-like chaperones superfamily protein
AT5G09430	-	2.19	NA	Alpha/beta-Hydrolases superfamily protein
AT5G52730	-	-1.90	NA	Copper transport protein family
AT2G13980	-	1.42	NA	Polynucleotidyl transferase
AT2G18270	-	2.28	NA	NA
AT3G30770	-	3.08	NA	Eukaryotic aspartyl protease family protein
AT4G02090	-	1.41	NA	NA
AT4G04650	-	2.75	NA	RNA-directed DNA polymerase
AT5G60650	-	1.13	NA	NA

Table 17. Differentially expressed genes either in *pip2;1 pip2;2 (DM)* or *pip2;1 pip2;2 pip2;4 (TM)* as compared to the wild type under DH HrH (red and green values represent fold change of significantly increased and decreased genes, respectively; black values represent non-significant fold changes with $\text{adj.}P \geq 0.05$; Black dashes “-” represent the low expressed genes that cannot be detected; NA, Not Assigned; The genes in bold are highly expressed in leaves).

AGI Code	Log ₂ FC		Name	Annotation
	DM	TM		
Major carbohydrates metabolism				
AT3G30720	1.78	2.74	<i>QQS</i>	Starch metabolism
Cell wall				
AT4G33840	-2.71	-	NA	Glycosyl hydrolase family 10 protein
AT4G14365	-1.04	-	<i>XBAT34</i>	XB3 ortholog 4 in Arabidopsis thaliana
AT3G24230	1.95	-	NA	Pectate lyase family protein
Amino acid metabolism				
AT4G28410	-1.47	-1.59	<i>RSA1</i>	Tyrosine transaminase family protein
Secondary metabolism				
AT5G36150	3.34	-	<i>PEN3</i>	Putative pentacyclic triterpene synthase 3
AT5G24140	-2.38	-	<i>SQP2</i>	Squalene monooxygenases 2
AT5G10990	-	-2.24	<i>SAUR69</i>	SAUR-like auxin-responsive protein family
AT1G23320	-	2.20	<i>TAR1</i>	Similar to the TAA1 tryptophan aminotransferase
AT1G04370	-	2.53	<i>ERF14</i>	ERF subfamily B-3 of ERF/AP2 transcription factor
Biotic stress				
AT2G32680	-1.12	-	<i>RLP23</i>	Receptor like protein 23
AT2G33080	-1.33	-	<i>RLP28</i>	Receptor like protein 28
AT2G43570	-1.30	-	<i>CHI</i>	Putative chitinase
Redox				
AT1G69880	-1.00	-	<i>TH8</i>	Thioredoxin H-type 8
Miscellaneous enzyme families				
AT5G37940	1.00	-	NA	Zinc-binding dehydrogenase family protein
AT2G29350	-1.29	-	<i>SAG13</i>	Senescence-associated gene 13
AT2G29460	-1.27	-	<i>GSTU4</i>	Glutathione transferase
AT3G26830	-1.15	-	<i>PAD3</i>	Phytoalexin deficient 3

AT3G52970	2.60	-	<i>CYP76G1</i>	Member of CYP76G
AT5G02900	2.46	-	<i>CYP96A13</i>	Member of CYP96A
AT1G61230	2.60	-	NA	Mannose-binding lectin superfamily protein
AT1G01590	1.00	-	<i>FRO1</i>	Ferric-chelate reductase 1
AT5G18470	-1.01	-	NA	Curculin-like (mannose-binding) lectin family protein
RNA.Transcription				
AT1G30455	-2.26	-2.82	NA	Transcription regulators
AT1G53490	-1.77	-1.98	<i>HEI10</i>	A RING finger-containing protein
AT5G22380	-1.28	-	<i>NAC090</i>	NAC domain containing protein 90
AT3G49950	1.91	-	NA	GRAS family transcription factor
AT5G56960	1.76	-	NA	bHLH DNA-binding family protein
Protein modification and degradation				
AT4G05250	2.07	-	NA	Ubiquitin-like superfamily protein
AT3G16555	-	-1.13	NA	F-box family protein
Signalling				
AT4G11890	-1.12	-	<i>ARCK1</i>	ABA- and osmotic-stress-inducible receptor-like kinase 1
AT4G23140	-1.11	-	<i>CRK6</i>	Cysteine-rich receptor-like protein kinase 6
AT4G23150	-1.06	-	<i>CRK7</i>	Cysteine-rich receptor-like protein kinase 7
AT5G41300	-4.00	-	NA	Receptor-like protein kinase-related family protein
Not assigned				
AT1G14780	-1.12	-	NA	Membrane attack complex
AT1G53480	-5.30	-5.37	<i>MRD1</i>	<i>mto 1</i> responding down
AT1G58225	-1.14	-	NA	NA
AT1G73810	-1.02	-	NA	NA
AT2G04037	3.47	-	NA	NA
AT2G04680	-1.77	-2.18	NA	Cysteine/Histidine-rich C1 domain family protein
AT2G16225	3.75	-	NA	Maternally expressed gene (MEG) family protein
AT2G19300	1.11	-	NA	NA
AT2G19320	4.49	-	NA	NA
AT2G25482	-1.55	-	NA	ECA1 gametogenesis related family protein
AT3G28310	-1.56	-1.76	NA	NA
AT3G29034	1.51	-	NA	NA
AT3G48209	-1.71	-2.22	NA	Plant thionin family protein
AT3G49796	-1.29	-	NA	NA
AT4G00700	-1.26	-	NA	C2 calcium/lipid-binding plant phosphoribosyltransferase
AT4G09775	2.22	-	NA	Ribonuclease H-like superfamily protein
AT4G16807	-1.36	-1.35	NA	NA
AT4G31740	-1.57	-	NA	Sec1/munc18-like (SM) proteins superfamily
AT5G03090	-2.63	-2.81	NA	Best protein match is <i>mto 1</i> responding down 1
AT5G08240	-1.04	-	NA	NA
AT5G22545	-1.05	-	NA	NA
AT5G46140	-1.02	-	NA	NA
AT5G52760	-1.19	-	NA	Copper transport protein family
AT2G41640	-	-1.00	NA	Glycosyltransferase family 61 protein
AT5G14020	-	3.28	NA	Targeting BRO1-like domain-containing protein

RESULTS

AT3G59260	-	2.12	NA	Putative pirin
AT1G55230	-	3.70	NA	NA
AT1G07710	3.13	-	NA	Ankyrin repeat family protein

Table 18. Differentially expressed genes either in *pip2;1 pip2;2 (DM)* or *pip2;1 pip2;2 pip2;4 (TM)* as compared to the wild type under DH LrH (red and green values represent fold change of significantly increased and decreased genes, respectively; black values represent non-significant fold changes with $\text{adj.}P \geq 0.05$; Black dashes “-” represent the low expressed genes that cannot be detected; NA, Not Assigned; The genes in bold are highly expressed in leaves).

AGI Code	Log ₂ FC		Name	Annotation
	DM	TM		
Major carbohydrate metabolism				
AT3G30720	1.72	2.24	<i>QQS</i>	Starch metabolism
TCA/Organic acid transformations				
AT5G04180	-	4.16	<i>ACA3</i>	Alpha carbonic anhydrase 3
Cell wall				
AT1G12040	1.27	-	<i>LRX1</i>	Leucine-rich repeat/extensin 1
AT4G16590	1.44	-	<i>CSLA01</i>	Cellulose synthase-like 1
AT3G08900	-1.54	-	<i>RGP3</i>	Reversibly glycosylated polypeptide 3
AT2G14620	-1.33	-	<i>XTH10</i>	Xyloglucan endotransglucosylase/hydrolase 10
AT1G74010	-1.11	-	NA	Calcium-dependent phosphotriesterase
AT2G47050	-	1.19	NA	Plant invertase/pectin methylesterase inhibitor
AT5G25310	-	3.23	NA	Exostosin family protein
AT1G23760	-	2.68	<i>PG3</i>	Polygalacturonase 3
AT2G43870	-	4.32	NA	Pectin lyase-like superfamily protein
Lipid metabolism				
AT1G68620	-1.38	-	NA	Alpha/beta-Hydrolases superfamily protein
AT3G12545	-	2.99	NA	Lipid-transfer protein
Amino acid metabolism				
AT5G14760	-	1.02	<i>AO</i>	L-aspartate oxidase
Hormone metabolism				
AT4G18350	-1.21	-	<i>NCED2</i>	9- <i>cis</i> -epoxycarotenoid dioxygenase
AT5G54510	-1.05	-	<i>DFL1</i>	IAA-amido synthase
AT1G68765	-1.01	-	<i>IDA</i>	Inflorescence deficient in abscission
AT5G07200	-4.18	-	<i>GA20OX3</i>	Gibberellin 20-oxidase
AT2G43820	-1.01	-	<i>SAGT1</i>	Salicylic acid glucosyltransferase 1
Biotic and abiotic stress				
AT4G19820	-1.05	-	NA	Glycosyl hydrolase family protein
AT1G57630	-1.46	-	NA	Toll-Interleukin-Resistance (TIR) domain family protein
AT4G14368	1.12	-	NA	Regulator of chromosome condensation family protein
AT5G62627	-3.74	-	NA	Encodes a defensin-like (DEFL) family protein.
AT3G01420	-1.79	-	<i>DOX1</i>	Plant alpha dioxygenase 1
AT1G33930	-	3.06	NA	P-loop containing nucleoside triphosphate hydrolases
Nucleotide metabolism				

AT4G29710	-	-2.11	NA	Alkaline-phosphatase-like family protein
Miscellaneous enzyme families				
AT2G46480	-3.19	-	<i>GAUT2</i>	Galacturonosyltransferase 2
AT1G31670	-1.50	-1.93	NA	Copper amine oxidase family protein
AT4G12270	-2.32	-	NA	Copper amine oxidase family protein
AT2G29350	-1.62	-	<i>SAG13</i>	Senescence-associated gene 13
AT2G29460	-1.33	-	<i>GSTU4</i>	Glutathione S-transferase 22
AT1G34540	-4.08	-	<i>CYP94D1</i>	Member of CYP94D
AT4G37430	-1.04	-	<i>CYP81F1</i>	Member of the CYP81F
AT3G52780	-1.33	-	<i>PAP20</i>	Protein serine/threonine phosphatase
AT3G53080	1.60	-	NA	D-galactoside/L-rhamnose binding SUEL lectin protein
AT1G61050	-	2.09	NA	Alpha 1,4-glycosyltransferase family protein
AT5G37170	-	-1.58	NA	O-methyltransferase family protein
AT1G53990	-	2.53	<i>GLIP3</i>	Contains lipase signature motif and GDSL domain
RNA.Transcription				
AT2G22750	1.15	-	NA	bHLH DNA-binding superfamily protein
AT4G38000	-1.15	-	<i>DOF4.7</i>	DNA binding with one finger 4.7
AT1G80730	1.95	-	<i>ZFP1</i>	Zinc finger protein 1
AT3G29340	-2.23	-	NA	zinc finger (C2H2 type) family protein
AT5G33210	-1.47	-	<i>SRS8</i>	A member of SHI gene family
AT3G15500	-1.40	-	<i>NAC3</i>	NAC-domain containing protein 3
AT5G46310	-1.92	-	NA	WRKY family transcription factor
AT5G18270	-1.07	-	<i>ANAC087</i>	NAC domain containing protein 87
AT4G31610	-1.44	-1.85	<i>REM1</i>	Reproductive meristems1
AT1G53490	-2.11	-1.99	<i>HEI10</i>	A RING finger-containing protein
AT4G08990	-	-2.05	NA	DNA (cytosine-5-)-methyltransferase family protein
AT5G56960	-	2.06	NA	bHLH DNA-binding family protein
AT5G49200	-	3.10	NA	WD-40 repeat family protein
DNA.Repair				
AT3G32330	-2.71	-2.45	NA	DNA repair protein-related
AT3G02680	1.71	-	<i>NBS1</i>	DNA repair and meiotic recombination protein
Protein modification and degradation				
AT5G45810	-1.03	-	<i>SnRK3.5</i>	Member of the SNF1-related kinase (SnRK) 3.5
AT5G40000	2.70	-	NA	P-loop containing nucleoside triphosphate hydrolases
AT4G03360	1.63	-	NA	Ubiquitin family protein
AT4G01023	-	2.20	NA	RING/U-box superfamily protein
AT4G12810	-	2.44	NA	F-box family protein
Signalling				
AT1G51870	2.34	-	NA	protein kinase family protein
AT4G04490	-1.15	-	<i>CRK36</i>	Cysteine-rich receptor-like protein kinase
AT4G03156	-2.12	-2.28	NA	small GTPase-related
Development				
AT3G53040	-1.59	-	NA	Putative late embryogenesis abundant protein
AT1G28330	-1.74	-	<i>DRM1</i>	dormancy-associated protein
AT4G35783	-1.05	-	<i>RTFL6</i>	ROTUNDIFOLIA like 6

RESULTS

Transport				
AT1G73220	-1.27	-	<i>OCT1</i>	organic cation/carnitine transporter1
AT3G10600	-1.48	-1.65	<i>CAT7</i>	Member of the cationic amino acid transporter
AT1G28220	-1.90	-1.55	<i>PUP3</i>	Proteins related to PUP1, a purine transporter
AT1G04560	-1.56	-	NA	AWPM-19-like family protein
AT3G02960	-2.02	-	NA	Heavy metal transport
AT5G55410	-1.49	-	NA	lipid-transfer protein
Not assigned				
AT1G12451	2.09	-	NA	NA
AT1G13520	-1.17	-	NA	NA
AT5G35830	-2.60	-	NA	Ankyrin repeat family protein
AT1G53480	-5.38	-5.00	<i>MRD1</i>	<i>mto</i> 1 responding down
AT1G68450	-1.08	-	<i>PDE337</i>	VQ motif-containing protein
AT1G72620	-3.08	-	NA	Alpha/beta-Hydrolases superfamily protein
AT2G05420	1.29	-	NA	TRAF-like family protein
AT2G10260	-1.62	-1.47	NA	NA
AT2G17740	-2.00	-	NA	Cysteine/Histidine-rich C1 domain family protein
AT2G27389	-1.24	-	NA	NA
AT2G31945	-1.25	-	NA	NA
AT3G09950	-1.19	-	NA	NA
AT3G12410	-2.85	-2.68	NA	Polynucleotidyl transferase
AT3G13950	-1.29	-	NA	NA
AT3G15760	-1.04	-	NA	NA
AT3G21520	-2.13	-	<i>DMP1</i>	DUF679 domain membrane protein 1
AT3G25950	-1.05	-	NA	TLC lipid-sensing domain containing protein
AT3G48344	-1.94	-	NA	NA
AT3G61930	-1.91	-	NA	NA
AT4G00140	-3.72	-	<i>EDA34</i>	embryo sac development arrest 34
AT4G32080	4.07	-	NA	NA
AT4G39670	-1.32	-	NA	Glycolipid transfer protein
AT5G03090	-2.72	-2.73	NA	Best protein match is <i>mto</i> 1 responding down 1
AT5G64190	-1.25	-	NA	NA
AT5G44540	-	-2.08	NA	Tapetum specific protein TAP35/TAP44
AT4G32785	-	-1.62	NA	NA
AT4G28005	-	-1.27	NA	NA
AT1G23610	-	-1.29	NA	NA
AT3G43420	-	-1.17	NA	NA
AT2G46840	-	1.41	<i>DUF4</i>	Member of the plant-specific DUF724 protein family
AT4G35025	-	1.11	NA	NA
AT1G07330	-	1.93	NA	NA
AT5G66340	-	2.13	NA	NA
AT5G53205	-	-2.40	NA	NA
AT5G41390	-	1.00	NA	PLAC8 family protein

3 DISCUSSION

3.1 Effect of high relative air humidity on the responses to heat stress and combined drought and heat stress

Heat stress lowers the relative air humidity if there is no water supplemented to the ambient atmosphere. This scenario is frequently occurring in natural climate conditions and is exerted in regular heat-stress studies in plant research. Consequently, plants suffer not only from heat stress, but also from the additional water deficit stress in air. To separate temperature and ambient water-deficit impacts, heat stress responses of *Arabidopsis* were explored in this study in both “classical” setting and by eliminating the additional water deficit stress *via* supplementing the ambient air with additional humidity. In addition, drought stress, as one of the most important water deficit stresses, occurs simultaneously with heat stress in the field. Therefore, the same strategy was used to explore the effect of high vs. regular low relative air humidity in response to combined drought and heat stresses.

3.1.1 High relative air humidity aggravates heat stress responses and induces specific transcriptional changes in response to heat stress

High temperature enhances transpiration to minimize the heat damage by transpiration-mediated leaf cooling (Crawford *et al.*, 2012). However, high relative air humidity prevents the transpiration-cooling and in turn aggravates the heat damage (Taiz and Zeiger, 2006). Transcriptome analysis revealed that heat stress with high relative air humidity (H HrH) resulted in a larger number of differentially expressed genes as compared to heat with low relative air humidity (H LrH) (Figure 6). Among these genes, 342 out of 1318 differentially expressed genes (26%) under H HrH were also detected in response to other more severe heat stress experiments at higher temperature or longer duration (data from Genevestigator) (Figure 12). In addition, the regular heat-responsive genes showed stronger changes in response to H HrH (Table 3). The heat responsive marker genes *HSFs* and *HSPs* in particular

also showed stronger changes under H HrH than under H LrH (Figure 10). These results indicate that high relative air humidity aggravates the heat stress responses also at the transcriptional level.

Previous studies have shown that regular heat stress induced transcriptional changes involved in various functional categories: *cellular metabolism*, *signal transduction*, *stress responses* and *transcription factors* (Lim *et al.*, 2006; Matsuura *et al.*, 2010; Mittal *et al.*, 2012; Zhang *et al.*, 2012). Similarly, heat stress with high relative air humidity also resulted in differentially expressed genes associated with these biological processes (Figure 8 and Figure 9). Although no specific functional categories were enriched under H HrH, high relative air humidity specifically deregulated 344 genes (26%) which were not related to regular heat stress in this or other published studies in response to heat stress (Table 4 and Table S1).

Among these genes, seven were associated with carbohydrate metabolism including sucrose degradation, raffinose biosynthesis and starch degradation. Inositol oxygenases (*MIOXs*) catalyze the oxidation of *myo*-inositol (Alford *et al.*, 2012) and the specific reduction of *MIOX1* indicates an overaccumulation of *myo*-inositol under H HrH. Raffinose biosynthesis is initiated by *GoISs* using UDP-galactose and *myo*-inositol as substrates. The activated galactose moieties donated by galactinol are subsequently added to sucrose by *RSs* to produce the trisaccharide raffinose and liberating *myo*-inositol. Thus the overaccumulation of *myo*-inositol may enhance raffinose biosynthesis (Panikulangara *et al.*, 2004; Egert *et al.*, 2013). In line with these changes, the genes encoding *GoIS4* and *RS6* were exclusively upregulated under H HrH, suggesting their specific roles in overaccumulation of raffinose as a signaling molecule, a potential osmolyte or an antioxidant under H HrH. On the other hand, the starch metabolism was also disturbed. Two genes, *BAM5* and *SEX4*, involved in starch degradation were detected to be specifically downregulated under H HrH. Starch is the major carbohydrate reserve in plants and the starch granules are composed of the glucose homopolymers amylose and amylopectin. Two enzymes, α -amylase, but primarily β -amylase could potentially produce maltose through hydrolysis of amylopectin and amylose. In

Arabidopsis, *BAM5* was a catalytically active cytosolic enzyme (Monroe and Preiss, 1990; Monroe *et al.*, 1991; Wang *et al.*, 1995). It has been shown that expression of *BAM5* is induced by sugars and the activity of *BAM5* is modulated under various light conditions (Caspar *et al.*, 1989). In addition, the glucan phosphatase *STARCH EXCESS4 (SEX4)* is a starch phosphatase which is essential for reversible starch phosphorylation in order to allow progressive starch degradation and its absence leads to a dramatic accumulation of starch in *Arabidopsis* (Kötting *et al.*, 2009; Silver *et al.*, 2014). Thus, downregulation of *BAM5* and *SEX4* suggests their specific role in reducing the starch degradation under H HrH. Altogether, these exclusively transcriptional changes associated with carbohydrate metabolism suggest their specific roles in leading to the upregulation of free carbohydrates including *myo*-inositol and raffinose, but downregulation of the condensed form starch. In fact, similar changes are known from metabolic studies in regular heat stress experiments (Kaplan *et al.*, 2004) or were predicted from the transcriptional profiles in response to regular heat stress (Table S3 and Table S4; Lim *et al.*, 2006), although invoking different genes than by H HrH conditions (e.g. *MIOX2*, *GoIS1* and *RS2*).

The plant cell wall is mainly composed of polysaccharides including cellulose, hemicelluloses and pectins. Cellulose synthase and cellulose synthase-like proteins are responsible for cell wall synthesis. In *Arabidopsis*, cellulose synthase-like genes are classified into six subfamilies based on the sequence similarity to cellulose synthase genes (*CSLA-E* and *CSLG*) (Richmond and Somerville, 2000). Among them, *CSLAs* have mannan synthase activity and synthesize the backbone of mannan, which is proposed to crosslink with cellulose and hemicellulose in the context of cell wall architecture. Therefore, exclusively upregulated *CSLA14* and downregulated *CSLG1* indicate their specific roles in modulating the cell wall components. In addition, the most abundant hemicellulose is xyloglucan which can crosslink to cellulose to restrain cell expansion. *XTHs* catalyze the cleavage of xyloglucan-cellulose crosslinks and are proposed to function in cell expansion and in turn impact plant growth and development (Campbell and Braam, 1999). It has been shown that repression of *XTH22* and *XTH30* causes

a reduction of the organ size (Claisse *et al.*, 2007) and overexpression of *XTH33* results in bigger leaves and wider stems (Ndamukong *et al.*, 2009). Together with the expansin genes and expansin-like genes which are known to have a cell wall-loosening activity and to be involved in cell expansion (Sampedro and Cosgrove, 2005), the exclusively upregulated *XTHs*, *EXP8* and *EXPL3* as well as the downregulated *EXP23* suggest their specific roles in modulating the cell wall properties and cell expansion under H HrH, which would be altered towards loosening the cell wall according to these transcriptional changes. Actually, cell wall modification was predicated from the transcriptional profiles in response to regular heat stress by invoking different genes (e.g. *EXPA10*, *EXPA15* and *XTH17*) (Table S3 and Table S4; Lim *et al.*, 2006; Prasch and Sonnewald, 2013).

Transcription factors play important regulatory roles in response to adverse environmental conditions. High relative air humidity results in specific changes of transcription factors *AP2/ERF*. As one of the largest transcription factor families, the *AP2/ERF* gene family can be classified into four subfamilies: *AP2*, *RAV*, *DREB* and *ERF*. It has been shown that the expression of *DREB26* is decreased in response to regular heat stress. Overexpression of *DREB26* results in early death at the vegetative stage and it is therefore impossible to further characterize their stress tolerance (Krishnaswamy *et al.*, 2011). In contrast, *DREB26* was specifically upregulated under H HrH, suggesting its specific regulatory role in response to H HrH.

In addition, other specific changed genes involved in stress responses, protein modification and other biological processes under H HrH are not well characterized, but these changes indicate their specific contributions in response to H HrH.

3.1.2 High relative air humidity shifts the combined stress responses from a predominant drought effect to a heat effect and induces specific transcriptional changes in response to combined drought and heat stresses

Previous studies have shown that drought effects predominantly contribute to combined drought and heat stresses. High relative air humidity suppresses transpiration and in turn alleviates the drought effect, but aggravates the heat effect in response to combined drought and heat stresses. Accordingly, a smaller number of drought-responsive genes, but a larger number of heat-responsive genes were detected under DH HrH than that under DH LrH in our study (Figure 15). In addition, the drought-responsive marker genes showed weaker changes, but heat-responsive marker genes showed stronger changes under DH HrH than that under DH LrH (Figure 16). Therefore, high relative air humidity shifts the combined stress responses from a predominant drought effect to a heat effect.

It has been shown that combined drought and regular heat stress induces transcriptional changes in various functional categories: *cellular metabolism*, *signal transduction*, *stress responses* and *transcription factors* (Rizhsky *et al.*, 2002; Rizhsky *et al.*, 2004; Prasch and Sonnewald, 2013). Similarly, combined drought and heat stress with high relative air humidity also resulted in differentially expressed genes associated with these biological processes (Figure 13 and Figure 14). Although no specific function categories were enriched under DH HrH, high relative air humidity specifically results in 142 differentially expressed genes (4%) in response to combined drought and heat stresses (Table 5 and Table S2). Among these changes, one gene encoding *KCS19* is associated with very long chain fatty acid biosynthesis. In plants, very long chain fatty acids are important biological components of lipids, such as phospholipids present in cell membranes and cuticular waxes deposited on leaf surfaces. The 3-ketoacyl-CoA synthases (*KCSs*) catalyze the first rate-limiting step of the fatty acid chain elongation. *KCS19* is specifically involved in very long fatty acid synthesis in

siliques and was differentially regulated under cold stress and osmotic stress (Joubès *et al.*, 2008). In contrast to previous studies, the expression of *KCS19* was also detected in rosettes and exclusively downregulated under DH HrH. This suggests a specific restriction of fatty acid chain elongation and may in turn reduce the wax component of leaf surfaces to improve the non-stomatal water loss in response to DH HrH. Actually, fatty acid elongation was also modified under DH LrH by invoking the different isoforms, such as *KCS3* and *KCS8* (Rizhsky *et al.*, 2004; Prasch and Sonnewald, 2013). In addition, a number of exclusively responsive genes under DH HrH were identified, but not well characterized, which may lead to specific responses to combined drought and heat stress with high relative air humidity.

In conclusion, high relative air humidity aggravates heat stress responses and in turn enhances the contribution of heat effects, but alleviates the contribution of drought effects in response to combined drought and heat stresses in comparison to low relative air humidity. In addition, high relative air humidity induces exclusively changed genes under H HrH and DH HrH. Further studies involving *Arabidopsis* mutants or overexpression lines with these genes may lead to a better understanding of specific effects of high relative air humidity in response to heat stress and combined drought and heat stresses.

3.2 The role of major *PIP2s* in leaves under well-watered condition and water stresses

Aquaporins facilitate water transport through membranes and show a high multiplicity of isoforms with 35 homologs, which can be further divided into four classes on the basis of their sequence homologies and subcellular localization in *Arabidopsis*. The plasma membrane intrinsic proteins *PIPs* with the two phylogenetic subfamilies *PIP1s* and *PIP2s* are localized in the plasma membrane and are considered to be important for transcellular water transport as well as water homeostasis in plants. Among these *PIPs*, *PIP2;1* and *PIP2;2* are extensively expressed in leaves and roots. They represent 39% and 34% of the total *PIPs* at the protein level in leaves and roots, respectively (Monneuse *et al.*, 2011). In *pip2;1 pip2;2*,

microarray-based transcriptome analysis revealed that there was no significant changes of the retained *PIPs* in comparison to wild type at the transcriptional level (Figure 24 and Figure 25), yet Western blot analysis revealed an additional, up to 50% repression of PIP1s at the protein level in both leaves and roots (Da Ines, 2008). Taking together these repression and the relative amount of PIPs estimated from a proteomic study of three-week-old leaves and seven-week-old roots (Monneuse *et al.*, 2011), around 60% and 40% of the total PIP proteins were expected to be repressed in leaves and roots, respectively, in *pip2;1 pip2;2*. Preliminary proteomic studies also indicated that no other *PIP* isoforms were significantly upregulated (Jin Zhao and Chen Liu, unpublished results from our laboratory). Therefore, there was no significant effect on *PIPs* expression and abundance as compensation for the loss of *PIP2;1* and *PIP2;2*. Activation of PIPs through phosphorylation or any other post-translational modification (Chaumont *et al.*, 2005b; Luu and Maurel, 2005) could be another way to compensate the loss of PIP2;1 and PIP2;2. However, it is unlikely that the function of these two major PIPs and other repressed isoforms in roots was fully compensated, since the root hydraulic conductivity was decreased in *pip2;1 pip2;2* (Péret *et al.*, 2012).

The functions of PIP2;1 and PIP2;2 for cell water permeability have been demonstrated by measurements of bursting rates in *Xenopus* oocytes (Kammerloher *et al.*, 1994). Both *pip2;1* and *pip2;2* T-DNA insertion mutations have resulted in reduction of hydraulic conductivity in roots and root cortex cells, respectively (Javot *et al.*, 2003; Péret *et al.*, 2012). The hydraulic conductivity of rosettes is also reduced in *pip2;1* single mutant under darkness (Prado *et al.*, 2013). However, the impact of the loss of *PIP2;1* and *PIP2;2* in leaves was surprisingly weak when physiological and molecular parameters were assessed in detail.

3.2.1 Marginal impact of the loss of major *PIP2s* in leaves under well-watered condition

The leaf water status is determined by root water transport (input) and transpiration demand (loss). In leaves, water is radially transported from the xylem to the mesophyll

across the bundle sheath cells. Bundle sheath cells constitute a layer with suberin deposits encircling the entire vascular tissue of the leaf, except at the leaf edges, to render the apoplast impermeable to xylem sap. They are suggested to play a critical role in the regulation of leaf hydraulic conductivity *via* the activity or abundance of aquaporins (Sack and Holbrook, 2006; Leegood, 2008; Buckley, 2015). It has been shown that the bundle sheath cells sensed the stress signalling within the xylem sap and in turn reduced leaf hydraulic conductivity mediated by downregulation of their aquaporin activity that consequently resulted in the decline of leaf water potential, which may lead to stomatal closure and reduction of transpiration rates (Shatil-Cohen *et al.*, 2011). In *Arabidopsis*, *PIP2;1* and *PIP2;2* are highly expressed in veins, especially *PIP2;1* is expressed in bundle sheath cells (Da Ines, 2008; Da Ines *et al.*, 2010; Prado *et al.*, 2013). Therefore, loss of functions of *PIP2;1* and *PIP2;2* in *Arabidopsis* may eventually reduce the leaf gas exchange. However, the transpiration rate and the stomatal conductance to water vapor were not significantly reduced in *pip2;1 pip2;2* in comparison to the wild type, but had a tendency to be reduced under well-watered condition (Figure 22). This tendency was getting more obvious when the root hydraulic conductivity was further restricted by the additional knockout of the root-specifically expressed *PIP2;4* or when the transpiration demand was further enhanced by reducing the relative air humidity to 20% (Figure 22). Similarly, Ehlert *et al.* (2009) had shown that reduction in root hydraulic conductivity had no effect on transpiration rates and stomatal conductance under conditions with low transpiration demand, but induced stomatal closure after increasing the evaporation demand (Ehlert *et al.*, 2009). Several other studies have also shown that antisense plants with decreased NtAQP1 or AtPIP1s expression reduced the transpiration rate and leaf water potential at well-watered condition with high transpiration demand (Siefritz *et al.*, 2002; Sade *et al.*, 2014). In addition, the antisense plants with reduced AtPIP1s and AtPIP2s displayed no effect on stomatal conductance, transpiration rate, plant hydraulic conductance and leaf water potential under well-watered condition with low transpiration demand (Martre *et al.*, 2002). In agreement with these studies, our studies have demonstrated that *PIP2;1* and *PIP2;2* as two ubiquitously and

highly expressed aquaporins play a role in leaf water relations, but their contribution to the leaf water status is dependent on both the transpiration demand and root water transport. To substantiate this hypothesis, more gas exchange measurements should be performed to confirm the tendency of different transpiration rates and stomatal conductance of water vapor in *pip2;1 pip2;2* in comparison to the wild type under well-watered condition, yet dependent on the relative air humidity. In addition, the leaf water potential and the leaf hydraulic conductance should be measured, which are expected to be reduced in *pip2;1 pip2;2* in comparison to the wild type, if the functional interpretation of the role of PIP2;1 and PIP2;2 were correct.

The water taken up from roots is not only lost to the atmosphere through transpiration of leaves (Sack and Holbrook, 2006), but a small portion of leaf water is also used to support expansion growth (Pantin *et al.*, 2012). Therefore, loss of *PIP2;1* and *PIP2;2* may impact the plant growth. However, our experiments indicated that leaf growth was not hampered in *pip2;1 pip2;2*. Kaldenhoff *et al.* (1998) also found that antisense plants that reduced the PIP1s had no effect on leaf growth, but root growth was enhanced (although this was not reproduced in other instances of knockdown or knockout plants) (Kaldenhoff *et al.*, 1998). These authors had suggested that the enhanced root growth compensated the reduced cellular water permeability to further support normal leaf growth. In contrast to this study, loss of PIP2;1 and PIP2;2 had no impact on root growth, but other impacts in *pip2;1 pip2;2* were indicated by transcriptional and metabolic analyses. Leaf expansion growth is driven by cell turgor. Thus, water transmembrane transport into expanding cells is required (Nonami and Boyer, 1993). To maintain the normal expansion growth in *pip2;1 pip2;2*, osmotic water potential could be reduced by depositing solutes to sustain water influx into expanding cells (Fricke and Peters, 2002). Transcriptional analysis showed that *QQS* was upregulated in *pip2;1 pip2;2*, which indicated that soluble sugars might overaccumulate in the cytosol (Li *et al.*, 2009). Zhao (2013) found a number of putative overaccumulated disaccharides and trisaccharides in *pip2;1 pip2;2* by non-targeted FT-ICR-MS (Zhao, 2013).

However, only a twofold enhancement of raffinose and of three unknown metabolites, which were co-regulated with QQS, had been detected by targeted GC-MS (Figure 29). Thus, the overaccumulation of these metabolites might not be so efficient in osmotic regulation, yet other molecules may have escaped the detection by these methods. In addition, leaf expansion growth is also dependent on cell wall relaxation. Transcriptional analysis found that genes associated with the functional category cell wall (*AGP5*, *EXPA23* and *PME17*) were downregulated in *pip2;1 pip2;2* in comparison to the wild type. Among these genes, *PME17* functions in demethylation of esterified homogalacturonan, a primary cell wall component, to allow the formation of a rigid gel by intermolecular Ca^{2+} bonds linking the free carboxylic acid groups. Thus, *PMEs* play an important role in cell wall stiffening (Hongo *et al.*, 2012). In turn, downregulation of *PME17* may result in cell wall relaxation. In addition, both *AGPs* and *EXPs* function in cell expansion. In particular, *EXPs* exerts acid-dependent wall-loosening for cell elongation (Willats and Knox, 1996). Thus, downregulation of *AGP5* and *EXPA23* may induce the cell wall rigidity. Although the final consequence of the cell wall plasticity is still obscure due to the potentially antagonistic effects of these differentially expressed genes, these changes indicate that the cell wall plasticity may be remodeled to support the normal growth in *pip2;1 pip2;2*.

In conclusion, loss of function of *PIP2;1* and *PIP2;2* marginally impacts the leaf water relations, but has no effect on leaf growth under well-watered condition. However, it is possible that these two major *PIPs* are relevant in the context of water stresses.

3.2.2 Marginal impact of loss of major *PIPs* in leaves in response to water stresses at molecular level

During drought stress and heat stress, two of the most important water stresses, plant water relations are regulated through changes in abundance of aquaporins (Maurel *et al.*, 2008). The expression of *PIPs* is generally downregulated in leaves under drought stress except for *PIP1;4* and *PIP2;5* (Figure 19), which is in agreement with previous studies (Alexandersson *et*

al., 2005; Alexandersson *et al.*, 2010). The downregulation of *PIPs* in leaves, especially in bundle sheath cells, would lead to stomata closure to avoid excess water loss when the root water supply is restricted under drought stress in accordance to the consideration of Shatil-Cohen *et al.* (2011). However, Martre *et al.* (2002) and our results showed that the repression of expression of *PIPs* is not sufficient to reduce the transpiration rate and stomata aperture under well-watered condition or drought stress with low transpiration demand as compared to the wild type (Martre *et al.*, 2002). This suggests that the repression of *PIPs* is a strategy of plants in response to drought stress, but not related to transpiration regulation. Furthermore, our results showed that the drought-responsive genes in wild type as compared to control condition were generally less deregulated in *pip2;1 pip2;2* (Table 9), suggesting loss of *PIP2;1* and *PIP2;2* alleviated the drought responses at transcriptional level. Rae *et al.* (2011) found that the transcription factor *RAP2.4B* positively regulated the expression of *PIPs*. *RAP2.4B* was induced by heat stress, which indicated that *PIPs* may be upregulated in response to heat (Rae *et al.*, 2011). In agreement with this study, the expression of *PIPs* were generally upregulated under regular heat stress except for *PIP1;4*, *PIP2;5* and *PIP2;8*. In addition, *PIPs* were also generally induced to a similar expression level at H HrH, when the additional water deficit in air was eliminated and the transpiration was restricted (Figure 19). These results suggest that the heat effect predominantly contributes to the upregulation of *PIPs* and the upregulation of *PIPs* is irrespective to the transpiration under heat stress. To further explore the functions of upregulated major *PIPs* under heat stress, transcriptional changes in response to heat stress in *pip2;1 pip2;2* were examined. *PIP2;1* and *PIP2;2* are highly expressed in leaves and loss of these two major *PIPs* were expected to aggravate the heat stress responses. Surprisingly, heat-responsive genes of the wild type were changed to a similar extent in *pip2;1 pip2;2* under either H LrH or H HrH as compared to control condition (Table 10 and Table 11). Thus, the role of upregulation of *PIP2;1* and *PIP2;2* in response to heat stress cannot be deduced from this finding. One possibility is that the excited activities of the remained *PIPs* (e.g. *PIP1;2*, *PIP2;6* and *PIP2;7*),

which are expressed in veins, may partially complement the loss-of-function of *PIP2;1* and *PIP2;2*. On the other hand, loss of *PIP2;1* and *PIP2;2* may only delay the optimal adjustment of leaf water relations, but not determine the final leaf water status. To support this hypothesis, several studies have shown that the regulation of *PIPs* expression responded quickly to changing environmental conditions (Siefritz *et al.*, 2004; Levin *et al.*, 2007; Caldeira *et al.*, 2014b; Caldeira *et al.*, 2014a). Rae *et al.* (2011) also showed that transcription factor *RAP2.4B*, which is targeted to *PIP* promoters, was highly induced after heating for 2 h, but started to decrease after heating for 6 h. So the dynamic changes of the water relations after heating could be more interesting to evaluate the *PIPs* functions. Therefore, regulation of *PIPs* along with the time after heating should be examined. Then the dynamic changes of leaf water potential and hydraulic conductivity should be measured in *pip* mutants and wild type to assess the functions of *PIPs* in regulation of water relations under heat stress. Furthermore, the dynamic changes at transcriptional and metabolic levels along with the time after heating could be interesting to evaluate other impacted biological processes due to loss of *PIPs* in response to heat stresses.

Drought stress and heat stress have opposite effects on the regulation of expression of *PIPs*. Therefore, it was interesting to study the regulation of *PIPs* under combined drought and heat stresses. Previous studies have shown that drought effects predominantly contributed to the response to a combined drought and regular heat stress scenario (Rizhsky *et al.*, 2004). In agreement with these studies, differential regulation of *PIPs* under DH LrH was similar to that under drought stress (Figure 19). However, high relative air humidity enhanced the heat stress responses and in turn aggravated the heat effect, but alleviated the drought effect (see 3.1). Therefore, the differential regulation of *PIPs* under DH HrH generally tended to be shifted from drought-related, suppressive effects to heat-related inductive responses (Figure 19). Among these *PIPs*, *PIP2;1* and *PIP2;2* were downregulated under DH LrH, similar to the situation under drought stress. Therefore, loss of *PIP2;1* and *PIP2;2* under DH LrH was expected to have impacts similar to those under drought stress. In agreement with our

expectation, the DH LrH-responsive genes were generally less deregulated in *pip2;1 pip2;2* than in the wild type, which was also found in the *pip* double mutant under drought stress (Table 9 and Table 13). In addition, *PIP2;1* and *PIP2;2* were not changed under DH HrH (Figure 19) and the DH HrH-responsive genes of the wild type showed similar changes in *pip2;1 pip2;2* (Table 12). Taken together, the regulation of *PIPs* under combined drought and heat stresses is determined by the predominant effect to allow optimal adjustment of the leaf water status under combined, yet antagonizing effects (Guyot *et al.*, 2012).

On the other hand, marginal changes were detected at the transcriptional level in *pip2;1 pip2;2* as compared to the wild type under various water stresses (Figure 30 and Table 14-18). Among these genes, *QQS* was upregulated in *pip2;1 pip2;2* under all water stresses, suggesting that soluble sugars might be overaccumulated in the cytosol to regulate the osmotic potential (Li *et al.*, 2009). In addition, cell wall modification was regulated by invoking different genes under various water stresses. The gene encoding *FUCOSYLTRANSFERASE 4 (FUT4)* functions in fucosylation of arabinogalactan proteins in leaves (Tryfona *et al.*, 2014) and was downregulated under drought stress, suggesting a reduced mechanical strength of the cell wall (Reiter *et al.*, 1993). The cell wall-associated genes *CELLULOSE SYNTHASE-LIKE A1 (CSLA01)*, which is involved in biosynthesis of mannan polysaccharides in the plant cell wall (Liepman *et al.*, 2007) and *LEUCINE-RICH REPEAT/EXTENSIN 1 (LRX1)*, which functions in cell expansion (Baumberger *et al.*, 2003) were upregulated under DH LrH. These results suggest that the reduction of osmotic potential by overaccumulation of soluble sugars may enhance the driving force of water influx into cells and in turn support normal cell growth assisted with enhanced cell extensibility by modification of cell wall components in response to water stresses when loss of PIP functions.

In conclusion, our results revealed that loss of *PIP2;1* and *PIP2;2* slightly reduce the transpiration water loss in leaves under well-watered condition and this reduction is dependent on root water supply as well as leaf water demand. These findings were

consistent with previous studies which showed that low relative air humidity increased the leaf hydraulic conductivity (Levin *et al.*, 2007) and that drought stress mimicked by xylem-fed ABA reduced the leaf hydraulic conductivity (Shatil-Cohen *et al.*, 2011) mediated by regulation of aquaporins. In addition, loss of PIP2;1 and PIP2;2 had no impact on leaf growth. Kaldenhoff *et al.* (1998) had found that improved root growth compensated the reduced root hydraulic conductance to support the normal growth in *Arabidopsis PIP1*-antisense plants. In contrast, root growth was not impacted in *pip2;1 pip2;2*, but the cellular osmotic potential and cell wall plasticity could be modified to support the normal growth. On the other hand, *PIPs* were deregulated under various water stresses. Our results showed that the expression of *PIPs* were downregulated under drought stress as well as DH LrH when drought stress is the predominant effect, and loss of PIP2;1 and PIP2;2 alleviated the stress responses based on the lowered transcriptional deregulation in comparison to wild type. In contrast, the expression of *PIPs* was upregulated under heat stress, irrespective of differences in relative air humidity. But the regulation of *PIP* expression was relatively shifted towards a heat effect along with the aggravated heat stress under combined drought and heat stress with high relative air humidity. Surprisingly, loss of PIP2;1 and PIP2;2 had no impact on the response to heat stress and combined drought and heat stress with high relative air humidity. Furthermore, loss of PIP2;1 and PIP2;2 may result in osmotic potential regulation and cell wall modification to regulate the water status under water stresses, and these changes may compensate the loss of the functions of PIP2;1 and PIP2;2. However, this compensation was still weak, especially under heat stress responses when the two major *PIPs* were upregulated. We speculate that the upregulation of *PIPs* may be a fast response to heat stress and play a critical role in speed up the water homeostasis after heating. Therefore, the dynamic changes in response to heat should be a focus of future research.

4 MATERIALS AND METHODS

4.1 Materials

4.1.1 Plant materials

Insertion lines and wild-type plants used in this study were *Arabidopsis thaliana* ecotype Columbia (Col-0). Information of *AtPIP2;1*, *AtPIP2;2* and *AtPIP2;4* T-DNA insertion lines were obtained by screening the publicly accessible SIGnAL T-DNA Express database of the SALK Institute (<http://signal.salk.edu/cgi-bin/tdnaexpress>) (Alonso *et al.*, 2003). The seeds were purchased from the Nottingham *Arabidopsis* Stock Center (NASC) or from the *Arabidopsis* Biological Resource Center (ABRC, Ohio state University, USA, <http://www.biosci.ohiostate.edu/pcmb/Facilities/abrc/abrchome.htm>). The loss-of-function mutants *pip2;1-2*, *pip2;2-3* and *pip2;4-1* were verified by RT-PCR at the cDNA level (Das Ines, 2008). The double mutant *pip2;1 pip2;2* and the triple mutant *pip2;1 pip2;2 pip2;4* used in this study were generated by crossing and verified by genotyping at the DNA level and by RT-PCR at the cDNA level (Da Ines, 2008).

4.1.2 Chemicals, buffers and media

Chemicals were purchased from Sigma and Roth at the highest purity available. Typical solutions, buffers and media were prepared according to common protocols used in molecular biology. The preparation of special media and solutions is described in the corresponding methods.

4.2 Methods

4.2.1 Methods of physiological characterization

4.2.1.1 Plant growth condition

Arabidopsis thaliana plants (Col-0, *pip2;1 pip2;2* and *pip2;1 pip2;2 pip2;4*) were grown on soil or *in vitro* cultures in a growth chamber with the following environmental parameters: 11 h/13 h light/dark cycle, 150-200 $\mu\text{mol m}^{-2} \text{s}^{-1}$ light intensity, 22-23°C temperature and 60% relative air humidity.

For plant growth on soil, seeds were placed on the pots (TO6D, 6 × 4.6 cm, Pöppelmann, Germany) filled with a 8 : 1 soil (Floragard B seeds, Germany) : quartz sand (Interseroh, Germany) mixture. For plant growth on *in vitro* cultures, seeds were surface-sterilized with 90% ethanol on filter papers in the sterile hood. This procedure was repeated twice after the seeds got completely dry. Then the sterile seeds were placed on the square Petri dishes (120 mm x 120 mm x 17 mm, Greiner bio-one, Germany) containing 70 ml ½ MS (Murashige & Skoog Medium including Vitamins, Duchefa Biochemie, Germany) medium with 1% sucrose and 0.5% (w/v) Gelrite (Duchefa Biochemie, Germany). The plates were arranged vertically in a rack to ensure root growth along the medium surface. In all cases, seeds were vernalized at 4°C in the darkness for two days to synchronize germination and were then placed in the growth chamber.

4.2.1.2 Growth measurements

Plant growth was observed and photographed after two weeks growth on ½ MS medium or after four weeks growth on soil. Five to seven detached rosettes and roots grown on ½ MS medium were pooled as one replicate and six biological replicates of fresh weight were measured. The areas of six individual rosettes grown on soil were measured by Image J (Version 1.46). Means \pm standard deviation (SD) were calculated.

4.2.1.3 Gas exchange measurements

Gas exchange measurements of four-week-old plants grown on soil were assayed using GFS-3000 portable gas-exchange system fitted with a special cuvette for *Arabidopsis* 3010-A (WALZ, Germany) in collaboration with Barbro Winkler (Research Unit Environmental Simulation, Helmholtz Zentrum München, Germany). The air flow to the cuvette was set at 700 mmol s⁻¹. During the measurements, the absolute CO₂ concentration, cuvette temperature, and light intensity in the cuvette were set at 390 ppm, 23°C and 350 μmol m⁻² s⁻¹, respectively. The relative air humidity was progressively changed at 20%, 40%, 60% and 75%. The transpiration rate, stomata conductance of water vapor, net photosynthesis and the internal CO₂ concentration in rosettes were recorded every 30 s for 8 min and the values of at last 3 min at each rH setting were averaged. Means ± SD were calculated (n = 8) and *p*-values were determined by the Student's *t* test.

4.2.1.4 Carbon isotope composition measurements

The measurements of carbon isotope composition were performed in collaboration with Franz Buegger (Institute of Soil Ecology, Helmholtz Zentrum München, Germany). Three four-week-old rosettes grown on soil were pooled and ground in the liquid nitrogen at 30 frequency s⁻¹ for 2 min 30 s using the mixer mill MM 400 (Retsch, Germany). The leaf powder was aliquoted into 2 ml Eppendorf tubes and was freeze-dried for 24 h using a Christ Alpha 1 – 5 Freeze drier (SciQuip, UK). Aliquots of 1.5 mg – 2.0 mg dry weight were transferred into tin capsules (3.3 × 5 mm, IVA Analysentechnik, Germany). Two replicates were required for each sample. Determination of total carbon and of ¹³C was performed in duplicates with an isotope ratio mass spectrometer (Delta V Advantage, Thermo Electron, Dreieich, Germany) coupled to an elemental analyzer (Euro EA, Eurovector, Milan, Italy). For calibration, a lab standard (acetanilide) and different international standards IAEA-CO-9 ($\delta^{13}\text{C}_{\text{V-PDB}} = -47.32\text{‰}$), IAEA-CH-7 ($\delta^{13}\text{C}_{\text{V-PDB}} = -32.15\text{‰}$) and IAEA-600 ($\delta^{13}\text{C}_{\text{V-PDB}} = -27.77\text{‰}$) were used. Means ± SD of three independent experiments including two to five biological

replicates for each experiment were calculated and *p*-values were determined by the Student's *t* test.

4.2.1.5 Relative water loss measurements

The relative water loss of rosettes was evaluated by measurements of the fresh weight of the detached rosettes. Whole rosettes were detached from four-week-old plants grown on soil, weighed and then left at room temperature (25°C, 55% rH) in a laminar flow bench with continuous ventilation. The rosettes were weighed every hour after being detached for five hours. The decline of the fresh weight was represented in percentage of the initial fresh weight. Three independent experiments were performed including measurements of three or four rosettes of each genotype for each experiment. Means \pm SD of three independent experiments were calculated and *p*-values were determined by the Student's *t* test.

4.2.2 Methods of transcriptome analysis

4.2.2.1 Plant growth conditions and water-deficit stress applications

For plant growth, the soil (Floragard B seeds, Germany) was mixed with quartz sand (Interseroh, Germany) in a ratio of 8:1 and poured into six-well packs (PL2838/48, 38 × 28 × 6 cm, Pöppelmann, Germany). The soil-sand mixture was pre-wetted with water and the seeds of three genotypes (Col-0, *pip2;1 pip2;2* and *pip2;1 pip2;2 pip2;4*) were sown on the surface of the soil. The seeds were vernalized at 4°C in the darkness for two days to synchronize germination and then were placed in the identical climate simulation chambers with well-defined operation and accurate climatic conditions including 11 h/13 h light/dark cycle, 200 $\mu\text{E m}^{-2} \text{s}^{-1}$ light intensity, 22°C temperature and 0.793 kPa vapor pressure deficit (in collaboration with the Environmental Simulation Research Unit, Helmholtz Zentrum München, Germany). Three-week-old plants were flooded with water up to 60% of the pot height for 15 min by an automatic flooding system (Zhao, 2013). After flooding, the plants used for drought stress (D) and combined drought and heat stresses (DH) were stopped

being watered and the soil moisture was regularly monitored. When the soil water content was decreased to $20.7 \pm 2.7\%$ of the initial water content after one week, heat stress was applied to both well-watered plants used for heat stress and drought-treated plants used for combined drought and heat stresses by increasing the temperature to 33°C for 6 hours from 11:00 a.m. to 5:00 p.m. (H LrH and DH LrH). In addition, increased temperature dramatically enhanced the vapor pressure deficit (VPD). In order to eliminate the effects of additional VPD enhancement associated with the increased temperature, additional air humidity supplementation accompanied by heat stress (84% rH at 33°C) was applied to both well-watered plants used for heat stress and drought-treated plants used for combined drought and heat stresses (H HrH and DH HrH). The plants used for control conditions were continuously watered (Control) (Table 19).

Table 19. Details of control condition and water stress conditions

	Control	H HrH	DH HrH
Water status	regular watering	regular watering	no watering
Temperature	22°C	33°C	33°C
Relative air humidity	70%	84%	84%
Vapor pressure deficit	0.793 kPa	0.793 kPa	0.793 kPa
Light/dark cycle	11 h/ 13h	11 h/13 h	11 h/13 h
Light intensity	$200 \mu\text{E m}^{-2} \text{s}^{-1}$	$200 \mu\text{E m}^{-2} \text{s}^{-1}$	$200 \mu\text{E m}^{-2} \text{s}^{-1}$
	D	H LrH	DH LrH
Water status	no watering	regular watering	no watering
Temperature	22°C	33°C	33°C
Relative air humidity	70%	37%	37%
Vapor pressure deficit	0.793 kPa	3.168 kPa	3.168 kPa
Light/dark cycle	11 h/13 h	11 h/13 h	11 h/13 h
Light intensity	$200 \mu\text{E m}^{-2} \text{s}^{-1}$	$200 \mu\text{E m}^{-2} \text{s}^{-1}$	$200 \mu\text{E m}^{-2} \text{s}^{-1}$

4.2.2.2 The arrangement of the replicates and harvest

Five replicates of each genotype were generated for each environmental scenario and were randomly distributed to exclude the position effects (Zhao, 2013). All of the samples were harvested after one-week drought stress (D) or/and six-hour heat stress (H and DH). The samples under control conditions (Control) were also harvested at the same time. During

harvesting, eight rosettes were pooled as one replicate, collected into plastic bags (4 oz. 118 ml, Whirl-Pak), immediately frozen in liquid nitrogen, and then stored at -80°C until use.

4.2.2.3 Isolation of the total RNA

The rosette samples were ground at 30 frequency s^{-1} for 2 min 30 s using the mixer mill MM 400 (Retsch, Germany) and then 90 mg – 100 mg powder were aliquoted into 2 ml Eppendorf tubes. The total RNA was extracted using the RNeasy plant mini kit (Qiagen, Hilden, Germany) applying a modified procedure. First, 900 μ l RLC Buffer were added into the sample tube immediately mixed well by vortexing. Then the homogenous solution was incubated at 600 rpm at 56°C for 3 min in a thermomixer. The mixture was transferred to QIAshredder (lilac) and centrifuged at 13000 rpm for 2 min. Then 600 μ l supernatant were transferred to a new 2 ml Eppendorf tube without disturbing the pellet and mixed well with 300 μ l ethanol by pipetting. The lysate was transferred into an RNeasy spin column (pink), centrifuged at 10000 rpm for 30 s and the flow-through was discarded. Then 350 μ l RW1 Buffer were added to the RNeasy spin column, centrifuged at 10000 rpm for 30s and the flow-through was again discarded. To avoid DNA contamination, DNase digestion was performed by applying 120 μ l DNase I stock solution (15 μ l DNase mixed with 105 μ l RDD Buffer) to the RNeasy spin column at room temperature for 25 min. Then 350 μ l RW1 Buffer were added to the RNeasy spin column and centrifuged at 10000 rpm for 30 s. Afterwards, 500 μ l RPE Buffer were added to the RNeasy spin column and centrifuged at 10000 rpm for 30 s. The flow-through was discarded and another 500 μ l RPE Buffer were added to the RNeasy spin column and centrifuged at 10000 rpm for 2 min. The RNeasy spin column was placed onto a new collection tube and then centrifuged at 10000 rpm for 1 min to remove the retained RPE Buffer. Afterwards, the RNeasy spin column was moved to a new 1.5 ml RNeasy-free tube and 30 μ l RNase-free H_2O were pipetted directly on the spin column membrane and centrifuged at 500 rpm for 10 s. The column was incubated at room temperature for 5 min and then centrifuged at 10000 rpm for 1 min. Another 30 μ l RNase-

free H₂O were pipetted to the spin column membrane and then centrifuged at 10000 rpm for 1 min. Finally, approximately 60 µl total RNA sample were collected.

4.2.2.4 RNA quality and quantity control

The quality and quantity of the total RNA was evaluated using an Agilent Bioanalyzer 2100 (Agilent Technologies, USA) and a Nanodrop ND-1000 spectrophotometer (Kisker-Biotech, Germany).

4.2.2.4.1 RNA 6000 Nano assay

All of the reagents including Agilent RNA 6000 Nano gel matrix, RNA 6000 Nano dye concentrate and RNA 6000 Nano marker were equilibrated to room temperature before use. In particular, the RNA 6000 Nano dye was protected from light. Several preparations needed to be done before experiments. Firstly, 500 µl Agilent RNA 6000 Nano gel matrix were added into a spin filter and centrifuged at 4000 rpm at room temperature for 10 min and then 65 µl filtered gel was aliquoted into a 0.5 ml RNase-free microfuge tube. Secondly, to avoid the decomposition of the RNA samples, the electrodes were cleaned by applying the electrode cleaner with 350 µl RNaseZAP for 1 min followed by 350 µl RNase-free H₂O for 5 min and then were left in air for 10 s for water evaporation on the electrodes before closing the lid. Thirdly, the base plate of the chip priming station was adjusted to position (C) and the adjustable clip was set to the top position and the plunger was positioned at 1 ml. Finally, the RNA ladder and the RNA samples were heat denatured at 70°C for 2 min before use.

Afterwards, the RNA 6000 Nano dye concentrate was vortexed for 10 s and spinned down in the microcentrifuge. Then 1 µl RNA 6000 Nano dye concentrate was added to the 65 µl filtered gel, mixed well by vortexing thoroughly and centrifuged at 14000 rpm at room temperature for 10 min. The new RNA Nano chip was placed on the chip priming station and 9.0 µl gel-dye mix was pipetted to the bottom of the well which was marked with ⑥. The chip priming station was closed and the plunger of the syringe was pressed down until it was

held by the clip. Thirty seconds later, the plunger was released and moved back to at least the 0.3 ml mark. After 5 s, the plunger was pulled back to the 1 ml position and the chip priming station was opened. Then 9.0 μ l gel-dye mix was pipetted to another two wells marked with **G**. Afterwards, 5 μ l RNA 6000 Nano marker was pipetted into each of the sample wells and also the well which was marked with the ladder symbol. Then 1 μ l RNA ladder was pipetted into the well which was marked with the ladder symbol and 1 μ l RNA sample was pipetted into each of the sample wells. The samples were mixed well horizontally using the bioanalyzer chip vortexer (IKA, Germany) at 2400 rpm at room temperature for 60 s. The chip was inserted into the Agilent 2100 Bioanalyzer and ran with the assay settings of Plant RNA Nano. After the assay was finished, the chip was immediately removed and the electrodes were cleaned by applying electrode cleaner with 350 μ l RNase-free H₂O for 5 min. The RNA samples with rRNA Ratio [25s/18s] values of 1.6 ± 0.2 and RNA Integrity Number (RIN) values of 7 ± 0.5 were chosen as good quality samples which were used for the microarray.

4.2.2.4.2 Nanodrop ND-1000 spectrophotometer

The Nanodrop ND-1000 spectrophotometer was chosen for checking RNA quality and quantity. Firstly, 1.5 μ l nuclease-free H₂O were pipetted on the loading area for initialization. RNA-40 was selected as the sample type and recording button was selected to save the results. After Blanking with 1.5 μ l nuclease-free H₂O, 1.5 μ l total RNA sample were loaded and measured. The RNA samples with both 260/230 ratio and 260/280 ratio more than two were selected as good quality samples and used for microarray analysis.

4.2.2.5 Agilent microarray analysis

Transcriptome analysis was performed using Agilent 8 \times 60 K microarrays followed the workflow of sample preparation and array processing (Figure 34).

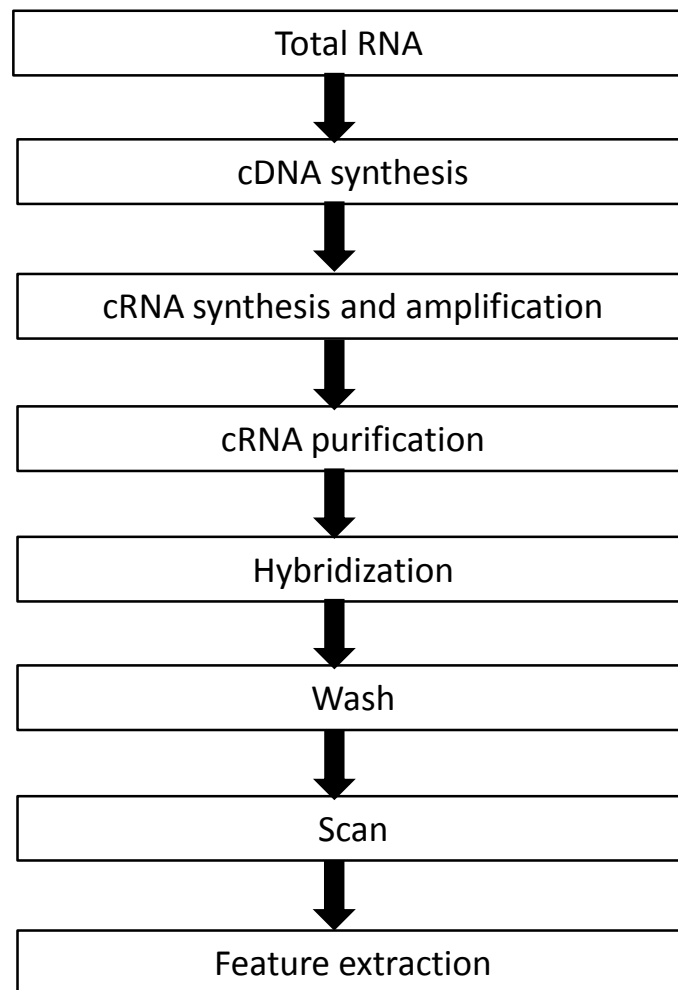


Figure 34. Scheme of sample preparation and array processing

4.2.2.5.1 One-color Spike Mix preparation

One-Color Spike Mix stock solution was vigorously mixed by a vortex mixer and was heated at 37°C for 5 min. The One-Color Spike Mix stock solution was vigorously mixed once again using a vortex mixer and was then briefly centrifuged. The first dilution was generated by mixing 2 µl of One-Color Spike Mix stock solution with 38 µl of Dilution Buffer, mixed thoroughly using a vortex mixer and then briefly centrifuged. The second dilution was generated by mixing 2 µl of the first dilution with 48 µl of Dilution Buffer, mixed thoroughly using a vortex mixer and again briefly centrifuged. The third dilution was created by mixing 2 µl of the second dilution with 38 µl of Dilution Buffer, mixed thoroughly using a vortex mixer and again briefly centrifuged.

4.2.2.5.2 Labeling reaction preparation

Two microliter of the third dilution of One-Color Spike Mix was pipetted into 100 ng of each total RNA sample. Then 1.8 μ l of T7 Promoter Primer Mix containing 0.8 μ l of T7 Promoter Primer and 1 μ l of Nuclease-free water were pipetted into the mix of spike dilution and total RNA. The mix was incubated in a circulating water bath at 65°C for 10 min to denature the primers as well as the templates and then was incubated on ice for 5 min. Afterwards, the 5 \times first strand buffer was prewarmed at 80°C for 5 min until the buffer components were resuspended. Then 4.7 μ l of cDNA Master Mix containing 2 μ l of 5 \times first strand buffer, 1 μ l of 0.1 M DTT, 10 mM dNTP mix and 1.2 μ l of AffinityScript RNase Block Mix were added into each sample tube and were gently mixed by pipetting. The mix was incubated in a circulating water bath at 40°C for 2 h followed by incubation at 70°C for 15 min and was then placed on ice for 5 min. Finally, 6 μ l of Transcription Master Mix containing 0.75 μ l of Nuclease-free water, 3.2 μ l of 5 \times Transcription Buffer, 0.6 μ l of 0.1 M DTT, 1 μ l of NTP mix, 0.21 μ l of T7 RNA Polymerase Blend and 0.24 μ l of Cyanine 3-CTP were added into each sample tube, gently mixed by pipetting and then incubated in a circulating water bath at 40°C for 2 h (Table 20).

Table 20. Preparation of Mix

	Component	Volume per reaction (μ l)
T7 Promoter Primer Mix	T7 Promoter Primer	0.8
	Nuclease-free water	1
cDNA Master Mix	5 \times First Strand Buffer	2
	0.1 M DTT	1
	10 mM dNTP mix	0.5
	AffinityScript RNase Block Mix	1.2
Transcription Master Mix	Nuclease-free water	0.75
	5 \times Transcription Buffer	3.2
	0.1 M DTT	0.6
	NTP mix	1
	T7 RNA Polymerase Blend	0.21
	Cyanine 3-CTP	0.24

4.2.2.5.3 Labeled and amplified RNA purification

RNeasy mini spin columns (Qiagen) were used for purification of the labeled and amplified cRNA samples. Firstly, 84 μl of nuclease-free water were added into each cRNA sample. Then 350 μl of RLT Buffer and 250 μl of ethanol were added into each sample tube and mixed thoroughly by pipetting. In total 700 μl of the cRNA sample were transferred into the RNeasy mini column and were centrifuged at 13000 rpm at 4°C for 30 s. Then 500 μl of RPE buffer were added into the RNeasy mini column after discarding the flow-through and were centrifuged at 13000 rpm at 4°C for 30 s. Another 500 μl of RPE buffer were added into the RNeasy mini column after discarding the flow-through and were centrifuged at 13000 rpm at 4°C for 60 s. To remove the remaining RPE buffer, the RNeasy mini column was transferred to a new collection tube and was centrifuged at 13000 rpm at 4°C for 30 s. Finally, 30 μl of RNase-free water were directly pipetted onto the RNeasy filter membrane and centrifuged at 13000 rpm at 4°C for 60 s after waiting for 60 s at room temperature to collect the cRNA sample.

4.2.2.5.4 cRNA quantification

The quantification of cRNA was assessed by the NanoDrop ND-1000 Spectrophotometer. Microarray measurement was selected and measured following the procedure described in 4.2.2.4.2. The yield and the specific activity of cRNA was calculated according to the formula of $(\text{Concentration of cRNA}) \times 30 \mu\text{l (elution volume)} / 1000 = \mu\text{g of cRNA}$ and $(\text{Concentration of Cy3} / \text{Concentration of cRNA}) \times 1000 = \text{pmol Cy3 per } \mu\text{g cRNA}$, respectively. The cRNA samples with more than 0.825 μg of the yield and at least 6 pmol Cy3 per μg cRNA of the specificity activity were used for hybridization.

4.2.2.5.5 Hybridization

The 10 \times Blocking Agent was incubated at 37°C for 5 min and then the Fragmentation mix was prepared for 8-pack microarray formats by mixing 600 ng of cRNA, 5 μl of 10 \times Blocking

Agent, Nuclease-free water to bring the volume to 24 μ l and 1 μ l of 25 \times Fragmentation Buffer. The Fragmentation mix was incubated at 60°C in a circulating water bath for exactly 30 min and was then cooled on ice immediately for 1 min. Then the hybridization mix was prepared by adding 25 μ l of 2 \times GE \times Hybridization Buffer HI-RPM into fragmentation mix, mixing well by pipetting, and then centrifuging at 13000 rpm at room temperature for 1 min. Afterwards, a new gasket slide was loaded into the Agilent SureHyb chamber base with the label facing up and 40 μ l of Hybridization mix were slowly dispensed in the middle of the gasket well. The array was slowly placed onto the gasket slide with the active side facing down. The cover of the SureHyb chamber was placed on the slides and hand-tightened using the clamps to assemble the chamber. The assembled chamber was vertically rotated to wet the gasket and assess the mobility of the bubbles and then incubated at 10 rpm at 65 °C for 17 h in the hybridization oven.

4.2.2.5.6 Microarray wash

The staining dishes, racks and stirs used for microarray wash should be carefully washed by rinsing with double-distilled water (ddH₂O) for five times. In particular, the staining dishes, racks and stirs used for Agilent Stabilization and Drying Solution were needed to be washed with acetonitrile for 5 min and then rinsed with ddH₂O for five times. The staining dishes, racks and stirs were left at room temperature for drying before use. Five staining dishes were filled in order with Wash Buffer 1 (Dish 1), Wash Buffer 1 (Dish 2), prewarmed Wash Buffer 2 (37°C, overnight; Dish 3), acetonitrile (Dish 4), and Stabilization and Drying Solution (Dish 5). Then the hybridization chamber was taken out of the oven and disassembled. The array-gasket sandwich was separated by grabbing the slides from their ends in Wash Buffer 1 (Dish 1). Then the array was immediately transferred to Wash Buffer 1 (Dish 2) and placed into the slide rack. One minute later, the slide rack was transferred to Wash Buffer 2 (Dish 3) for 1 min followed by washing in Acetonitrile for 10 s. Then the slide rack was transferred into Stabilization and Drying Solution (Dish 5) and was slowly moved out of the solution after 30 s.

4.2.2.5.7 Slide scan and figure extraction

The slides were scanned using the Agilent Microarray Scanner. The slides were placed into the slide holder with the Agilent barcode facing up. The slot number and Profile AgilentG3_GX_1Color were set for 8 × 60 K microarray scan. The scan settings were verified with the dye channel green, scan area (61 × 21.6 mm), scan resolution 3 μm as well as tiff 20 bit and then the scan was performed. Microarray data extraction was performed using the Agilent Feature Extraction Software with the extract set of GE1_1010_Sep10.

4.2.3 GC-MS measurements

Metabolite measurements using GC–TOF–MS were performed in collaboration with Dr. Martin Lehmann (Faculty of Biology, Ludwig-Maximilians-Universität München). The metabolites for measurements were extracted and derivatized using a modified method described by Roessner *et al.* (2001), Lisec *et al.* (2006) and Erban *et al.* (2007). 50 mg and 100 mg fresh weight of the rosettes were used for regular mode and concentrated mode measurement, respectively.

4.2.4 Statistical analysis

The gene expression analysis was done together with Dr. Elisabeth Georgii (Institute of Biochemical Plant Pathology, Helmholtz Zentrum München). Further analyses on data from targeted metabolome measurements and the integrative analysis were done by Dr. Elisabeth Georgii (Institute of Biochemical Plant Pathology, Helmholtz Zentrum München).

4.2.4.1 Gene expression analysis

The computational analysis of gene expression was done with the Bioconductor 2.13 software package limma, version 3.18.13 (Smyth, 2005). Firstly, the data were preprocessed by background correction and quantile normalization. Secondly, linear models were applied for all genes simultaneously to analyze treatment effects and genotype effects, respectively,

and to compute differential expression statistics for specific comparisons. For this purpose, transcriptomic measurements using microarrays from all three independent experiments were combined, accounting for the independent experiments as a random effect in the linear models. The knockout genes *PIP2;1*, *PIP2;2* and *PIP2;4* (AT3G53420, AT2G37170 and AT5G60660) were excluded from further analysis. For gene set enrichment analysis, differentially expressed genes with adjusted p-value smaller than 0.05 and absolute log₂ fold change greater than 1 were checked using MapMan3.5.1R2. For visualization, the fixed effects from the linear models (means of specific genotype-condition combinations) were subjected to dimension reduction *via* principal component analysis in R.

4.2.4.2 Metabolomic analysis

The targeted metabolomic data derived from GC-MS measurements were preprocessed by log₂ transformation and quantile normalization. Then a linear model analysis with LIMMA (Smyth, 2005) was performed, analogously to the gene expression analysis.

4.2.4.3 Integrative analysis

Samples applied for both transcriptomic and metabolomic measurements were selected and the corresponding data were corrected for batch effects of the independent experiments using LIMMA (Smyth, 2005). Then Spearman correlation tests between transcript and metabolite abundances were computed and FDR-adjusted in R. The significant associations (adjusted p-value<0.05) around specific genes of interest were visualized with Cytoscape, version 3.1.1.

4.2.5 Data mining from public expression data

The expression of heat stress with high relative air humidity responsive genes under regular heat stress was extracted *via* Genevestigator database (<https://www.genevestigator.com/gv/plant.jsp>). Eight regular heat stresses were selected

and their Genevestigator experiment IDs were AT-00645, AT-00500, AT-00120, AT-00402, AT-00387 and AT-00439.

4.2.6 Co-expression analysis

Differentially expressed genes with adjust p-value smaller than 0.05 and absolute log₂ fold change greater than 1 in *pip2;1 pip2;2* and *pip2;1 pip2;2 pip2;4* under various environmental scenarios were applied for co-expression analysis to explore the functions of uncharacterized genes *via* ATTED-II databases (<http://atted.jp>).

SUPPLEMENTARY MATERIALS

Table S1. Specifically altered genes that were lowly expressed and even downregulated in rosettes of wild type under H HrH compared to control condition (green values represent fold change of significantly decreased genes)

AGI	Gene Name	Log ₂ FC	adj.P
Carbohydrate metabolism			
AT4G02280	<i>SUS3</i>	-1.50	0.00
AT5G49190	<i>SUS2</i>	-1.07	0.00
Cell wall			
AT4G02250	<i>Plant invertase/pectin methylesterase inhibitor superfamily protein</i>	-14.12	0.00
AT5G39280	<i>EXP23</i>	-3.63	0.00
AT1G60760	<i>Plant invertase/pectin methylesterase inhibitor superfamily protein</i>	-3.58	0.00
Secondary metabolism			
AT2G19070	<i>SHT</i>	-3.92	0.00
AT4G35160	<i>O-methyltransferase family protein</i>	-2.32	0.00
AT5G38120	<i>4CL8</i>	-1.92	0.00
AT4G15870	<i>TS1</i>	-1.84	0.00
AT4G23590	<i>Tyrosine transaminase family protein</i>	-1.36	0.00
AT1G18140	<i>LAC1</i>	-1.20	0.00
Hormone metabolism			
AT3G23240	<i>ERF1</i>	-1.20	0.00
Transport			
AT3G05960	<i>STP6</i>	-1.95	0.02
AT3G45700	<i>Major facilitator superfamily protein</i>	-1.87	0.01
AT1G34580	<i>Major facilitator superfamily protein</i>	-1.81	0.00
AT2G28170	<i>CHX7</i>	-1.79	0.03
AT3G09990	<i>Nucleoside transporter family protein</i>	-1.30	0.02
AT1G54720	<i>Major facilitator superfamily protein</i>	-1.28	0.02
AT1G27940	<i>PGP13</i>	-1.16	0.00
AT4G04760	<i>Major facilitator superfamily protein</i>	-1.14	0.00
AT2G25810	<i>TIP4;1</i>	-1.13	0.00
RNA			
AT1G66390	<i>MYB90</i>	-1.72	0.00
AT3G62610	<i>MYB11</i>	-1.41	0.00
AT5G64810	<i>WRKY51</i>	-1.24	0.00
AT2G37260	<i>WRKY44</i>	-1.20	0.00
AT4G00540	<i>MYB3R2</i>	-1.05	0.01
N-metabolism			
AT3G03910	<i>GDH3</i>	-1.27	0.00
Amino acid metabolism			
AT2G13810	<i>ALD1</i>	-1.11	0.00
Metal handling			
AT5G23980	<i>FRO4</i>	-1.03	0.00
Stress			
AT5G38350	<i>Disease resistance protein</i>	-3.23	0.00
AT5G60553	<i>Defensin-like family protein</i>	-2.59	0.02
AT5G25530	<i>DNAJ heat shock family protein</i>	-1.42	0.03
AT5G23950	<i>Calcium-dependent lipid-binding family protein</i>	-1.40	0.00
AT2G21490	<i>LEA</i>	-1.29	0.00
AT5G46871	<i>Defensin-like family protein</i>	-1.29	0.00
AT2G43580	<i>Chitinase family protein</i>	-1.10	0.01
Miscellaneous enzyme families			
AT3G11825	<i>Protease inhibitor/LTP family protein</i>	-2.36	0.00
AT5G53610	<i>Carbohydrate-binding X8 domain superfamily protein</i>	-2.11	0.03
AT3G22620	<i>Bifunctional inhibitor/lipid-transfer protein</i>	-1.79	0.00
AT4G12825	<i>Protease inhibitor/LTP family protein</i>	-1.70	0.04

AT3G46660	UGT76E12	-1.59	0.00
AT5G07475	Cupredoxin superfamily protein	-1.47	0.00
AT5G59580	UGT76E1	-1.26	0.00
AT1G62620	Flavin-binding monooxygenase family protein	-1.22	0.00
AT5G55410	Bifunctional inhibitor/lipid-transfer protein	-1.22	0.00
AT4G01380	plastocyanin-like domain-containing protein	-1.14	0.00
AT5G17030	UGT78D3	-1.13	0.01
AT1G02940	GSTF5	-1.11	0.00
AT3G20140	CYP705A23	-1.09	0.01
RNA			
AT3G50330	HEC2	-3.74	0.01
AT4G13610	MEE57	-1.82	0.02
AT5G39540	F-box associated ubiquitination effector family protein	-1.67	0.04
AT5G21960	DREB subfamily A-5 of ERF/AP2 transcription factor family	-1.38	0.04
AT5G53040	RKD4	-1.26	0.01
AT2G27220	BLH5	-1.18	0.00
AT1G34410	ARF21	-1.10	0.04
AT3G03260	HGD8	-1.02	0.00
AT5G17490	RGL3	-1.02	0.00
AT5G41315	GL3	-1.00	0.00
DNA			
AT2G05642	Nucleic acid-binding, OB-fold-like protein	-2.72	0.00
Protein			
AT2G27535	ribosomal protein L10A family protein	-1.95	0.01
AT2G17890	CPK16	-1.91	0.04
AT2G32510	MAPKKK17	-1.27	0.00
AT5G28080	WNK9	-1.25	0.00
AT4G17480	alpha/beta-Hydrolases superfamily protein	-1.21	0.00
AT5G26010	Protein phosphatase 2C family protein	-1.09	0.00

Table S2. Specifically altered genes that were lowly expressed and even downregulated in rosettes of wild type under DH HrH compared to control condition (green values represent fold change of significantly decreased genes)

AGI	Gene Name	Log ₂ FC	adj.P
Carbohydrate metabolism			
AT1G72000	<i>A/N-InvF</i>	-1.09	0.00
AT3G28340	<i>GoIS8</i>	-1.30	0.00
Cell wall			
AT1G49490	<i>Leucine-rich repeat (LRR) family protein</i>	-1.01	0.00
AT5G39280	<i>EXPA23</i>	-4.05	0.00
AT5G44840	<i>Pectin lyase-like superfamily protein</i>	-2.50	0.01
Hormone metabolism			
AT4G21340	<i>B70</i>	-1.04	0.00
Transport			
AT1G16370	<i>OCT6</i>	-1.32	0.00
AT2G13620	<i>CHX15</i>	-1.51	0.00
AT4G19680	<i>IRT2</i>	-1.49	0.04
Stress			
AT1G09260	NA	-3.40	0.00
AT1G77093	NA	-1.11	0.02
Miscellaneous enzyme families			
AT1G30700	NA	-1.05	0.00
AT4G02250	NA	-11.84	0.00
AT4G38310	NA	-1.48	0.03
RNA			
AT1G10585	NA	-1.52	0.00
AT3G28470	<i>MYB35</i>	-5.83	0.00

SUPPLEMENTARY MATERIALS

AT4G15250	NA	-3.34	0.00
AT4G39250	<i>RL1</i>	-2.34	0.00
AT5G04150	<i>BHLH101</i>	-1.16	0.00
Protein			
AT2G17890	<i>CPK16</i>	-1.74	0.04
AT5G11940	NA	-2.64	0.01
AT5G17140	NA	-1.69	0.02
AT5G38386	NA	-1.84	0.03
AT5G39560	NA	-2.35	0.00
AT5G56820	NA	-2.01	0.01
Signalling			
AT1G01560	<i>MPK11</i>	-1.19	0.00
AT3G05310	<i>MIRO3</i>	-2.85	0.02
Cell			
AT5G58180	<i>YKT62</i>	-4.27	0.01
Development			
AT2G36985	<i>ROT4</i>	-1.35	0.00
AT5G07930	<i>MCT2</i>	-1.61	0.00
AT5G37900	NA	-3.71	0.00
AT5G52250	<i>EFO1</i>	-1.02	0.00

Table S3. Differentially expressed genes under H HrH excluding the really specifically altered genes in Table 4 and Table S1

AGI	Gene Name	Log ₂ FC	adj.P	AGI	Gene Name	Log ₂ FC	adj.P
AT1G01190	CYP78A8	-1.66	0.00	AT3G57700	NA	-1.02	0.00
AT1G01305	NA	-1.67	0.00	AT3G57780	NA	-1.09	0.00
AT1G01680	ATPUB54	-1.94	0.00	AT3G62700	ABCC14	-1.00	0.00
AT1G02820	NA	-3.14	0.00	AT3G62740	BGLU7	-1.01	0.00
AT1G02930	ATGST1	-2.60	0.00	AT3G62780	NA	-1.13	0.00
AT1G05680	UGT74E2	-1.48	0.00	AT3G62950	NA	-1.00	0.00
AT1G06000	NA	-2.24	0.00	AT3G62960	NA	-1.53	0.00
AT1G06540	NA	-1.20	0.00	AT3G63160	NA	-1.24	0.00
AT1G06830	NA	-2.48	0.00	AT4G01390	NA	-1.07	0.00
AT1G09350	AtGolS3	-3.76	0.00	AT4G01700	NA	-1.32	0.00
AT1G09780	iPGAM1	-1.84	0.00	AT4G02110	NA	-1.51	0.00
AT1G15520	ABCG40	-2.07	0.00	AT4G02360	NA	-1.06	0.00
AT1G17170	ATGSTU24	-1.70	0.00	AT4G02850	NA	-2.34	0.00
AT1G17545	NA	-4.42	0.00	AT4G04450	AtWRKY42	-1.01	0.00
AT1G19050	ARR7	-1.89	0.00	AT4G07820	NA	-1.04	0.00
AT1G23640	NA	-1.20	0.00	AT4G08770	Prx37	-1.49	0.00
AT1G31690	NA	-2.85	0.00	AT4G08870	ARGAH2	-1.89	0.00
AT1G35230	AGP5	-1.95	0.00	AT4G09510	A/N-Invl	-1.01	0.00
AT1G57630	NA	-2.13	0.00	AT4G10290	NA	-1.49	0.00
AT1G67670	NA	-2.17	0.00	AT4G10500	NA	-1.29	0.00
AT1G67810	SUFE2	-1.08	0.00	AT4G11310	NA	-1.28	0.00
AT1G73810	NA	-2.76	0.00	AT4G11320	NA	-1.84	0.00
AT1G75040	PR-5	-2.07	0.00	AT4G11370	RHA1A	-1.27	0.00
AT1G78922	NA	-1.27	0.00	AT4G11521	NA	-1.18	0.00
AT1G79400	ATCHX2	-1.36	0.00	AT4G13210	NA	-1.46	0.00
AT2G04450	ATNUDT6	-1.80	0.00	AT4G13410	ATCSLA15	-1.77	0.00
AT2G14610	ATPR1	-1.51	0.00	AT4G13930	SHM4	-1.11	0.00
AT2G17680	NA	-4.26	0.01	AT4G14090	NA	-3.59	0.00
AT2G18328	ATRL4	-1.25	0.00	AT4G14400	ACD6	-1.10	0.00
AT2G18690	NA	-1.46	0.00	AT4G16000	NA	-2.18	0.00
AT2G21650	ATRL2	-1.35	0.00	AT4G16590	ATCSLA01	-1.19	0.00
AT2G25130	NA	-1.59	0.00	AT4G16740	ATTPS03	-2.77	0.00
AT2G26400	ARD	-1.65	0.00	AT4G16750	NA	-1.06	0.00
AT2G26560	PLA	-1.59	0.00	AT4G17090	BAM3	-1.68	0.00

AT2G30040	MAPKKK14	-2.60	0.01	AT4G17695	KAN3	-1.05	0.00
AT2G30770	CYP71A13	-1.89	0.00	AT4G18170	ATWRKY28	-1.54	0.00
AT2G35970	NA	-1.75	0.00	AT4G19120	ERD3	-1.05	0.00
AT2G35980	ATNHL10	-1.26	0.00	AT4G21200	ATGA2OX8	-1.03	0.00
AT2G43590	NA	-1.74	0.00	AT4G21215	NA	-1.52	0.00
AT3G04570	AHL19	-1.90	0.00	AT4G21380	ARK3	-1.08	0.00
AT3G09940	ATMDAR3	-2.41	0.00	AT4G21400	CRK28	-2.00	0.00
AT3G15356	NA	-1.96	0.00	AT4G21760	BGLU47	-1.23	0.00
AT3G17609	HYH	-1.22	0.00	AT4G21830	ATMSRB7	-1.35	0.00
AT3G19350	MPC	-2.00	0.00	AT4G22470	NA	-1.02	0.00
AT3G21460	NA	-1.98	0.00	AT4G22530	NA	-1.10	0.00
AT3G22421	NA	-2.93	0.00	AT4G22870	NA	-4.92	0.00
AT3G26830	CYP71B15	-1.74	0.00	AT4G22880	ANS	-4.16	0.00
AT3G28510	NA	-2.30	0.00	AT4G23020	NA	-1.71	0.00
AT3G28580	NA	-1.12	0.00	AT4G23200	CRK12	-1.00	0.00
AT3G32050	NA	-1.28	0.01	AT4G23430	AtTic32-IVa	-1.03	0.00
AT3G43630	NA	-3.18	0.00	AT4G23496	SP1L5	-1.04	0.00
AT3G44350	NAC061	-1.09	0.00	AT4G23990	ATCSLG3	-1.57	0.00
AT3G44990	ATXTR8	-2.13	0.00	AT4G24960	ATHVA22D	-1.10	0.00
AT3G49340	NA	-1.35	0.00	AT4G25110	AtMC2	-1.06	0.00
AT3G50510	LBD28	-1.33	0.01	AT4G25480	ATCBF3	-1.66	0.00
AT3G50970	LTI30	-4.58	0.00	AT4G26960	NA	-1.00	0.00
AT3G51240	F3'H	-3.08	0.00	AT4G27520	AtENODL2	-1.22	0.00
AT3G53260	ATPAL2	-1.51	0.00	AT4G27560	NA	-1.93	0.00
AT3G55120	A11	-1.83	0.00	AT4G27570	NA	-2.08	0.00
AT3G55646	NA	-1.30	0.00	AT4G27820	BGLU9	-1.14	0.00
AT3G57240	BG3	-1.81	0.00	AT4G28250	ATEXPB3	-1.67	0.00
AT3G57260	AtPR2	-1.49	0.00	AT4G28550	NA	-1.04	0.00
AT3G59480	NA	-2.36	0.00	AT4G29110	NA	-1.18	0.00
AT3G62930	NA	-1.03	0.00	AT4G29690	NA	-2.04	0.00
AT4G00280	NA	-1.52	0.00	AT4G29700	NA	-1.38	0.00
AT4G10190	NA	-3.01	0.01	AT4G31870	ATGPX7	-2.19	0.00
AT4G10820	NA	-2.23	0.00	AT4G32870	NA	-2.00	0.00
AT4G11290	NA	-1.34	0.00	AT4G34930	NA	-1.03	0.00
AT4G12490	NA	-1.69	0.00	AT4G34950	NA	-1.79	0.00
AT4G12500	NA	-1.00	0.01	AT4G35180	LHT7	-1.26	0.00
AT4G13790	NA	-2.14	0.00	AT4G35320	NA	-1.42	0.00
AT4G14690	ELIP2	-1.83	0.00	AT4G37400	CYP81F3	-1.56	0.00
AT4G15660	NA	-1.50	0.00	AT4G39030	EDS5	-1.56	0.00
AT4G15670	NA	-1.44	0.00	AT4G39380	NA	-1.19	0.00
AT4G15680	NA	-1.81	0.00	AT4G39780	NA	-1.34	0.00
AT4G19810	ChiC	-1.26	0.00	AT4G39795	NA	-2.13	0.00
AT4G23210	CRK13	-1.01	0.00	AT5G01170	NA	-1.18	0.00
AT4G29610	NA	-1.09	0.00	AT5G01500	TAAC	-1.07	0.00
AT4G29740	ATCKX4	-1.08	0.00	AT5G01790	NA	-1.32	0.00
AT4G30650	NA	-2.62	0.00	AT5G01900	ATWRKY62	-1.77	0.00
AT4G33390	NA	-1.56	0.00	AT5G02270	ABCI20	-1.18	0.00
AT4G34550	NA	-2.51	0.00	AT5G02350	NA	-1.00	0.00
AT5G02570	NA	-1.16	0.00	AT5G03210	AtDIP2	-1.23	0.00
AT5G07100	WRKY26	-1.40	0.00	AT5G03350	NA	-2.37	0.00
AT5G07930	MCT2	-1.07	0.00	AT5G04160	NA	-1.14	0.00
AT5G07990	CYP75B1	-2.40	0.00	AT5G04620	ATBIOF	-1.28	0.00
AT5G08640	ATFLS1	-3.00	0.00	AT5G05340	NA	-1.18	0.00
AT5G09470	DIC3	-1.81	0.00	AT5G05580	AtFAD8	-1.74	0.00
AT5G13930	ATCHS	-3.27	0.00	AT5G05840	NA	-1.02	0.00
AT5G18290	SIP1;2	-1.16	0.00	AT5G06060	NA	-1.13	0.00
AT5G22520	NA	-1.46	0.00	AT5G06570	NA	-1.56	0.00
AT5G24200	NA	-2.48	0.00	AT5G07010	ATST2A	-2.52	0.00
AT5G26220	NA	-1.77	0.00	AT5G07720	NA	-1.11	0.00
AT5G26290	NA	-2.84	0.00	AT5G08020	ATRPA70B	-1.34	0.00
AT5G39670	NA	-1.36	0.00	AT5G08100	ASPGA1	-1.12	0.00
AT5G40070	NA	-5.27	0.01	AT5G08570	NA	-1.12	0.00

SUPPLEMENTARY MATERIALS

AT5G43520	NA	-1.19	0.00	AT5G10390	NA	-2.26	0.00
AT5G44420	LCR77	-2.38	0.00	AT5G10400	NA	-1.30	0.00
AT5G44565	NA	-1.62	0.00	AT5G10760	NA	-1.21	0.00
AT5G44568	NA	-1.27	0.00	AT5G11590	TINY2	-1.79	0.00
AT5G46600	NA	-1.44	0.00	AT5G11610	NA	-1.14	0.00
AT5G48880	KAT5	-2.48	0.00	AT5G12340	NA	-1.36	0.00
AT5G52940	NA	-1.00	0.00	AT5G12420	NA	-1.04	0.00
AT5G54020	NA	-2.30	0.00	AT5G12470	NA	-1.54	0.00
AT5G57760	NA	-1.58	0.00	AT5G12910	NA	-2.17	0.00
AT5G61160	AACT1	-1.70	0.00	AT5G13170	AtSWEET15	-1.13	0.02
AT5G62310	IRE	-1.48	0.00	AT5G13320	GDG1	-1.45	0.00
AT5G62920	ARR6	-1.55	0.00	AT5G13650	SVR3	-1.12	0.00
AT5G63087	NA	-2.54	0.00	AT5G14570	ATNRT2.7	-1.20	0.00
AT1G01250	NA	-1.62	0.00	AT5G14700	NA	-1.01	0.00
AT1G01390	NA	-1.59	0.00	AT5G15190	NA	-1.44	0.00
AT1G01560	ATMPK11	-1.29	0.00	AT5G15650	ATRGP2	-1.14	0.00
AT1G01600	CYP86A4	-1.05	0.00	AT5G15760	NA	-1.20	0.00
AT1G01790	ATKEA1	-1.17	0.00	AT5G16350	NA	-1.08	0.00
AT1G02450	NIMIN-1	-1.40	0.00	AT5G17050	UGT78D2	-2.05	0.00
AT1G03495	NA	-3.29	0.00	AT5G17220	ATGSTF12	-3.49	0.00
AT1G03940	NA	-3.34	0.00	AT5G17780	NA	-1.59	0.00
AT1G04020	ATBARD1	-1.14	0.00	AT5G18550	NA	-1.15	0.00
AT1G04110	SDD1	-1.18	0.00	AT5G18840	NA	-1.45	0.00
AT1G04570	NA	-2.00	0.00	AT5G19250	NA	-1.17	0.00
AT1G06690	NA	-1.98	0.00	AT5G19470	NUDT24	-1.43	0.02
AT1G06960	NA	-1.06	0.00	AT5G19800	NA	-1.39	0.00
AT1G07180	ATNDI1	-1.38	0.00	AT5G22300	AtNIT4	-1.88	0.00
AT1G07270	NA	-1.09	0.00	AT5G22390	NA	-1.19	0.00
AT1G07450	NA	-1.65	0.00	AT5G22630	ADT5	-1.05	0.00
AT1G07610	MT1C	-1.85	0.00	AT5G22880	H2B	-1.45	0.00
AT1G08165	NA	-1.39	0.00	AT5G24470	APRR5	-1.08	0.00
AT1G08890	NA	-1.05	0.00	AT5G24850	CRY3	-1.12	0.00
AT1G09200	NA	-1.58	0.00	AT5G24880	NA	-1.37	0.00
AT1G09240	ATNAS3	-2.14	0.00	AT5G25250	NA	-1.39	0.00
AT1G09500	NA	-1.09	0.00	AT5G25260	NA	-1.89	0.00
AT1G10070	ATBCAT-2	-2.22	0.00	AT5G26170	ATWRKY50	-1.31	0.00
AT1G10585	NA	-1.41	0.00	AT5G26690	NA	-2.24	0.00
AT1G11210	NA	-1.11	0.00	AT5G26731	NA	-1.57	0.02
AT1G11220	NA	-1.04	0.00	AT5G27420	ATL31	-1.06	0.00
AT1G12370	PHR1	-1.26	0.00	AT5G33290	XGD1	-1.07	0.00
AT1G13470	NA	-1.51	0.00	AT5G33370	NA	-1.18	0.00
AT1G13750	NA	-1.11	0.00	AT5G35970	NA	-1.16	0.00
AT1G14170	NA	-1.09	0.00	AT5G36220	CYP81D1	-1.09	0.00
AT1G14250	NA	-2.21	0.00	AT5G38690	NA	-1.14	0.00
AT1G14580	NA	-1.36	0.00	AT5G38930	NA	-1.31	0.00
AT1G14870	AtPCR2	-1.32	0.00	AT5G38940	NA	-1.58	0.00
AT1G14880	AtPCR1	-2.09	0.00	AT5G39240	NA	-1.12	0.00
AT1G17190	ATGSTU26	-1.07	0.00	AT5G39520	NA	-2.30	0.00
AT1G18150	ATMPK8	-1.07	0.00	AT5G39610	ANAC092	-1.37	0.00
AT1G18265	NA	-1.60	0.00	AT5G40780	LHT1	-1.52	0.00
AT1G18360	NA	-1.21	0.00	AT5G41880	POLA3	-1.12	0.00
AT1G18710	AtMYB47	-1.26	0.00	AT5G41900	NA	-1.17	0.00
AT1G19200	NA	-1.33	0.00	AT5G42070	NA	-1.27	0.00
AT1G19640	JMT	-1.04	0.00	AT5G42800	DFR	-4.42	0.00
AT1G19940	AtGH9B5	-1.97	0.00	AT5G42860	NA	-1.36	0.00
AT1G19960	NA	-1.50	0.00	AT5G43250	NF-YC13	-1.10	0.00
AT1G20450	ERD10	-1.38	0.00	AT5G43860	ATCLH2	-1.49	0.00
AT1G20490	NA	-1.86	0.00	AT5G44110	ABC121	-1.49	0.00
AT1G20693	HMG	-1.08	0.00	AT5G44390	NA	-1.07	0.00
AT1G21520	NA	-1.64	0.00	AT5G45280	NA	-2.28	0.00
AT1G23140	NA	-1.18	0.00	AT5G45470	NA	-1.26	0.00
AT1G23200	NA	-1.34	0.00	AT5G45700	NA	-1.02	0.00

AT1G24070	ATCSLA10	-1.35	0.00	AT5G46230	NA	-1.77	0.00
AT1G24470	ATKCR2	-2.25	0.00	AT5G46830	ATNIG1	-1.47	0.00
AT1G25422	NA	-2.46	0.00	AT5G50200	ATNRT3.1	-1.08	0.00
AT1G26770	AT-EXP10	-1.24	0.00	AT5G50560	NA	-1.22	0.00
AT1G27760	ATSAT32	-1.07	0.00	AT5G50800	AtSWEET13	-1.10	0.00
AT1G28480	GRX480	-1.14	0.00	AT5G52310	COR78	-3.49	0.00
AT1G28680	NA	-1.15	0.00	AT5G52810	NA	-1.54	0.00
AT1G29395	COR413-TM1	-1.46	0.00	AT5G54060	UF3GT	-3.70	0.00
AT1G29720	NA	-1.67	0.00	AT5G54970	NA	-1.12	0.00
AT1G30620	HSR8	-1.15	0.00	AT5G55340	NA	-1.03	0.00
AT1G30700	NA	-1.51	0.00	AT5G55400	NA	-1.28	0.00
AT1G31190	IMPL1	-1.34	0.00	AT5G55570	NA	-1.98	0.00
AT1G32900	GBSS1	-1.29	0.00	AT5G57050	ABI2	-1.11	0.00
AT1G33960	AIG1	-1.77	0.00	AT5G57123	NA	-1.56	0.00
AT1G35720	ANNAT1	-1.06	0.00	AT5G58700	ATPLC4	-1.28	0.00
AT1G43800	NA	-1.06	0.01	AT5G58830	NA	-1.23	0.00
AT1G52030	F-ATMBP	-1.55	0.00	AT5G59090	ATSBT4.12	-1.05	0.00
AT1G52040	ATMBP	-1.76	0.00	AT5G59130	NA	-1.37	0.00
AT1G52290	AtPERK15	-1.11	0.00	AT5G59670	NA	-2.48	0.00
AT1G52530	NA	-1.02	0.00	AT5G59690	NA	-1.04	0.00
AT1G52770	NA	-1.68	0.00	AT5G59870	HTA6	-2.09	0.00
AT1G52890	ANAC019	-2.17	0.00	AT5G59970	NA	-1.52	0.00
AT1G53040	NA	-1.05	0.00	AT5G60540	ATPDX2	-1.12	0.00
AT1G53542	NA	-1.01	0.00	AT5G60900	RLK1	-1.35	0.00
AT1G54000	GLL22	-1.02	0.00	AT5G61000	ATRPA70D	-1.29	0.00
AT1G55110	AtIDD7	-1.22	0.00	AT5G61412	NA	-1.61	0.00
AT1G56020	NA	-1.03	0.00	AT5G62210	NA	-1.96	0.00
AT1G56120	NA	-1.10	0.00	AT5G64630	FAS2	-1.05	0.00
AT1G56430	ATNAS4	-1.07	0.00	AT5G65020	ANNAT2	-1.02	0.00
AT1G56600	AtGolS2	-1.16	0.00	AT5G65360	NA	-1.39	0.00
AT1G57560	AtMYB50	-1.83	0.00	AT5G67210	IRX15-L	-1.31	0.00
AT1G57590	NA	-1.75	0.00	AT1G03410	2A6	1.40	0.00
AT1G58270	ZW9	-1.37	0.00	AT1G07350	SR45a	2.40	0.00
AT1G61120	GES	-2.26	0.00	AT1G07400	NA	6.10	0.00
AT1G63220	NA	-1.09	0.00	AT1G09140	ATSRP30	1.70	0.00
AT1G63580	NA	-1.07	0.00	AT1G13080	CYP71B2	1.49	0.00
AT1G63710	CYP86A7	-1.93	0.00	AT1G15960	ATNRAMP6	1.03	0.00
AT1G64170	ATCHX16	-1.11	0.00	AT1G27420	NA	1.79	0.00
AT1G64390	AtGH9C2	-1.19	0.00	AT1G30190	NA	1.44	0.00
AT1G64890	NA	-1.20	0.00	AT1G34792	NA	1.02	0.02
AT1G64910	NA	-1.78	0.00	AT1G53540	NA	7.81	0.00
AT1G65450	NA	-1.34	0.00	AT1G59860	NA	4.90	0.00
AT1G65470	FAS1	-1.26	0.00	AT1G62510	NA	2.72	0.00
AT1G65690	NA	-1.36	0.00	AT1G65486	NA	1.58	0.00
AT1G66050	ORTH5	-1.24	0.00	AT1G65490	NA	2.14	0.00
AT1G67330	NA	-1.07	0.00	AT1G71000	NA	2.10	0.00
AT1G67800	NA	-1.16	0.00	AT1G72660	NA	6.24	0.00
AT1G67940	ABC117	-1.09	0.00	AT1G73040	NA	1.11	0.00
AT1G70580	AOAT2	-1.10	0.00	AT1G74310	ATHSP101	4.51	0.00
AT1G70640	NA	-1.96	0.00	AT2G19310	NA	2.22	0.00
AT1G72000	A/N-InvF	-1.25	0.00	AT2G20560	NA	2.85	0.00
AT1G72700	NA	-1.10	0.00	AT2G21560	NA	1.19	0.00
AT1G73805	SARD1	-1.03	0.00	AT2G22770	NAI1	1.47	0.00
AT1G74000	SS3	-1.20	0.00	AT2G26150	ATHSFA2	4.43	0.00
AT1G74010	NA	-1.31	0.00	AT2G29300	NA	1.45	0.00
AT1G74290	NA	-1.11	0.00	AT2G29500	NA	6.72	0.00
AT1G74300	NA	-1.16	0.00	AT2G37180	PIP2;3	1.91	0.00
AT1G74640	NA	-1.04	0.00	AT2G37900	NA	1.24	0.00
AT1G74890	ARR15	-1.61	0.00	AT2G38255	NA	1.80	0.00
AT1G75150	NA	-1.16	0.00	AT2G45920	NA	1.39	0.00
AT1G75600	NA	-1.55	0.00	AT2G47180	AtGolS1	1.72	0.00
AT1G76020	NA	-1.77	0.00	AT3G12580	ATHSP70	5.41	0.00

SUPPLEMENTARY MATERIALS

AT1G76690	ATOPR2	-1.36	0.00	AT3G24500	ATMBF1C	4.10	0.00
AT1G76790	IGMT5	-2.28	0.00	AT3G29810	COBL2	2.40	0.00
AT1G77760	GNR1	-1.48	0.00	AT3G45680	NA	1.65	0.00
AT1G78210	NA	-1.07	0.00	AT3G46230	ATHSP17.4	7.31	0.00
AT1G78370	ATGSTU20	-1.16	0.00	AT3G47340	ASN1	1.63	0.00
AT1G78440	ATGA2OX1	-2.63	0.00	AT3G47360	ATHSD3	1.10	0.00
AT1G78570	ATRHM1	-1.26	0.00	AT3G53230	NA	1.60	0.00
AT1G79080	NA	-1.03	0.00	AT4G00670	NA	1.29	0.00
AT1G79410	AtOCT5	-1.44	0.00	AT4G10240	NA	1.72	0.03
AT1G79460	ATKS	-1.59	0.00	AT4G11960	PGRL1B	1.13	0.00
AT1G80160	GLYI7	-1.19	0.00	AT4G12400	Hop3	6.48	0.00
AT2G01830	AHK4	-1.32	0.00	AT4G14819	NA	1.31	0.00
AT2G02990	ATRNS1	-2.73	0.00	AT4G18550	AtDSEL	1.40	0.00
AT2G03090	ATEXP15	-1.03	0.00	AT4G19430	NA	4.50	0.00
AT2G04032	ZIP7	-1.53	0.00	AT4G20820	NA	1.06	0.00
AT2G04080	NA	-1.10	0.00	AT4G21320	HSA32	3.73	0.00
AT2G14560	LURP1	-1.88	0.00	AT4G21650	NA	1.06	0.00
AT2G15620	ATHNIR	-1.03	0.00	AT4G23493	NA	2.86	0.00
AT2G15970	COR413-PM1	-1.20	0.00	AT4G30540	NA	2.01	0.00
AT2G16060	AHB1	-1.19	0.00	AT4G31351	NA	1.90	0.00
AT2G16430	ATPAP10	-1.11	0.00	AT4G31354	NA	1.90	0.00
AT2G16890	NA	-1.22	0.00	AT4G33420	NA	2.49	0.00
AT2G17280	NA	-1.03	0.00	AT4G39675	NA	1.27	0.00
AT2G17470	ALMT6	-1.60	0.00	AT5G10946	NA	1.30	0.00
AT2G18210	NA	-1.07	0.00	AT5G12030	AT-HSP17.6A	7.10	0.00
AT2G19190	FRK1	-1.29	0.00	AT5G18065	NA	1.22	0.00
AT2G19800	MIOX2	-1.34	0.00	AT5G18340	NA	1.86	0.00
AT2G19990	PR-1-LIKE	-1.03	0.00	AT5G25450	NA	5.00	0.00
AT2G20290	ATXIG	-1.08	0.00	AT5G42965	NA	1.55	0.00
AT2G22590	NA	-1.69	0.00	AT5G46490	NA	2.27	0.00
AT2G23910	NA	-1.91	0.00	AT5G47600	NA	2.59	0.00
AT2G24850	TAT	-1.82	0.00	AT5G51440	NA	6.36	0.00
AT2G24970	NA	-1.14	0.00	AT5G52570	B2	1.20	0.00
AT2G25510	NA	-1.19	0.00	AT5G52640	ATHS83	5.06	0.00
AT2G25625	NA	-1.33	0.00	AT5G54165	NA	1.79	0.00
AT2G26440	NA	-1.45	0.00	AT5G57785	NA	1.61	0.00
AT2G27402	NA	-1.12	0.00	AT5G59310	LTP4	1.48	0.00
AT2G28740	HIS4	-1.42	0.00	AT5G62020	AT-HSFB2A	1.47	0.00
AT2G28900	ATOEP16-1	-1.15	0.00	AT5G64510	TIN1	3.78	0.00
AT2G29090	CYP707A2	-1.89	0.00	AT5G66110	HIPP27	2.33	0.00
AT2G29170	NA	-1.01	0.00	AT1G01750	ADF11	1.59	0.01
AT2G30420	ETC2	-1.00	0.00	AT1G02980	ATCUL2	2.19	0.00
AT2G30540	NA	-1.22	0.00	AT1G05820	ATSPPL5	1.26	0.00
AT2G30830	NA	-1.01	0.00	AT1G10455	NA	1.12	0.01
AT2G31270	ATCDT1A	-1.10	0.00	AT1G10550	XET	1.07	0.00
AT2G31390	NA	-1.51	0.00	AT1G11000	ATMLO4	1.02	0.00
AT2G32590	EMB2795	-1.13	0.00	AT1G11740	NA	1.17	0.00
AT2G33380	AtCLO3	-1.13	0.00	AT1G12080	NA	1.43	0.00
AT2G34930	NA	-2.12	0.00	AT1G13700	PGL1	1.28	0.00
AT2G35070	NA	-1.36	0.00	AT1G18620	NA	1.22	0.00
AT2G36470	NA	-1.26	0.00	AT1G21910	DREB26	1.19	0.00
AT2G36500	NA	-1.46	0.00	AT1G22890	NA	1.27	0.00
AT2G36590	ATPROT3	-1.76	0.00	AT1G24095	NA	1.23	0.00
AT2G36880	MAT3	-1.35	0.00	AT1G28450	AGL58	2.54	0.02
AT2G37040	ATPAL1	-1.75	0.00	AT1G29418	NA	1.13	0.00
AT2G37560	ATORC2	-1.12	0.00	AT1G29490	NA	1.31	0.00
AT2G37710	RLK	-1.29	0.00	AT1G32170	XTH30	1.21	0.00
AT2G37720	TBL15	-2.06	0.00	AT1G33811	NA	1.10	0.00
AT2G37770	AKR4C9	-1.31	0.00	AT1G34315	NA	1.49	0.00
AT2G37960	NA	-1.49	0.00	AT1G34930	NA	1.21	0.02
AT2G38740	NA	-1.21	0.00	AT1G36060	NA	1.75	0.00
AT2G39240	NA	-1.25	0.00	AT1G36940	NA	1.12	0.00

AT2G39710	NA	-1.10	0.00	AT1G50060	NA	2.25	0.02
AT2G40080	ELF4	-1.14	0.00	AT1G50080	NA	1.47	0.03
AT2G40130	NA	-1.36	0.00	AT1G51120	NA	1.54	0.03
AT2G40390	NA	-1.61	0.00	AT1G51920	NA	1.30	0.00
AT2G40670	ARR16	-1.85	0.00	AT1G57990	ATPUP18	1.02	0.00
AT2G40750	ATWRKY54	-1.52	0.00	AT1G60470	AtGolS4	2.07	0.02
AT2G40840	DPE2	-1.08	0.00	AT1G64561	NA	1.70	0.00
AT2G42530	COR15B	-2.10	0.00	AT1G65040	AtHrd1B	1.52	0.00
AT2G42540	COR15	-3.38	0.00	AT1G65200	NA	1.34	0.01
AT2G45080	cycp3;1	-1.04	0.00	AT1G68840	AtRAV2	1.16	0.00
AT2G45220	NA	-1.13	0.00	AT1G70985	NA	1.26	0.00
AT2G45760	BAL	-1.51	0.00	AT1G70990	NA	1.43	0.00
AT2G46400	ATWRKY46	-1.08	0.00	AT1G71400	AtRLP12	1.11	0.00
AT2G47190	ATMYB2	-1.35	0.00	AT1G72060	NA	1.36	0.00
AT2G47460	ATMYB12	-1.05	0.00	AT1G73540	NUDT21	1.02	0.00
AT2G47670	NA	-1.21	0.00	AT1G74670	GASA6	1.87	0.00
AT2G47780	NA	-1.16	0.00	AT2G01300	NA	1.58	0.00
AT2G47870	NA	-1.86	0.00	AT2G01860	EMB975	1.21	0.00
AT2G47880	NA	-2.55	0.00	AT2G05540	NA	1.62	0.00
AT3G01550	ATPPT2	-1.01	0.00	AT2G06020	NA	2.65	0.00
AT3G01920	NA	-1.02	0.00	AT2G19500	ATCKX2	1.46	0.00
AT3G01960	NA	-1.25	0.00	AT2G23348	NA	1.16	0.00
AT3G02230	ATRGP1	-1.21	0.00	AT2G23690	NA	1.17	0.00
AT3G03250	AtUGP1	-1.34	0.00	AT2G25230	AtMYB100	2.67	0.05
AT3G03350	NA	-1.13	0.00	AT2G26860	NA	1.07	0.00
AT3G03480	CHAT	-1.22	0.00	AT2G28630	KCS12	1.43	0.00
AT3G03780	ATMS2	-1.47	0.00	AT2G31083	AtCLE5	1.26	0.04
AT3G05640	NA	-1.08	0.00	AT2G31110	TBL40	1.22	0.00
AT3G05660	AtRLP33	-1.31	0.00	AT2G31150	NA	1.15	0.00
AT3G05800	AIF1	-1.40	0.00	AT2G33250	NA	1.27	0.00
AT3G05980	NA	-1.45	0.00	AT2G37060	NF-YB8	1.54	0.00
AT3G06035	NA	-1.37	0.00	AT2G40610	ATEXP8	1.56	0.00
AT3G06890	NA	-1.40	0.00	AT2G40740	ATWRKY55	1.26	0.00
AT3G07195	NA	-1.39	0.00	AT2G44195	NA	1.54	0.00
AT3G08870	NA	-1.09	0.00	AT2G45180	NA	1.07	0.00
AT3G09270	ATGSTU8	-1.51	0.00	AT2G46220	NA	1.42	0.00
AT3G09540	NA	-1.47	0.00	AT2G48130	NA	1.02	0.04
AT3G10340	PAL4	-1.14	0.00	AT3G02380	ATCOL2	1.12	0.00
AT3G11480	ATBSMT1	-1.16	0.03	AT3G07000	NA	1.11	0.00
AT3G12170	NA	-1.14	0.00	AT3G08940	LHCB4.2	1.02	0.00
AT3G13060	ECT5	-1.09	0.00	AT3G10405	NA	1.03	0.00
AT3G13650	NA	-1.23	0.00	AT3G15578	NA	1.91	0.00
AT3G14000	ATBRXL2	-1.05	0.00	AT3G16150	ASPGB1	1.13	0.01
AT3G14280	NA	-1.35	0.00	AT3G16240	AQP1	1.06	0.00
AT3G14395	NA	-1.25	0.00	AT3G16580	NA	1.40	0.04
AT3G14440	ATNCED3	-1.14	0.00	AT3G18773	NA	1.08	0.00
AT3G14720	ATMPK19	-1.00	0.00	AT3G19508	NA	1.11	0.00
AT3G14740	NA	-1.70	0.00	AT3G22060	NA	1.07	0.00
AT3G14890	NA	-1.16	0.00	AT3G23637	DVL21	1.00	0.00
AT3G15030	MEE35	-1.11	0.00	AT3G24715	NA	1.07	0.00
AT3G19660	NA	-1.31	0.00	AT3G25050	XTH3	1.77	0.01
AT3G20370	NA	-1.35	0.00	AT3G25880	NA	1.15	0.01
AT3G21560	UGT84A2	-1.42	0.00	AT3G26800	NA	1.27	0.00
AT3G21950	NA	-1.12	0.00	AT3G27027	NA	1.08	0.00
AT3G22142	NA	-1.21	0.00	AT3G27030	NA	1.06	0.00
AT3G22160	NA	-1.00	0.00	AT3G27860	NA	1.00	0.00
AT3G22231	PCC1	-2.09	0.00	AT3G30350	RGF4	2.24	0.00
AT3G22600	NA	-1.71	0.00	AT3G42800	NA	1.55	0.00
AT3G23810	ATSAAH2	-1.66	0.00	AT3G45960	ATEXLA3	1.39	0.00
AT3G23870	NA	-1.24	0.00	AT3G46770	NA	1.08	0.00
AT3G24982	ATRLP40	-1.49	0.00	AT3G50190	NA	1.20	0.00
AT3G25100	CDC45	-1.24	0.00	AT3G50720	NA	2.18	0.04

SUPPLEMENTARY MATERIALS

AT3G25180	CYP82G1	-2.56	0.00	AT3G52480	NA	1.02	0.00
AT3G25760	AOC1	-1.02	0.00	AT3G52670	NA	1.05	0.00
AT3G25882	NIMIN-2	-2.34	0.00	AT3G56000	ATCSLA14	1.40	0.00
AT3G26960	NA	-1.14	0.00	AT3G57958	NA	1.06	0.03
AT3G27300	G6PD5	-1.06	0.00	AT4G01330	NA	1.14	0.00
AT3G27360	NA	-1.20	0.00	AT4G03156	NA	1.08	0.00
AT3G27400	NA	-1.49	0.00	AT4G03566	NA	2.85	0.01
AT3G27640	NA	-1.16	0.00	AT4G05170	NA	1.65	0.02
AT3G28007	AtSWEET4	-1.76	0.00	AT4G08250	NA	1.03	0.00
AT3G28220	NA	-2.42	0.00	AT4G10910	NA	1.15	0.00
AT3G28540	NA	-1.21	0.00	AT4G14100	NA	1.04	0.00
AT3G29575	AFP3	-1.68	0.00	AT4G15560	AtCLA1	1.04	0.00
AT3G29590	AT5MAT	-3.54	0.00	AT4G18970	NA	1.34	0.00
AT3G44450	NA	-1.20	0.00	AT4G19080	NA	1.26	0.00
AT3G44860	FAMT	-1.59	0.00	AT4G19620	NA	2.98	0.00
AT3G44870	NA	-1.54	0.00	AT4G26280	NA	5.84	0.00
AT3G44970	NA	-1.27	0.00	AT4G27420	ABCG9	1.12	0.05
AT3G45140	ATLOX2	-1.62	0.00	AT4G27654	NA	1.02	0.05
AT3G45410	NA	-1.06	0.00	AT4G28395	A7	6.16	0.00
AT3G45930	NA	-1.37	0.00	AT4G28405	NA	1.13	0.01
AT3G46320	NA	-1.85	0.00	AT4G28420	NA	1.16	0.00
AT3G46880	NA	-1.04	0.00	AT4G34770	NA	1.20	0.00
AT3G46940	DUT1	-1.62	0.00	AT4G37610	BT5	1.02	0.00
AT3G46970	ATPHS2	-1.08	0.00	AT4G37800	XTH7	1.54	0.00
AT3G47480	NA	-1.43	0.00	AT4G38825	NA	1.46	0.00
AT3G48020	NA	-1.26	0.00	AT4G39500	CYP96A11	1.39	0.03
AT3G48080	NA	-2.32	0.00	AT4G39700	NA	1.05	0.00
AT3G48490	NA	-1.12	0.00	AT5G02000	NA	2.43	0.00
AT3G48990	NA	-1.03	0.00	AT5G03020	NA	1.19	0.00
AT3G49110	ATPCA	-1.12	0.00	AT5G10250	DOT3	1.22	0.00
AT3G49120	ATPCB	-1.38	0.00	AT5G14730	NA	1.18	0.00
AT3G50760	GATL2	-1.48	0.00	AT5G15830	AtbZIP3	1.51	0.00
AT3G51470	NA	-1.10	0.00	AT5G18404	NA	1.04	0.00
AT3G52310	ABCG27	-1.54	0.00	AT5G20250	DIN10	1.86	0.00
AT3G52630	NA	-1.18	0.00	AT5G22940	F8H	1.04	0.00
AT3G53650	NA	-1.41	0.00	AT5G24110	ATWRKY30	1.17	0.00
AT3G53730	NA	-1.49	0.00	AT5G26800	NA	1.04	0.00
AT3G54560	HTA11	-1.13	0.00	AT5G28770	AtbZIP63	1.20	0.00
AT3G54750	NA	-1.10	0.00	AT5G39910	NA	2.25	0.00
AT3G54950	PLA	-1.02	0.00	AT5G48530	NA	1.03	0.00
AT3G55970	ATJRG21	-1.15	0.00	AT5G49360	ATBXL1	2.13	0.00
AT3G56170	CAN	-1.05	0.00	AT5G57560	TCH4	1.04	0.02
AT3G56260	NA	-1.87	0.00	AT5G58360	ATOFP3	1.30	0.00
AT3G56380	ARR17	-1.43	0.00	AT5G66270	NA	1.01	0.00
AT3G56710	SIB1	-1.13	0.00	AT5G67610	NA	1.39	0.00
AT3G56870	NA	-1.25	0.00				

Table S4. Specifically changed genes under H LrH

AGI	Gene Name	Log ₂ FC	adj.P	AGI	Gene Name	Log ₂ FC	adj.P
AT1G02390	ATGPAT2	1.15	0.00	AT4G33550	NA	1.49	0.00
AT1G07430	HAI2	1.53	0.00	AT4G36950	MAPKKK21	1.15	0.01
AT1G11080	scpl31	1.35	0.01	AT5G03210	AtDIP2	1.38	0.00
AT1G12940	ATNRT2.5	1.78	0.00	AT5G07260	NA	1.59	0.00
AT1G17010	NA	1.05	0.00	AT5G07330	NA	1.38	0.04
AT1G20160	ATSBT5.2	1.01	0.00	AT5G08090	NA	1.15	0.01
AT1G22480	NA	1.02	0.00	AT5G13210	NA	1.05	0.00
AT1G22990	HIPP22	1.36	0.00	AT5G13620	NA	3.48	0.02
AT1G29230	ATCIPK18	1.47	0.00	AT5G14490	NAC085	2.10	0.01
AT1G31520	NA	2.22	0.00	AT5G15500	NA	1.50	0.00
AT1G43160	RAP2.6	1.56	0.01	AT5G16850	ATTERT	1.75	0.00
AT1G47915	NA	1.71	0.01	AT5G17540	NA	1.08	0.00

AT1G49450	NA	1.02	0.00	AT5G19470	NUDT24	1.49	0.05
AT1G52720	NA	1.24	0.00	AT5G20260	NA	2.66	0.00
AT1G53680	ATGSTU28	3.55	0.00	AT5G25140	CYP71B13	1.28	0.00
AT1G57650	NA	2.64	0.02	AT5G26140	ATLOG9	1.18	0.02
AT1G57670	NA	1.12	0.00	AT5G28237	NA	1.28	0.00
AT1G60190	AtPUB19	1.71	0.00	AT5G37060	ATCHX24	1.66	0.03
AT1G60450	AtGolS7	2.77	0.00	AT5G37760	NA	1.18	0.00
AT1G64590	NA	1.56	0.00	AT5G38760	NA	1.18	0.02
AT1G65352	NA	2.28	0.03	AT5G39640	NA	1.06	0.00
AT1G67960	POD1	1.54	0.01	AT5G40790	NA	1.06	0.01
AT1G68040	NA	1.47	0.02	AT5G43690	NA	1.38	0.01
AT1G68270	NA	2.78	0.04	AT5G45810	CIPK19	1.09	0.00
AT1G69100	NA	2.18	0.04	AT5G46040	NA	1.59	0.00
AT1G72770	HAB1	1.01	0.00	AT5G48605	NA	1.86	0.00
AT1G75160	NA	1.57	0.03	AT5G50050	NA	1.18	0.05
AT2G05330	NA	2.92	0.02	AT5G52730	NA	1.68	0.00
AT2G10920	NA	1.50	0.01	AT5G53710	NA	1.25	0.00
AT2G15130	NA	1.30	0.02	AT5G55440	NA	1.12	0.02
AT2G18140	NA	2.41	0.01	AT5G59220	HAI1	2.07	0.00
AT2G20880	AtERF53	1.19	0.00	AT5G59320	LTP3	2.22	0.00
AT2G24610	ATCNGC14	1.34	0.01	AT5G59330	NA	1.93	0.00
AT2G27690	CYP94C1	1.17	0.00	AT5G63450	CYP94B1	2.52	0.00
AT2G28780	NA	1.01	0.03	AT5G64750	ABR1	1.30	0.02
AT2G29820	NA	1.22	0.00	AT1G02920	ATGST11	-1.57	0.00
AT2G30830	NA	1.11	0.00	AT1G06160	ORA59	-1.37	0.00
AT2G33380	AtCLO3	1.29	0.00	AT1G09080	BIP3	-1.34	0.00
AT2G34600	JAZ7	1.47	0.01	AT1G21110	IGMT3	-1.17	0.00
AT2G36650	NA	1.08	0.00	AT1G22690	NA	-1.29	0.03
AT2G36750	UGT73C1	1.01	0.01	AT1G24530	NA	-1.27	0.00
AT2G37170	PIP2;2	1.01	0.00	AT1G25340	AtMYB116	-2.93	0.01
AT2G38600	NA	1.15	0.01	AT1G25550	NA	-1.08	0.00
AT2G38823	NA	1.43	0.00	AT1G26380	NA	-1.21	0.00
AT2G39640	NA	1.37	0.04	AT1G27020	NA	-1.26	0.00
AT2G41480	NA	1.25	0.00	AT1G50040	NA	-1.06	0.01
AT2G42760	NA	1.19	0.00	AT1G55230	NA	-1.79	0.02
AT2G46270	GBF3	1.73	0.00	AT1G66090	NA	-1.12	0.03
AT3G01620	NA	1.70	0.00	AT1G66100	NA	-1.12	0.04
AT3G05720	IMPA-7	2.29	0.00	AT1G66700	PXMT1	-1.27	0.00
AT3G08860	PYD4	1.22	0.01	AT1G78410	NA	-1.78	0.00
AT3G11480	ATBSMT1	1.43	0.01	AT2G02930	ATGSTF3	-1.40	0.00
AT3G15280	NA	1.01	0.00	AT2G05380	GRP3S	-1.25	0.00
AT3G18518	DVL7	1.46	0.02	AT2G07774	NA	-1.09	0.00
AT3G20590	NA	1.41	0.00	AT2G11810	ATMGD3	-1.06	0.03
AT3G21890	NA	1.01	0.00	AT2G14700	NA	-1.96	0.02
AT3G22740	HMT3	1.04	0.00	AT2G18190	NA	-1.16	0.01
AT3G24517	NA	1.08	0.03	AT2G18890	NA	-1.01	0.00
AT3G28270	NA	1.60	0.00	AT2G22810	ACC4	-1.05	0.00
AT3G28600	NA	1.54	0.03	AT2G30750	CYP71A12	-1.04	0.00
AT3G28870	NA	2.88	0.05	AT2G31540	NA	-1.03	0.02
AT3G42990	NA	1.09	0.03	AT2G36970	NA	-1.08	0.02
AT3G44210	NA	3.61	0.00	AT2G38940	ATPT2	-1.08	0.00
AT3G44718	NA	1.12	0.05	AT3G02040	AtGDPD1	-1.35	0.00
AT3G46340	NA	3.38	0.01	AT3G04720	HEL	-1.51	0.00
AT3G48520	CYP94B3	2.31	0.00	AT3G15720	NA	-1.18	0.00
AT3G48630	NA	2.72	0.03	AT3G16530	NA	-2.42	0.00
AT3G49460	NA	3.07	0.00	AT3G23550	NA	-2.00	0.00
AT3G52720	ACA1	1.02	0.00	AT3G48360	ATBT2	-1.60	0.00
AT3G53980	NA	1.31	0.01	AT3G54150	NA	-1.22	0.00
AT3G54260	TBL36	1.04	0.00	AT3G55180	NA	-1.65	0.01
AT3G54870	ARK1	2.80	0.00	AT3G56980	BHLH039	-2.44	0.01
AT3G55590	NA	1.25	0.02	AT3G63110	ATIPT3	-1.07	0.00
AT3G56920	NA	2.56	0.02	AT4G02520	ATGSTF2	-1.32	0.00

SUPPLEMENTARY MATERIALS

AT3G60790	NA	4.42	0.00	AT4G06746	DEAR5	-2.07	0.00
AT4G02360	NA	1.03	0.00	AT4G15700	NA	-1.11	0.03
AT4G08570	NA	1.88	0.00	AT4G16260	NA	-2.24	0.00
AT4G08990	NA	1.52	0.00	AT4G19380	NA	-1.03	0.00
AT4G09775	NA	1.83	0.01	AT4G21840	ATMSRB8	-1.18	0.02
AT4G10700	NA	1.38	0.01	AT4G25630	ATFIB2	-1.03	0.00
AT4G13580	NA	1.07	0.03	AT4G32090	NA	-1.63	0.02
AT4G19690	ATIRT1	1.07	0.00	AT5G02260	ATEXP9	-1.25	0.00
AT4G21930	NA	1.57	0.00	AT5G15430	NA	-1.80	0.01
AT4G23670	NA	1.05	0.00	AT5G18470	NA	-1.22	0.00
AT4G26288	NA	1.02	0.01	AT5G20150	ATSPX1	-1.14	0.00
AT4G28365	AtENODL3	1.74	0.00	AT5G20790	NA	-1.95	0.00
AT4G29930	NA	1.08	0.00	AT5G41300	NA	-3.06	0.01
AT4G30270	MERI-5	1.14	0.00	AT5G52760	NA	-1.04	0.02
AT4G30450	NA	1.00	0.00	AT5G55565	NA	-1.97	0.02
AT4G30460	NA	1.32	0.00	AT5G57220	CYP81F2	-2.24	0.00
AT4G31760	NA	1.25	0.03				

Table S5. Differentially expressed genes under DH HrH excluding the really specifically altered genes in Table 5 and Table S2

AGI	Gene	Log ₂ FC	adj.P	AGI	Gene	Log ₂ FC	adj.P
AT1G01190	CYP78A8	-1.63	0.00	AT5G66590	NA	-1.27	0.00
AT1G01200	ATRAB-A3	-1.55	0.00	AT5G66640	DAR3	-1.19	0.00
AT1G01300	NA	-1.20	0.00	AT5G66770	NA	-1.08	0.00
AT1G01390	NA	-2.77	0.00	AT5G67100	ICU2	-1.28	0.00
AT1G01600	CYP86A4	-1.91	0.00	AT5G67260	CYCD3;2	-1.04	0.00
AT1G01790	ATKEA1	-1.83	0.00	AT5G67270	ATEB1C	-1.43	0.00
AT1G02360	NA	-2.19	0.00	AT5G67385	NA	-1.67	0.00
AT1G02450	NIMIN-1	-2.17	0.00	AT5G67390	NA	-1.51	0.00
AT1G02730	ATCSLD5	-1.43	0.00	AT5G67460	NA	-1.40	0.00
AT1G02920	ATGST11	-2.51	0.00	AT1G01090	PDH-E1	-1.02	0.00
AT1G02930	ATGST1	-2.74	0.00	AT1G01180	NA	-1.11	0.00
AT1G02950	ATGSTF4	-1.44	0.00	AT1G01340	ACBK1	-1.61	0.00
AT1G03020	NA	-1.53	0.00	AT1G01680	ATPUB54	-1.35	0.00
AT1G03230	NA	-1.26	0.00	AT1G02820	NA	-1.81	0.00
AT1G03780	AtTPX2	-1.98	0.00	AT1G04280	NA	-1.33	0.00
AT1G03870	FLA9	-2.07	0.00	AT1G05020	NA	-1.09	0.00
AT1G04020	ATBARD1	-2.50	0.00	AT1G05620	NSH2	-1.04	0.00
AT1G04040	NA	-2.08	0.00	AT1G05770	NA	-1.03	0.00
AT1G04110	SDD1	-2.38	0.00	AT1G07180	ATNDI1	-1.16	0.00
AT1G04430	NA	-1.38	0.00	AT1G07610	MT1C	-2.12	0.00
AT1G04520	PDLP2	-2.24	0.00	AT1G10060	ATBCAT-1	-1.32	0.00
AT1G04640	LIP2	-1.26	0.00	AT1G11310	ATMLO2	-1.23	0.00
AT1G04680	NA	-1.23	0.00	AT1G11330	NA	-1.11	0.00
AT1G04760	ATVAMP726	-1.29	0.00	AT1G12090	ELP	-1.06	0.00
AT1G04800	NA	-3.17	0.00	AT1G12850	NA	-1.10	0.00
AT1G05010	ACO4	-1.14	0.00	AT1G13670	NA	-1.00	0.00
AT1G05210	NA	-1.35	0.00	AT1G14080	ATFUT6	-1.12	0.00
AT1G05440	NA	-2.12	0.00	AT1G14170	NA	-1.30	0.00
AT1G05575	NA	-1.92	0.00	AT1G17890	GER2	-1.02	0.00
AT1G05680	UGT74E2	-2.01	0.00	AT1G18990	NA	-1.25	0.04
AT1G05760	RTM1	-1.11	0.00	AT1G20070	NA	-1.31	0.00
AT1G05805	NA	-1.26	0.00	AT1G20480	NA	-1.12	0.00
AT1G06000	NA	-1.76	0.00	AT1G21540	NA	-1.10	0.00
AT1G06080	ADS1	-1.98	0.00	AT1G22360	AtUGT85A2	-1.10	0.00
AT1G06160	ORA59	-3.67	0.00	AT1G22400	ATUGT85A1	-1.14	0.00
AT1G06350	NA	-1.40	0.00	AT1G23140	NA	-1.18	0.00
AT1G06360	NA	-1.54	0.00	AT1G24530	NA	-1.09	0.00
AT1G06690	NA	-1.24	0.00	AT1G25422	NA	-1.45	0.00
AT1G06830	NA	-4.53	0.00	AT1G28480	GRX480	-1.15	0.00

AT1G06960	NA	-1.45	0.00	AT1G29630	NA	-1.03	0.00
AT1G07070	NA	-1.14	0.00	AT1G31670	NA	-1.21	0.00
AT1G07090	LSH6	-1.03	0.00	AT1G33790	NA	-1.11	0.00
AT1G07240	UGT71C5	-1.17	0.00	AT1G33960	AIG1	-3.10	0.00
AT1G07260	UGT71C3	-1.38	0.00	AT1G43800	NA	-1.61	0.00
AT1G07270	NA	-1.51	0.00	AT1G43910	NA	-1.04	0.00
AT1G07370	ATPCNA1	-2.03	0.00	AT1G52530	NA	-1.10	0.00
AT1G07450	NA	-2.07	0.00	AT1G52770	NA	-1.15	0.00
AT1G07650	NA	-1.04	0.00	AT1G53625	NA	-1.20	0.00
AT1G08160	NA	-1.87	0.00	AT1G56720	NA	-1.03	0.00
AT1G08165	NA	-1.53	0.00	AT1G57630	NA	-2.65	0.00
AT1G08260	ABO4	-1.02	0.00	AT1G57990	ATPUP18	-1.88	0.00
AT1G08550	AVDE1	-1.40	0.00	AT1G64980	NA	-1.01	0.00
AT1G08560	ATSYP111	-1.74	0.00	AT1G65930	ciCDH	-1.02	0.00
AT1G08810	AtMYB60	-1.63	0.00	AT1G67180	NA	-1.22	0.00
AT1G08840	emb2411	-1.73	0.00	AT1G67800	NA	-1.13	0.00
AT1G08930	ERD6	-2.35	0.00	AT1G69890	NA	-1.16	0.00
AT1G09080	BIP3	-1.25	0.00	AT1G71030	ATMYBL2	-1.13	0.00
AT1G09200	NA	-2.72	0.00	AT1G73370	ATSUS6	-1.22	0.00
AT1G09340	CRB	-1.20	0.00	AT1G73760	NA	-1.02	0.00
AT1G09350	AtGolS3	-3.08	0.00	AT1G73805	SARD1	-1.19	0.00
AT1G09390	NA	-1.43	0.00	AT1G74300	NA	-1.25	0.00
AT1G09450	AtHaspin	-1.87	0.00	AT1G76690	ATOPR2	-1.21	0.00
AT1G09470	NA	-1.16	0.00	AT1G77700	NA	-1.03	0.00
AT1G09630	ATRA-B-A2A	-1.40	0.00	AT1G78830	NA	-1.10	0.00
AT1G09750	NA	-1.98	0.00	AT1G79340	AtMC4	-1.03	0.00
AT1G09780	iPGAM1	-2.00	0.00	AT1G79680	ATWAKL10	-1.25	0.00
AT1G09932	NA	-1.60	0.00	AT1G80340	ATGA3OX2	-1.26	0.02
AT1G10020	NA	-2.20	0.00	AT2G02990	ATRNS1	-1.60	0.00
AT1G10340	NA	-1.15	0.00	AT2G06255	ELF4-L3	-1.00	0.00
AT1G10470	ARR4	-1.47	0.00	AT2G15390	FUT4	-1.21	0.00
AT1G10780	NA	-1.19	0.00	AT2G16280	KCS9	-1.15	0.00
AT1G10850	NA	-1.27	0.00	AT2G17620	CYCB2;1	-1.16	0.00
AT1G10990	NA	-3.01	0.00	AT2G19570	AT-CDA1	-1.29	0.00
AT1G11112	NA	-1.01	0.00	AT2G19590	ACO1	-1.46	0.00
AT1G11350	CBRLK1	-1.26	0.00	AT2G19880	NA	-1.05	0.00
AT1G11450	NA	-1.24	0.00	AT2G22920	SCPL12	-1.07	0.00
AT1G11545	XTH8	-3.13	0.00	AT2G22990	SCPL8	-1.05	0.00
AT1G11580	ATPMEPCRA	-1.26	0.00	AT2G23290	AtMYB70	-1.20	0.00
AT1G11670	NA	-1.80	0.00	AT2G23620	ATMES1	-1.16	0.00
AT1G11850	NA	-2.87	0.00	AT2G25450	NA	-1.34	0.00
AT1G12080	NA	-1.73	0.00	AT2G26080	AtGLDP2	-1.08	0.00
AT1G12110	ATNRT1	-1.65	0.00	AT2G27430	NA	-1.00	0.00
AT1G12310	NA	-1.18	0.00	AT2G30040	MAPKKK14	-2.95	0.00
AT1G12370	PHR1	-1.57	0.00	AT2G31390	NA	-1.65	0.00
AT1G12500	NA	-1.20	0.00	AT2G32960	AtPFA-DSP2	-1.75	0.00
AT1G12900	GAPA-2	-1.11	0.00	AT2G33600	NA	-1.13	0.00
AT1G13110	CYP71B7	-2.34	0.00	AT2G36500	NA	-1.47	0.00
AT1G13170	ORP1D	-1.25	0.00	AT2G37430	NA	-1.24	0.00
AT1G13210	ACA.I	-1.20	0.00	AT2G37710	RLK	-1.11	0.00
AT1G13260	EDF4	-2.27	0.00	AT2G37720	TBL15	-2.31	0.00
AT1G13420	ATST4B	-1.03	0.00	AT2G38240	NA	-2.16	0.00
AT1G13470	NA	-1.64	0.00	AT2G39200	ATMLO12	-1.03	0.00
AT1G13750	NA	-1.38	0.00	AT2G40390	NA	-1.45	0.00
AT1G14250	NA	-1.40	0.00	AT2G42580	TTL3	-1.03	0.00
AT1G14290	SBH2	-1.20	0.00	AT2G42900	NA	-1.15	0.00
AT1G14390	NA	-1.51	0.00	AT2G44450	BGLU15	-1.04	0.00
AT1G14430	NA	-2.30	0.00	AT2G44930	NA	-1.05	0.00
AT1G14870	AtPCR2	-2.07	0.00	AT2G45750	NA	-1.01	0.00
AT1G14880	AtPCR1	-4.30	0.00	AT2G47000	ABCB4	-1.12	0.00
AT1G15125	NA	-2.68	0.00	AT2G47880	NA	-1.94	0.00
AT1G15140	NA	-1.27	0.00	AT3G02600	ATLPP3	-1.03	0.00

SUPPLEMENTARY MATERIALS

AT1G15520	ABCG40	-1.96	0.00	AT3G03600	RPS2	-1.05	0.00
AT1G15570	CYCA2;3	-1.09	0.00	AT3G08630	NA	-1.09	0.00
AT1G15660	CENP-C	-1.16	0.00	AT3G11800	NA	-1.37	0.00
AT1G15690	ATAVP3	-1.11	0.00	AT3G11840	PUB24	-1.23	0.00
AT1G16070	AtTLP8	-1.02	0.00	AT3G14770	AtSWEET2	-1.37	0.00
AT1G16330	CYCB3;1	-1.33	0.00	AT3G14790	ATRHM3	-1.06	0.00
AT1G16390	ATOCT3	-3.68	0.00	AT3G19680	NA	-1.06	0.00
AT1G16630	NA	-1.65	0.00	AT3G20270	NA	-1.02	0.00
AT1G16640	NA	-1.47	0.00	AT3G23550	NA	-4.38	0.00
AT1G17170	ATGSTU24	-1.99	0.00	AT3G25670	NA	-1.03	0.00
AT1G17190	ATGSTU26	-1.23	0.00	AT3G26080	NA	-1.05	0.00
AT1G17430	NA	-1.37	0.00	AT3G26210	CYP71B23	-1.11	0.00
AT1G17600	NA	-1.15	0.00	AT3G26830	CYP71B15	-1.77	0.00
AT1G17700	PRA1.F1	-1.07	0.00	AT3G27120	NA	-1.02	0.00
AT1G17860	NA	-1.64	0.00	AT3G28320	NA	-1.54	0.00
AT1G18140	ATLAC1	-1.28	0.00	AT3G46130	ATMYB48	-1.31	0.00
AT1G18150	ATMPK8	-1.24	0.00	AT3G48260	WNK3	-1.29	0.00
AT1G18250	ATLP-1	-1.53	0.00	AT3G49620	DIN11	-2.58	0.00
AT1G18265	NA	-1.37	0.00	AT3G50140	NA	-1.22	0.00
AT1G18370	ATNACK1	-3.04	0.00	AT3G51330	NA	-1.03	0.00
AT1G18400	BEE1	-1.41	0.00	AT3G52110	NA	-1.26	0.00
AT1G18810	NA	-1.53	0.00	AT3G57700	NA	-1.19	0.00
AT1G19050	ARR7	-1.91	0.00	AT3G59140	ABCC10	-1.05	0.00
AT1G19450	NA	-1.94	0.00	AT3G60130	BGLU16	-1.14	0.00
AT1G19670	ATCLH1	-1.73	0.00	AT3G62720	ATXT1	-1.10	0.00
AT1G19710	NA	-1.08	0.00	AT3G62960	NA	-1.26	0.00
AT1G19720	NA	-1.27	0.00	AT4G00330	CRCK2	-1.12	0.00
AT1G19940	AtGH9B5	-2.94	0.00	AT4G04745	NA	-1.58	0.00
AT1G19950	HVA22H	-1.14	0.00	AT4G10500	NA	-1.19	0.00
AT1G19960	NA	-2.25	0.00	AT4G13790	NA	-1.29	0.00
AT1G19990	NA	-1.06	0.00	AT4G14390	NA	-1.17	0.00
AT1G20010	TUB5	-1.73	0.00	AT4G16000	NA	-1.18	0.00
AT1G20190	ATEXP11	-1.91	0.00	AT4G18470	SNI1	-1.11	0.00
AT1G20330	CVP1	-1.10	0.00	AT4G19420	NA	-1.05	0.00
AT1G20693	HMG	-1.20	0.00	AT4G19810	ChiC	-1.03	0.00
AT1G20840	AtTMT1	-1.43	0.00	AT4G21400	CRK28	-1.33	0.00
AT1G21060	NA	-1.45	0.00	AT4G22530	NA	-1.36	0.00
AT1G21070	NA	-1.47	0.00	AT4G26470	NA	-1.05	0.00
AT1G21100	IGMT1	-1.75	0.00	AT4G26910	NA	-1.14	0.00
AT1G21110	IGMT3	-1.71	0.00	AT4G28550	NA	-1.14	0.00
AT1G21120	IGMT2	-2.16	0.00	AT4G28720	YUC8	-1.03	0.00
AT1G21130	IGMT4	-1.98	0.00	AT4G30310	NA	-1.03	0.00
AT1G21270	WAK2	-1.53	0.00	AT4G30340	ATDGK7	-1.10	0.00
AT1G21520	NA	-1.91	0.00	AT4G30670	NA	-1.24	0.00
AT1G22150	SULTR1;3	-1.45	0.00	AT4G31400	CTF7	-1.04	0.00
AT1G22330	NA	-2.30	0.00	AT4G33666	NA	-1.04	0.00
AT1G22690	NA	-3.43	0.00	AT4G34610	BLH6	-1.07	0.00
AT1G23030	NA	-1.42	0.00	AT4G35160	NA	-1.37	0.00
AT1G23110	NA	-1.50	0.01	AT4G37260	ATMYB73	-1.33	0.00
AT1G23170	NA	-1.47	0.00	AT4G39270	NA	-1.25	0.00
AT1G23390	NA	-2.09	0.00	AT4G39810	NA	-1.02	0.00
AT1G23640	NA	-1.17	0.00	AT5G01830	NA	-1.08	0.00
AT1G23790	NA	-2.15	0.00	AT5G04270	NA	-1.38	0.00
AT1G24120	ARL1	-1.03	0.00	AT5G04930	ALA1	-1.01	0.00
AT1G24147	NA	-2.20	0.00	AT5G06980	NA	-1.15	0.00
AT1G24170	GATL8	-1.56	0.00	AT5G11950	LOG8	-1.02	0.00
AT1G24180	IAR4	-1.16	0.00	AT5G12340	NA	-1.54	0.00
AT1G24575	NA	-1.51	0.00	AT5G12420	NA	-1.46	0.00
AT1G24610	NA	-1.01	0.00	AT5G15650	ATRGP2	-1.01	0.00
AT1G25230	NA	-1.72	0.00	AT5G16570	GLN1;4	-1.10	0.04
AT1G25275	NA	-1.59	0.00	AT5G20150	ATSPX1	-1.05	0.00
AT1G25425	CLE43	-1.20	0.00	AT5G22920	NA	-1.01	0.00

AT1G25450	CER60	-1.24	0.00	AT5G25930	NA	-1.56	0.00
AT1G26290	NA	-1.16	0.00	AT5G33290	XGD1	-1.24	0.00
AT1G26380	NA	-1.11	0.00	AT5G34830	NA	-1.13	0.00
AT1G26570	ATUGD1	-1.58	0.00	AT5G36220	CYP81D1	-1.02	0.00
AT1G26760	ATXR1	-1.65	0.00	AT5G37010	NA	-1.20	0.00
AT1G26770	AT-EXP10	-1.51	0.00	AT5G37600	ATGLN1;1	-1.15	0.00
AT1G26945	KDR	-1.08	0.00	AT5G40780	LHT1	-1.74	0.00
AT1G27020	NA	-3.65	0.00	AT5G43170	AZF3	-1.31	0.00
AT1G27130	ATGSTU13	-1.54	0.00	AT5G44070	ARA8	-1.07	0.00
AT1G27460	NPGR1	-1.43	0.00	AT5G45530	NA	-1.36	0.00
AT1G27880	NA	-1.12	0.00	AT5G45830	ATDOG1	-1.05	0.00
AT1G28010	ABCB14	-1.28	0.00	AT5G50560	NA	-1.06	0.00
AT1G29270	NA	-1.18	0.00	AT5G55180	NA	-1.58	0.00
AT1G29280	ATWRKY65	-1.70	0.00	AT5G60280	NA	-1.01	0.00
AT1G29430	NA	-1.47	0.00	AT5G61412	NA	-1.95	0.00
AT1G29440	NA	-1.27	0.00	AT5G61590	NA	-1.63	0.00
AT1G29450	NA	-1.80	0.00	AT5G62280	NA	-2.27	0.00
AT1G29460	NA	-1.11	0.00	AT5G62680	NA	-1.00	0.00
AT1G29660	NA	-2.18	0.00	AT5G62865	NA	-1.49	0.00
AT1G29720	NA	-1.95	0.00	AT5G63060	NA	-1.12	0.00
AT1G30250	NA	-1.37	0.00	AT5G64110	NA	-1.17	0.00
AT1G30420	ABCC11	-1.09	0.00	AT1G01160	GIF2	1.13	0.00
AT1G30455	NA	-2.63	0.00	AT1G01250	NA	1.12	0.00
AT1G30520	AAE14	-1.09	0.00	AT1G01480	ACS2	1.31	0.02
AT1G30530	UGT78D1	-1.25	0.00	AT1G01710	NA	1.57	0.00
AT1G30690	NA	-1.07	0.00	AT1G01720	ANAC002	1.47	0.00
AT1G31190	IMPL1	-1.44	0.00	AT1G01810	NA	1.25	0.00
AT1G31200	ATPP2-A9	-1.74	0.00	AT1G02050	LAP6	1.15	0.00
AT1G31490	NA	-1.57	0.00	AT1G02205	CER1	2.68	0.00
AT1G31550	NA	-1.22	0.00	AT1G02310	MAN1	1.37	0.00
AT1G31580	CXC750	-1.92	0.00	AT1G02390	ATGPAT2	2.78	0.00
AT1G31690	NA	-3.79	0.00	AT1G02700	NA	2.78	0.00
AT1G32080	AtLrgB	-1.10	0.00	AT1G02770	NA	1.82	0.00
AT1G33240	AT-GTL1	-1.20	0.00	AT1G03070	NA	3.74	0.00
AT1G33590	NA	-1.63	0.00	AT1G03410	2A6	1.59	0.00
AT1G33600	NA	-1.82	0.00	AT1G03470	NA	1.59	0.00
AT1G33610	NA	-1.60	0.00	AT1G03550	NA	1.59	0.00
AT1G33670	NA	-1.41	0.00	AT1G03760	NA	1.23	0.00
AT1G33930	NA	-1.18	0.02	AT1G04220	KCS2	2.69	0.00
AT1G34010	NA	-1.49	0.00	AT1G04560	NA	1.69	0.00
AT1G34355	ATPS1	-1.20	0.00	AT1G04970	NA	1.16	0.00
AT1G34760	GF14	-1.16	0.00	AT1G05100	MAPKKK18	2.42	0.00
AT1G35230	AGP5	-1.75	0.00	AT1G05340	NA	4.63	0.00
AT1G35580	A/N-InvG	-1.54	0.00	AT1G05870	NA	1.56	0.00
AT1G36940	NA	-1.16	0.00	AT1G05894	NA	1.04	0.00
AT1G37130	ATNR2	-1.47	0.00	AT1G06090	NA	1.08	0.00
AT1G43670	AtcFBP	-1.49	0.00	AT1G06110	SKIP16	1.31	0.00
AT1G44000	NA	-1.18	0.00	AT1G06430	FTSH8	1.27	0.00
AT1G44830	NA	-1.62	0.00	AT1G06570	HPD	1.10	0.00
AT1G44900	ATMCM2	-1.25	0.00	AT1G06790	NA	2.72	0.00
AT1G45130	BGAL5	-1.04	0.00	AT1G07120	NA	1.59	0.00
AT1G45180	NA	-1.30	0.00	AT1G07230	NPC1	1.39	0.00
AT1G45191	BGLU1	-1.52	0.00	AT1G07350	SR45a	3.12	0.00
AT1G45474	Lhca5	-1.16	0.00	AT1G07380	NA	1.36	0.00
AT1G47210	CYCA3;2	-1.55	0.00	AT1G07390	AtRLP1	1.16	0.00
AT1G47395	NA	-2.74	0.00	AT1G07400	NA	7.18	0.00
AT1G47400	NA	-2.44	0.00	AT1G07430	HAI2	4.06	0.00
AT1G47480	NA	-1.32	0.00	AT1G07500	NA	5.13	0.00
AT1G47485	NA	-1.48	0.00	AT1G07720	KCS3	1.51	0.00
AT1G47760	AGL102	-1.17	0.00	AT1G07870	NA	1.43	0.00
AT1G47840	HXK3	-1.12	0.00	AT1G07900	LBD1	2.85	0.00
AT1G48480	RKL1	-2.04	0.00	AT1G07985	NA	1.80	0.00

SUPPLEMENTARY MATERIALS

AT1G49220	NA	-1.34	0.00	AT1G08300	NVL	1.71	0.00
AT1G49730	NA	-1.25	0.00	AT1G08460	ATHDA8	1.22	0.00
AT1G49870	NA	-1.35	0.00	AT1G09070	(AT)SRC2	1.27	0.00
AT1G49975	NA	-1.21	0.00	AT1G09140	ATSRP30	2.45	0.00
AT1G50010	TUA2	-1.02	0.00	AT1G09500	NA	1.44	0.00
AT1G50040	NA	-1.60	0.00	AT1G09530	PAP3	1.49	0.00
AT1G50240	FU	-1.68	0.00	AT1G09950	RAS1	1.54	0.00
AT1G50490	UBC20	-1.15	0.00	AT1G10240	FRS11	1.35	0.00
AT1G51070	bHLH115	-1.19	0.00	AT1G11100	NA	1.45	0.00
AT1G51790	NA	-1.34	0.00	AT1G11170	NA	1.13	0.00
AT1G51800	IOS1	-1.58	0.00	AT1G11190	BFN1	1.10	0.00
AT1G51805	NA	-1.89	0.00	AT1G11270	NA	1.06	0.00
AT1G51820	NA	-1.55	0.00	AT1G11910	APA1	1.03	0.00
AT1G51890	NA	-1.47	0.00	AT1G12064	NA	2.89	0.00
AT1G51940	NA	-1.05	0.00	AT1G12210	RFL1	1.30	0.00
AT1G52190	NA	-1.27	0.00	AT1G12290	NA	1.38	0.00
AT1G52200	NA	-3.17	0.00	AT1G12950	RSH2	1.59	0.00
AT1G52270	NA	-1.07	0.00	AT1G13050	NA	1.03	0.00
AT1G52290	AtPERK15	-1.90	0.00	AT1G13990	NA	1.43	0.00
AT1G52342	NA	-1.36	0.00	AT1G14300	NA	1.18	0.00
AT1G52510	NA	-1.24	0.00	AT1G14890	NA	1.25	0.00
AT1G52910	NA	-1.54	0.00	AT1G15230	NA	1.30	0.00
AT1G53040	NA	-1.64	0.00	AT1G15240	NA	1.33	0.00
AT1G53140	DRP5A	-2.19	0.00	AT1G15340	MBD10	1.09	0.00
AT1G53230	TCP3	-1.95	0.00	AT1G15510	ATECB2	1.45	0.00
AT1G53290	NA	-1.11	0.00	AT1G15550	ATGA3OX1	2.55	0.00
AT1G53310	ATPEPC1	-1.32	0.00	AT1G15960	ATNRAMP6	2.07	0.00
AT1G53350	NA	-1.23	0.00	AT1G16030	Hsp70b	3.69	0.00
AT1G53430	NA	-2.17	0.00	AT1G16515	NA	2.32	0.00
AT1G53440	NA	-1.45	0.00	AT1G16850	NA	2.72	0.00
AT1G53520	NA	-1.49	0.00	AT1G17020	ATSRG1	2.61	0.00
AT1G53542	NA	-1.10	0.00	AT1G17460	TRFL3	1.47	0.00
AT1G53700	PK3AT	-1.92	0.00	AT1G17744	NA	3.17	0.00
AT1G54000	GLL22	-1.65	0.00	AT1G17830	NA	1.98	0.00
AT1G54010	NA	-2.86	0.00	AT1G17870	ATEGY3	4.71	0.00
AT1G54385	NA	-2.03	0.00	AT1G17940	NA	2.24	0.00
AT1G54410	NA	-1.15	0.00	AT1G17950	ATMYB52	1.04	0.00
AT1G54820	NA	-1.49	0.00	AT1G18750	AGL65	1.03	0.00
AT1G55120	ATFRUCT5	-1.86	0.00	AT1G19060	NA	1.23	0.00
AT1G55160	NA	-1.09	0.00	AT1G19490	NA	1.41	0.00
AT1G55260	NA	-1.06	0.00	AT1G19530	NA	1.09	0.00
AT1G55330	AGP21	-2.66	0.00	AT1G19630	CYP722A1	1.33	0.00
AT1G55450	NA	-1.49	0.00	AT1G19980	NA	1.38	0.00
AT1G56120	NA	-1.74	0.00	AT1G20160	ATSBT5.2	2.15	0.00
AT1G56430	ATNAS4	-2.40	0.00	AT1G20225	NA	1.20	0.00
AT1G57560	AtMYB50	-2.38	0.00	AT1G20350	ATTIM17-1	2.05	0.00
AT1G57770	NA	-1.41	0.00	AT1G20850	XCP2	1.29	0.00
AT1G58370	ATXYN1	-1.08	0.00	AT1G20890	NA	1.20	0.00
AT1G58602	NA	-2.37	0.00	AT1G20920	NA	1.47	0.00
AT1G59710	NA	-1.64	0.00	AT1G21000	NA	1.11	0.00
AT1G59870	ABCG36	-1.60	0.00	AT1G21400	NA	1.80	0.00
AT1G59960	NA	-1.05	0.00	AT1G21410	SKP2A	1.65	0.00
AT1G60010	NA	-1.03	0.00	AT1G21460	AtSWEET1	1.65	0.00
AT1G60060	NA	-1.10	0.00	AT1G21550	NA	2.88	0.00
AT1G60760	NA	-3.40	0.00	AT1G21580	NA	1.28	0.00
AT1G60870	MEE9	-1.07	0.00	AT1G21670	NA	1.00	0.00
AT1G61070	LCR66	-1.15	0.00	AT1G21890	NA	1.24	0.00
AT1G61120	GES	-2.24	0.00	AT1G22160	NA	1.26	0.00
AT1G61170	NA	-1.59	0.00	AT1G22190	RAP2.4	1.27	0.00
AT1G61450	NA	-1.52	0.00	AT1G22370	AtUGT85A5	1.33	0.00
AT1G61575	NA	-1.02	0.00	AT1G22380	AtUGT85A3	1.17	0.00
AT1G62200	AtPTR6	-1.25	0.00	AT1G22480	NA	3.12	0.00

AT1G62380	ACO2	-1.95	0.00	AT1G22985	CRF7	1.39	0.00
AT1G62480	NA	-2.15	0.00	AT1G22990	HIPP22	6.42	0.00
AT1G62640	KAS	-1.11	0.00	AT1G23040	NA	1.15	0.00
AT1G62780	NA	-1.42	0.00	AT1G23050	NA	1.41	0.00
AT1G62790	NA	-1.67	0.00	AT1G23330	NA	1.02	0.00
AT1G63000	NRS/ER	-1.08	0.00	AT1G23550	SRO2	1.02	0.00
AT1G63100	NA	-2.07	0.00	AT1G23860	At-RSZ21	1.97	0.00
AT1G63220	NA	-2.59	0.00	AT1G24095	NA	1.64	0.00
AT1G63260	TET10	-1.60	0.00	AT1G24265	NA	1.23	0.00
AT1G63310	NA	-1.13	0.00	AT1G24330	NA	1.08	0.00
AT1G63580	NA	-1.24	0.00	AT1G24580	NA	2.55	0.00
AT1G63710	CYP86A7	-2.19	0.00	AT1G24600	NA	2.95	0.00
AT1G63940	MDAR6	-1.34	0.00	AT1G25211	NA	1.44	0.00
AT1G64170	ATCHX16	-2.30	0.00	AT1G25530	NA	1.03	0.00
AT1G64450	NA	-1.08	0.00	AT1G25540	MED25	1.24	0.00
AT1G64640	AtENODL8	-1.36	0.00	AT1G26580	NA	1.45	0.00
AT1G64650	NA	-1.03	0.00	AT1G26800	NA	1.57	0.00
AT1G64770	NDF2	-1.21	0.00	AT1G27170	NA	1.11	0.00
AT1G65060	4CL3	-1.03	0.00	AT1G27200	NA	1.15	0.00
AT1G65295	NA	-1.49	0.00	AT1G27385	NA	1.08	0.00
AT1G65470	FAS1	-2.11	0.00	AT1G27420	NA	2.40	0.00
AT1G65570	NA	-4.75	0.00	AT1G27590	NA	2.09	0.00
AT1G65590	ATHEX1	-1.55	0.00	AT1G27650	ATU2AF35A	1.10	0.00
AT1G65710	NA	-1.50	0.00	AT1G28260	NA	1.38	0.00
AT1G65960	GAD2	-1.20	0.00	AT1G28330	DRM1	1.82	0.00
AT1G65985	NA	-1.98	0.00	AT1G28370	ATERF11	1.31	0.00
AT1G66050	ORTH5	-2.25	0.00	AT1G29240	NA	1.16	0.00
AT1G66100	NA	-5.11	0.00	AT1G29418	NA	1.90	0.00
AT1G66150	TMK1	-1.14	0.00	AT1G29465	NA	1.67	0.00
AT1G66200	ATGSR2	-1.19	0.00	AT1G29640	NA	2.72	0.00
AT1G66350	RGL	-1.14	0.00	AT1G29680	NA	2.39	0.02
AT1G66370	AtMYB113	-1.31	0.00	AT1G30190	NA	4.58	0.00
AT1G66620	NA	-1.59	0.00	AT1G30220	ATINT2	3.72	0.00
AT1G66700	PXMT1	-1.48	0.00	AT1G30500	NF-YA7	1.52	0.00
AT1G66940	NA	-3.40	0.00	AT1G30970	SUF4	1.16	0.00
AT1G67260	TCP1	-1.28	0.00	AT1G31600	AtTRM9	1.15	0.00
AT1G67330	NA	-1.89	0.00	AT1G31750	NA	1.21	0.00
AT1G67630	EMB2814	-1.39	0.00	AT1G31760	NA	1.58	0.00
AT1G67670	NA	-2.01	0.00	AT1G31820	NA	1.43	0.00
AT1G67790	NA	-1.55	0.00	AT1G31835	NA	1.23	0.00
AT1G67810	SUFE2	-3.45	0.00	AT1G32100	ATPRR1	1.29	0.00
AT1G68590	NA	-1.25	0.00	AT1G32560	AtLEA4-1	2.06	0.00
AT1G68780	NA	-1.30	0.00	AT1G32583	NA	2.05	0.00
AT1G69040	ACR4	-1.01	0.00	AT1G32870	ANAC013	1.28	0.00
AT1G69520	NA	-1.23	0.00	AT1G32950	NA	1.65	0.00
AT1G69530	AT-EXP1	-1.75	0.00	AT1G33102	NA	1.15	0.00
AT1G69770	CMT3	-1.11	0.00	AT1G33260	NA	1.11	0.00
AT1G69780	ATHB13	-1.16	0.00	AT1G33640	NA	1.31	0.00
AT1G69900	NA	-1.51	0.00	AT1G33700	NA	1.59	0.00
AT1G70090	GATL9	-1.48	0.00	AT1G33800	NA	1.08	0.00
AT1G70270	NA	-3.64	0.00	AT1G34042	NA	2.76	0.00
AT1G71140	NA	-3.36	0.00	AT1G34630	NA	1.25	0.00
AT1G71760	NA	-1.10	0.00	AT1G34792	NA	1.00	0.02
AT1G71880	ATSUC1	-1.16	0.00	AT1G35660	NA	1.80	0.00
AT1G72250	NA	-1.32	0.00	AT1G36060	NA	1.16	0.00
AT1G72416	NA	-1.75	0.00	AT1G36070	NA	1.20	0.00
AT1G72450	JAZ6	-1.53	0.00	AT1G36980	NA	1.18	0.00
AT1G72610	ATGER1	-2.87	0.00	AT1G42980	NA	1.21	0.00
AT1G72670	iqd8	-1.71	0.00	AT1G44414	NA	2.35	0.00
AT1G72730	NA	-1.38	0.00	AT1G45249	ABF2	1.52	0.00
AT1G72910	NA	-1.25	0.00	AT1G45616	AtRLP6	2.57	0.00
AT1G72920	NA	-1.24	0.00	AT1G45976	SBP1	1.18	0.00

SUPPLEMENTARY MATERIALS

AT1G72930	TIR	-1.67	0.00	AT1G46768	RAP2.1	1.13	0.00
AT1G73110	NA	-1.10	0.00	AT1G47510	5PTASE11	1.52	0.00
AT1G73325	NA	-1.69	0.00	AT1G47960	ATC/VIF1	3.94	0.00
AT1G73620	NA	-1.43	0.00	AT1G48000	AtMYB112	1.82	0.00
AT1G73830	BEE3	-1.10	0.00	AT1G48020	ATPMEI1	1.51	0.00
AT1G74000	SS3	-1.20	0.00	AT1G48320	NA	1.14	0.00
AT1G74290	NA	-1.19	0.00	AT1G48430	NA	1.05	0.00
AT1G74440	NA	-1.39	0.00	AT1G48750	NA	2.27	0.00
AT1G74690	IQD31	-1.12	0.00	AT1G48840	NA	1.17	0.00
AT1G74710	ATIC51	-1.37	0.00	AT1G49170	NA	1.32	0.00
AT1G74730	NA	-1.13	0.00	AT1G49200	NA	1.14	0.00
AT1G74790	NA	-1.09	0.00	AT1G49405	NA	2.62	0.00
AT1G74890	ARR15	-2.35	0.00	AT1G49450	NA	2.57	0.00
AT1G75030	ATLP-3	-1.86	0.00	AT1G49530	GGPS6	1.30	0.00
AT1G75040	PR-5	-2.95	0.00	AT1G50260	NTMC2T5.1	1.14	0.00
AT1G75150	NA	-1.93	0.00	AT1G50400	NA	2.10	0.00
AT1G75190	NA	-1.83	0.00	AT1G50520	CYP705A27	1.57	0.00
AT1G75250	ATRL6	-1.83	0.00	AT1G50590	NA	1.09	0.00
AT1G75600	NA	-2.03	0.00	AT1G51130	NA	1.26	0.00
AT1G75640	NA	-1.20	0.00	AT1G51200	NA	1.52	0.00
AT1G75690	LQY1	-1.33	0.00	AT1G51380	NA	1.81	0.00
AT1G75960	NA	-1.69	0.00	AT1G51402	NA	1.56	0.00
AT1G76020	NA	-1.25	0.00	AT1G52080	AR791	1.06	0.00
AT1G76090	SMT3	-1.21	0.00	AT1G52560	NA	5.71	0.00
AT1G76160	sks5	-1.35	0.00	AT1G52690	LEA7	6.41	0.00
AT1G76190	NA	-1.83	0.00	AT1G52720	NA	1.04	0.00
AT1G76240	NA	-3.28	0.00	AT1G52790	NA	1.05	0.05
AT1G76310	CYCB2;4	-1.58	0.00	AT1G52827	ATCDT1	1.13	0.00
AT1G76680	ATOPR1	-2.06	0.00	AT1G52920	GCR2	1.51	0.00
AT1G76740	NA	-1.02	0.00	AT1G52990	NA	1.30	0.00
AT1G76790	IGMT5	-1.30	0.00	AT1G53080	NA	1.86	0.00
AT1G77330	NA	-1.60	0.00	AT1G53100	NA	1.81	0.00
AT1G77690	LAX3	-1.37	0.00	AT1G53280	AtDJ1B	1.06	0.00
AT1G77760	GNR1	-2.73	0.00	AT1G53540	NA	9.64	0.00
AT1G78210	NA	-1.32	0.00	AT1G54050	NA	3.04	0.00
AT1G78270	AtUGT85A4	-2.52	0.00	AT1G54100	ALDH7B4	1.77	0.00
AT1G78300	14-3-3OMEGA	-1.13	0.00	AT1G54120	NA	1.10	0.00
AT1G78370	ATGSTU20	-1.43	0.00	AT1G54160	NF-YA5	1.36	0.00
AT1G78410	NA	-1.19	0.00	AT1G54575	NA	1.36	0.00
AT1G78430	RIP2	-1.87	0.00	AT1G54830	NF-YC3	1.02	0.00
AT1G78450	NA	-1.30	0.00	AT1G55040	NA	1.11	0.00
AT1G78460	NA	-1.56	0.00	AT1G55280	NA	1.14	0.00
AT1G78530	NA	-1.66	0.00	AT1G55530	NA	1.23	0.00
AT1G78570	ATRHM1	-1.21	0.00	AT1G55760	NA	1.41	0.00
AT1G78820	NA	-1.31	0.00	AT1G56170	ATHAP5B	2.87	0.00
AT1G78890	NA	-1.24	0.00	AT1G56280	ATDI19	1.01	0.00
AT1G78922	NA	-1.53	0.00	AT1G56440	TPR5	1.75	0.00
AT1G78995	NA	-1.14	0.00	AT1G56600	AtGolS2	1.81	0.00
AT1G79080	NA	-1.44	0.00	AT1G57590	NA	1.39	0.00
AT1G79400	ATCHX2	-1.77	0.00	AT1G58340	BCD1	1.78	0.00
AT1G79410	AtOCT5	-2.10	0.00	AT1G58360	AAP1	1.15	0.00
AT1G79770	NA	-1.30	0.00	AT1G58470	ATRBP1	1.32	0.00
AT1G79790	AtcpFHy1	-1.92	0.00	AT1G58520	RXW8	1.17	0.00
AT1G80050	APT2	-1.56	0.00	AT1G59640	BPE	1.28	0.00
AT1G80560	ATIMD2	-1.35	0.00	AT1G59740	NA	1.00	0.00
AT2G02930	ATGSTF3	-3.14	0.00	AT1G59860	NA	5.73	0.00
AT2G02950	PKS1	-1.65	0.00	AT1G60190	AtPUB19	4.00	0.00
AT2G03350	NA	-1.44	0.00	AT1G60470	AtGolS4	1.55	0.03
AT2G03420	NA	-1.52	0.00	AT1G60970	NA	4.16	0.00
AT2G03760	ATST1	-1.54	0.00	AT1G61255	NA	1.06	0.00
AT2G03980	NA	-1.79	0.00	AT1G61340	NA	1.17	0.00
AT2G04032	ZIP7	-1.64	0.00	AT1G61580	ARP2	1.81	0.00

AT2G04450	ATNUDT6	-2.64	0.00	AT1G61800	ATGPT2	1.43	0.00
AT2G04650	NA	-1.34	0.00	AT1G61970	NA	1.36	0.00
AT2G04780	FLA7	-1.96	0.00	AT1G62290	NA	2.88	0.00
AT2G05160	NA	-1.35	0.00	AT1G62510	NA	4.84	0.00
AT2G05380	GRP3S	-1.58	0.00	AT1G62700	ANAC026	1.02	0.00
AT2G05642	NA	-2.87	0.00	AT1G63840	NA	1.34	0.00
AT2G05810	NA	-1.16	0.00	AT1G64110	DAA1	4.28	0.00
AT2G06850	EXGT-A1	-2.68	0.00	AT1G64561	NA	2.67	0.00
AT2G06925	ATSPLA2-ALPHA	-1.69	0.00	AT1G64660	ATMGL	2.30	0.00
AT2G07170	NA	-1.85	0.00	AT1G65000	NA	1.05	0.00
AT2G10940	NA	-1.36	0.00	AT1G65890	AAE12	1.10	0.00
AT2G11810	ATMGD3	-2.09	0.00	AT1G65980	TPX1	1.44	0.00
AT2G12462	NA	-1.48	0.00	AT1G66080	NA	2.22	0.00
AT2G13820	AtXYP2	-1.27	0.00	AT1G66390	ATMYB90	1.21	0.01
AT2G14247	NA	-2.84	0.00	AT1G66500	NA	2.65	0.00
AT2G14560	LURP1	-3.53	0.00	AT1G66510	NA	1.59	0.00
AT2G14610	ATPR1	-2.80	0.00	AT1G67120	NA	1.46	0.00
AT2G15042	NA	-1.09	0.00	AT1G67265	DVL3	3.07	0.00
AT2G15080	AtRLP19	-1.16	0.00	AT1G67360	NA	1.33	0.00
AT2G15090	KCS8	-1.52	0.00	AT1G67370	ASY1	1.47	0.00
AT2G15620	ATHNIR	-1.17	0.00	AT1G67856	NA	2.25	0.00
AT2G15760	NA	-1.41	0.00	AT1G67920	NA	3.45	0.00
AT2G16060	AHB1	-2.87	0.00	AT1G68360	NA	1.16	0.00
AT2G16380	NA	-1.43	0.00	AT1G68490	NA	1.25	0.00
AT2G16430	ATPAP10	-1.24	0.00	AT1G68500	NA	1.83	0.00
AT2G16440	MCM4	-1.19	0.00	AT1G68570	NA	1.14	0.00
AT2G16630	NA	-1.21	0.00	AT1G69260	AFP1	2.96	0.00
AT2G16660	NA	-2.82	0.00	AT1G69280	NA	1.38	0.00
AT2G16850	PIP2;8	-1.18	0.00	AT1G69295	PDCB4	1.06	0.00
AT2G17230	EXL5	-1.93	0.00	AT1G69410	ATELF5A-3	1.12	0.00
AT2G17470	ALMT6	-1.39	0.00	AT1G69430	NA	1.16	0.00
AT2G17630	NA	-1.60	0.00	AT1G69480	NA	2.52	0.00
AT2G17880	NA	-1.22	0.00	AT1G69490	ANAC029	1.30	0.00
AT2G18190	NA	-1.24	0.00	AT1G69540	AGL94	1.07	0.00
AT2G18210	NA	-1.79	0.00	AT1G69790	NA	1.46	0.00
AT2G18300	NA	-2.71	0.00	AT1G70300	KUP6	2.81	0.00
AT2G18328	ATRL4	-2.76	0.00	AT1G70510	ATK1	1.27	0.00
AT2G18670	NA	-1.01	0.00	AT1G70720	NA	1.65	0.00
AT2G18690	NA	-2.18	0.00	AT1G70920	ATHB18	2.44	0.00
AT2G18890	NA	-1.49	0.00	AT1G71000	NA	4.83	0.00
AT2G18969	NA	-1.23	0.00	AT1G71260	ATWHY2	1.58	0.00
AT2G19190	FRK1	-1.73	0.00	AT1G71330	ATNAP5	2.43	0.00
AT2G19680	NA	-1.39	0.00	AT1G71340	AtGDPD4	1.58	0.00
AT2G19800	MIOX2	-1.83	0.00	AT1G71960	ABCG25	1.46	0.00
AT2G20290	ATXIG	-1.67	0.00	AT1G72040	NA	1.09	0.00
AT2G20562	NA	-1.12	0.00	AT1G72090	NA	1.47	0.00
AT2G20590	NA	-1.85	0.00	AT1G72100	NA	1.30	0.00
AT2G20610	ALF1	-1.24	0.00	AT1G72240	NA	1.49	0.00
AT2G20950	NA	-1.20	0.00	AT1G72650	TRFL6	1.43	0.00
AT2G20980	MCM10	-1.26	0.00	AT1G72660	NA	7.03	0.00
AT2G21140	ATPRP2	-1.95	0.00	AT1G72770	HAB1	2.33	0.00
AT2G21540	ATSFH3	-1.25	0.00	AT1G72840	NA	1.13	0.00
AT2G21650	ATRL2	-4.56	0.00	AT1G73010	ATPS2	1.56	0.00
AT2G21790	ATRNR1	-1.27	0.00	AT1G73040	NA	2.47	0.00
AT2G22122	NA	-1.30	0.00	AT1G73066	NA	1.92	0.00
AT2G22170	NA	-1.18	0.00	AT1G73210	NA	1.11	0.00
AT2G22425	NA	-1.13	0.00	AT1G73220	AtOCT1	1.76	0.00
AT2G22610	NA	-1.76	0.00	AT1G73330	ATDR4	1.47	0.00
AT2G22795	NA	-1.00	0.00	AT1G73680	ALPHA	1.33	0.00
AT2G22810	ACC4	-2.25	0.00	AT1G73690	AT;CDKD;1	1.70	0.00
AT2G22890	NA	-1.04	0.00	AT1G73780	NA	1.30	0.00
AT2G23130	AGP17	-1.83	0.00	AT1G73880	UGT89B1	1.06	0.00

SUPPLEMENTARY MATERIALS

AT2G23560	ATMES7	-1.05	0.00	AT1G74180	AtRLP14	1.03	0.00
AT2G23600	ACL	-1.41	0.00	AT1G74310	ATHSP101	5.31	0.00
AT2G23680	NA	-1.46	0.00	AT1G74860	NA	2.07	0.00
AT2G23770	NA	-1.43	0.00	AT1G75400	NA	1.07	0.00
AT2G24210	TPS10	-3.32	0.00	AT1G75860	NA	1.09	0.00
AT2G24490	ATRPA2	-1.78	0.00	AT1G76065	NA	2.02	0.00
AT2G24600	NA	-1.19	0.00	AT1G76080	ATCDSP32	1.03	0.00
AT2G24850	TAT	-1.90	0.00	AT1G76820	NA	1.97	0.00
AT2G24970	NA	-1.95	0.00	AT1G77000	ATSKP2;2	1.04	0.00
AT2G25060	AtENODL14	-2.44	0.00	AT1G77010	NA	1.03	0.00
AT2G25130	NA	-1.93	0.00	AT1G77450	NAC032	1.94	0.00
AT2G25200	NA	-1.21	0.00	AT1G77520	NA	1.64	0.00
AT2G25510	NA	-1.58	0.00	AT1G77570	NA	1.11	0.00
AT2G25735	NA	-2.14	0.00	AT1G77880	NA	2.03	0.00
AT2G25810	TIP4;1	-1.35	0.00	AT1G78070	NA	1.18	0.00
AT2G26040	PYL2	-1.26	0.00	AT1G78340	ATGSTU22	2.27	0.00
AT2G26180	IQD6	-1.65	0.00	AT1G78610	MSL6	1.51	0.00
AT2G26190	NA	-1.17	0.00	AT1G78670	ATGGH3	1.21	0.00
AT2G26360	NA	-1.14	0.00	AT1G78780	NA	1.42	0.00
AT2G26400	ARD	-3.02	0.00	AT1G78930	NA	1.97	0.00
AT2G26440	NA	-2.63	0.00	AT1G79260	NA	1.20	0.00
AT2G26520	NA	-1.64	0.00	AT1G79270	ECT8	1.52	0.00
AT2G26530	AR781	-1.96	0.00	AT1G79520	NA	1.84	0.00
AT2G26560	PLA	-3.86	0.00	AT1G79900	ATMBAC2	2.47	0.00
AT2G26650	AKT1	-1.12	0.00	AT1G80110	ATPP2-B11	1.55	0.00
AT2G26710	BAS1	-1.07	0.00	AT1G80130	NA	1.68	0.00
AT2G26730	NA	-1.03	0.00	AT1G80160	GLYI7	2.70	0.00
AT2G26760	CYCB1;4	-1.68	0.00	AT1G80320	NA	2.89	0.00
AT2G27030	ACAM-2	-1.05	0.00	AT1G80660	AHA9	2.08	0.00
AT2G27130	NA	-1.26	0.00	AT1G80670	RAE1	1.01	0.00
AT2G27402	NA	-4.08	0.00	AT1G80970	NA	1.06	0.00
AT2G27420	NA	-2.20	0.00	AT2G01008	NA	1.84	0.00
AT2G28085	NA	-1.97	0.00	AT2G01100	NA	1.07	0.00
AT2G28160	ATBHLH029	-1.07	0.00	AT2G02350	AtPP2-B9	1.64	0.00
AT2G28620	NA	-1.87	0.00	AT2G02750	NA	1.40	0.00
AT2G28720	NA	-1.08	0.00	AT2G03200	NA	1.29	0.00
AT2G28740	HIS4	-2.34	0.00	AT2G03570	NA	1.06	0.00
AT2G28950	ATEXP6	-1.01	0.00	AT2G03890	ATPI4K	1.16	0.00
AT2G29170	NA	-2.04	0.00	AT2G04030	AtHsp90.5	1.67	0.00
AT2G29550	TUB7	-1.36	0.00	AT2G04240	XERICO	1.97	0.00
AT2G29570	ATPCNA2	-1.28	0.00	AT2G05540	NA	1.31	0.00
AT2G29980	AtFAD3	-1.37	0.00	AT2G05580	NA	1.32	0.01
AT2G30010	TBL45	-2.88	0.00	AT2G05630	ATG8D	1.03	0.00
AT2G30420	ETC2	-1.64	0.00	AT2G07671	NA	2.86	0.00
AT2G30424	TCL2	-1.83	0.00	AT2G07706	NA	1.71	0.00
AT2G30600	NA	-1.45	0.00	AT2G11891	NA	2.03	0.00
AT2G30620	NA	-1.35	0.00	AT2G12400	NA	1.50	0.00
AT2G30766	NA	-2.79	0.00	AT2G13960	NA	1.69	0.00
AT2G30770	CYP71A13	-1.59	0.00	AT2G15240	NA	1.02	0.00
AT2G30820	NA	-1.66	0.00	AT2G16720	ATMYB7	1.28	0.00
AT2G30930	NA	-2.02	0.00	AT2G16990	NA	1.57	0.00
AT2G30942	NA	-1.48	0.00	AT2G17036	NA	2.04	0.00
AT2G31230	ATERF15	-1.26	0.00	AT2G17040	NAC036	1.20	0.00
AT2G31270	ATCDT1A	-2.00	0.00	AT2G17787	NA	1.13	0.00
AT2G31360	ADS2	-1.16	0.00	AT2G17900	ASHR1	2.37	0.00
AT2G31750	UGT74D1	-1.74	0.00	AT2G17975	NA	1.21	0.00
AT2G32100	ATOF16	-1.31	0.00	AT2G18050	HIS1-3	1.85	0.00
AT2G32200	NA	-1.07	0.00	AT2G18370	NA	1.20	0.00
AT2G32380	NA	-1.27	0.00	AT2G18550	ATHB21	1.45	0.00
AT2G32590	EMB2795	-1.64	0.00	AT2G18780	NA	1.19	0.00
AT2G32690	ATGRP23	-1.00	0.00	AT2G19240	NA	1.00	0.00
AT2G33050	AtRLP26	-1.08	0.00	AT2G19310	NA	2.74	0.00

AT2G33330	PDLP3	-2.29	0.00	AT2G19350	NA	1.02	0.00
AT2G33400	NA	-1.06	0.00	AT2G19810	AtOZF1	1.32	0.00
AT2G33520	NA	-3.18	0.00	AT2G19930	NA	1.22	0.00
AT2G33560	BUBR1	-1.96	0.00	AT2G20400	NA	1.41	0.00
AT2G34010	NA	-1.55	0.00	AT2G20560	NA	4.00	0.00
AT2G34060	NA	-1.78	0.00	AT2G20585	NFD6	1.70	0.00
AT2G34190	NA	-1.08	0.00	AT2G20770	GCL2	1.65	0.00
AT2G34300	NA	-1.04	0.00	AT2G21130	NA	1.02	0.00
AT2G34430	LHB1B1	-1.15	0.00	AT2G21710	EMB2219	1.32	0.00
AT2G34510	NA	-1.12	0.00	AT2G21820	NA	4.47	0.00
AT2G34530	NA	-1.17	0.00	AT2G22345	NA	1.62	0.01
AT2G34930	NA	-3.56	0.00	AT2G22420	NA	1.89	0.00
AT2G34940	BP80-3;2	-1.30	0.00	AT2G22470	AGP2	2.30	0.00
AT2G35190	ATNPSN11	-1.70	0.00	AT2G22680	WAVH1	1.18	0.00
AT2G35970	NA	-2.91	0.00	AT2G22850	AtbZIP6	1.11	0.00
AT2G35980	ATNHL10	-1.64	0.00	AT2G24540	AFR	1.20	0.00
AT2G36050	ATOFFP15	-1.28	0.00	AT2G24960	NA	1.32	0.00
AT2G36200	NA	-2.15	0.00	AT2G25090	CIPK16	1.74	0.00
AT2G36310	NSH1	-1.41	0.00	AT2G25140	CLPB-M	2.48	0.00
AT2G36320	NA	-1.27	0.00	AT2G25460	NA	1.67	0.00
AT2G36470	NA	-1.95	0.00	AT2G25820	ESE2	1.49	0.00
AT2G36590	ATPROT3	-1.93	0.00	AT2G25910	NA	1.27	0.00
AT2G36880	MAT3	-1.83	0.00	AT2G26030	NA	1.07	0.00
AT2G36881	NA	-1.27	0.00	AT2G26150	ATHSFA2	5.40	0.00
AT2G36970	NA	-2.37	0.00	AT2G26860	NA	1.70	0.00
AT2G37025	TRFL8	-1.11	0.00	AT2G27550	ATC	3.09	0.00
AT2G37100	NA	-1.02	0.00	AT2G27580	NA	1.10	0.00
AT2G37130	NA	-2.12	0.00	AT2G27830	NA	1.11	0.00
AT2G37460	NA	-1.67	0.00	AT2G28110	FRA8	1.09	0.00
AT2G37470	NA	-1.17	0.00	AT2G28400	NA	1.80	0.00
AT2G37560	ATORC2	-1.95	0.00	AT2G28500	LBD11	2.05	0.00
AT2G37620	AAc1	-1.05	0.00	AT2G29130	ATLAC2	1.32	0.00
AT2G37640	ATEXP3	-1.81	0.00	AT2G29263	NA	1.01	0.01
AT2G37950	NA	-2.04	0.00	AT2G29300	NA	2.04	0.00
AT2G37960	NA	-2.12	0.00	AT2G29500	NA	7.77	0.00
AT2G38120	AUX1	-1.00	0.00	AT2G30480	NA	2.04	0.00
AT2G38310	PYL4	-1.81	0.00	AT2G30540	NA	1.28	0.00
AT2G38620	CDKB1;2	-2.02	0.00	AT2G30550	NA	1.16	0.00
AT2G38700	ATMVD1	-1.02	0.00	AT2G31083	AtCLE5	1.16	0.04
AT2G38750	ANNAT4	-1.02	0.00	AT2G31350	GLX2-5	1.20	0.00
AT2G38810	HTA8	-1.35	0.00	AT2G31970	ATRAD50	1.15	0.00
AT2G38860	YLS5	-1.09	0.00	AT2G32090	NA	1.23	0.00
AT2G39180	ATCRR2	-1.08	0.00	AT2G32120	HSP70T-2	5.07	0.00
AT2G39220	PLA	-1.14	0.00	AT2G32130	NA	1.66	0.00
AT2G40150	TBL28	-1.37	0.00	AT2G32140	NA	1.32	0.00
AT2G40230	NA	-1.04	0.00	AT2G32340	NA	2.15	0.00
AT2G40260	NA	-1.08	0.00	AT2G32870	NA	1.15	0.00
AT2G40330	PYL6	-2.03	0.01	AT2G32880	NA	1.05	0.00
AT2G40490	HEME2	-1.19	0.00	AT2G33000	NA	1.25	0.00
AT2G40550	ETG1	-1.08	0.00	AT2G33060	AtRLP27	1.60	0.00
AT2G40610	ATEXP8	-1.85	0.00	AT2G33070	ATNSP2	1.00	0.00
AT2G40670	ARR16	-2.62	0.00	AT2G33280	NA	1.80	0.00
AT2G40750	ATWRKY54	-2.89	0.00	AT2G33380	AtCLO3	1.49	0.00
AT2G41100	ATCAL4	-1.44	0.00	AT2G33590	NA	1.68	0.00
AT2G41450	NA	-1.58	0.00	AT2G33735	NA	1.57	0.00
AT2G41560	ACA4	-1.40	0.00	AT2G33740	CUTA	1.30	0.00
AT2G41730	NA	-1.24	0.00	AT2G34730	NA	1.20	0.00
AT2G41880	AGK1	-1.29	0.00	AT2G34850	MEE25	1.81	0.00
AT2G42110	NA	-1.74	0.00	AT2G35060	KUP11	1.09	0.00
AT2G42200	AtSPL9	-1.19	0.00	AT2G35070	NA	2.78	0.00
AT2G42260	PYM	-1.67	0.00	AT2G35300	AtLEA4-2	1.92	0.00
AT2G42380	ATBZIP34	-1.37	0.00	AT2G35550	ATBPC7	1.37	0.00

SUPPLEMENTARY MATERIALS

AT2G42610	LSH10	-1.45	0.00	AT2G35750	NA	1.42	0.00
AT2G42770	NA	-1.02	0.00	AT2G35950	EDA12	1.59	0.00
AT2G42870	HLH1	-1.39	0.00	AT2G36030	NA	1.68	0.00
AT2G42990	NA	-1.08	0.00	AT2G36053	NA	1.60	0.00
AT2G43040	NPG1	-1.25	0.00	AT2G36261	NA	1.25	0.00
AT2G43150	NA	-1.31	0.00	AT2G36460	NA	1.16	0.00
AT2G43360	BIO2	-1.29	0.00	AT2G36640	ATECP63	2.93	0.00
AT2G43520	ATTI2	-1.35	0.00	AT2G36730	NA	1.23	0.00
AT2G43535	NA	-1.58	0.00	AT2G36750	UGT73C1	3.24	0.00
AT2G43550	NA	-1.93	0.00	AT2G36780	NA	1.15	0.00
AT2G44230	NA	-1.60	0.00	AT2G36854	NA	1.18	0.00
AT2G44240	NA	-1.53	0.00	AT2G36900	ATMEMB11	1.08	0.00
AT2G44490	BGLU26	-1.26	0.00	AT2G36950	NA	1.19	0.00
AT2G44580	NA	-2.02	0.00	AT2G37090	IRX9	1.14	0.00
AT2G44740	CYCP4;1	-2.67	0.00	AT2G37150	NA	1.88	0.00
AT2G44790	UCC2	-1.47	0.00	AT2G37200	NA	1.47	0.00
AT2G45080	cycp3;1	-1.32	0.00	AT2G37340	AT-RS2Z33	1.68	0.00
AT2G45300	NA	-1.15	0.00	AT2G37530	NA	1.15	0.00
AT2G45470	AGP8	-1.58	0.00	AT2G37760	AKR4C8	1.47	0.00
AT2G45970	CYP86A8	-1.21	0.00	AT2G37770	AKR4C9	1.56	0.00
AT2G46330	AGP16	-2.31	0.00	AT2G37900	NA	2.86	0.00
AT2G46870	NGA1	-1.04	0.00	AT2G38255	NA	2.61	0.00
AT2G47130	AtSDR3	-1.25	0.00	AT2G38340	DREB19	2.15	0.00
AT2G47240	CER8	-1.67	0.00	AT2G38530	LP2	1.05	0.00
AT2G47370	NA	-1.20	0.00	AT2G38600	NA	1.19	0.00
AT2G47910	CRR6	-1.14	0.00	AT2G38800	NA	1.42	0.00
AT2G47930	AGP26	-1.08	0.00	AT2G38820	NA	1.80	0.00
AT2G48020	NA	-1.91	0.00	AT2G39020	NA	1.15	0.00
AT2G48030	NA	-1.43	0.00	AT2G39110	NA	2.18	0.00
AT3G01290	AtHIR2	-1.89	0.00	AT2G39230	LOJ	1.09	0.00
AT3G01480	ATCYP38	-1.08	0.00	AT2G39570	ACR9	1.29	0.00
AT3G01550	ATPPT2	-2.72	0.00	AT2G39800	ATP5CS	2.34	0.00
AT3G01680	SEOR1	-1.27	0.00	AT2G40170	ATEM6	1.04	0.00
AT3G01690	NA	-1.17	0.00	AT2G40320	TBL33	1.08	0.00
AT3G01750	NA	-1.51	0.00	AT2G40350	NA	1.21	0.00
AT3G01920	NA	-1.09	0.00	AT2G40470	ASL11	1.33	0.00
AT3G01960	NA	-1.18	0.00	AT2G40711	NA	1.78	0.00
AT3G02040	AtGDPD1	-1.45	0.00	AT2G41070	ATBZIP12	1.60	0.00
AT3G02120	NA	-3.17	0.00	AT2G41150	NA	1.00	0.00
AT3G02230	ATRGP1	-1.50	0.00	AT2G41190	NA	3.86	0.00
AT3G02570	MEE31	-1.49	0.00	AT2G41200	NA	1.48	0.00
AT3G02640	NA	-2.74	0.00	AT2G41210	PIP5K5	1.83	0.00
AT3G02820	NA	-1.15	0.00	AT2G41330	NA	1.49	0.00
AT3G03000	NA	-2.29	0.00	AT2G41410	NA	1.30	0.00
AT3G03130	NA	-2.32	0.00	AT2G41440	NA	1.22	0.00
AT3G03250	AtUGP1	-1.16	0.00	AT2G41480	NA	1.27	0.00
AT3G03260	HDG8	-1.64	0.00	AT2G41870	NA	1.45	0.00
AT3G03350	NA	-1.27	0.00	AT2G41905	NA	1.95	0.00
AT3G03780	ATMS2	-1.73	0.00	AT2G42270	NA	1.35	0.00
AT3G03820	NA	-1.38	0.00	AT2G42330	NA	2.44	0.00
AT3G03840	NA	-1.27	0.00	AT2G42395	NA	1.79	0.00
AT3G03850	NA	-2.18	0.00	AT2G42560	NA	3.09	0.00
AT3G03910	GDH3	-1.40	0.00	AT2G42920	NA	1.11	0.00
AT3G03990	NA	-1.46	0.00	AT2G43570	CHI	1.49	0.00
AT3G04210	NA	-2.92	0.00	AT2G43580	NA	2.04	0.00
AT3G04290	ATLTL1	-2.61	0.00	AT2G43800	NA	1.76	0.00
AT3G04570	AHL19	-1.70	0.00	AT2G43840	UGT74F1	1.04	0.00
AT3G04720	HEL	-3.89	0.00	AT2G43930	NA	1.45	0.00
AT3G04780	NA	-1.08	0.00	AT2G45360	NA	1.20	0.00
AT3G04790	EMB3119	-1.48	0.00	AT2G45380	NA	1.47	0.00
AT3G04910	ATWNK1	-1.40	0.00	AT2G45610	NA	1.31	0.00
AT3G05020	ACP	-1.12	0.00	AT2G45680	NA	1.17	0.00

AT3G05140	RBK2	-1.26	0.00	AT2G45920	NA	2.17	0.00
AT3G05330	ATN	-1.59	0.00	AT2G46240	ATBAG6	3.17	0.00
AT3G05470	NA	-1.07	0.00	AT2G46270	GBF3	3.60	0.00
AT3G05600	NA	-2.17	0.00	AT2G46610	At-RS31a	1.65	0.00
AT3G05625	NA	-1.22	0.00	AT2G46680	ATHB-7	3.14	0.00
AT3G05727	NA	-1.63	0.00	AT2G46760	NA	1.17	0.00
AT3G05730	NA	-3.23	0.00	AT2G46800	ATCDF1	1.71	0.00
AT3G05740	RECQ1	-1.28	0.00	AT2G46830	AtCCA1	1.39	0.00
AT3G05800	AIF1	-1.68	0.00	AT2G46940	NA	2.24	0.00
AT3G05910	NA	-1.31	0.00	AT2G46950	CYP709B2	1.07	0.00
AT3G06070	NA	-2.37	0.00	AT2G47180	AtGolS1	3.38	0.00
AT3G06080	TBL10	-1.23	0.00	AT2G47560	NA	1.39	0.00
AT3G06145	NA	-1.37	0.00	AT2G47770	ATTSP0	5.85	0.00
AT3G06740	GATA15	-1.70	0.00	AT2G47780	NA	2.67	0.00
AT3G06750	NA	-1.11	0.00	AT2G47950	NA	1.11	0.00
AT3G06770	NA	-1.68	0.00	AT2G48100	NA	1.08	0.00
AT3G06840	NA	-1.61	0.00	AT3G01100	ATHYP1	1.12	0.00
AT3G06868	NA	-1.23	0.00	AT3G01210	NA	1.22	0.00
AT3G06880	NA	-1.23	0.00	AT3G01350	NA	1.48	0.00
AT3G06890	NA	-1.44	0.00	AT3G01520	NA	1.23	0.00
AT3G06985	LCR44	-1.21	0.00	AT3G01570	NA	1.12	0.00
AT3G07010	NA	-2.49	0.00	AT3G01770	ATBET10	1.62	0.00
AT3G07170	NA	-1.12	0.00	AT3G02140	AFP4	1.90	0.00
AT3G07195	NA	-1.17	0.00	AT3G02210	COBL1	1.59	0.00
AT3G07390	AIR12	-1.04	0.00	AT3G02390	NA	1.29	0.00
AT3G07460	NA	-1.81	0.00	AT3G02490	NA	1.21	0.00
AT3G07470	NA	-2.07	0.00	AT3G03030	NA	1.14	0.00
AT3G07480	NA	-1.10	0.00	AT3G03170	NA	3.16	0.00
AT3G07525	ATATG10	-1.17	0.00	AT3G03230	NA	1.95	0.00
AT3G08580	AAC1	-1.11	0.00	AT3G03270	NA	1.24	0.00
AT3G08600	NA	-1.12	0.00	AT3G03310	ATLCAT3	1.47	0.00
AT3G08770	LTP6	-1.23	0.00	AT3G03330	NA	1.22	0.00
AT3G08920	NA	-1.07	0.00	AT3G03341	NA	1.94	0.00
AT3G09010	NA	-1.26	0.00	AT3G03470	CYP89A9	1.40	0.00
AT3G09020	NA	-2.12	0.00	AT3G03480	CHAT	1.52	0.00
AT3G09270	ATGSTU8	-1.68	0.00	AT3G03520	NPC3	1.11	0.00
AT3G09480	NA	-1.75	0.00	AT3G03950	ECT1	1.22	0.00
AT3G09580	NA	-1.43	0.00	AT3G04000	NA	2.38	0.00
AT3G09780	ATCRR1	-1.08	0.00	AT3G04070	NAC047	1.11	0.00
AT3G09940	ATMDAR3	-2.07	0.00	AT3G04160	NA	1.69	0.00
AT3G09990	NA	-1.36	0.01	AT3G04240	SEC	1.08	0.00
AT3G10050	OMR1	-1.47	0.00	AT3G04710	TPR10	1.50	0.00
AT3G10260	NA	-1.17	0.00	AT3G05165	NA	1.23	0.00
AT3G10520	AHB2	-1.91	0.00	AT3G05640	NA	1.26	0.00
AT3G10610	NA	-1.38	0.00	AT3G05650	AtRLP32	1.86	0.00
AT3G10660	ATCPK2	-1.22	0.00	AT3G05790	LON4	1.38	0.00
AT3G10720	NA	-1.89	0.00	AT3G06400	CHR11	1.03	0.00
AT3G11110	NA	-1.36	0.00	AT3G06520	NA	1.41	0.00
AT3G11210	NA	-1.12	0.00	AT3G07090	NA	1.39	0.00
AT3G11520	CYC2	-1.77	0.00	AT3G07150	NA	3.24	0.00
AT3G12110	ACT11	-1.24	0.00	AT3G07273	NA	1.17	0.00
AT3G12145	FLOR1	-1.52	0.00	AT3G07350	NA	1.06	0.00
AT3G12150	NA	-1.09	0.00	AT3G07770	AtHsp90-6	1.81	0.00
AT3G12170	NA	-2.37	0.00	AT3G08020	NA	1.05	0.00
AT3G12610	DRT100	-1.82	0.00	AT3G08690	ATUBC11	1.16	0.00
AT3G12700	NA	-1.33	0.00	AT3G08860	PYD4	2.21	0.00
AT3G12710	NA	-1.14	0.00	AT3G08970	ATERDJ3A	2.84	0.00
AT3G12870	NA	-2.13	0.00	AT3G09100	NA	1.10	0.00
AT3G13060	ECT5	-1.24	0.00	AT3G09350	Fes1A	1.95	0.00
AT3G13110	ATSERAT2;2	-1.16	0.00	AT3G09720	NA	1.22	0.00
AT3G13650	NA	-1.23	0.00	AT3G09770	LOG2	1.01	0.00
AT3G13750	BGAL1	-1.51	0.00	AT3G10020	NA	2.42	0.00

SUPPLEMENTARY MATERIALS

AT3G13790	ATBFRUCT1	-2.71	0.00	AT3G10030	NA	1.20	0.00
AT3G13930	NA	-1.08	0.00	AT3G10190	NA	1.23	0.00
AT3G14020	NF-YA6	-1.12	0.00	AT3G10250	NA	1.01	0.00
AT3G14220	NA	-1.10	0.00	AT3G10815	NA	1.53	0.00
AT3G14310	ATPME3	-1.89	0.00	AT3G10985	ATWI-12	1.16	0.00
AT3G14740	NA	-2.55	0.00	AT3G11020	DREB2	1.03	0.00
AT3G14760	NA	-1.22	0.00	AT3G11410	AHG3	2.17	0.00
AT3G14820	NA	-2.58	0.00	AT3G11420	NA	1.20	0.00
AT3G14840	NA	-1.42	0.00	AT3G11690	NA	2.04	0.00
AT3G14850	TBL41	-1.77	0.00	AT3G11930	NA	1.05	0.00
AT3G14890	NA	-1.14	0.00	AT3G12050	NA	1.95	0.00
AT3G15030	MEE35	-1.33	0.00	AT3G12300	NA	1.08	0.00
AT3G15060	AtRABA1g	-1.65	0.00	AT3G12510	NA	1.46	0.00
AT3G15356	NA	-4.43	0.00	AT3G12530	PSF2	1.24	0.00
AT3G15450	NA	-1.78	0.00	AT3G12580	ATHSP70	6.28	0.00
AT3G15540	IAA19	-1.38	0.00	AT3G12770	MEF22	1.28	0.00
AT3G15550	NA	-1.75	0.00	AT3G12860	NA	1.67	0.00
AT3G15570	NA	-1.74	0.00	AT3G12915	NA	1.16	0.00
AT3G15620	UVR3	-1.38	0.00	AT3G12955	NA	2.05	0.00
AT3G15630	NA	-2.21	0.00	AT3G13020	NA	1.24	0.00
AT3G15680	NA	-1.35	0.00	AT3G13130	NA	1.61	0.00
AT3G15720	NA	-1.21	0.00	AT3G13224	NA	1.82	0.00
AT3G15820	ROD1	-1.02	0.00	AT3G13672	NA	2.51	0.00
AT3G15850	ADS3	-1.03	0.00	AT3G13784	AtcwINV5	5.04	0.00
AT3G16070	NA	-1.19	0.00	AT3G14200	NA	1.05	0.00
AT3G16180	NA	-1.02	0.00	AT3G14360	NA	2.83	0.00
AT3G16240	AQP1	-1.81	0.00	AT3G14440	ATNCED3	1.85	0.00
AT3G16410	NSP4	-2.62	0.00	AT3G14560	NA	2.89	0.00
AT3G16420	JAL30	-1.63	0.00	AT3G14590	NTMC2T6.2	2.43	0.00
AT3G16460	JAL34	-1.08	0.00	AT3G14595	NA	1.08	0.00
AT3G16530	NA	-5.99	0.00	AT3G15000	NA	1.05	0.00
AT3G16660	NA	-1.78	0.00	AT3G15280	NA	1.82	0.00
AT3G16670	NA	-4.13	0.00	AT3G15340	PPI2	2.43	0.00
AT3G16690	AtSWEET16	-1.20	0.00	AT3G15350	NA	1.17	0.00
AT3G16700	NA	-1.16	0.00	AT3G15357	NA	1.34	0.00
AT3G17390	MAT4	-1.70	0.00	AT3G15400	ATA20	1.26	0.00
AT3G17609	HYH	-1.06	0.00	AT3G15500	ANAC055	1.02	0.00
AT3G17640	NA	-1.49	0.00	AT3G15534	NA	2.50	0.00
AT3G17680	NA	-1.35	0.00	AT3G15670	NA	1.42	0.00
AT3G17780	NA	-1.03	0.00	AT3G15780	NA	1.67	0.00
AT3G18050	NA	-1.01	0.00	AT3G15790	ATMBD11	1.07	0.00
AT3G18080	BGLU44	-1.38	0.00	AT3G15990	SULTR3;4	1.04	0.00
AT3G18130	RACK1C	-1.14	0.00	AT3G16050	A37	2.98	0.00
AT3G18730	BRU1	-1.27	0.00	AT3G16400	ATMLP-470	1.23	0.00
AT3G18780	ACT2	-1.09	0.00	AT3G16650	NA	1.14	0.00
AT3G19010	NA	-1.10	0.00	AT3G16920	ATCTL2	1.39	0.00
AT3G19050	POK2	-1.53	0.00	AT3G17180	scpl33	1.91	0.00
AT3G19350	MPC	-1.98	0.00	AT3G17460	NA	1.72	0.00
AT3G19360	NA	-1.01	0.00	AT3G17520	NA	6.23	0.00
AT3G19400	NA	-1.08	0.00	AT3G17611	ATRBL14	1.99	0.00
AT3G19480	NA	-1.19	0.00	AT3G17630	ATCHX19	1.48	0.00
AT3G19550	NA	-1.40	0.00	AT3G17740	NA	1.43	0.00
AT3G19660	NA	-1.86	0.00	AT3G17790	ATACP5	1.10	0.00
AT3G19850	NA	-1.18	0.00	AT3G17800	NA	1.39	0.00
AT3G19930	ATSTP4	-1.21	0.00	AT3G17980	AtC2	1.40	0.00
AT3G20150	NA	-1.64	0.00	AT3G18280	NA	1.58	0.00
AT3G20370	NA	-1.68	0.00	AT3G19100	NA	1.28	0.00
AT3G20450	NA	-1.57	0.00	AT3G19580	AZF2	1.13	0.00
AT3G20570	AtENODL9	-1.38	0.00	AT3G19620	NA	2.02	0.00
AT3G20670	HTA13	-1.28	0.00	AT3G20100	CYP705A19	1.32	0.00
AT3G20790	NA	-1.09	0.00	AT3G20250	APUM5	1.19	0.00
AT3G21080	NA	-1.57	0.00	AT3G20300	NA	1.41	0.00

AT3G21510	AHP1	-1.20	0.00	AT3G20310	ATERF-7	1.86	0.00
AT3G21950	NA	-2.44	0.00	AT3G20500	ATPAP18	1.10	0.00
AT3G22142	NA	-2.71	0.00	AT3G20660	AtOCT4	1.05	0.00
AT3G22210	NA	-2.07	0.00	AT3G20810	JMJ30	2.09	0.00
AT3G22231	PCC1	-3.90	0.00	AT3G21150	BBX32	1.21	0.00
AT3G22235	NA	-3.53	0.00	AT3G21240	4CL2	1.27	0.00
AT3G22400	ATLOX5	-1.35	0.00	AT3G21250	ABCC8	1.03	0.00
AT3G23172	NA	-1.60	0.03	AT3G21260	GLTP3	1.50	0.00
AT3G23390	NA	-1.03	0.00	AT3G21600	NA	1.79	0.00
AT3G23510	NA	-1.26	0.00	AT3G21660	NA	2.40	0.00
AT3G23530	NA	-1.40	0.00	AT3G21740	APO4	1.18	0.00
AT3G23670	KINESIN-12B	-2.31	0.00	AT3G21890	NA	1.46	0.00
AT3G23730	XTH16	-3.02	0.00	AT3G22560	NA	2.81	0.00
AT3G23740	NA	-1.09	0.00	AT3G22830	AT-HSFA6B	4.11	0.00
AT3G23805	RALFL24	-1.36	0.00	AT3G22840	ELIP	2.71	0.00
AT3G23810	ATSAHH2	-2.15	0.00	AT3G22910	NA	1.02	0.00
AT3G23880	NA	-1.06	0.00	AT3G22942	AGG2	1.03	0.00
AT3G23890	ATTOPII	-1.91	0.00	AT3G23000	ATSR2	1.64	0.00
AT3G24420	NA	-1.77	0.00	AT3G23020	NA	1.21	0.00
AT3G24503	ALDH1A	-1.13	0.00	AT3G23260	NA	2.15	0.00
AT3G25100	CDC45	-2.65	0.00	AT3G23920	BAM1	1.67	0.00
AT3G25180	CYP82G1	-2.31	0.00	AT3G24100	NA	2.50	0.00
AT3G25600	NA	-1.36	0.00	AT3G24500	ATMBF1C	5.06	0.00
AT3G25700	NA	-1.13	0.00	AT3G24520	AT-HSFC1	2.40	0.00
AT3G25717	DVL6	-1.32	0.00	AT3G24750	NA	1.63	0.00
AT3G25882	NIMIN-2	-2.90	0.00	AT3G25290	NA	1.80	0.00
AT3G25980	MAD2	-1.75	0.00	AT3G25620	ABCG21	1.05	0.00
AT3G26200	CYP71B22	-3.09	0.00	AT3G25870	NA	1.64	0.00
AT3G26320	CYP71B36	-1.42	0.00	AT3G26350	NA	2.00	0.00
AT3G26490	NA	-1.30	0.00	AT3G26510	NA	1.57	0.00
AT3G26520	GAMMA-TIP2	-1.17	0.00	AT3G26742	NA	2.37	0.00
AT3G26680	ATSNM1	-1.15	0.00	AT3G26790	FUS3	1.21	0.00
AT3G26700	NA	-1.18	0.00	AT3G26800	NA	1.57	0.00
AT3G26780	MEF14	-1.23	0.00	AT3G26920	NA	1.04	0.00
AT3G27050	NA	-1.07	0.00	AT3G27025	NA	3.43	0.00
AT3G27060	ATTSO2	-2.52	0.00	AT3G27170	ATCLC-B	1.76	0.00
AT3G27360	NA	-2.19	0.00	AT3G27200	NA	1.10	0.00
AT3G27500	NA	-1.15	0.00	AT3G27210	NA	2.00	0.00
AT3G27640	NA	-2.29	0.00	AT3G27250	NA	1.58	0.00
AT3G27690	LHCB2	-1.74	0.00	AT3G27860	NA	1.17	0.00
AT3G27750	EMB3123	-1.03	0.00	AT3G28007	AtSWEET4	1.55	0.00
AT3G28130	NA	-1.00	0.00	AT3G28270	NA	3.13	0.00
AT3G28180	ATCSLC04	-2.02	0.00	AT3G29140	NA	1.47	0.00
AT3G28220	NA	-2.41	0.00	AT3G29575	AFP3	2.58	0.00
AT3G28510	NA	-3.00	0.00	AT3G29810	COBL2	2.13	0.00
AT3G28580	NA	-2.22	0.00	AT3G30210	ATMYB121	1.71	0.00
AT3G28910	ATMYB30	-1.28	0.00	AT3G42860	NA	1.42	0.00
AT3G28930	AIG2	-2.29	0.00	AT3G43210	ATNACK2	1.28	0.00
AT3G29034	NA	-1.24	0.00	AT3G43520	NA	1.33	0.00
AT3G30180	BR6OX2	-1.78	0.00	AT3G44290	NAC060	1.19	0.00
AT3G30775	AT-POX	-1.20	0.00	AT3G44440	NA	2.10	0.00
AT3G32050	NA	-1.41	0.00	AT3G45420	NA	2.08	0.00
AT3G42725	NA	-1.52	0.00	AT3G45680	NA	1.92	0.00
AT3G42800	NA	-1.07	0.00	AT3G46230	ATHSP17.4	9.00	0.00
AT3G43720	NA	-1.68	0.00	AT3G46450	NA	1.30	0.00
AT3G43800	ATGSTU27	-1.33	0.00	AT3G46920	NA	1.31	0.00
AT3G44050	NA	-1.25	0.00	AT3G47080	NA	1.22	0.00
AT3G44350	NAC061	-1.20	0.00	AT3G47110	NA	1.12	0.00
AT3G44450	NA	-2.88	0.00	AT3G47360	ATHSD3	1.04	0.00
AT3G44755	NA	-1.49	0.00	AT3G47580	NA	1.31	0.00
AT3G44970	NA	-1.66	0.00	AT3G47600	ATMYB94	1.50	0.00
AT3G44990	ATXTR8	-1.14	0.00	AT3G48020	NA	2.25	0.00

SUPPLEMENTARY MATERIALS

AT3G45140	ATLOX2	-2.05	0.00	AT3G48240	NA	3.27	0.00
AT3G45260	NA	-1.18	0.00	AT3G48330	ATPIMT1	1.13	0.00
AT3G45640	ATMAPK3	-1.03	0.00	AT3G48390	NA	1.67	0.00
AT3G45650	NAXT1	-1.02	0.00	AT3G48510	NA	2.15	0.00
AT3G45810	NA	-1.82	0.00	AT3G48520	CYP94B3	1.29	0.03
AT3G45850	NA	-1.30	0.00	AT3G48580	XTH11	1.13	0.00
AT3G45860	CRK4	-1.18	0.00	AT3G48790	NA	1.54	0.00
AT3G45930	NA	-2.37	0.00	AT3G48830	NA	3.26	0.00
AT3G45980	H2B	-1.73	0.00	AT3G49130	NA	3.02	0.00
AT3G46030	HTB11	-1.31	0.00	AT3G49320	NA	1.90	0.00
AT3G46110	NA	-1.57	0.00	AT3G49570	LSU3	1.37	0.00
AT3G46320	NA	-3.74	0.00	AT3G49580	LSU1	1.45	0.00
AT3G46650	NA	-1.42	0.00	AT3G49760	AtbZIP5	1.59	0.01
AT3G46820	TOPP5	-1.54	0.00	AT3G50410	OBP1	1.17	0.00
AT3G46940	DUT1	-2.62	0.00	AT3G50540	NA	1.48	0.00
AT3G47380	NA	-2.22	0.00	AT3G50770	CML41	1.74	0.00
AT3G47480	NA	-1.72	0.00	AT3G50910	NA	1.30	0.00
AT3G47800	NA	-1.33	0.00	AT3G50940	NA	1.76	0.00
AT3G47820	PUB39	-1.21	0.00	AT3G50980	XERO1	2.41	0.00
AT3G47830	NA	-1.08	0.00	AT3G51810	AT3	1.65	0.00
AT3G48080	NA	-2.62	0.00	AT3G51860	ATCAX3	1.89	0.00
AT3G48100	ARR5	-1.39	0.00	AT3G52780	ATPAP20	1.10	0.00
AT3G48160	DEL1	-1.27	0.00	AT3G53100	NA	1.28	0.00
AT3G48360	ATBT2	-2.50	0.00	AT3G53160	UGT73C7	1.24	0.00
AT3G48490	NA	-1.84	0.00	AT3G53230	NA	2.57	0.00
AT3G48540	NA	-1.47	0.00	AT3G53370	NA	1.46	0.00
AT3G48720	DCF	-2.85	0.00	AT3G53630	NA	1.54	0.00
AT3G49110	ATPCA	-2.31	0.00	AT3G53690	NA	1.32	0.00
AT3G49260	iqd21	-1.67	0.00	AT3G53960	NA	1.08	0.00
AT3G49670	BAM2	-1.51	0.00	AT3G53970	NA	1.17	0.00
AT3G49720	NA	-1.28	0.00	AT3G53980	NA	5.55	0.00
AT3G49930	NA	-1.65	0.00	AT3G54000	NA	1.77	0.00
AT3G49940	LBD38	-1.84	0.00	AT3G54390	NA	1.78	0.00
AT3G49960	NA	-1.32	0.00	AT3G55840	NA	2.20	0.00
AT3G50010	NA	-1.41	0.00	AT3G55910	NA	2.46	0.00
AT3G50060	MYB77	-1.00	0.00	AT3G56270	NA	1.27	0.00
AT3G50120	NA	-1.77	0.00	AT3G56320	NA	1.27	0.00
AT3G50270	NA	-1.61	0.00	AT3G56470	NA	1.07	0.00
AT3G50280	NA	-1.03	0.00	AT3G56880	NA	1.05	0.00
AT3G50480	HR4	-1.05	0.00	AT3G56960	PIP5K4	1.44	0.00
AT3G50560	NA	-1.69	0.00	AT3G57010	NA	1.02	0.00
AT3G50740	UGT72E1	-1.05	0.00	AT3G57360	NA	1.12	0.00
AT3G50750	BEH1	-1.35	0.00	AT3G57520	AtSIP2	1.78	0.00
AT3G50900	NA	-1.46	0.00	AT3G57590	NA	1.21	0.00
AT3G51080	GATA6	-1.07	0.00	AT3G57810	NA	1.01	0.00
AT3G51160	GMD2	-1.61	0.00	AT3G57880	NA	2.03	0.00
AT3G51230	NA	-2.10	0.00	AT3G58150	NA	1.25	0.00
AT3G51280	NA	-2.87	0.00	AT3G58270	NA	1.22	0.00
AT3G51290	NA	-1.05	0.00	AT3G58810	ATMTP3	1.31	0.00
AT3G51470	NA	-2.18	0.00	AT3G58930	NA	1.26	0.00
AT3G51720	NA	-1.79	0.00	AT3G59150	NA	1.12	0.00
AT3G51740	IMK2	-2.15	0.00	AT3G59280	TXR1	1.07	0.00
AT3G51930	NA	-1.15	0.00	AT3G59350	NA	1.07	0.00
AT3G52290	IQD3	-1.08	0.00	AT3G59440	NA	1.04	0.00
AT3G52370	FLA15	-1.02	0.00	AT3G59530	LAP3	1.73	0.00
AT3G52430	ATPAD4	-1.54	0.00	AT3G59750	NA	1.67	0.00
AT3G52630	NA	-2.22	0.00	AT3G59820	NA	1.24	0.00
AT3G52690	NA	-3.21	0.01	AT3G60300	NA	1.51	0.00
AT3G53010	NA	-1.21	0.00	AT3G60670	NA	1.18	0.00
AT3G53190	NA	-1.47	0.00	AT3G60690	NA	1.09	0.00
AT3G53232	DVL20	-1.10	0.00	AT3G61420	NA	1.37	0.00
AT3G53260	ATPAL2	-1.86	0.00	AT3G61450	ATSYP73	1.44	0.00

AT3G53650	NA	-1.67	0.00	AT3G61630	CRF6	1.46	0.00
AT3G53730	NA	-2.18	0.00	AT3G61830	ARF18	1.06	0.00
AT3G54120	NA	-1.72	0.00	AT3G61890	ATHB-12	2.44	0.00
AT3G54150	NA	-2.89	0.00	AT3G61900	NA	1.04	0.00
AT3G54250	NA	-1.20	0.00	AT3G62090	PIF6	1.72	0.00
AT3G54400	NA	-1.48	0.00	AT3G62190	NA	1.10	0.00
AT3G54560	HTA11	-2.42	0.00	AT3G62260	NA	1.62	0.00
AT3G54630	NA	-1.12	0.00	AT3G62330	NA	1.16	0.00
AT3G54640	TRP3	-1.35	0.00	AT3G62430	NA	1.52	0.00
AT3G54650	FBL17	-1.95	0.00	AT3G62730	NA	1.69	0.00
AT3G54690	SETH3	-1.25	0.00	AT3G62770	ATG18a	1.91	0.00
AT3G54750	NA	-1.81	0.00	AT3G62990	NA	2.21	0.00
AT3G54920	PMR6	-1.00	0.00	AT3G63010	ATGID1B	1.26	0.00
AT3G55130	ABCG19	-1.59	0.00	AT3G63060	EDL3	1.38	0.00
AT3G55330	PPL1	-1.03	0.00	AT3G63530	BB	1.37	0.00
AT3G55520	NA	-1.09	0.00	AT4G00040	NA	1.20	0.00
AT3G55646	NA	-1.48	0.00	AT4G00700	NA	1.05	0.00
AT3G55660	ATROPGEF6	-1.37	0.00	AT4G00820	iqd17	1.02	0.00
AT3G56060	NA	-1.76	0.00	AT4G00940	NA	1.25	0.00
AT3G56090	ATFER3	-1.09	0.00	AT4G01060	CPL3	1.71	0.00
AT3G56100	IMK3	-1.64	0.00	AT4G01120	ATBZIP54	1.64	0.00
AT3G56300	NA	-1.18	0.00	AT4G01280	NA	1.24	0.00
AT3G56380	ARR17	-1.74	0.00	AT4G01610	NA	1.34	0.00
AT3G56650	NA	-1.62	0.00	AT4G01870	NA	1.12	0.00
AT3G56870	NA	-2.20	0.00	AT4G01985	NA	5.12	0.00
AT3G56970	BHLH038	-1.32	0.00	AT4G01990	NA	1.11	0.00
AT3G57060	NA	-1.21	0.00	AT4G02140	NA	1.46	0.00
AT3G57240	BG3	-1.74	0.00	AT4G02210	NA	1.36	0.00
AT3G57780	NA	-1.42	0.00	AT4G02280	ATSUS3	1.75	0.00
AT3G58120	ATBZIP61	-1.82	0.00	AT4G02360	NA	2.22	0.00
AT3G58650	NA	-1.57	0.00	AT4G02380	AtLEA5	1.34	0.00
AT3G58850	HLH2	-1.51	0.00	AT4G03030	NA	1.09	0.00
AT3G58990	IPMI1	-1.49	0.00	AT4G03230	NA	1.11	0.00
AT3G59220	ATPIRIN1	-1.71	0.00	AT4G03320	AtTic20-IV	2.33	0.00
AT3G59480	NA	-2.61	0.00	AT4G03430	EMB2770	1.20	0.00
AT3G59550	ATRAD21.2	-1.24	0.00	AT4G03820	NA	1.22	0.00
AT3G59760	ATCS-C	-1.36	0.00	AT4G04020	FIB	1.80	0.00
AT3G59900	ARGOS	-1.39	0.00	AT4G04180	NA	1.12	0.00
AT3G59970	MTHFR1	-1.66	0.00	AT4G04810	ATMSRB4	1.13	0.00
AT3G60200	NA	-1.07	0.00	AT4G05100	AtMYB74	2.01	0.00
AT3G60245	NA	-1.01	0.00	AT4G05170	NA	1.89	0.01
AT3G60290	NA	-2.01	0.00	AT4G06676	NA	1.00	0.00
AT3G60840	MAP65-4	-1.17	0.00	AT4G08250	NA	1.62	0.00
AT3G61440	ATCYSC1	-1.47	0.00	AT4G08570	NA	6.37	0.00
AT3G61610	NA	-1.34	0.00	AT4G10250	ATHSP22.0	9.41	0.00
AT3G61840	NA	-1.53	0.00	AT4G10925	NA	1.12	0.00
AT3G62110	NA	-1.90	0.00	AT4G11220	BTI2	2.07	0.00
AT3G62150	ABCB21	-2.23	0.00	AT4G11350	NA	1.94	0.00
AT3G62160	NA	-1.22	0.00	AT4G11660	AT-HSFB2B	2.35	0.00
AT3G62780	NA	-1.42	0.00	AT4G11845	NA	1.02	0.00
AT3G63110	ATIPT3	-2.41	0.00	AT4G11910	NA	1.02	0.00
AT3G63160	NA	-1.24	0.00	AT4G11960	PGRL1B	1.77	0.00
AT4G00020	BRCA2(IV)	-1.40	0.00	AT4G12005	NA	1.46	0.00
AT4G00280	NA	-1.40	0.01	AT4G12080	AHL1	1.15	0.00
AT4G00370	ANTR2	-1.07	0.00	AT4G12382	NA	1.09	0.00
AT4G00400	AtGPAT8	-1.73	0.00	AT4G12400	Hop3	6.79	0.00
AT4G00890	NA	-1.23	0.00	AT4G12410	NA	2.09	0.00
AT4G00950	MEE47	-1.08	0.00	AT4G12560	CPR1	1.29	0.00
AT4G00960	NA	-1.37	0.00	AT4G12580	NA	3.06	0.00
AT4G00970	CRK41	-2.34	0.00	AT4G13560	UNE15	1.06	0.00
AT4G01270	NA	-1.11	0.00	AT4G13750	EMB2597	1.21	0.00
AT4G01380	NA	-1.77	0.00	AT4G13800	NA	1.08	0.00

SUPPLEMENTARY MATERIALS

AT4G01390	NA	-1.66	0.00	AT4G14010	RALFL32	1.26	0.00
AT4G01690	HEMG1	-1.16	0.00	AT4G14250	NA	1.35	0.00
AT4G01700	NA	-2.02	0.00	AT4G14270	NA	1.83	0.00
AT4G01730	NA	-1.97	0.00	AT4G14716	ARD1	1.18	0.00
AT4G01950	ATGPAT3	-1.02	0.00	AT4G14819	NA	3.73	0.00
AT4G02060	MCM7	-1.82	0.00	AT4G15090	FAR1	1.29	0.00
AT4G02110	NA	-2.47	0.00	AT4G15570	MAA3	1.17	0.00
AT4G02330	ATPMEPCRB	-1.21	0.00	AT4G15730	NA	1.22	0.00
AT4G02520	ATGSTF2	-3.26	0.00	AT4G15780	ATVAMP724	1.68	0.00
AT4G02800	NA	-1.90	0.00	AT4G15910	ATDI21	2.03	0.00
AT4G02850	NA	-3.73	0.00	AT4G16190	NA	1.11	0.00
AT4G03100	NA	-1.78	0.00	AT4G16215	NA	1.00	0.00
AT4G03140	NA	-1.63	0.00	AT4G16280	FCA	2.21	0.00
AT4G03150	NA	-1.29	0.00	AT4G16444	NA	1.41	0.00
AT4G03210	XTH9	-1.73	0.00	AT4G16600	NA	1.40	0.00
AT4G03450	NA	-1.66	0.00	AT4G16680	NA	1.62	0.00
AT4G04210	PUX4	-1.04	0.00	AT4G17030	AT-EXPR	3.77	0.00
AT4G04450	AtWRKY42	-1.06	0.00	AT4G17230	SCL13	1.12	0.00
AT4G04570	CRK40	-1.63	0.00	AT4G17250	NA	1.43	0.00
AT4G04695	CPK31	-1.36	0.00	AT4G17280	NA	1.38	0.00
AT4G04700	CPK27	-1.16	0.00	AT4G17410	NA	1.13	0.00
AT4G04840	ATMSRB6	-4.23	0.00	AT4G17440	NA	1.60	0.00
AT4G05190	ATK5	-1.87	0.00	AT4G17550	AtG3Pp4	1.09	0.00
AT4G06746	DEAR5	-3.86	0.00	AT4G17730	ATSYP23	1.09	0.00
AT4G08097	NA	-4.36	0.00	AT4G17840	NA	1.03	0.00
AT4G08555	NA	-1.17	0.00	AT4G18280	NA	2.55	0.00
AT4G08870	ARGAH2	-1.68	0.00	AT4G18490	NA	1.53	0.00
AT4G09060	NA	-1.48	0.00	AT4G18550	AtDSEL	1.25	0.00
AT4G09420	NA	-1.21	0.00	AT4G18660	NA	1.26	0.00
AT4G09510	A/N-Invl	-1.09	0.00	AT4G18780	ATCESA8	1.07	0.00
AT4G10120	ATSPS4F	-1.58	0.00	AT4G18980	AtS40-3	1.56	0.00
AT4G10190	NA	-2.55	0.02	AT4G19080	NA	1.66	0.00
AT4G10820	NA	-2.11	0.00	AT4G19090	NA	1.08	0.00
AT4G11080	3xHMG-box1	-2.14	0.00	AT4G19220	NA	1.01	0.00
AT4G11190	NA	-1.47	0.00	AT4G19230	CYP707A1	1.54	0.00
AT4G11290	NA	-2.95	0.00	AT4G19430	NA	2.32	0.00
AT4G11320	NA	-1.19	0.00	AT4G20060	EMB1895	1.10	0.00
AT4G11521	NA	-1.97	0.00	AT4G20480	NA	1.01	0.00
AT4G11530	CRK34	-1.04	0.00	AT4G20820	NA	2.53	0.00
AT4G12300	CYP706A4	-1.09	0.00	AT4G21320	HSA32	5.54	0.00
AT4G12310	CYP706A5	-1.10	0.00	AT4G21410	CRK29	1.07	0.00
AT4G12320	CYP706A6	-1.69	0.00	AT4G21440	ATM4	1.13	0.00
AT4G12330	CYP706A7	-1.17	0.00	AT4G21550	VAL3	1.31	0.00
AT4G12420	SKU5	-1.59	0.00	AT4G21570	NA	1.33	0.00
AT4G12490	NA	-1.93	0.00	AT4G21650	NA	3.04	0.00
AT4G12500	NA	-1.78	0.00	AT4G21930	NA	2.95	0.00
AT4G12620	ATORC1B	-1.08	0.00	AT4G22220	ATISU1	1.03	0.00
AT4G12730	FLA2	-3.28	0.00	AT4G22280	NA	1.17	0.00
AT4G12810	NA	-2.94	0.00	AT4G22390	NA	1.57	0.00
AT4G12870	NA	-1.70	0.00	AT4G22740	NA	1.42	0.00
AT4G12980	NA	-1.77	0.00	AT4G22780	ACR7	1.07	0.00
AT4G13210	NA	-2.18	0.00	AT4G22950	AGL19	1.28	0.00
AT4G13340	LRX3	-1.20	0.00	AT4G23420	NA	1.01	0.00
AT4G13370	NA	-1.53	0.00	AT4G23493	NA	4.19	0.00
AT4G13410	ATCSLA15	-1.76	0.00	AT4G23520	NA	1.03	0.00
AT4G13690	NA	-1.07	0.00	AT4G23670	NA	1.80	0.00
AT4G13930	SHM4	-1.63	0.00	AT4G23680	NA	2.04	0.00
AT4G14120	NA	-1.11	0.00	AT4G23870	NA	1.38	0.00
AT4G14150	KINESIN-12A	-1.24	0.00	AT4G23880	NA	1.80	0.00
AT4G14310	NA	-1.46	0.00	AT4G24000	ATCSLG2	2.88	0.00
AT4G14330	NA	-1.34	0.00	AT4G24050	NA	1.18	0.00
AT4G14400	ACD6	-2.32	0.00	AT4G24910	NA	1.20	0.00

AT4G14650	NA	-1.41	0.00	AT4G25000	AMY1	2.04	0.00
AT4G14680	APS3	-1.05	0.00	AT4G25200	ATHSP23.6-MITO	9.08	0.00
AT4G14690	ELIP2	-1.39	0.00	AT4G25433	NA	1.17	0.00
AT4G14770	ATTCX2	-1.16	0.00	AT4G25580	NA	1.28	0.00
AT4G14940	AO1	-1.54	0.00	AT4G25850	ORP4B	1.39	0.00
AT4G15210	AT-BETA-AMY	-1.39	0.00	AT4G26080	ABI1	1.36	0.00
AT4G15500	UGT84A4	-1.62	0.00	AT4G26220	NA	1.97	0.00
AT4G15510	NA	-1.04	0.00	AT4G26800	NA	1.04	0.00
AT4G15630	NA	-1.85	0.00	AT4G27130	NA	1.28	0.00
AT4G15660	NA	-1.77	0.00	AT4G27390	NA	1.20	0.00
AT4G15670	NA	-1.19	0.01	AT4G27410	ANAC072	2.78	0.00
AT4G15690	NA	-1.29	0.00	AT4G27580	NA	1.51	0.00
AT4G15760	MO1	-1.14	0.00	AT4G27654	NA	2.19	0.00
AT4G15830	NA	-1.96	0.00	AT4G27657	NA	1.57	0.00
AT4G15870	ATTS1	-2.29	0.00	AT4G27670	HSP21	8.16	0.00
AT4G15960	NA	-1.27	0.00	AT4G27990	ATYLMG1-2	1.21	0.00
AT4G16120	ATSEB1	-1.44	0.00	AT4G28150	NA	1.47	0.00
AT4G16260	NA	-3.01	0.00	AT4G28200	NA	1.12	0.00
AT4G16370	ATOPT3	-1.45	0.00	AT4G28370	NA	1.26	0.00
AT4G16740	ATTPS03	-1.98	0.00	AT4G28590	MRL7	1.29	0.00
AT4G16880	NA	-2.22	0.00	AT4G28703	NA	1.24	0.00
AT4G16980	NA	-2.03	0.00	AT4G29070	NA	1.06	0.00
AT4G16990	RLM3	-1.34	0.00	AT4G29400	NA	1.14	0.00
AT4G17000	NA	-1.69	0.00	AT4G29770	NA	3.30	0.00
AT4G17090	BAM3	-1.22	0.00	AT4G29980	NA	1.22	0.00
AT4G17100	NA	-1.12	0.00	AT4G30450	NA	2.18	0.00
AT4G17240	NA	-1.50	0.00	AT4G30460	NA	3.69	0.00
AT4G17810	NA	-1.31	0.00	AT4G30470	NA	2.02	0.00
AT4G18195	ATPUP8	-1.53	0.00	AT4G30490	NA	1.62	0.00
AT4G18197	ATPUP7	-2.27	0.00	AT4G30540	NA	1.04	0.01
AT4G18205	NA	-2.59	0.00	AT4G30570	NA	1.99	0.00
AT4G18250	NA	-1.93	0.00	AT4G30630	NA	1.22	0.00
AT4G18440	NA	-1.10	0.00	AT4G30830	NA	1.42	0.00
AT4G18480	CH-42	-1.06	0.00	AT4G30960	ATCIPK6	1.37	0.00
AT4G18760	AtRLP51	-1.33	0.00	AT4G31290	NA	1.13	0.00
AT4G18790	ATNRAMP5	-3.19	0.00	AT4G31351	NA	2.60	0.00
AT4G18970	NA	-1.15	0.00	AT4G31354	NA	2.59	0.00
AT4G19120	ERD3	-1.68	0.00	AT4G32295	NA	1.31	0.00
AT4G19380	NA	-2.53	0.00	AT4G32450	NA	1.72	0.00
AT4G19410	NA	-3.04	0.00	AT4G32850	PAP(IV)	1.16	0.00
AT4G19530	NA	-1.32	0.00	AT4G32920	NA	1.90	0.00
AT4G19985	NA	-1.07	0.00	AT4G33040	NA	1.15	0.00
AT4G20230	NA	-1.25	0.00	AT4G33150	LKR	1.51	0.00
AT4G20760	NA	-1.13	0.00	AT4G33420	NA	2.10	0.00
AT4G20780	CML42	-2.08	0.00	AT4G33550	NA	4.75	0.00
AT4G20970	NA	-1.63	0.00	AT4G33905	NA	2.19	0.00
AT4G21070	ATBRCA1	-1.21	0.00	AT4G33940	NA	1.07	0.00
AT4G21200	ATGA2OX8	-1.47	0.00	AT4G34000	ABF3	2.27	0.00
AT4G21210	ATRP1	-1.19	0.00	AT4G34060	DML3	1.28	0.00
AT4G21215	NA	-1.19	0.00	AT4G34230	ATCAD5	1.49	0.00
AT4G21270	ATK1	-1.53	0.00	AT4G34370	ARI1	1.03	0.00
AT4G21380	ARK3	-1.05	0.00	AT4G34710	ADC2	1.58	0.00
AT4G21760	BGLU47	-1.63	0.00	AT4G34860	A/N-InvB	1.57	0.00
AT4G21840	ATMSRB8	-1.26	0.00	AT4G34990	AtMYB32	1.33	0.00
AT4G21850	ATMSRB9	-2.30	0.00	AT4G35190	LOG5	1.07	0.00
AT4G21870	NA	-1.29	0.00	AT4G35280	DAZ2	1.40	0.00
AT4G22010	sks4	-2.28	0.00	AT4G35295	NA	1.58	0.00
AT4G22485	NA	-2.94	0.00	AT4G35560	DAW1	1.19	0.00
AT4G22490	NA	-1.32	0.00	AT4G36600	NA	3.48	0.00
AT4G22505	NA	-1.94	0.00	AT4G36690	ATU2AF65A	1.13	0.00
AT4G22513	NA	-2.48	0.00	AT4G36740	ATHB40	1.57	0.00
AT4G22517	NA	-2.69	0.00	AT4G36900	DEAR4	1.83	0.00

SUPPLEMENTARY MATERIALS

AT4G22520	NA	-1.53	0.00	AT4G36925	NA	1.50	0.00
AT4G22690	CYP706A1	-1.02	0.00	AT4G36930	SPT	1.81	0.00
AT4G22710	CYP706A2	-1.38	0.00	AT4G37150	ATMES9	1.15	0.00
AT4G23030	NA	-1.19	0.00	AT4G37180	NA	1.00	0.00
AT4G23210	CRK13	-1.34	0.00	AT4G37730	AtbZIP7	2.22	0.00
AT4G23290	CRK21	-2.34	0.00	AT4G37970	ATCAD6	2.05	0.00
AT4G23320	CRK24	-1.14	0.00	AT4G38010	NA	1.27	0.00
AT4G23470	NA	-1.30	0.00	AT4G38020	NA	1.67	0.00
AT4G23496	SP1L5	-1.53	0.00	AT4G38060	NA	1.12	0.00
AT4G23610	NA	-1.18	0.00	AT4G38080	NA	1.35	0.00
AT4G23710	VAG2	-1.54	0.00	AT4G38230	ATCPK26	1.02	0.00
AT4G23800	3xHMG-box2	-1.18	0.00	AT4G38380	NA	1.58	0.00
AT4G23820	NA	-2.69	0.00	AT4G38440	IYO	1.51	0.00
AT4G24265	NA	-2.15	0.00	AT4G39210	APL3	1.27	0.00
AT4G24275	NA	-1.38	0.00	AT4G39360	NA	2.04	0.00
AT4G24340	NA	-1.66	0.00	AT4G39700	NA	1.63	0.00
AT4G24350	NA	-2.91	0.00	AT4G39800	ATIPS1	1.15	0.00
AT4G24620	PGI	-1.05	0.00	AT4G39952	NA	1.19	0.00
AT4G24780	NA	-1.59	0.00	AT4G39955	NA	1.39	0.00
AT4G24930	NA	-1.33	0.00	AT4G40010	SNRK2-7	2.61	0.00
AT4G25030	NA	-1.42	0.00	AT5G01200	NA	1.97	0.00
AT4G25050	ACP4	-1.57	0.00	AT5G01360	TBL3	1.05	0.00
AT4G25110	AtMC2	-3.00	0.00	AT5G01520	AIRP2	1.76	0.00
AT4G25260	NA	-1.43	0.00	AT5G01600	ATFER1	1.24	0.00
AT4G25900	NA	-1.13	0.00	AT5G01760	NA	1.19	0.00
AT4G26530	NA	-1.60	0.00	AT5G01820	ATCIPK14	1.11	0.00
AT4G26540	NA	-1.57	0.00	AT5G01940	NA	1.39	0.00
AT4G26660	NA	-2.90	0.00	AT5G02020	SIS	3.02	0.00
AT4G26690	GDPDL3	-1.19	0.00	AT5G02320	ATMYB3R5	1.15	0.00
AT4G26860	NA	-1.31	0.00	AT5G02430	NA	1.08	0.00
AT4G26960	NA	-2.02	0.00	AT5G02550	NA	1.16	0.00
AT4G27230	HTA2	-1.12	0.00	AT5G02640	NA	1.70	0.00
AT4G27270	NA	-1.19	0.00	AT5G03190	CPUORF47	2.25	0.00
AT4G27300	NA	-1.39	0.00	AT5G03210	AtDIP2	3.50	0.00
AT4G27310	NA	-1.47	0.00	AT5G03560	NA	1.78	0.00
AT4G27440	PORB	-1.39	0.00	AT5G03830	NA	1.60	0.00
AT4G27550	ATTPS4	-1.29	0.00	AT5G03970	NA	1.12	0.00
AT4G27595	NA	-1.36	0.00	AT5G03990	NA	1.68	0.00
AT4G27720	NA	-1.18	0.00	AT5G04000	NA	1.08	0.00
AT4G27740	NA	-1.24	0.00	AT5G04010	NA	2.02	0.00
AT4G27820	BGLU9	-1.18	0.00	AT5G04200	AtMC9	1.12	0.00
AT4G28000	NA	-2.12	0.00	AT5G04210	NA	1.21	0.00
AT4G28080	NA	-1.02	0.00	AT5G04250	NA	1.14	0.00
AT4G28190	ULT	-1.61	0.00	AT5G04370	NAMT1	1.87	0.00
AT4G28310	NA	-2.21	0.00	AT5G04410	NAC2	1.27	0.00
AT4G28430	NA	-1.57	0.00	AT5G04760	NA	1.60	0.00
AT4G28560	RIC7	-1.15	0.00	AT5G05110	NA	1.51	0.00
AT4G28660	PSB28	-1.12	0.00	AT5G05130	NA	1.43	0.00
AT4G28780	NA	-2.78	0.00	AT5G05220	NA	4.18	0.00
AT4G29030	NA	-1.24	0.00	AT5G05400	NA	2.06	0.00
AT4G29050	NA	-2.25	0.00	AT5G05410	DREB2	2.77	0.00
AT4G29110	NA	-1.28	0.00	AT5G05480	NA	1.33	0.00
AT4G29140	ADS1	-1.30	0.00	AT5G05490	ATREC8	1.90	0.00
AT4G29270	NA	-1.30	0.00	AT5G05960	NA	1.36	0.00
AT4G29310	NA	-2.09	0.00	AT5G06510	NF-YA10	1.65	0.00
AT4G29610	NA	-2.24	0.00	AT5G06540	NA	1.26	0.00
AT4G29690	NA	-2.03	0.00	AT5G06760	AtLEA4-5	4.65	0.00
AT4G29700	NA	-1.91	0.00	AT5G06820	SRF2	1.28	0.00
AT4G29740	ATCKX4	-3.50	0.00	AT5G06990	NA	1.17	0.00
AT4G29905	NA	-1.01	0.00	AT5G07080	NA	1.10	0.00
AT4G30010	NA	-1.18	0.00	AT5G07330	NA	6.63	0.00
AT4G30020	NA	-1.14	0.00	AT5G07500	PEI1	1.12	0.00

AT4G30110	ATHMA2	-1.02	0.00	AT5G07880	ATSNAP29	1.31	0.00
AT4G30140	CDEF1	-1.95	0.00	AT5G07920	ATDGK1	1.32	0.00
AT4G30190	AHA2	-1.29	0.00	AT5G08230	NA	1.40	0.00
AT4G30270	MERI-5	-1.32	0.00	AT5G08400	NA	1.19	0.00
AT4G30280	ATXTH18	-1.44	0.00	AT5G09480	NA	1.80	0.00
AT4G30610	BRS1	-2.44	0.00	AT5G09530	PELPK1	1.32	0.00
AT4G30650	NA	-1.70	0.00	AT5G09930	ABCF2	1.85	0.00
AT4G30860	ASHR3	-1.58	0.00	AT5G10080	NA	1.47	0.00
AT4G31500	ATR4	-2.19	0.00	AT5G10100	TPPI	1.36	0.00
AT4G31590	ATCSLC05	-1.25	0.00	AT5G10140	AGL25	1.06	0.00
AT4G31805	NA	-1.23	0.00	AT5G10300	ATMESS	1.80	0.00
AT4G31840	AtENODL15	-3.10	0.00	AT5G10695	NA	1.77	0.00
AT4G31870	ATGPX7	-1.43	0.00	AT5G10930	CIPK5	2.45	0.00
AT4G32000	NA	-1.18	0.00	AT5G10946	NA	2.52	0.00
AT4G32090	NA	-1.47	0.01	AT5G11090	NA	2.13	0.00
AT4G32280	IAA29	-1.76	0.00	AT5G11100	ATSYTD	1.16	0.00
AT4G32800	NA	-1.14	0.00	AT5G11110	ATSPS2F	1.22	0.00
AT4G32890	GATA9	-1.47	0.00	AT5G12020	HSP17.6II	6.92	0.00
AT4G33220	ATPME44	-1.24	0.00	AT5G12030	AT-HSP17.6A	8.90	0.00
AT4G33270	AtCDC20.1	-1.12	0.00	AT5G12840	ATHAP2A	1.37	0.00
AT4G33360	FLDH	-1.95	0.00	AT5G12870	ATMYB46	1.41	0.00
AT4G33390	NA	-1.38	0.00	AT5G13170	AtSWEET15	5.69	0.00
AT4G33470	ATHDA14	-1.15	0.00	AT5G13330	Rap2.6L	1.58	0.00
AT4G33625	NA	-1.15	0.00	AT5G13820	ATBP-1	1.50	0.00
AT4G34220	NA	-1.09	0.00	AT5G13880	NA	1.42	0.00
AT4G34550	NA	-2.43	0.00	AT5G14800	AT-P5C1	1.55	0.00
AT4G34730	NA	-1.47	0.00	AT5G15190	NA	2.93	0.00
AT4G34740	ASE2	-1.40	0.00	AT5G15250	ATFTSH6	8.52	0.00
AT4G34750	NA	-1.80	0.00	AT5G15254	NA	1.62	0.00
AT4G34760	NA	-1.18	0.00	AT5G15270	NA	1.88	0.00
AT4G34770	NA	-1.91	0.00	AT5G15500	NA	3.17	0.00
AT4G34790	NA	-2.28	0.00	AT5G15630	COBL4	1.34	0.00
AT4G34810	NA	-1.44	0.00	AT5G15860	ATPCME	1.88	0.00
AT4G34881	NA	-1.33	0.00	AT5G16110	NA	1.34	0.00
AT4G34930	NA	-1.90	0.00	AT5G16200	NA	2.10	0.00
AT4G34950	NA	-1.67	0.00	AT5G16550	NA	1.02	0.00
AT4G35030	NA	-1.27	0.00	AT5G16600	AtMYB43	2.91	0.00
AT4G35060	HIPP25	-1.32	0.00	AT5G16960	NA	1.17	0.00
AT4G35180	LHT7	-1.53	0.00	AT5G17220	ATGSTF12	1.17	0.01
AT4G35250	NA	-1.33	0.00	AT5G17420	ATCESA7	1.22	0.00
AT4G35350	XCP1	-1.26	0.00	AT5G17850	NA	1.10	0.00
AT4G35620	CYCB2;2	-1.39	0.00	AT5G18065	NA	1.42	0.00
AT4G35630	PSAT	-1.58	0.00	AT5G18340	NA	2.57	0.00
AT4G35770	ATSEN1	-2.27	0.00	AT5G18930	BUD2	1.35	0.00
AT4G36030	ARO3	-1.87	0.00	AT5G18980	NA	1.16	0.00
AT4G36110	NA	-1.77	0.00	AT5G19470	NUDT24	3.32	0.00
AT4G36230	NA	-1.10	0.00	AT5G19740	NA	1.53	0.00
AT4G36250	ALDH3F1	-1.15	0.00	AT5G19875	NA	3.60	0.00
AT4G36410	UBC17	-1.52	0.00	AT5G19890	NA	1.35	0.00
AT4G36500	NA	-2.32	0.00	AT5G20520	WAV2	1.13	0.00
AT4G36540	BEE2	-1.90	0.00	AT5G20930	TSL	1.07	0.00
AT4G36570	ATRL3	-1.51	0.00	AT5G22000	RHF2A	1.63	0.00
AT4G36670	AtPLT6	-2.11	0.00	AT5G22290	FSQ6	1.36	0.00
AT4G37240	NA	-3.29	0.00	AT5G22460	NA	1.55	0.00
AT4G37400	CYP81F3	-1.40	0.00	AT5G22540	NA	1.11	0.00
AT4G37450	AGP18	-1.47	0.00	AT5G22770	alpha-ADR	1.33	0.00
AT4G37490	CYC1	-1.63	0.00	AT5G22860	NA	1.65	0.00
AT4G37610	BT5	-1.73	0.00	AT5G23050	AAE17	1.30	0.00
AT4G37630	CYCD5;1	-1.55	0.00	AT5G23230	NIC2	1.45	0.00
AT4G37700	NA	-1.38	0.00	AT5G24090	ATCHIA	1.48	0.00
AT4G37800	XTH7	-1.58	0.00	AT5G24155	NA	2.16	0.00
AT4G38420	sks9	-1.94	0.00	AT5G24770	ATVSP2	1.82	0.00

SUPPLEMENTARY MATERIALS

AT4G38510	NA	-1.13	0.00	AT5G24800	ATBZIP9	1.36	0.00
AT4G38540	NA	-1.51	0.00	AT5G25110	CIPK25	1.71	0.00
AT4G38620	ATMYB4	-1.26	0.00	AT5G25220	KNAT3	1.56	0.00
AT4G38660	NA	-1.27	0.00	AT5G25240	NA	1.20	0.00
AT4G38770	ATPRP4	-1.11	0.00	AT5G25280	NA	3.55	0.00
AT4G38781	NA	-1.67	0.01	AT5G25390	SHN3	2.15	0.00
AT4G38850	ATSAUR15	-1.91	0.00	AT5G25450	NA	5.72	0.00
AT4G38860	NA	-1.83	0.00	AT5G25560	NA	1.47	0.00
AT4G39030	EDS5	-2.32	0.00	AT5G25610	ATRD22	1.52	0.00
AT4G39050	NA	-1.13	0.00	AT5G25620	YUC6	1.30	0.00
AT4G39120	HISN7	-1.09	0.00	AT5G25754	NA	1.11	0.00
AT4G39320	NA	-1.70	0.00	AT5G26180	NA	1.34	0.00
AT4G39380	NA	-1.52	0.00	AT5G27460	NA	1.07	0.00
AT4G39630	NA	-1.82	0.00	AT5G27660	NA	1.66	0.00
AT4G39640	GGT1	-2.16	0.00	AT5G28080	WNK9	2.07	0.00
AT4G39710	FKBP16-2	-1.36	0.00	AT5G30500	GoIS10	2.14	0.00
AT4G39770	TPPH	-1.81	0.00	AT5G35320	NA	2.08	0.00
AT4G39780	NA	-2.42	0.00	AT5G35560	NA	1.62	0.00
AT4G39795	NA	-2.46	0.00	AT5G35660	NA	3.70	0.00
AT4G39940	AKN2	-1.14	0.00	AT5G37260	CIR1	1.58	0.00
AT4G39950	CYP79B2	-2.01	0.00	AT5G37300	WSD1	2.14	0.00
AT4G39960	NA	-1.12	0.00	AT5G37340	NA	1.64	0.00
AT4G39970	NA	-1.16	0.00	AT5G37440	NA	1.14	0.00
AT4G39990	ATGB3	-1.10	0.00	AT5G37478	NA	1.02	0.00
AT5G01015	NA	-2.62	0.00	AT5G37540	NA	1.49	0.00
AT5G01170	NA	-1.43	0.00	AT5G37550	NA	1.09	0.00
AT5G01240	LAX1	-1.10	0.00	AT5G37670	NA	4.04	0.00
AT5G01420	NA	-1.21	0.00	AT5G38730	NA	1.15	0.00
AT5G01500	TAAC	-1.50	0.00	AT5G39330	NA	1.20	0.00
AT5G01790	NA	-1.37	0.00	AT5G39520	NA	1.57	0.00
AT5G01870	NA	-1.72	0.00	AT5G39640	NA	1.03	0.00
AT5G01900	ATWRKY62	-1.80	0.00	AT5G39740	OLI7	2.06	0.00
AT5G01910	NA	-1.72	0.00	AT5G39850	NA	1.91	0.00
AT5G02090	NA	-1.26	0.00	AT5G39940	NA	1.24	0.00
AT5G02540	NA	-1.60	0.00	AT5G40020	NA	1.39	0.00
AT5G02570	NA	-1.51	0.00	AT5G40382	NA	3.60	0.00
AT5G02760	NA	-3.73	0.00	AT5G40570	NA	1.43	0.00
AT5G02820	BIN5	-1.08	0.00	AT5G40790	NA	4.07	0.00
AT5G02890	NA	-2.78	0.00	AT5G40800	NA	2.31	0.00
AT5G03040	iqd2	-1.24	0.00	AT5G41360	ATXPB2	1.00	0.00
AT5G03120	NA	-1.55	0.00	AT5G42180	PER64	1.05	0.00
AT5G03300	ADK2	-1.12	0.00	AT5G42200	NA	1.00	0.00
AT5G03350	NA	-3.80	0.00	AT5G42290	NA	2.91	0.01
AT5G03390	NA	-1.56	0.00	AT5G42370	NA	1.44	0.00
AT5G03545	AT4	-1.05	0.03	AT5G42820	ATU2AF35B	1.19	0.00
AT5G03670	NA	-2.10	0.00	AT5G42900	COR27	1.53	0.00
AT5G03870	NA	-2.10	0.00	AT5G42965	NA	2.53	0.00
AT5G03995	NA	-1.64	0.00	AT5G43150	NA	1.98	0.00
AT5G04160	NA	-1.90	0.00	AT5G43290	ATWRKY49	1.62	0.00
AT5G04230	ATPAL3	-1.15	0.00	AT5G43300	AtGDPD3	2.21	0.00
AT5G04310	NA	-1.54	0.00	AT5G43400	NA	1.22	0.00
AT5G04620	ATBIOF	-1.55	0.00	AT5G43620	NA	1.74	0.00
AT5G04820	ATOFFP13	-1.11	0.00	AT5G43660	NA	1.08	0.00
AT5G05240	NA	-1.69	0.00	AT5G43730	NA	1.10	0.00
AT5G05250	NA	-2.59	0.00	AT5G43840	AT-HSFA6A	3.91	0.00
AT5G05300	NA	-1.45	0.00	AT5G43850	ARD4	1.67	0.00
AT5G05440	PYL5	-1.30	0.00	AT5G43920	NA	1.22	0.00
AT5G05510	NA	-1.15	0.00	AT5G44310	NA	1.90	0.01
AT5G05580	AtFAD8	-2.67	0.00	AT5G44660	NA	1.21	0.00
AT5G05730	AMT1	-1.19	0.00	AT5G44980	NA	1.35	0.00
AT5G05820	NA	-1.44	0.00	AT5G45310	NA	1.78	0.00
AT5G05860	UGT76C2	-1.31	0.00	AT5G45630	NA	4.99	0.00

AT5G05890	NA	-2.05	0.00	AT5G45690	NA	2.39	0.02
AT5G05940	ATROPGEF5	-1.03	0.00	AT5G46460	NA	1.55	0.00
AT5G06060	NA	-1.32	0.00	AT5G46490	NA	1.94	0.00
AT5G06570	NA	-1.71	0.00	AT5G47020	NA	1.02	0.00
AT5G06870	ATPGIP2	-2.00	0.00	AT5G47160	NA	2.37	0.00
AT5G07000	ATST2B	-1.34	0.00	AT5G47530	NA	1.47	0.00
AT5G07010	ATST2A	-2.33	0.00	AT5G47550	NA	3.68	0.00
AT5G07100	WRKY26	-2.96	0.00	AT5G47560	ATSDAT	1.35	0.00
AT5G07110	PRA1.B6	-2.14	0.00	AT5G47590	NA	1.04	0.00
AT5G07460	ATMSRA2	-1.19	0.00	AT5G47600	NA	2.97	0.00
AT5G07570	NA	-2.86	0.01	AT5G47610	NA	3.74	0.00
AT5G07580	NA	-1.84	0.00	AT5G47640	NF-YB2	1.14	0.00
AT5G07590	NA	-1.42	0.00	AT5G47670	L1L	1.69	0.00
AT5G07720	NA	-2.01	0.00	AT5G47830	NA	2.18	0.00
AT5G08000	E13L3	-1.17	0.00	AT5G48470	NA	1.82	0.00
AT5G08020	ATRA70B	-2.64	0.00	AT5G48480	NA	1.26	0.00
AT5G08050	NA	-1.13	0.00	AT5G48650	NA	1.61	0.00
AT5G08100	ASPGA1	-1.17	0.00	AT5G48850	ATSDI1	1.25	0.00
AT5G08260	scpl35	-1.56	0.00	AT5G49290	ATRLP56	1.14	0.00
AT5G08570	NA	-1.28	0.00	AT5G49700	NA	1.21	0.00
AT5G08640	ATFLS1	-2.32	0.00	AT5G49990	NA	2.24	0.00
AT5G09240	NA	-1.37	0.00	AT5G50240	AtPIMT2	2.00	0.00
AT5G09470	DIC3	-2.91	0.00	AT5G50260	CEP1	1.02	0.00
AT5G09870	CESA5	-1.02	0.00	AT5G50360	NA	4.96	0.00
AT5G10170	ATMIPS3	-1.03	0.00	AT5G51170	NA	1.72	0.00
AT5G10220	ANN6	-1.23	0.00	AT5G51440	NA	6.42	0.00
AT5G10260	AtRABH1e	-2.11	0.00	AT5G51620	NA	1.30	0.00
AT5G10390	NA	-3.45	0.00	AT5G51680	NA	2.42	0.00
AT5G10400	NA	-2.03	0.00	AT5G51890	NA	2.10	0.00
AT5G10760	NA	-1.86	0.00	AT5G52300	LTI65	2.64	0.00
AT5G10770	NA	-1.33	0.00	AT5G52390	NA	2.32	0.00
AT5G10840	NA	-1.23	0.00	AT5G52570	B2	2.31	0.00
AT5G11000	NA	-1.07	0.00	AT5G52640	ATHS83	5.81	0.00
AT5G11230	NA	-1.02	0.00	AT5G53090	NA	1.60	0.00
AT5G11410	NA	-1.40	0.00	AT5G53120	ATSPDS3	1.27	0.00
AT5G11420	NA	-1.33	0.00	AT5G53710	NA	4.47	0.00
AT5G11610	NA	-1.46	0.00	AT5G53730	NA	1.33	0.00
AT5G11670	ATNADP-ME2	-1.13	0.00	AT5G53870	AtENODL1	2.98	0.00
AT5G11920	AtcwINV6	-1.12	0.00	AT5G54080	HGO	1.46	0.00
AT5G12130	ATTERC	-1.14	0.00	AT5G54165	NA	4.58	0.00
AT5G12470	NA	-2.18	0.00	AT5G54870	NA	1.02	0.00
AT5G12860	DIT1	-1.13	0.00	AT5G54950	NA	1.02	0.00
AT5G12910	NA	-3.60	0.00	AT5G55750	NA	1.02	0.04
AT5G12940	NA	-2.22	0.00	AT5G56160	NA	1.03	0.00
AT5G13060	ABAP1	-2.05	0.00	AT5G56380	NA	1.47	0.00
AT5G13430	NA	-1.08	0.00	AT5G56520	NA	1.22	0.00
AT5G14120	NA	-1.30	0.00	AT5G56540	AGP14	1.28	0.00
AT5G14200	ATIMD1	-1.10	0.00	AT5G56600	PFN3	1.38	0.00
AT5G14330	NA	-1.46	0.00	AT5G57040	NA	1.08	0.00
AT5G14360	NA	-1.80	0.00	AT5G57050	ABI2	1.68	0.00
AT5G14570	ATNRT2.7	-1.10	0.00	AT5G57100	NA	1.19	0.00
AT5G14730	NA	-1.48	0.00	AT5G57150	NA	1.76	0.00
AT5G14740	BETA	-1.08	0.00	AT5G57560	TCH4	1.06	0.02
AT5G15350	AtENODL17	-1.51	0.00	AT5G57565	NA	1.66	0.00
AT5G15530	BCCP2	-2.26	0.00	AT5G57785	NA	1.07	0.00
AT5G15760	NA	-1.36	0.00	AT5G57790	NA	2.21	0.00
AT5G15770	AtGNA1	-1.28	0.00	AT5G57900	SKIP1	1.25	0.00
AT5G16030	NA	-1.99	0.00	AT5G57910	NA	1.33	0.00
AT5G16080	AtCXE17	-1.43	0.00	AT5G58070	ATTIL	1.29	0.00
AT5G16170	NA	-1.53	0.00	AT5G58110	NA	1.91	0.00
AT5G16190	ATCSLA11	-1.20	0.00	AT5G58470	TAF15b	1.28	0.00
AT5G16230	NA	-1.38	0.00	AT5G58590	RANBP1	1.97	0.00

SUPPLEMENTARY MATERIALS

AT5G16250	NA	-2.93	0.00	AT5G58660	NA	1.32	0.00
AT5G16350	NA	-1.67	0.00	AT5G58770	NA	2.03	0.00
AT5G16590	LRR1	-1.40	0.00	AT5G58860	CYP86	1.05	0.00
AT5G16940	NA	-1.12	0.00	AT5G58920	NA	1.10	0.00
AT5G17030	UGT78D3	-1.07	0.01	AT5G59220	HAI1	6.41	0.00
AT5G17160	NA	-2.24	0.00	AT5G59310	LTP4	7.60	0.00
AT5G17630	NA	-1.10	0.00	AT5G59320	LTP3	5.86	0.00
AT5G17670	NA	-1.24	0.00	AT5G59330	NA	5.81	0.00
AT5G17920	ATCIMS	-1.46	0.00	AT5G59440	ATTMPK.1	1.29	0.00
AT5G18020	NA	-1.38	0.00	AT5G59570	BOA	1.55	0.00
AT5G18030	NA	-1.23	0.00	AT5G59720	HSP18.2	8.06	0.00
AT5G18050	NA	-1.03	0.00	AT5G59845	NA	2.79	0.00
AT5G18060	NA	-1.01	0.00	AT5G60360	AALP	1.21	0.00
AT5G18080	SAUR24	-1.01	0.00	AT5G60580	NA	1.74	0.00
AT5G18280	APY2	-1.32	0.00	AT5G60610	NA	1.40	0.00
AT5G18430	NA	-2.57	0.00	AT5G60650	NA	1.17	0.00
AT5G18470	NA	-1.36	0.00	AT5G60910	AGL8	1.34	0.00
AT5G18600	NA	-1.15	0.00	AT5G61510	NA	1.00	0.00
AT5G19110	NA	-2.00	0.00	AT5G61820	NA	1.39	0.00
AT5G19190	NA	-2.56	0.00	AT5G61880	NA	1.42	0.00
AT5G19220	ADG2	-1.24	0.00	AT5G61990	NA	1.00	0.00
AT5G19230	NA	-1.98	0.00	AT5G62020	AT-HSFB2A	3.03	0.00
AT5G19240	NA	-1.32	0.00	AT5G62040	BFT	5.17	0.00
AT5G19250	NA	-2.43	0.00	AT5G62090	SLK2	1.35	0.00
AT5G19750	NA	-1.40	0.00	AT5G62130	NA	1.30	0.00
AT5G19770	TUA3	-1.96	0.00	AT5G62150	NA	2.20	0.00
AT5G19780	TUA5	-1.31	0.00	AT5G62190	PRH75	1.22	0.00
AT5G19800	NA	-1.77	0.00	AT5G62200	NA	1.61	0.00
AT5G20030	NA	-1.32	0.00	AT5G62470	ATMYB96	1.13	0.00
AT5G20110	NA	-1.42	0.00	AT5G62480	ATGSTU9	1.23	0.00
AT5G20340	BG5	-2.78	0.01	AT5G62520	SRO5	1.73	0.00
AT5G20630	ATGER3	-1.67	0.00	AT5G62575	SDH7	1.20	0.00
AT5G20790	NA	-2.98	0.00	AT5G63130	NA	1.57	0.00
AT5G20820	NA	-1.63	0.00	AT5G63160	BT1	1.59	0.00
AT5G22110	ATDPB2	-1.25	0.00	AT5G63350	NA	3.44	0.00
AT5G22140	NA	-1.22	0.00	AT5G63370	NA	1.14	0.00
AT5G22300	AtNIT4	-1.52	0.00	AT5G63830	NA	1.44	0.00
AT5G22310	NA	-1.13	0.00	AT5G63930	NA	1.08	0.00
AT5G22390	NA	-1.69	0.00	AT5G64180	NA	1.36	0.00
AT5G22520	NA	-1.86	0.00	AT5G64430	NA	1.09	0.00
AT5G22530	NA	-1.03	0.00	AT5G64450	NA	1.39	0.00
AT5G22570	ATWRKY38	-3.11	0.00	AT5G64510	TIN1	3.54	0.00
AT5G22580	NA	-1.92	0.00	AT5G64710	NA	1.54	0.00
AT5G22880	H2B	-2.74	0.00	AT5G64870	NA	1.51	0.00
AT5G22940	F8H	-1.02	0.00	AT5G65040	NA	1.27	0.00
AT5G23020	IMS2	-1.18	0.00	AT5G65140	TPPJ	1.45	0.00
AT5G23210	SCPL34	-1.19	0.00	AT5G65380	NA	1.06	0.00
AT5G23400	NA	-1.69	0.00	AT5G65850	NA	1.39	0.00
AT5G23420	HMGB6	-1.91	0.00	AT5G66052	NA	1.72	0.00
AT5G23530	AtCXE18	-1.20	0.00	AT5G66090	NA	1.75	0.00
AT5G23840	NA	-1.05	0.00	AT5G66110	HIPP27	3.63	0.00
AT5G23910	NA	-2.29	0.00	AT5G66240	NA	1.29	0.00
AT5G24105	AGP41	-1.60	0.00	AT5G66400	ATDI8	3.50	0.00
AT5G24200	NA	-3.43	0.00	AT5G66460	AtMAN7	2.49	0.00
AT5G24420	PGL5	-1.69	0.00	AT5G66480	NA	1.98	0.00
AT5G24570	NA	-1.16	0.00	AT5G66690	UGT72E2	1.64	0.00
AT5G24640	NA	-1.06	0.00	AT5G66960	NA	1.65	0.00
AT5G24655	LSU4	-1.45	0.00	AT5G67110	ALC	1.99	0.00
AT5G24850	CRY3	-1.96	0.00	AT5G67310	CYP81G1	1.15	0.00
AT5G25090	AtENODL13	-2.58	0.00	AT5G67610	NA	1.57	0.00
AT5G25190	ESE3	-1.76	0.00	AT1G01660	NA	1.30	0.00
AT5G25250	NA	-1.69	0.00	AT1G01725	NA	1.14	0.00

AT5G25370	PLDALPHA3	-1.06	0.00	AT1G01920	NA	1.12	0.00
AT5G25460	NA	-1.05	0.00	AT1G02300	NA	1.00	0.00
AT5G25980	BGLU37	-1.00	0.00	AT1G03170	FAF2	1.40	0.00
AT5G26000	AtTGG1	-1.07	0.00	AT1G03360	ATRRP4	1.16	0.00
AT5G26170	ATWRKY50	-1.39	0.00	AT1G04130	AtTPR2	1.06	0.00
AT5G26220	NA	-1.32	0.00	AT1G04980	ATPDI10	1.13	0.00
AT5G26230	MAKR1	-1.48	0.00	AT1G05730	NA	1.23	0.00
AT5G26290	NA	-3.00	0.00	AT1G05970	NA	1.18	0.00
AT5G26667	PYR6	-1.17	0.00	AT1G07830	NA	1.09	0.00
AT5G26670	NA	-1.60	0.00	AT1G09710	NA	1.14	0.00
AT5G26690	NA	-2.55	0.00	AT1G10800	NA	1.04	0.00
AT5G26850	NA	-1.49	0.00	AT1G10960	ATFD1	1.45	0.00
AT5G27290	NA	-1.28	0.00	AT1G11230	NA	1.08	0.00
AT5G27380	GSH2	-1.55	0.00	AT1G11475	NRPB10	1.15	0.00
AT5G27780	NA	-1.05	0.00	AT1G13080	CYP71B2	1.05	0.00
AT5G28050	NA	-1.08	0.00	AT1G14360	ATUTR3	1.33	0.00
AT5G28290	ATNEK3	-1.05	0.00	AT1G15830	NA	1.14	0.00
AT5G28630	NA	-1.56	0.00	AT1G15850	NA	1.03	0.00
AT5G28770	AtbZIP63	-1.08	0.00	AT1G18800	NRP2	1.17	0.00
AT5G33370	NA	-2.79	0.00	AT1G19160	NA	1.02	0.02
AT5G35735	NA	-1.15	0.00	AT1G19610	LCR78	1.24	0.00
AT5G35740	NA	-2.67	0.00	AT1G21140	NA	1.08	0.00
AT5G35970	NA	-1.69	0.00	AT1G28290	AGP31	1.01	0.00
AT5G36120	CCB3	-1.03	0.00	AT1G28430	CYP705A24	1.06	0.00
AT5G36890	BGLU42	-1.03	0.00	AT1G28760	NA	1.14	0.00
AT5G38020	NA	-1.96	0.00	AT1G29030	NA	1.07	0.00
AT5G38110	ASF1B	-1.24	0.00	AT1G34160	NA	1.04	0.00
AT5G38430	NA	-1.06	0.00	AT1G48970	NA	1.03	0.00
AT5G38520	NA	-1.07	0.00	AT1G49940	NA	1.01	0.00
AT5G38690	NA	-1.62	0.00	AT1G51670	NA	1.04	0.00
AT5G38930	NA	-1.89	0.00	AT1G54250	ATRPABC16.5	1.27	0.00
AT5G38940	NA	-2.19	0.00	AT1G54310	NA	1.21	0.00
AT5G38970	ATBR6OX	-1.01	0.00	AT1G56650	ATMYB75	1.27	0.00
AT5G39240	NA	-1.79	0.00	AT1G58150	NA	1.20	0.00
AT5G39320	NA	-2.46	0.00	AT1G58170	NA	1.66	0.00
AT5G39550	ORTH1	-1.75	0.00	AT1G61620	NA	1.03	0.00
AT5G39670	NA	-1.95	0.00	AT1G62975	NA	1.10	0.00
AT5G39760	AtHB23	-1.08	0.00	AT1G64600	NA	1.13	0.00
AT5G39860	BHLH136	-2.37	0.00	AT1G64720	CP5	1.17	0.00
AT5G40070	NA	-5.46	0.01	AT1G65040	AtHrd1B	1.14	0.00
AT5G40180	NA	-1.26	0.00	AT1G65490	NA	1.83	0.00
AT5G40450	NA	-2.14	0.00	AT1G65560	NA	1.09	0.00
AT5G40610	NA	-1.32	0.00	AT1G68930	NA	1.07	0.00
AT5G40730	AGP24	-1.67	0.00	AT1G69100	NA	3.98	0.00
AT5G41140	NA	-1.52	0.00	AT1G71790	NA	1.09	0.00
AT5G41880	POLA3	-1.75	0.00	AT1G72645	NA	1.25	0.00
AT5G42070	NA	-2.26	0.00	AT1G74560	NRP1	1.10	0.00
AT5G42240	scpl42	-1.08	0.00	AT1G75120	RRA1	1.25	0.00
AT5G42250	NA	-1.34	0.00	AT1G76460	NA	1.10	0.00
AT5G42530	NA	-1.02	0.00	AT1G76610	NA	1.07	0.00
AT5G42860	NA	-1.67	0.00	AT1G76955	NA	1.13	0.00
AT5G43250	NF-YC13	-1.83	0.00	AT1G77480	NA	1.04	0.00
AT5G43520	NA	-1.12	0.00	AT1G77885	NA	1.22	0.00
AT5G43580	UPI	-1.43	0.00	AT1G78680	ATGGH2	1.23	0.00
AT5G43630	TZP	-1.25	0.00	AT1G78750	NA	1.36	0.00
AT5G43745	NA	-1.20	0.00	AT1G79310	AtMC7	1.00	0.00
AT5G43910	NA	-1.25	0.00	AT1G80890	NA	1.04	0.00
AT5G44020	NA	-3.67	0.00	AT2G02770	NA	1.11	0.00
AT5G44110	ABCI21	-2.28	0.00	AT2G02810	ATUTR1	1.16	0.00
AT5G44130	FLA13	-1.55	0.00	AT2G04860	NA	1.01	0.00
AT5G44340	TUB4	-2.12	0.00	AT2G07772	NA	1.61	0.00
AT5G44390	NA	-1.41	0.00	AT2G07779	NA	1.53	0.00

SUPPLEMENTARY MATERIALS

AT5G44420	LCR77	-6.23	0.00	AT2G17525	NA	1.11	0.00
AT5G44520	NA	-1.02	0.00	AT2G17870	ATCSP3	1.05	0.00
AT5G44565	NA	-2.26	0.00	AT2G18510	emb2444	1.07	0.00
AT5G44568	NA	-3.64	0.00	AT2G21320	NA	1.63	0.00
AT5G44578	NA	-2.08	0.00	AT2G21560	NA	1.19	0.00
AT5G44582	NA	-1.17	0.00	AT2G21640	NA	1.42	0.00
AT5G44585	NA	-1.12	0.00	AT2G22410	SLO1	1.04	0.00
AT5G44620	CYP706A3	-1.37	0.00	AT2G23348	NA	1.24	0.00
AT5G44635	MCM6	-1.24	0.00	AT2G24100	ASG1	1.21	0.00
AT5G44680	NA	-1.23	0.00	AT2G24830	NA	1.05	0.00
AT5G45000	NA	-2.18	0.00	AT2G29660	NA	1.05	0.00
AT5G45280	NA	-2.21	0.00	AT2G30000	NA	1.00	0.00
AT5G45470	NA	-1.81	0.00	AT2G30790	PSBP-2	1.09	0.00
AT5G45480	NA	-1.12	0.00	AT2G31150	NA	1.32	0.00
AT5G45490	NA	-1.76	0.00	AT2G31600	NA	1.10	0.00
AT5G45540	NA	-1.04	0.00	AT2G31830	NA	1.47	0.00
AT5G45700	NA	-2.88	0.00	AT2G31890	ATRAP	1.17	0.00
AT5G45750	AtRABA1c	-1.17	0.00	AT2G32530	ATCSLB03	1.16	0.00
AT5G45820	CIPK20	-1.45	0.00	AT2G32830	PHT1;5	1.18	0.00
AT5G45930	CHL	-1.12	0.00	AT2G32920	ATPDI9	1.11	0.00
AT5G45940	AtNUDX11	-1.40	0.00	AT2G33250	NA	1.08	0.00
AT5G45950	NA	-1.45	0.00	AT2G35430	NA	1.04	0.00
AT5G46230	NA	-2.13	0.00	AT2G37180	PIP2;3	1.82	0.00
AT5G46240	KAT1	-1.36	0.00	AT2G39120	WTF9	1.02	0.00
AT5G46330	FLS2	-2.07	0.00	AT2G39580	NA	1.06	0.00
AT5G46570	BSK2	-1.00	0.00	AT2G41160	NA	1.25	0.00
AT5G46600	NA	-1.70	0.00	AT2G42760	NA	1.05	0.00
AT5G46800	BOU	-1.15	0.00	AT2G44460	BGLU28	1.19	0.00
AT5G46810	NA	-1.18	0.04	AT2G44510	NA	1.04	0.00
AT5G47220	ATERF-2	-1.23	0.00	AT2G44810	DAD1	2.62	0.01
AT5G47360	NA	-1.06	0.00	AT2G45510	CYP704A2	1.16	0.00
AT5G47380	NA	-1.69	0.00	AT2G45900	NA	1.21	0.00
AT5G47910	ATRBOHD	-1.24	0.00	AT2G47420	DIM1A	1.11	0.00
AT5G48375	BGLU39	-1.01	0.00	AT2G47790	NA	1.09	0.00
AT5G48460	NA	-1.69	0.00	AT3G01820	NA	1.08	0.00
AT5G48540	NA	-1.87	0.00	AT3G05780	LON3	1.09	0.00
AT5G48830	NA	-1.64	0.00	AT3G05810	NA	1.10	0.00
AT5G48880	KAT5	-1.90	0.00	AT3G06710	NA	1.12	0.00
AT5G48900	NA	-1.44	0.00	AT3G07860	NA	1.23	0.00
AT5G49160	DDM2	-1.17	0.00	AT3G09700	NA	1.05	0.00
AT5G49170	NA	-1.84	0.00	AT3G10120	NA	1.10	0.00
AT5G49215	NA	-1.86	0.00	AT3G10450	SCPL7	1.28	0.00
AT5G49460	ACLB-2	-1.26	0.00	AT3G10940	LSF2	1.24	0.00
AT5G49470	NA	-1.09	0.00	AT3G13470	Cpn60beta2	1.40	0.00
AT5G49630	AAP6	-2.23	0.00	AT3G15590	NA	1.01	0.00
AT5G50335	NA	-1.09	0.00	AT3G17668	ENA	1.09	0.00
AT5G50740	NA	-1.88	0.00	AT3G19508	NA	1.19	0.00
AT5G50915	NA	-1.21	0.00	AT3G20180	NA	1.46	0.00
AT5G51560	NA	-1.49	0.00	AT3G20440	BE1	1.06	0.00
AT5G51850	NA	-1.76	0.00	AT3G23637	DVL21	1.91	0.00
AT5G52220	NA	-1.60	0.00	AT3G23930	NA	1.25	0.00
AT5G52810	NA	-1.68	0.00	AT3G24000	NA	1.02	0.00
AT5G52882	NA	-2.06	0.00	AT3G25190	NA	1.15	0.00
AT5G52940	NA	-1.56	0.00	AT3G25230	ATFKBP62	1.57	0.00
AT5G52950	NA	-1.23	0.00	AT3G28740	CYP81D11	1.01	0.00
AT5G53490	NA	-1.40	0.00	AT3G29680	NA	1.09	0.00
AT5G53592	NA	-1.09	0.00	AT3G44950	NA	1.19	0.00
AT5G53880	NA	-1.34	0.00	AT3G45940	NA	1.78	0.00
AT5G54020	NA	-1.86	0.00	AT3G46770	NA	1.41	0.00
AT5G54130	NA	-1.23	0.00	AT3G51500	NA	1.02	0.00
AT5G54190	PORA	-1.23	0.00	AT3G51910	AT-HSFA7A	1.06	0.00
AT5G54330	NA	-2.06	0.01	AT3G52670	NA	1.19	0.00

AT5G54490	PBP1	-1.48	0.00	AT3G53830	NA	1.46	0.00
AT5G54610	ANK	-1.36	0.00	AT3G53940	NA	1.08	0.00
AT5G54630	NA	-1.17	0.00	AT3G60360	EDA14	1.07	0.00
AT5G54670	ATK3	-1.07	0.00	AT3G60910	NA	1.01	0.00
AT5G54710	NA	-2.44	0.00	AT3G62200	NA	1.03	0.00
AT5G54720	NA	-1.45	0.00	AT3G62560	NA	1.14	0.00
AT5G54970	NA	-2.15	0.00	AT4G00335	RHB1A	1.09	0.00
AT5G55340	NA	-1.50	0.00	AT4G00670	NA	1.13	0.00
AT5G55460	NA	-1.76	0.00	AT4G02980	ABP	1.24	0.00
AT5G55480	GDPDL4	-1.08	0.00	AT4G08590	ORL1	1.03	0.00
AT5G55510	NA	-1.04	0.00	AT4G09150	NA	1.12	0.00
AT5G55520	NA	-2.39	0.00	AT4G09890	NA	1.27	0.00
AT5G55570	NA	-2.27	0.00	AT4G09920	NA	1.02	0.00
AT5G55820	WYR	-1.41	0.00	AT4G10330	NA	1.09	0.00
AT5G55830	NA	-1.78	0.00	AT4G11240	TOPP7	1.09	0.00
AT5G56580	ANQ1	-1.90	0.00	AT4G12740	NA	1.05	0.00
AT5G56720	c-NAD-MDH3	-1.47	0.00	AT4G12750	NA	1.10	0.00
AT5G56840	NA	-2.07	0.00	AT4G13195	CLE44	1.26	0.00
AT5G56870	BGAL4	-1.75	0.00	AT4G19560	CYCT1;2	1.19	0.00
AT5G57123	NA	-1.43	0.00	AT4G20020	NA	1.05	0.00
AT5G57220	CYP81F2	-2.91	0.00	AT4G20140	GSO1	1.08	0.00
AT5G57490	ATVDAC4	-1.05	0.00	AT4G24260	ATGH9A3	1.03	0.00
AT5G57760	NA	-3.94	0.00	AT4G25470	ATCBF2	1.07	0.00
AT5G57770	NA	-1.03	0.00	AT4G25980	NA	1.42	0.00
AT5G57780	P1R1	-1.14	0.00	AT4G26780	AR192	1.28	0.00
AT5G58670	ATPLC	-1.31	0.00	AT4G27370	ATVIIIIB	1.30	0.00
AT5G58890	AGL82	-1.72	0.01	AT4G28040	NA	1.02	0.00
AT5G58900	NA	-1.15	0.00	AT4G29340	PRF4	1.24	0.00
AT5G59080	NA	-1.13	0.00	AT4G32150	ATVAMP711	1.06	0.00
AT5G59240	NA	-1.14	0.00	AT4G32480	NA	2.08	0.00
AT5G59580	UGT76E1	-1.72	0.00	AT4G36910	CBSX1	1.43	0.00
AT5G59613	NA	-1.08	0.00	AT4G37140	ATMES20	1.17	0.00
AT5G59670	NA	-2.77	0.00	AT4G39550	NA	1.20	0.00
AT5G59680	NA	-1.27	0.00	AT5G01110	NA	1.01	0.00
AT5G59690	NA	-1.80	0.00	AT5G01920	STN8	1.03	0.00
AT5G59870	HTA6	-4.16	0.00	AT5G03455	ACR2	1.01	0.00
AT5G59970	NA	-2.66	0.00	AT5G03720	AT-HSFA3	1.28	0.00
AT5G60270	NA	-1.34	0.00	AT5G03780	TRFL10	1.08	0.00
AT5G60540	ATPDX2	-1.18	0.00	AT5G09225	NA	1.00	0.00
AT5G60860	AtRABA1f	-1.37	0.00	AT5G09570	NA	1.23	0.00
AT5G60880	BASL	-1.18	0.00	AT5G10530	NA	1.32	0.00
AT5G60930	NA	-1.81	0.00	AT5G13270	RARE1	1.02	0.00
AT5G61000	ATRAPA70D	-2.74	0.00	AT5G15450	APG6	1.14	0.00
AT5G61160	AACT1	-4.86	0.00	AT5G17540	NA	1.15	0.00
AT5G61440	ACHT5	-2.19	0.00	AT5G18820	Cpn60alpha2	1.16	0.00
AT5G61570	NA	-1.18	0.00	AT5G19473	NA	1.03	0.00
AT5G61660	NA	-1.07	0.00	AT5G23480	NA	1.35	0.00
AT5G62310	IRE	-1.37	0.02	AT5G23690	NA	1.03	0.00
AT5G62360	NA	-3.92	0.00	AT5G24110	ATWRKY30	1.22	0.00
AT5G62630	HIPL2	-1.63	0.00	AT5G25475	NA	1.08	0.00
AT5G62920	ARR6	-1.26	0.00	AT5G26310	UGT72E3	1.11	0.00
AT5G63087	NA	-3.10	0.00	AT5G26800	NA	1.02	0.00
AT5G63140	ATPAP29	-1.36	0.00	AT5G26880	AGL26	1.13	0.00
AT5G63180	NA	-2.65	0.00	AT5G37400	NA	1.04	0.00
AT5G63680	NA	-1.08	0.00	AT5G37970	NA	1.44	0.01
AT5G63810	BGAL10	-1.31	0.00	AT5G37990	NA	1.41	0.00
AT5G63850	AAP4	-1.65	0.00	AT5G38070	NA	1.03	0.00
AT5G63980	ALX8	-1.03	0.00	AT5G38565	NA	1.07	0.00
AT5G64050	ATERS	-1.11	0.00	AT5G41400	NA	1.24	0.00
AT5G64120	NA	-1.81	0.00	AT5G42060	NA	1.22	0.00
AT5G64290	DCT	-1.32	0.00	AT5G42580	CYP705A12	1.09	0.00
AT5G64410	ATOPT4	-1.34	0.00	AT5G44780	NA	1.07	0.00

SUPPLEMENTARY MATERIALS

AT5G64460	NA	-1.11	0.00	AT5G47090	NA	1.12	0.00
AT5G64630	FAS2	-1.32	0.00	AT5G49390	NA	1.10	0.00
AT5G64810	ATWRKY51	-1.20	0.00	AT5G53920	NA	1.24	0.00
AT5G65010	ASN2	-1.71	0.00	AT5G56030	AtHsp90.2	1.11	0.00
AT5G65020	ANNAT2	-1.36	0.00	AT5G57140	ATPAP28	1.04	0.00
AT5G65310	ATHB-5	-1.16	0.00	AT5G58140	NPL1	1.07	0.00
AT5G65360	NA	-2.52	0.00	AT5G62370	NA	1.04	0.00
AT5G65390	AGP7	-1.04	0.00	AT5G63670	SPT42	1.19	0.00
AT5G65683	WAVH2	-1.12	0.00	AT5G63760	ARI15	1.05	0.00
AT5G65730	XTH6	-3.36	0.00	AT5G64280	DiT2.2	1.00	0.00
AT5G65810	CGR3	-1.39	0.00	AT5G65300	NA	1.04	0.00
AT5G66000	NA	-1.03	0.00	AT5G65490	NA	1.05	0.00
AT5G66230	NA	-2.77	0.00	AT5G66270	NA	1.14	0.00
AT5G66280	GMD1	-1.45	0.00	AT5G67290	NA	1.06	0.00
AT5G66330	NA	-1.48	0.00				

Table S6. Specifically changed genes under DH LrH

AGI	Gene Name	Log ₂ FC	adj.P	AGI	Gene Name	Log ₂ FC	adj.P
AT1G01110	IQD18	-1.04	0.00	AT5G60210	RIP5	-1.17	0.00
AT1G01420	UGT72B3	-1.34	0.00	AT5G60720	NA	-1.05	0.00
AT1G01430	TBL25	-1.19	0.00	AT5G60770	ATNRT2.4	-1.46	0.05
AT1G01590	ATFRO1	-1.28	0.00	AT5G60800	NA	-1.92	0.00
AT1G02180	NA	-1.12	0.00	AT5G61270	PIF7	-1.11	0.00
AT1G02230	ANAC004	-1.21	0.00	AT5G61340	NA	-1.07	0.00
AT1G02460	NA	-1.11	0.00	AT5G61420	AtMYB28	-1.58	0.00
AT1G03010	NA	-1.07	0.00	AT5G61720	NA	-1.88	0.04
AT1G03160	FZL	-1.12	0.00	AT5G61740	ABCA10	-1.09	0.00
AT1G03660	NA	-1.12	0.00	AT5G62730	NA	-1.83	0.00
AT1G04160	ATXIB	-1.10	0.00	AT5G63780	SHA1	-1.70	0.00
AT1G04250	AXR3	-1.46	0.00	AT5G64040	PSAN	-1.31	0.00
AT1G05205	NA	-1.09	0.00	AT5G64620	ATC/VIF2	-1.01	0.00
AT1G05300	ZIP5	-1.08	0.00	AT5G64800	CLE21	-1.27	0.00
AT1G05810	ARA	-1.35	0.00	AT5G64900	ATPEP1	-1.79	0.00
AT1G05835	NA	-1.39	0.00	AT5G65165	SDH2-3	-1.20	0.00
AT1G06420	NA	-1.01	0.00	AT5G65420	CYCD4;1	-1.37	0.00
AT1G07050	NA	-1.77	0.00	AT5G65440	NA	-1.10	0.00
AT1G07490	DVL9	-1.46	0.00	AT5G65700	BAM1	-1.45	0.00
AT1G07880	ATMPK13	-1.20	0.00	AT5G65970	ATMLO10	-1.20	0.00
AT1G09415	NIMIN-3	-1.06	0.00	AT5G65980	NA	-1.27	0.03
AT1G10030	ERG28	-1.11	0.00	AT5G66005	NA	-1.01	0.00
AT1G10200	WLIM1	-1.20	0.00	AT5G66260	NA	-1.01	0.00
AT1G10770	NA	-1.10	0.00	AT5G66310	NA	-1.68	0.00
AT1G11220	NA	-1.10	0.00	AT5G66510	GAMMA	-1.15	0.00
AT1G11440	NA	-1.17	0.00	AT5G66520	NA	-1.59	0.00
AT1G11740	NA	-1.41	0.00	AT5G66750	ATDDM1	-1.03	0.00
AT1G11860	NA	-1.55	0.00	AT5G66800	NA	-1.16	0.00
AT1G12000	NA	-1.26	0.00	AT5G66920	sks17	-1.48	0.00
AT1G12020	NA	-1.28	0.00	AT5G67280	RLK	-1.54	0.00
AT1G12960	NA	-1.01	0.00	AT5G67420	ASL39	-1.49	0.00
AT1G13250	GATL3	-1.47	0.00	AT3G63000	NPL41	1.00	0.00
AT1G13430	ATST4C	-1.09	0.03	AT1G01240	NA	1.86	0.00
AT1G14150	PQL1	-1.27	0.00	AT1G01280	CYP703	1.17	0.00
AT1G14190	NA	-1.07	0.00	AT1G01453	NA	2.24	0.00
AT1G14210	NA	-1.06	0.00	AT1G01470	LEA14	1.97	0.00
AT1G14240	NA	-1.06	0.00	AT1G01570	NA	1.09	0.00
AT1G14345	NA	-1.32	0.00	AT1G01580	ATFRO2	1.79	0.00
AT1G14380	IQD28	-1.03	0.00	AT1G01640	NA	1.12	0.00
AT1G14440	AtHB31	-1.04	0.00	AT1G02220	ANAC003	1.29	0.00
AT1G14460	NA	-1.19	0.00	AT1G02400	ATGA2OX4	1.30	0.00
AT1G14580	NA	-1.00	0.00	AT1G02470	NA	1.90	0.00
AT1G15000	scpl50	-1.40	0.00	AT1G02610	NA	1.40	0.00

AT1G15410	NA	-1.30	0.00	AT1G02660	NA	2.65	0.00
AT1G15820	CP24	-1.07	0.00	AT1G02816	NA	1.13	0.00
AT1G16410	BUS1	-1.39	0.00	AT1G02860	BAH1	1.02	0.00
AT1G16880	ACR11	-1.14	0.00	AT1G03200	NA	1.31	0.00
AT1G17140	ICR1	-1.16	0.00	AT1G03990	NA	1.83	0.00
AT1G17220	FUG1	-1.02	0.00	AT1G04390	NA	1.01	0.00
AT1G17455	ELF4-L4	-1.07	0.00	AT1G04830	NA	1.35	0.00
AT1G17545	NA	-4.14	0.00	AT1G05330	NA	1.15	0.00
AT1G17560	HLL	-1.61	0.00	AT1G05400	NA	1.09	0.00
AT1G17650	GLYR2	-1.13	0.00	AT1G05510	NA	2.13	0.00
AT1G18090	NA	-1.43	0.00	AT1G05530	UGT2	1.21	0.00
AT1G18650	PDCB3	-1.29	0.00	AT1G05560	UGT1	1.44	0.00
AT1G19920	APS2	-1.12	0.00	AT1G05890	ARI5	1.18	0.00
AT1G20020	ATLFNR2	-1.12	0.00	AT1G05940	CAT9	1.07	0.00
AT1G20950	NA	-1.13	0.00	AT1G06148	NA	1.02	0.00
AT1G21050	NA	-1.44	0.00	AT1G06180	ATMYB13	1.27	0.00
AT1G21500	NA	-1.42	0.00	AT1G06520	ATGPAT1	1.42	0.00
AT1G21810	NA	-1.00	0.00	AT1G06810	NA	1.02	0.00
AT1G22170	NA	-1.20	0.00	AT1G07040	NA	1.51	0.00
AT1G22630	NA	-1.22	0.00	AT1G07520	NA	1.10	0.00
AT1G22650	A/N-InvD	-1.37	0.00	AT1G07590	NA	1.16	0.00
AT1G23000	NA	-1.03	0.00	AT1G08210	NA	1.01	0.00
AT1G23060	NA	-1.11	0.00	AT1G08315	NA	1.23	0.00
AT1G23080	ATPIN7	-1.34	0.00	AT1G08340	NA	1.06	0.00
AT1G23205	NA	-1.98	0.00	AT1G08500	AtENODL18	1.09	0.00
AT1G23360	MENG	-1.12	0.00	AT1G08570	ACHT4	1.40	0.00
AT1G23410	NA	-1.37	0.00	AT1G08920	ESL1	1.67	0.00
AT1G23480	ATCSLA03	-1.27	0.00	AT1G09400	NA	1.34	0.00
AT1G23830	NA	-1.06	0.00	AT1G09510	NA	2.41	0.00
AT1G23840	NA	-1.36	0.00	AT1G10040	NA	1.46	0.00
AT1G24020	MLP423	-1.66	0.00	AT1G10050	NA	1.06	0.00
AT1G24625	ZFP7	-1.04	0.00	AT1G10070	ATBCAT-2	2.11	0.00
AT1G26100	NA	-1.06	0.00	AT1G10740	NA	1.02	0.00
AT1G26200	NA	-1.09	0.01	AT1G11210	NA	1.27	0.00
AT1G26540	NA	-1.10	0.00	AT1G11710	NA	1.02	0.00
AT1G26600	CLE9	-1.22	0.00	AT1G11925	NA	1.05	0.00
AT1G26960	AtHB23	-1.26	0.00	AT1G11960	NA	1.08	0.00
AT1G27120	NA	-1.04	0.00	AT1G12420	ACR8	2.13	0.00
AT1G27210	NA	-1.13	0.00	AT1G12805	NA	1.04	0.00
AT1G27710	NA	-3.42	0.00	AT1G13140	CYP86C3	1.23	0.00
AT1G28110	SCPL45	-1.61	0.00	AT1G13360	NA	1.25	0.00
AT1G28510	NA	-1.03	0.00	AT1G13520	NA	1.45	0.00
AT1G28600	NA	-1.07	0.00	AT1G13700	PGL1	1.03	0.00
AT1G28670	ARAB-1	-1.26	0.00	AT1G13740	AFP2	1.30	0.00
AT1G29070	NA	-1.05	0.00	AT1G14490	NA	1.68	0.00
AT1G29310	NA	-1.12	0.00	AT1G14720	ATXTH28	1.02	0.00
AT1G29470	NA	-1.13	0.00	AT1G14730	NA	1.98	0.00
AT1G29510	SAUR68	-1.53	0.00	AT1G14800	NA	1.41	0.00
AT1G29530	NA	-1.13	0.00	AT1G15310	ATHSRP54A	1.68	0.00
AT1G29670	NA	-1.35	0.00	AT1G15330	NA	2.20	0.00
AT1G29920	AB165	-1.09	0.00	AT1G15430	NA	1.05	0.00
AT1G31180	ATIMD3	-1.23	0.00	AT1G15540	NA	1.14	0.00
AT1G31335	NA	-1.14	0.00	AT1G15800	NA	1.15	0.00
AT1G31420	FEI1	-1.02	0.00	AT1G16120	WAKL1	1.22	0.00
AT1G31710	NA	-1.19	0.00	AT1G16130	WAKL2	2.28	0.00
AT1G32060	PRK	-1.35	0.00	AT1G16950	NA	1.07	0.00
AT1G32470	NA	-1.66	0.00	AT1G17230	NA	1.14	0.00
AT1G32780	NA	-1.74	0.00	AT1G17240	AtRLP2	1.01	0.00
AT1G33170	NA	-1.43	0.00	AT1G17550	HAB2	1.58	0.00
AT1G33811	NA	-2.14	0.00	AT1G17680	NA	1.14	0.00
AT1G34065	SAMC2	-1.07	0.00	AT1G18100	E12A11	1.56	0.00
AT1G34570	NA	-1.12	0.00	AT1G19180	JAZ1	1.94	0.00

SUPPLEMENTARY MATERIALS

AT1G34580	NA	-1.35	0.00	AT1G19190	NA	1.88	0.00
AT1G35260	MLP165	-1.47	0.00	AT1G19200	NA	1.34	0.00
AT1G35625	NA	-2.44	0.02	AT1G19470	NA	1.11	0.00
AT1G35680	RPL21C	-1.04	0.00	AT1G19660	NA	1.18	0.00
AT1G42970	GAPB	-1.01	0.00	AT1G19970	NA	1.12	0.00
AT1G43610	NA	-1.10	0.00	AT1G20180	NA	1.85	0.00
AT1G43710	emb1075	-1.04	0.00	AT1G20440	AtCOR47	1.76	0.00
AT1G44318	hemb2	-1.20	0.00	AT1G21790	NA	1.67	0.00
AT1G44920	NA	-1.18	0.00	AT1G22080	NA	1.58	0.00
AT1G45010	NA	-1.38	0.00	AT1G22490	NA	1.10	0.00
AT1G45207	NA	-1.14	0.00	AT1G22570	NA	1.27	0.00
AT1G47380	NA	-1.09	0.00	AT1G22640	ATMYB3	1.38	0.00
AT1G47740	NA	-1.03	0.00	AT1G22930	NA	1.59	0.00
AT1G48610	NA	-1.33	0.00	AT1G23070	NA	1.14	0.00
AT1G49010	NA	-1.01	0.00	AT1G23120	NA	1.36	0.00
AT1G49230	NA	-1.53	0.00	AT1G23200	NA	1.44	0.00
AT1G49430	LACS2	-1.49	0.00	AT1G23610	NA	1.32	0.00
AT1G49580	NA	-1.15	0.00	AT1G23710	NA	1.06	0.00
AT1G50110	NA	-1.09	0.00	AT1G23850	NA	1.01	0.00
AT1G50575	NA	-1.18	0.00	AT1G23960	NA	1.02	0.00
AT1G50732	NA	-1.08	0.00	AT1G24140	NA	1.13	0.00
AT1G51060	HTA10	-1.08	0.00	AT1G24145	NA	1.07	0.00
AT1G51080	NA	-1.08	0.00	AT1G24480	NA	1.23	0.00
AT1G51405	NA	-1.12	0.00	AT1G25560	EDF1	1.16	0.00
AT1G52140	NA	-1.01	0.00	AT1G27150	NA	1.02	0.00
AT1G52220	NA	-1.04	0.00	AT1G27461	NA	1.25	0.00
AT1G52830	IAA6	-1.18	0.00	AT1G27670	NA	1.20	0.00
AT1G53180	NA	-1.02	0.00	AT1G27730	STZ	2.22	0.00
AT1G53240	mMDH1	-1.44	0.00	AT1G28220	ATPUP3	1.79	0.00
AT1G53300	TTL1	-1.24	0.00	AT1G28360	ATERF12	1.32	0.00
AT1G53633	NA	-1.19	0.00	AT1G28650	NA	1.06	0.00
AT1G53840	ATPME1	-1.32	0.00	AT1G29050	TBL38	1.14	0.00
AT1G54020	NA	-1.20	0.00	AT1G29230	ATCIPK18	1.17	0.00
AT1G54450	NA	-1.06	0.00	AT1G29620	NA	1.90	0.00
AT1G54690	G-H2AX	-1.15	0.00	AT1G29760	NA	1.03	0.00
AT1G55200	NA	-1.30	0.00	AT1G30100	ATNCED5	1.08	0.00
AT1G55480	ZKT	-1.10	0.00	AT1G30135	JAZ8	1.09	0.00
AT1G55910	ZIP11	-1.16	0.00	AT1G30640	NA	1.23	0.00
AT1G56670	NA	-1.40	0.00	AT1G30820	NA	1.52	0.00
AT1G57800	ORTH3	-1.44	0.00	AT1G32375	NA	1.22	0.00
AT1G57820	ORTH2	-1.21	0.00	AT1G32450	NRT1.5	1.50	0.00
AT1G58080	ATATP-PRT1	-1.07	0.00	AT1G32690	NA	1.34	0.00
AT1G58160	NA	-1.35	0.00	AT1G32920	NA	1.56	0.00
AT1G58290	AtHEMA1	-1.03	0.00	AT1G33055	NA	1.33	0.00
AT1G60550	DHNS	-1.11	0.00	AT1G33480	NA	1.11	0.00
AT1G60600	ABC4	-1.08	0.00	AT1G33560	ADR1	1.24	0.00
AT1G60660	ATCB5LP	-1.57	0.00	AT1G34060	NA	1.12	0.00
AT1G60950	ATFD2	-1.19	0.00	AT1G34180	NAC016	1.33	0.00
AT1G62400	HT1	-1.24	0.00	AT1G35720	ANNAT1	1.04	0.00
AT1G62520	NA	-1.31	0.00	AT1G43160	RAP2.6	2.81	0.00
AT1G62560	FMO	-1.15	0.00	AT1G43245	NA	1.09	0.00
AT1G62630	NA	-1.10	0.00	AT1G43700	SUE3	1.05	0.00
AT1G63470	NA	-1.07	0.00	AT1G44800	NA	1.54	0.00
AT1G63650	ATMYC-2	-1.23	0.00	AT1G47128	RD21	1.00	0.00
AT1G64090	RTNLB3	-1.06	0.00	AT1G47915	NA	1.20	0.00
AT1G64390	AtGH9C2	-1.40	0.00	AT1G48370	YSL8	1.02	0.00
AT1G64530	NA	-1.15	0.00	AT1G48500	JAZ4	1.12	0.00
AT1G65010	NA	-1.54	0.00	AT1G49330	NA	1.19	0.00
AT1G65190	NA	-1.44	0.00	AT1G52565	NA	3.16	0.00
AT1G65450	NA	-1.18	0.00	AT1G52650	NA	1.25	0.00
AT1G65620	AS2	-1.02	0.00	AT1G52855	NA	1.65	0.00
AT1G65845	NA	-1.43	0.00	AT1G52890	ANAC019	2.98	0.00

AT1G65860	FMO	-1.19	0.00	AT1G53110	NA	1.16	0.00
AT1G66570	ATSUC7	-1.71	0.00	AT1G53170	ATERF-8	1.27	0.00
AT1G66970	GDPDL1	-1.25	0.00	AT1G53210	NA	1.22	0.00
AT1G66980	GDPDL2	-1.03	0.00	AT1G53470	MSL4	1.56	0.00
AT1G67050	NA	-1.42	0.00	AT1G53580	ETHE1	1.20	0.00
AT1G67090	RBCS1A	-1.16	0.00	AT1G53680	ATGSTU28	1.77	0.00
AT1G67350	NA	-1.10	0.00	AT1G53780	NA	1.10	0.00
AT1G67470	NA	-1.03	0.00	AT1G54130	AT-RSH3	1.03	0.00
AT1G67700	NA	-1.20	0.00	AT1G54560	ATXIE	1.13	0.00
AT1G67740	PSBY	-1.21	0.00	AT1G54570	NA	1.27	0.00
AT1G67750	NA	-1.30	0.00	AT1G54775	NA	1.00	0.00
AT1G67830	ATFXG1	-1.34	0.00	AT1G54860	NA	1.19	0.00
AT1G67910	NA	-1.17	0.00	AT1G55510	BCDH	1.31	0.00
AT1G67940	ABCI17	-1.01	0.00	AT1G55600	ATWRKY10	2.25	0.00
AT1G67980	CCOAMT	-1.10	0.00	AT1G55740	AtSIP1	1.06	0.00
AT1G68060	ATMAP70-1	-1.18	0.00	AT1G56320	NA	1.32	0.00
AT1G68330	NA	-1.43	0.00	AT1G57780	NA	1.81	0.00
AT1G68520	NA	-1.10	0.00	AT1G58030	CAT2	1.03	0.00
AT1G68560	ATXYL1	-1.33	0.00	AT1G58270	ZW9	2.13	0.00
AT1G68585	NA	-1.40	0.00	AT1G61890	NA	1.39	0.00
AT1G68650	NA	-1.08	0.00	AT1G62000	NA	1.02	0.00
AT1G68840	AtRAV2	-1.28	0.00	AT1G62305	NA	1.41	0.00
AT1G69080	NA	-1.18	0.00	AT1G62370	NA	1.52	0.00
AT1G69320	CLE10	-1.10	0.00	AT1G62570	FMO	2.69	0.00
AT1G69325	NA	-1.04	0.00	AT1G62620	NA	2.53	0.00
AT1G69420	NA	-1.04	0.00	AT1G62760	NA	1.94	0.00
AT1G69523	NA	-1.17	0.00	AT1G62810	NA	1.46	0.00
AT1G69650	NA	-1.13	0.03	AT1G63010	NA	1.24	0.00
AT1G69810	ATWRKY36	-1.03	0.00	AT1G63720	NA	1.46	0.00
AT1G69910	NA	-1.26	0.00	AT1G64107	NA	1.52	0.00
AT1G70410	ATBCA4	-1.34	0.00	AT1G64810	APO1	1.06	0.00
AT1G70560	CKRC1	-1.25	0.00	AT1G64990	GTG1	1.00	0.00
AT1G70710	ATGH9B1	-1.24	0.00	AT1G65090	NA	1.42	0.00
AT1G72070	NA	-1.11	0.00	AT1G65690	NA	1.75	0.00
AT1G72430	NA	-1.20	0.00	AT1G65720	NA	1.03	0.00
AT1G72940	NA	-1.25	0.00	AT1G65840	ATPAO4	1.04	0.00
AT1G72970	EDA17	-1.34	0.00	AT1G67300	NA	1.36	0.00
AT1G73020	NA	-1.03	0.00	AT1G67340	NA	1.77	0.00
AT1G73630	NA	-1.33	0.00	AT1G67650	NA	1.45	0.00
AT1G74070	NA	-1.40	0.00	AT1G68020	ATTPS6	1.41	0.00
AT1G74670	GASA6	-1.71	0.00	AT1G68340	NA	1.29	0.00
AT1G75500	WAT1	-1.83	0.00	AT1G68440	NA	1.47	0.00
AT1G75590	NA	-1.07	0.00	AT1G68450	PDE337	1.14	0.00
AT1G75680	AtGH9B7	-1.03	0.00	AT1G68530	CER6	1.08	0.00
AT1G75750	GASA1	-2.56	0.00	AT1G68620	NA	2.04	0.00
AT1G75780	TUB1	-1.45	0.00	AT1G68690	AtPERK9	1.14	0.00
AT1G75820	ATCLV1	-1.10	0.00	AT1G68765	IDA	2.42	0.00
AT1G75880	NA	-1.39	0.00	AT1G68795	CLE12	1.66	0.00
AT1G76450	NA	-1.12	0.00	AT1G68850	NA	1.28	0.00
AT1G76870	NA	-1.41	0.00	AT1G69270	RPK1	1.60	0.00
AT1G76880	NA	-1.09	0.00	AT1G69360	NA	1.15	0.00
AT1G76890	AT-GT2	-1.25	0.00	AT1G69610	NA	1.75	0.00
AT1G76952	IDL5	-1.45	0.00	AT1G69800	NA	1.13	0.00
AT1G76990	ACR3	-1.43	0.00	AT1G69840	NA	1.41	0.00
AT1G77460	NA	-1.18	0.00	AT1G70130	NA	1.77	0.00
AT1G77730	NA	-1.61	0.05	AT1G70140	ATFH8	1.33	0.00
AT1G77750	NA	-1.09	0.00	AT1G70500	NA	1.11	0.00
AT1G77940	NA	-1.06	0.00	AT1G71050	HIPP20	1.44	0.00
AT1G77990	AST56	-1.04	0.00	AT1G71090	NA	1.03	0.00
AT1G78770	APC6	-1.18	0.00	AT1G71110	NA	1.30	0.00
AT1G78970	ATLUP1	-1.57	0.00	AT1G71240	NA	1.01	0.00
AT1G80280	NA	-1.85	0.00	AT1G71360	NA	1.24	0.00

SUPPLEMENTARY MATERIALS

AT1G80640	NA	-1.12	0.00	AT1G71910	NA	1.19	0.00
AT1G80850	NA	-1.44	0.00	AT1G72120	NA	1.39	0.00
AT2G01420	ATPIN4	-1.24	0.00	AT1G72125	NA	1.51	0.00
AT2G01670	NUDT17	-1.25	0.00	AT1G72620	NA	2.84	0.00
AT2G01755	NA	-1.22	0.00	AT1G73000	PYL3	1.96	0.00
AT2G01910	ATMAP65-6	-1.14	0.00	AT1G73165	CLE1	1.17	0.00
AT2G01918	PQL3	-1.44	0.00	AT1G73390	NA	1.19	0.00
AT2G02020	AtPTR4	-1.33	0.00	AT1G73810	NA	1.62	0.00
AT2G02070	AtIDD5	-1.47	0.00	AT1G74010	NA	2.10	0.00
AT2G02100	LCR69	-1.04	0.00	AT1G74020	SS2	1.89	0.00
AT2G02450	ANAC034	-1.25	0.00	AT1G74740	ATCPK30	1.35	0.00
AT2G02850	ARPN	-1.23	0.00	AT1G76070	NA	1.34	0.00
AT2G03550	NA	-1.02	0.00	AT1G76130	AMY2	1.59	0.00
AT2G04845	NA	-1.09	0.00	AT1G76590	NA	1.30	0.00
AT2G05070	LHCB2	-1.22	0.00	AT1G76650	CML38	1.53	0.00
AT2G05100	LHCB2	-1.49	0.00	AT1G76705	NA	1.07	0.00
AT2G05790	NA	-1.06	0.00	AT1G77120	ADH	1.98	0.00
AT2G05990	ENR1	-1.09	0.00	AT1G77145	NA	1.59	0.00
AT2G06904	NA	-2.15	0.01	AT1G77200	NA	1.18	0.00
AT2G07340	PFD1	-1.26	0.00	AT1G77290	NA	1.04	0.00
AT2G07690	MCM5	-1.04	0.00	AT1G78310	NA	1.27	0.00
AT2G14580	ATPRB1	-1.28	0.00	AT1G78380	ATGSTU19	1.35	0.00
AT2G14660	NA	-1.30	0.00	AT1G79250	AGC1.7	1.50	0.00
AT2G14700	NA	-1.72	0.01	AT1G79360	ATOCT2	1.05	0.00
AT2G14750	AKN1	-1.22	0.00	AT1G79370	CYP79C1	1.11	0.00
AT2G15050	LTP	-1.47	0.00	AT1G79450	ALIS5	1.34	0.00
AT2G15280	NA	-1.04	0.00	AT1G80120	NA	1.02	0.00
AT2G15300	NA	-1.21	0.00	AT1G80570	NA	1.19	0.00
AT2G16535	NA	-1.00	0.00	AT1G80610	NA	1.48	0.00
AT2G18620	NA	-1.43	0.00	AT1G80820	ATCCR2	1.79	0.00
AT2G18650	MEE16	-1.51	0.00	AT1G80840	ATWRKY40	2.07	0.00
AT2G18730	ATDGK3	-1.13	0.00	AT2G01340	At17.1	1.79	0.00
AT2G18940	NA	-1.09	0.00	AT2G01890	ATPAP8	2.05	0.00
AT2G19460	NA	-1.30	0.00	AT2G02390	ATGSTZ1	1.03	0.00
AT2G19550	NA	-1.01	0.00	AT2G02710	PLP	1.14	0.00
AT2G19690	PLA2-BETA	-1.18	0.00	AT2G03160	ASK19	1.15	0.00
AT2G19780	NA	-1.01	0.00	AT2G03240	NA	1.14	0.00
AT2G19970	NA	-1.02	0.00	AT2G03850	NA	1.22	0.00
AT2G19990	PR-1-LIKE	-1.74	0.00	AT2G04350	LACS8	1.41	0.00
AT2G20240	NA	-1.07	0.00	AT2G05360	NA	1.62	0.00
AT2G20515	NA	-1.33	0.00	AT2G07215	NA	2.29	0.00
AT2G20570	ATGLK1	-1.23	0.00	AT2G10260	NA	1.53	0.00
AT2G20680	AtMAN2	-1.04	0.00	AT2G10920	NA	1.23	0.00
AT2G20875	EPF1	-1.66	0.00	AT2G14160	NA	1.74	0.00
AT2G21200	NA	-1.08	0.00	AT2G14620	XTH10	1.06	0.00
AT2G21210	NA	-1.51	0.00	AT2G15960	NA	1.23	0.00
AT2G21220	NA	-1.27	0.00	AT2G16770	bZIP23	1.01	0.00
AT2G21530	NA	-1.08	0.00	AT2G17520	ATIRE1-2	1.09	0.00
AT2G22230	NA	-1.13	0.00	AT2G17570	NA	1.04	0.00
AT2G22250	AAT	-1.08	0.00	AT2G17860	NA	2.78	0.00
AT2G22930	NA	-1.02	0.00	AT2G18090	NA	1.11	0.00
AT2G23010	SCPL9	-1.75	0.00	AT2G18260	ATSYP112	1.09	0.00
AT2G23360	NA	-1.09	0.00	AT2G18340	NA	2.00	0.00
AT2G23670	YCF37	-1.16	0.00	AT2G20320	NA	1.08	0.00
AT2G23690	NA	-1.40	0.00	AT2G20784	NA	1.05	0.00
AT2G23700	NA	-1.19	0.00	AT2G21490	LEA	1.50	0.00
AT2G24060	NA	-1.12	0.00	AT2G22690	NA	1.01	0.00
AT2G24090	NA	-1.30	0.00	AT2G22770	NAI1	1.63	0.00
AT2G24170	NA	-1.18	0.00	AT2G22860	ATPSK2	1.79	0.00
AT2G24395	NA	-1.16	0.00	AT2G23110	NA	2.53	0.00
AT2G24560	NA	-1.11	0.00	AT2G23450	NA	1.30	0.00
AT2G24645	NA	-1.13	0.00	AT2G23810	TET8	1.30	0.00

AT2G24700	NA	-1.09	0.00	AT2G24550	NA	1.07	0.00
AT2G25000	ATWRKY60	-1.09	0.00	AT2G24610	ATCNGC14	1.47	0.00
AT2G25480	NA	-1.71	0.00	AT2G24615	NA	1.08	0.00
AT2G25840	OVA4	-1.10	0.00	AT2G25240	NA	1.14	0.00
AT2G26550	HO2	-1.30	0.00	AT2G25344	LCR14	1.42	0.00
AT2G26640	KCS11	-1.01	0.00	AT2G25625	NA	1.14	0.00
AT2G26910	ABC32	-1.06	0.00	AT2G25690	NA	1.10	0.00
AT2G26975	NA	-1.21	0.00	AT2G25760	NA	1.12	0.00
AT2G27050	AtEIL1	-1.12	0.00	AT2G25890	NA	1.79	0.00
AT2G27380	ATEPR1	-1.53	0.00	AT2G25940	ALPHA-VPE	1.40	0.00
AT2G27590	NA	-1.06	0.00	AT2G26310	NA	1.29	0.00
AT2G27820	ADT3	-1.22	0.00	AT2G26940	NA	1.24	0.00
AT2G27970	CKS2	-1.16	0.00	AT2G27389	NA	2.01	0.00
AT2G28080	NA	-1.29	0.00	AT2G27500	NA	1.41	0.00
AT2G28140	NA	-1.61	0.00	AT2G28200	NA	1.48	0.00
AT2G28630	KCS12	-1.14	0.00	AT2G28840	XBAT31	1.41	0.00
AT2G28660	NA	-1.52	0.00	AT2G29120	ATGLR2.7	1.26	0.00
AT2G28900	ATOEP16-1	-1.14	0.00	AT2G29140	APUM3	1.15	0.00
AT2G28930	APK1B	-1.08	0.00	AT2G29350	SAG13	1.56	0.00
AT2G29180	NA	-1.36	0.00	AT2G29380	HAI3	3.44	0.00
AT2G29290	NA	-1.22	0.00	AT2G29450	AT103-1A	1.12	0.00
AT2G29890	ATVLN1	-1.26	0.00	AT2G29460	ATGSTU4	1.90	0.00
AT2G29940	ABC31	-1.11	0.00	AT2G30020	NA	2.06	0.00
AT2G30695	NA	-1.07	0.00	AT2G30140	NA	1.13	0.00
AT2G31030	ORP1B	-1.62	0.05	AT2G30210	LAC3	1.14	0.00
AT2G31730	NA	-1.49	0.00	AT2G30300	NA	1.12	0.00
AT2G31790	NA	-1.34	0.00	AT2G30690	NA	1.14	0.00
AT2G32220	NA	-1.00	0.00	AT2G31260	APG9	1.00	0.00
AT2G32280	NA	-1.26	0.00	AT2G31470	DOR	1.43	0.00
AT2G32390	ATGLR3.5	-1.11	0.00	AT2G31945	NA	3.38	0.00
AT2G32487	NA	-1.27	0.00	AT2G31960	ATGSL03	1.06	0.00
AT2G32500	NA	-1.33	0.00	AT2G32510	MAPKKK17	2.43	0.00
AT2G32540	ATCSLB04	-1.13	0.00	AT2G32800	AP4.3A	2.09	0.00
AT2G32810	BGAL9	-1.03	0.00	AT2G33080	AtRLP28	2.20	0.00
AT2G33370	NA	-1.04	0.00	AT2G33460	RIC1	1.30	0.00
AT2G33750	ATPUP2	-1.19	0.00	AT2G33700	NA	1.03	0.00
AT2G33850	NA	-1.31	0.00	AT2G33775	RALFL19	1.75	0.00
AT2G34620	NA	-1.27	0.00	AT2G34123	NA	1.54	0.00
AT2G34670	NA	-1.26	0.00	AT2G34500	CYP710A1	1.37	0.00
AT2G35370	GDCH	-1.09	0.00	AT2G34600	JAZ7	2.16	0.00
AT2G35410	NA	-1.07	0.00	AT2G34810	NA	1.63	0.00
AT2G35612	NA	-1.54	0.04	AT2G35600	ATBRXL1	1.16	0.00
AT2G35700	ATERF38	-1.39	0.00	AT2G35730	NA	1.40	0.00
AT2G35860	FLA16	-1.08	0.00	AT2G35900	NA	1.02	0.00
AT2G35880	NA	-1.06	0.00	AT2G36770	NA	2.40	0.00
AT2G35960	NHL12	-1.40	0.00	AT2G36800	DOGT1	1.86	0.00
AT2G36400	AtGRF3	-1.02	0.00	AT2G37670	NA	1.10	0.00
AT2G36430	NA	-1.38	0.00	AT2G37750	NA	1.76	0.00
AT2G36570	NA	-1.25	0.00	AT2G37970	SOUL-1	1.16	0.00
AT2G36620	RPL24A	-1.18	0.00	AT2G38250	NA	1.59	0.00
AT2G36885	NA	-1.27	0.00	AT2G38380	NA	1.13	0.00
AT2G37080	RIP3	-1.05	0.00	AT2G38400	AGT3	1.41	0.00
AT2G37230	NA	-1.11	0.00	AT2G38490	CIPK22	1.26	0.00
AT2G37380	MAKR3	-1.99	0.00	AT2G38540	ATLTP1	1.16	0.00
AT2G37390	NAKR2	-1.27	0.00	AT2G39050	ArathEULS3	1.93	0.00
AT2G37450	NA	-1.03	0.00	AT2G39400	NA	1.29	0.00
AT2G37585	NA	-1.10	0.00	AT2G40000	ATHSPRO2	1.58	0.00
AT2G37925	COPT4	-1.21	0.00	AT2G40370	LAC5	1.14	0.00
AT2G38110	ATGPAT6	-1.05	0.00	AT2G40990	NA	1.58	0.00
AT2G38140	PSRP4	-1.16	0.00	AT2G41220	GLU2	1.05	0.00
AT2G38160	NA	-1.44	0.00	AT2G42620	MAX2	1.17	0.00
AT2G38230	ATPDX1.1	-1.12	0.00	AT2G42890	AML2	1.12	0.00

SUPPLEMENTARY MATERIALS

AT2G39390	NA	-1.12	0.00	AT2G43420	NA	1.01	0.00
AT2G39470	PPL2	-1.09	0.00	AT2G43500	NA	1.06	0.00
AT2G39705	DVL11	-1.10	0.00	AT2G43590	NA	1.53	0.00
AT2G39880	AtMYB25	-1.32	0.00	AT2G43710	FAB2	1.08	0.00
AT2G39900	WLIM2a	-1.47	0.00	AT2G43820	ATSAGT1	1.04	0.00
AT2G40400	NA	-1.60	0.00	AT2G44770	NA	1.29	0.00
AT2G41510	ATCKX1	-1.13	0.00	AT2G45210	NA	1.78	0.00
AT2G41680	NTRC	-1.27	0.00	AT2G45500	NA	1.19	0.00
AT2G41940	ZFP8	-1.31	0.00	AT2G45570	CYP76C2	2.52	0.00
AT2G42220	NA	-1.59	0.00	AT2G45600	NA	1.42	0.00
AT2G42320	NA	-1.03	0.00	AT2G46020	ATBRM	1.01	0.00
AT2G42530	COR15B	-1.23	0.00	AT2G46140	NA	1.41	0.00
AT2G42690	NA	-1.03	0.00	AT2G46480	GAUT2	2.57	0.00
AT2G43000	NAC042	-1.04	0.00	AT2G46510	AIB	1.31	0.00
AT2G43030	NA	-1.14	0.00	AT2G46520	NA	1.12	0.00
AT2G43050	ATPMEPCRD	-1.36	0.00	AT2G46660	CYP78A6	1.33	0.00
AT2G43100	ATLEUD1	-1.31	0.00	AT2G47190	ATMYB2	2.02	0.00
AT2G43440	NA	-1.16	0.00	AT2G47410	NA	1.21	0.00
AT2G43510	ATTI1	-1.73	0.00	AT2G47600	ATMHX	1.00	0.00
AT2G44210	NA	-1.60	0.00	AT2G47670	NA	1.32	0.00
AT2G44690	ARAC9	-1.23	0.00	AT2G47870	NA	1.39	0.00
AT2G44830	NA	-1.08	0.00	AT2G48090	NA	1.06	0.00
AT2G44940	NA	-1.58	0.00	AT3G01320	SNL1	1.20	0.00
AT2G45180	NA	-1.53	0.00	AT3G01420	ALPHA-DOX1	1.77	0.00
AT2G45190	AFO	-1.22	0.00	AT3G01590	NA	1.00	0.00
AT2G45310	GAE4	-1.19	0.00	AT3G01830	NA	1.04	0.00
AT2G45850	NA	-1.07	0.00	AT3G01961	NA	1.23	0.00
AT2G46160	NA	-1.11	0.00	AT3G02150	PTF1	1.07	0.00
AT2G46570	LAC6	-1.18	0.00	AT3G02370	NA	1.03	0.00
AT2G46650	ATCB5-C	-1.28	0.00	AT3G02410	ICME-LIKE2	1.38	0.00
AT2G46740	NA	-1.01	0.00	AT3G02800	AtPFA-DSP3	1.42	0.00
AT2G46820	PSAP	-1.32	0.00	AT3G02850	SKOR	1.15	0.00
AT2G46880	ATPAP14	-1.56	0.03	AT3G02875	ILR1	1.19	0.00
AT2G46970	PIL1	-1.04	0.00	AT3G02910	NA	1.09	0.00
AT2G47010	NA	-1.35	0.00	AT3G02960	NA	1.20	0.00
AT2G47440	NA	-1.08	0.00	AT3G02990	ATHSFA1E	1.75	0.00
AT2G47840	AtTic20-II	-1.00	0.00	AT3G03272	NA	2.64	0.00
AT2G48070	RPH1	-1.07	0.00	AT3G03460	NA	1.23	0.00
AT3G01120	AtCGS1	-1.12	0.00	AT3G03650	EDA5	1.30	0.00
AT3G01140	AtMYB106	-1.47	0.00	AT3G04050	NA	1.16	0.00
AT3G01190	NA	-1.43	0.03	AT3G04060	NAC046	1.67	0.00
AT3G01330	DEL3	-1.30	0.00	AT3G04360	NA	1.85	0.00
AT3G01440	PQL1	-1.46	0.00	AT3G04530	ATPPCK2	1.00	0.00
AT3G01450	NA	-1.43	0.00	AT3G05260	NA	2.04	0.00
AT3G01500	ATBCA1	-1.01	0.00	AT3G05390	NA	1.12	0.00
AT3G01510	LSF1	-1.06	0.00	AT3G05400	NA	1.12	0.00
AT3G01516	NA	-1.17	0.00	AT3G05580	TOPP9	1.07	0.00
AT3G01810	NA	-1.14	0.00	AT3G05630	PDLZ2	1.24	0.00
AT3G01860	NA	-1.30	0.00	AT3G06170	NA	1.29	0.00
AT3G01940	NA	-1.14	0.00	AT3G06420	ATG8H	1.51	0.00
AT3G02170	LNG2	-1.24	0.00	AT3G06480	NA	1.00	0.00
AT3G02180	SP1L3	-1.11	0.00	AT3G06500	A/N-InvC	1.15	0.00
AT3G02250	NA	-1.22	0.00	AT3G07700	NA	1.14	0.00
AT3G02870	VTC4	-1.19	0.00	AT3G07970	QRT2	1.53	0.00
AT3G02920	ATRPA32B	-1.00	0.00	AT3G08040	ATFRD3	1.03	0.00
AT3G02930	NA	-1.38	0.00	AT3G09060	NA	1.35	0.00
AT3G03190	ATGSTF11	-1.10	0.00	AT3G09390	ATMT-1	1.35	0.00
AT3G04140	NA	-1.33	0.00	AT3G09450	NA	1.05	0.00
AT3G04630	WDL1	-1.29	0.00	AT3G09950	NA	2.28	0.00
AT3G05980	NA	-1.57	0.00	AT3G10200	NA	1.12	0.00
AT3G06035	NA	-1.35	0.00	AT3G10320	NA	1.80	0.00
AT3G06120	MUTE	-1.21	0.00	AT3G10340	PAL4	2.08	0.00

AT3G06130	NA	-1.29	0.00	AT3G10410	CPY	1.04	0.00
AT3G06140	NA	-1.11	0.00	AT3G10500	NAC053	1.47	0.00
AT3G06470	NA	-1.21	0.00	AT3G10600	CAT7	1.26	0.00
AT3G06680	NA	-1.13	0.00	AT3G10740	ARAF	1.39	0.00
AT3G07270	NA	-1.10	0.00	AT3G10780	NA	1.24	0.00
AT3G07510	NA	-1.34	0.00	AT3G10800	BZIP28	1.13	0.00
AT3G07990	SCPL27	-1.41	0.00	AT3G11430	ATGPAT5	1.10	0.00
AT3G08660	NA	-1.23	0.00	AT3G11480	ATBSMT1	1.91	0.00
AT3G08680	NA	-1.29	0.00	AT3G11773	NA	1.05	0.00
AT3G09050	NA	-1.16	0.00	AT3G11880	NA	1.07	0.00
AT3G09162	NA	-1.08	0.00	AT3G12410	NA	2.35	0.00
AT3G09730	NA	-1.14	0.00	AT3G12830	NA	1.48	0.00
AT3G10080	NA	-1.13	0.00	AT3G12960	NA	2.84	0.00
AT3G10185	NA	-1.01	0.00	AT3G13090	ABCC6	1.03	0.00
AT3G10230	AtLCY	-1.11	0.00	AT3G13857	NA	1.05	0.00
AT3G10570	CYP77A6	-1.15	0.00	AT3G13950	NA	1.15	0.00
AT3G10840	NA	-1.46	0.00	AT3G14067	NA	1.11	0.00
AT3G11090	LBD21	-1.21	0.00	AT3G14070	ATCCX3	1.34	0.00
AT3G11630	NA	-1.03	0.00	AT3G14280	NA	1.00	0.00
AT3G11720	NA	-1.10	0.00	AT3G14570	ATGSL04	1.16	0.00
AT3G13437	NA	-1.07	0.00	AT3G14880	NA	1.82	0.00
AT3G13690	NA	-1.15	0.00	AT3G15290	NA	1.09	0.00
AT3G13960	AtGRF5	-1.17	0.00	AT3G15740	NA	1.13	0.00
AT3G14190	NA	-1.03	0.00	AT3G15760	NA	2.17	0.00
AT3G14210	ESM1	-1.79	0.00	AT3G16030	CES101	1.69	0.00
AT3G14260	NA	-1.53	0.00	AT3G16150	ASPGB1	1.06	0.00
AT3G14930	HEME1	-1.28	0.00	AT3G16340	ABCG29	1.18	0.00
AT3G15520	NA	-1.24	0.00	AT3G16640	TCTP	1.03	0.00
AT3G16250	NDF4	-1.25	0.00	AT3G16940	NA	1.05	0.00
AT3G16560	NA	-1.03	0.00	AT3G16990	NA	1.65	0.00
AT3G16780	NA	-1.23	0.00	AT3G17000	UBC32	2.12	0.00
AT3G16870	GATA17	-1.21	0.00	AT3G17010	NA	1.02	0.00
AT3G17120	NA	-1.24	0.00	AT3G17770	NA	1.08	0.00
AT3G17360	POK1	-1.08	0.00	AT3G18560	NA	1.46	0.00
AT3G17840	RLK902	-1.21	0.00	AT3G18700	NA	2.50	0.00
AT3G18010	WOX1	-1.02	0.00	AT3G19150	ACK1	1.03	0.00
AT3G18460	NA	-1.15	0.01	AT3G19240	NA	1.08	0.00
AT3G18710	ATPUB29	-1.16	0.00	AT3G19270	CYP707A4	1.08	0.00
AT3G18715	IDL4	-1.24	0.00	AT3G19290	ABF4	1.39	0.00
AT3G18773	NA	-1.40	0.00	AT3G19500	NA	1.56	0.00
AT3G18890	AtTic62	-1.06	0.00	AT3G20910	NF-YA9	1.23	0.00
AT3G19880	NA	-13.88	0.00	AT3G21120	NA	1.39	0.00
AT3G20015	NA	-1.59	0.00	AT3G21270	ADOF2	1.83	0.00
AT3G20470	ATGRP-5	-1.15	0.00	AT3G21520	AtDMP1	3.41	0.00
AT3G21055	PSBTN	-1.48	0.00	AT3G21710	NA	1.05	0.00
AT3G21190	NA	-1.09	0.00	AT3G21790	NA	1.07	0.00
AT3G21330	NA	-1.24	0.01	AT3G22370	AOX1A	1.40	0.00
AT3G21870	CYCP2;1	-1.21	0.00	AT3G22420	ATWINK2	1.10	0.00
AT3G22120	CWLP	-1.26	0.00	AT3G22460	OASA2	1.43	0.00
AT3G22790	NA	-1.34	0.00	AT3G22600	NA	1.51	0.00
AT3G23010	AtRLP36	-1.01	0.00	AT3G22620	NA	2.80	0.00
AT3G23760	NA	-1.11	0.00	AT3G23240	ATERF1	1.47	0.00
AT3G24850	NA	-1.37	0.01	AT3G25719	NA	1.21	0.00
AT3G25070	RIN4	-1.17	0.00	AT3G25950	NA	1.51	0.00
AT3G25130	NA	-1.09	0.00	AT3G26280	CYP71B4	1.23	0.00
AT3G25500	AFH1	-1.23	0.00	AT3G26290	CYP71B26	1.02	0.00
AT3G25730	EDF3	-1.09	0.00	AT3G26855	NA	1.85	0.00
AT3G25900	ATHMT-1	-1.05	0.00	AT3G26910	NA	1.40	0.00
AT3G25905	CLE27	-1.24	0.00	AT3G27440	UKL5	1.38	0.00
AT3G26470	NA	-1.35	0.00	AT3G27870	NA	1.15	0.00
AT3G26570	ORF02	-1.30	0.00	AT3G28210	PMZ	1.99	0.00
AT3G26650	GAPA	-1.13	0.00	AT3G29000	NA	2.08	0.00

SUPPLEMENTARY MATERIALS

AT3G26960	NA	-1.04	0.00	AT3G29090	ATPME31	1.04	0.00
AT3G27400	NA	-1.59	0.00	AT3G29250	AtSDR4	1.76	0.00
AT3G27830	RPL12	-1.04	0.00	AT3G29340	NA	1.93	0.00
AT3G28040	NA	-1.06	0.00	AT3G29390	RIK	1.03	0.00
AT3G28500	NA	-1.20	0.00	AT3G32330	NA	2.22	0.00
AT3G28550	NA	-1.35	0.00	AT3G43420	NA	1.23	0.00
AT3G28857	PRE5	-1.75	0.00	AT3G44540	FAR4	1.01	0.00
AT3G28860	ABCB19	-1.58	0.00	AT3G44880	ACD1	1.94	0.00
AT3G28960	NA	-1.66	0.00	AT3G45010	scpl48	1.14	0.00
AT3G29375	NA	-1.08	0.00	AT3G45730	NA	1.19	0.00
AT3G30320	NA	-1.29	0.02	AT3G45880	NA	1.27	0.00
AT3G43148	NA	-4.38	0.00	AT3G45970	ATEXLA1	1.78	0.00
AT3G43600	AAO2	-1.18	0.00	AT3G46660	UGT76E12	4.05	0.00
AT3G43630	NA	-3.51	0.00	AT3G46700	NA	1.89	0.00
AT3G43960	NA	-1.18	0.00	AT3G46930	NA	1.50	0.00
AT3G44310	ATNIT1	-1.28	0.00	AT3G47340	ASN1	1.28	0.00
AT3G44320	AtNIT3	-1.27	0.00	AT3G47790	ABCA8	1.21	0.00
AT3G44780	NA	-3.57	0.01	AT3G48000	ALDH2	1.11	0.00
AT3G44890	RPL9	-1.07	0.00	AT3G48344	NA	2.03	0.00
AT3G45050	NA	-1.05	0.00	AT3G48690	ATCXE12	1.27	0.00
AT3G45230	NA	-1.35	0.00	AT3G49160	NA	1.16	0.00
AT3G45430	NA	-1.18	0.00	AT3G49210	NA	1.47	0.00
AT3G45780	JK224	-1.16	0.00	AT3G49530	ANAC062	1.16	0.00
AT3G46550	FLA4	-1.21	0.00	AT3G49590	ATG13	1.00	0.00
AT3G46900	COPT2	-1.04	0.00	AT3G49790	NA	1.02	0.00
AT3G46970	ATPHS2	-1.13	0.00	AT3G50390	NA	1.85	0.00
AT3G47010	NA	-1.17	0.00	AT3G50400	NA	1.65	0.00
AT3G47070	NA	-1.16	0.00	AT3G50970	LTI30	1.64	0.00
AT3G48550	NA	-1.66	0.00	AT3G51130	NA	1.02	0.00
AT3G48730	GSA2	-1.05	0.00	AT3G51895	AST12	1.08	0.00
AT3G48970	NA	-1.96	0.00	AT3G51960	ATBZIP24	1.67	0.00
AT3G49680	ATBCAT-3	-1.23	0.00	AT3G51990	NA	1.10	0.00
AT3G49900	NA	-1.26	0.00	AT3G52350	NA	1.18	0.00
AT3G50022	NA	-1.53	0.01	AT3G52790	NA	1.09	0.00
AT3G50240	KICP-02	-1.07	0.00	AT3G52820	ATPAP22	2.06	0.00
AT3G50450	HR1	-1.22	0.00	AT3G52850	ATELP	1.12	0.00
AT3G50470	HR3	-1.26	0.00	AT3G53040	NA	4.72	0.00
AT3G50510	LBD28	-1.47	0.01	AT3G54020	AtIPCS1	1.13	0.00
AT3G50570	NA	-1.43	0.00	AT3G54200	NA	1.37	0.00
AT3G50630	ICK2	-1.01	0.00	AT3G54680	NA	1.37	0.00
AT3G50790	NA	-1.08	0.00	AT3G54820	PIP2;5	1.11	0.00
AT3G51400	NA	-1.73	0.00	AT3G55430	NA	1.40	0.00
AT3G52500	NA	-1.33	0.00	AT3G55440	ATCTIMC	1.06	0.00
AT3G52720	ACA1	-1.38	0.00	AT3G55610	P5CS2	1.54	0.00
AT3G53530	NAKR3	-1.24	0.00	AT3G55640	NA	1.21	0.00
AT3G53850	NA	-1.00	0.00	AT3G55880	SUE4	1.91	0.00
AT3G54180	CDC2B	-1.34	0.00	AT3G55940	NA	1.14	0.00
AT3G54350	emb1967	-1.13	0.00	AT3G55980	ATSZF1	1.53	0.00
AT3G54470	NA	-1.03	0.00	AT3G56080	NA	1.06	0.00
AT3G54600	NA	-1.44	0.00	AT3G56530	NAC064	3.44	0.00
AT3G55230	NA	-1.12	0.00	AT3G56780	NA	1.12	0.00
AT3G55515	DVL8	-1.10	0.00	AT3G56790	NA	1.52	0.00
AT3G55630	ATDFD	-1.28	0.00	AT3G57020	NA	2.12	0.00
AT3G55800	SBPASE	-1.40	0.00	AT3G57380	NA	1.47	0.00
AT3G56020	NA	-1.04	0.00	AT3G57510	ADPG1	1.74	0.00
AT3G56370	NA	-1.24	0.00	AT3G57680	NA	2.56	0.00
AT3G56480	NA	-1.28	0.00	AT3G58450	NA	1.43	0.00
AT3G56810	NA	-1.72	0.00	AT3G59460	NA	1.05	0.00
AT3G56910	PSRP5	-1.34	0.00	AT3G59580	NA	1.25	0.00
AT3G56950	SIP2	-1.13	0.00	AT3G60040	NA	1.26	0.00
AT3G57130	BOP1	-1.25	0.00	AT3G60110	NA	1.02	0.00
AT3G57160	NA	-1.07	0.00	AT3G60280	UCC3	2.09	0.00

AT3G57500	NA	-1.22	0.00	AT3G60570	ATEXPB5	1.19	0.00
AT3G57860	GIG1	-1.37	0.00	AT3G61060	AtPP2-A13	1.97	0.00
AT3G59980	NA	-1.19	0.00	AT3G61290	NA	1.32	0.00
AT3G60320	NA	-1.26	0.00	AT3G61400	NA	1.71	0.00
AT3G60380	NA	-1.09	0.00	AT3G61930	NA	1.92	0.00
AT3G60440	NA	-1.24	0.00	AT3G61980	NA	1.01	0.00
AT3G60540	NA	-1.01	0.00	AT3G62040	NA	1.01	0.00
AT3G60580	NA	-1.07	0.00	AT3G62590	NA	2.22	0.00
AT3G60630	ATHAM2	-1.05	0.00	AT3G62660	GATL7	1.08	0.00
AT3G60700	NA	-1.17	0.00	AT3G63040	NA	1.71	0.00
AT3G60900	FLA10	-1.26	0.00	AT3G63050	NA	1.40	0.00
AT3G61820	NA	-1.46	0.00	AT4G00050	UNE10	1.22	0.00
AT3G62030	CYP20-3	-1.28	0.00	AT4G00140	EDA34	2.36	0.00
AT3G62060	NA	-1.05	0.00	AT4G00220	JLO	1.13	0.00
AT3G62390	TBL6	-1.11	0.00	AT4G00305	NA	1.55	0.00
AT3G62610	ATMYB11	-1.28	0.00	AT4G00430	PIP1;4	1.46	0.00
AT3G63300	FKD1	-1.16	0.00	AT4G00440	NA	1.03	0.00
AT3G63510	NA	-1.00	0.00	AT4G00695	NA	1.02	0.00
AT4G00165	NA	-1.38	0.00	AT4G00900	ATECA2	1.01	0.00
AT4G00180	YAB3	-1.17	0.00	AT4G01026	PYL7	1.10	0.00
AT4G00480	ATMYC1	-1.30	0.00	AT4G01250	AtWRKY22	1.05	0.00
AT4G00770	NA	-1.59	0.00	AT4G01360	NA	2.34	0.00
AT4G01080	TBL26	-1.74	0.00	AT4G01430	NA	1.80	0.00
AT4G01460	NA	-1.03	0.00	AT4G01910	NA	1.04	0.00
AT4G01895	NA	-1.04	0.00	AT4G02090	NA	1.27	0.00
AT4G02100	NA	-1.18	0.00	AT4G02190	NA	1.14	0.00
AT4G02270	RHS13	-1.35	0.00	AT4G02390	APP	1.24	0.00
AT4G02290	AtGH9B13	-1.32	0.00	AT4G03420	NA	1.34	0.00
AT4G02530	NA	-1.22	0.00	AT4G04490	CRK36	2.23	0.00
AT4G03190	AFB1	-1.13	0.00	AT4G04710	CPK22	1.18	0.00
AT4G03270	CYCD6;1	-1.07	0.00	AT4G05020	NDB2	1.13	0.00
AT4G03330	ATSYP123	-1.15	0.00	AT4G05091	NA	1.04	0.00
AT4G04220	AtRLP46	-1.06	0.00	AT4G05497	NA	1.32	0.00
AT4G04630	NA	-1.04	0.00	AT4G06534	NA	1.01	0.00
AT4G04640	ATPC1	-1.03	0.00	AT4G07408	NA	1.06	0.00
AT4G05030	NA	-1.15	0.02	AT4G07740	NA	1.15	0.00
AT4G05090	NA	-1.00	0.00	AT4G08990	NA	2.40	0.00
AT4G07820	NA	-1.48	0.00	AT4G09030	AGP10	1.18	0.00
AT4G08400	NA	-1.33	0.00	AT4G09965	NA	1.39	0.00
AT4G08950	EXO	-1.69	0.00	AT4G10845	NA	1.01	0.00
AT4G09160	NA	-1.32	0.00	AT4G10910	NA	1.07	0.00
AT4G09650	ATPD	-1.47	0.00	AT4G12000	NA	1.11	0.00
AT4G10740	NA	-2.12	0.02	AT4G12270	NA	2.14	0.00
AT4G11310	NA	-1.02	0.00	AT4G12570	UPL5	1.07	0.00
AT4G11820	FKP1	-1.12	0.00	AT4G13010	NA	1.03	0.00
AT4G12030	BASS5	-1.73	0.00	AT4G13110	NA	1.23	0.00
AT4G12390	PME1	-1.35	0.00	AT4G14000	NA	1.03	0.00
AT4G12480	EARL11	-1.42	0.00	AT4G14290	NA	1.39	0.00
AT4G12540	NA	-1.21	0.00	AT4G14370	NA	1.06	0.00
AT4G12830	NA	-1.65	0.00	AT4G14500	NA	1.03	0.00
AT4G12880	AtENODL19	-1.07	0.00	AT4G14860	AtOFP11	2.26	0.00
AT4G13500	NA	-1.13	0.00	AT4G15056	NA	2.56	0.00
AT4G13840	NA	-1.09	0.00	AT4G15248	NA	1.95	0.00
AT4G14040	EDA38	-1.66	0.00	AT4G15610	NA	1.25	0.00
AT4G14300	NA	-1.09	0.00	AT4G16195	NA	2.76	0.00
AT4G15160	NA	-1.27	0.00	AT4G16620	NA	1.18	0.00
AT4G15620	NA	-1.52	0.00	AT4G16750	NA	1.38	0.00
AT4G15680	NA	-1.97	0.00	AT4G16760	ACX1	1.45	0.00
AT4G16140	NA	-1.34	0.00	AT4G16960	NA	1.04	0.00
AT4G16380	NA	-1.21	0.00	AT4G17020	NA	1.19	0.00
AT4G16515	RGF6	-1.55	0.00	AT4G17850	NA	3.15	0.00
AT4G16563	NA	-1.73	0.00	AT4G18050	ABCB9	1.07	0.00

SUPPLEMENTARY MATERIALS

AT4G16590	ATCSLA01	-1.29	0.00	AT4G18350	ATNCED2	1.09	0.00
AT4G16807	NA	-1.35	0.00	AT4G18425	NA	1.17	0.00
AT4G16820	PLA- β 2	-1.01	0.00	AT4G18580	NA	1.14	0.00
AT4G16860	RPP4	-1.20	0.00	AT4G18830	ATOPF5	1.28	0.00
AT4G17160	ATRAB2B	-1.23	0.00	AT4G18940	NA	1.71	0.00
AT4G17360	NA	-1.03	0.00	AT4G19390	NA	1.53	0.00
AT4G17460	HAT1	-1.67	0.00	AT4G19720	NA	1.20	0.00
AT4G17480	NA	-1.24	0.00	AT4G19810	ChiC	1.41	0.00
AT4G17490	ATERF6	-1.34	0.00	AT4G20390	NA	1.07	0.00
AT4G17600	LIL3:1	-1.35	0.00	AT4G21323	NA	1.07	0.00
AT4G17695	KAN3	-1.07	0.00	AT4G21490	NDB3	1.03	0.00
AT4G17870	PYR1	-1.01	0.00	AT4G21620	NA	1.03	0.00
AT4G18030	NA	-1.40	0.00	AT4G21680	NRT1.8	2.04	0.00
AT4G18080	NA	-1.96	0.01	AT4G22240	NA	1.53	0.00
AT4G18370	DEG5	-1.17	0.00	AT4G22820	NA	2.04	0.00
AT4G18670	NA	-1.25	0.00	AT4G22920	ATNYE1	1.53	0.00
AT4G18740	NA	-1.08	0.00	AT4G23120	NA	2.23	0.00
AT4G19030	AT-NLM1	-1.12	0.00	AT4G23450	AIRP1	1.70	0.00
AT4G19170	CCD4	-1.16	0.00	AT4G23630	BTI1	1.01	0.00
AT4G19830	NA	-1.06	0.00	AT4G23750	CRF2	1.13	0.00
AT4G20430	NA	-1.02	0.00	AT4G23882	NA	1.99	0.00
AT4G20890	TUB9	-1.03	0.00	AT4G24380	NA	1.25	0.00
AT4G21280	PSBQ	-1.43	0.00	AT4G24400	ATCIPK8	1.11	0.00
AT4G21366	NA	-1.04	0.00	AT4G24450	ATGWD2	1.02	0.00
AT4G21445	NA	-1.05	0.00	AT4G24800	ECIP1	1.17	0.00
AT4G21970	NA	-1.07	0.00	AT4G24960	ATHVA22D	1.70	0.00
AT4G22130	SRF8	-1.12	0.00	AT4G25180	NA	1.02	0.00
AT4G22230	NA	-1.31	0.00	AT4G25390	NA	1.34	0.00
AT4G22560	NA	-1.33	0.00	AT4G25790	NA	1.45	0.00
AT4G22800	NA	-1.11	0.00	AT4G25800	NA	1.06	0.00
AT4G23020	NA	-1.07	0.00	AT4G25810	XTH23	1.32	0.00
AT4G23060	IQD22	-1.43	0.00	AT4G26200	ACS7	1.55	0.00
AT4G23130	CRK5	-1.02	0.00	AT4G26250	AtGolS6	1.19	0.00
AT4G23790	TBL24	-1.29	0.00	AT4G26580	NA	1.08	0.00
AT4G24090	NA	-1.21	0.00	AT4G26701	NA	1.04	0.00
AT4G24810	NA	-1.27	0.00	AT4G27260	GH3.5	1.03	0.00
AT4G25080	CHLM	-1.30	0.00	AT4G27350	NA	1.06	0.00
AT4G25240	SKS1	-1.41	0.00	AT4G27520	AtENODL2	1.68	0.00
AT4G25350	SHB1	-1.02	0.00	AT4G27800	PPH1	1.11	0.00
AT4G25420	AT2301	-1.72	0.00	AT4G28005	NA	1.91	0.00
AT4G25630	ATFIB2	-1.13	0.00	AT4G28110	AtMYB41	1.16	0.00
AT4G25870	NA	-1.08	0.00	AT4G28350	NA	1.45	0.00
AT4G25890	NA	-1.20	0.00	AT4G29190	AtOZF2	1.38	0.00
AT4G26760	MAP65-2	-1.37	0.00	AT4G29305	LCR25	2.62	0.00
AT4G27240	NA	-1.29	0.00	AT4G29710	NA	1.27	0.00
AT4G27420	ABCG9	-1.60	0.02	AT4G29780	NA	1.88	0.00
AT4G27730	ATOPT6	-1.11	0.00	AT4G29930	NA	1.43	0.00
AT4G27950	CRF4	-1.01	0.00	AT4G30120	ATHMA3	1.14	0.00
AT4G27970	SLAH2	-1.37	0.00	AT4G30710	QWRF8	1.01	0.00
AT4G28680	TYRDC	-1.11	0.00	AT4G31160	DCAF1	1.04	0.00
AT4G28790	NA	-1.18	0.00	AT4G31240	NA	1.54	0.00
AT4G29060	emb2726	-1.06	0.00	AT4G31610	ATREM1	1.58	0.00
AT4G29240	NA	-1.04	0.00	AT4G31860	NA	1.22	0.00
AT4G29360	NA	-1.03	0.00	AT4G32050	NA	1.02	0.00
AT4G29480	NA	-1.06	0.00	AT4G32250	NA	1.34	0.00
AT4G29720	ATPAO5	-1.20	0.00	AT4G32810	ATCCD8	1.06	0.00
AT4G30130	NA	-1.10	0.00	AT4G32870	NA	1.95	0.00
AT4G30230	NA	-1.64	0.00	AT4G33020	ATZIP9	1.08	0.00
AT4G30410	NA	-1.54	0.00	AT4G33280	NA	1.06	0.00
AT4G30680	NA	-1.11	0.00	AT4G33467	NA	4.16	0.00
AT4G30980	LRL2	-1.16	0.00	AT4G33910	NA	1.26	0.00
AT4G30993	NA	-1.05	0.00	AT4G33950	ATOST1	1.16	0.00

AT4G31620	NA	-1.52	0.00	AT4G34131	UGT73B3	1.31	0.00
AT4G31890	NA	-1.63	0.00	AT4G34135	UGT73B2	1.00	0.00
AT4G32330	NA	-1.28	0.00	AT4G34180	NA	1.02	0.00
AT4G32710	PERK14	-1.14	0.00	AT4G34410	RRTF1	3.03	0.00
AT4G33130	NA	-1.07	0.00	AT4G34940	ARO1	1.36	0.00
AT4G33530	KUP5	-1.08	0.00	AT4G35300	TMT2	1.18	0.00
AT4G34138	UGT73B1	-1.19	0.00	AT4G35420	DRL1	1.02	0.00
AT4G34160	CYCD3	-1.29	0.00	AT4G35500	NA	1.52	0.00
AT4G34800	NA	-1.07	0.00	AT4G35783	DVL17	1.29	0.00
AT4G35900	FD	-1.10	0.00	AT4G35790	ATPLDELTA	1.41	0.00
AT4G36470	NA	-1.27	0.00	AT4G35985	NA	1.26	0.00
AT4G36550	NA	-1.39	0.00	AT4G36610	NA	1.60	0.00
AT4G36770	NA	-1.19	0.00	AT4G36700	NA	1.79	0.00
AT4G37040	MAP1D	-1.10	0.00	AT4G36730	GBF1	1.18	0.00
AT4G37080	NA	-1.09	0.00	AT4G36950	MAPKKK21	2.49	0.00
AT4G37110	NA	-1.15	0.00	AT4G36980	NA	1.02	0.00
AT4G37300	MEE59	-1.17	0.00	AT4G37030	NA	1.38	0.00
AT4G37520	NA	-1.29	0.00	AT4G37220	NA	1.05	0.00
AT4G37540	LBD39	-1.27	0.00	AT4G37370	CYP81D8	1.61	0.00
AT4G37670	NAGS2	-1.02	0.00	AT4G37420	NA	1.25	0.00
AT4G37740	AtGRF2	-1.27	0.00	AT4G37430	CYP81F1	2.70	0.00
AT4G37750	ANT	-1.44	0.00	AT4G37470	NA	1.08	0.00
AT4G37770	ACS8	-1.14	0.00	AT4G37790	HAT22	1.24	0.00
AT4G37810	NA	-1.10	0.00	AT4G37990	ATCAD8	1.36	0.00
AT4G38520	NA	-1.14	0.00	AT4G38000	DOF4.7	1.28	0.00
AT4G38840	NA	-1.49	0.00	AT4G38730	NA	1.28	0.00
AT4G38970	FBA2	-1.23	0.00	AT4G39670	NA	3.67	0.00
AT4G39010	AtGH9B18	-1.03	0.00	AT5G01225	NA	1.79	0.00
AT4G39190	NA	-1.06	0.00	AT5G01380	NA	1.46	0.00
AT4G39840	NA	-1.35	0.00	AT5G01720	NA	1.32	0.00
AT5G01370	ACI1	-1.12	0.00	AT5G02000	NA	1.33	0.00
AT5G01410	ATPDX1	-1.18	0.00	AT5G02420	NA	2.01	0.00
AT5G02220	NA	-1.56	0.00	AT5G02490	AtHsp70-2	1.51	0.00
AT5G02830	NA	-1.01	0.00	AT5G02502	NA	1.17	0.00
AT5G02940	NA	-1.14	0.00	AT5G02880	UPL4	1.13	0.00
AT5G03150	JKD	-1.34	0.00	AT5G02970	NA	1.11	0.00
AT5G03850	NA	-1.06	0.00	AT5G03100	NA	1.20	0.00
AT5G03960	IQD12	-1.04	0.00	AT5G03230	NA	1.18	0.00
AT5G04190	PKS4	-1.07	0.00	AT5G04340	C2H2	1.02	0.00
AT5G04430	BTR1	-1.13	0.00	AT5G04660	CYP77A4	1.59	0.00
AT5G04690	NA	-1.08	0.00	AT5G05230	NA	1.01	0.00
AT5G04950	ATNAS1	-2.80	0.00	AT5G05260	CYP79A2	1.33	0.00
AT5G04960	NA	-1.82	0.02	AT5G05350	NA	1.19	0.00
AT5G05180	NA	-1.25	0.00	AT5G06230	TBL9	1.34	0.00
AT5G06290	2-Cys	-1.36	0.00	AT5G06320	NHL3	1.01	0.00
AT5G06790	NA	-1.38	0.00	AT5G06370	NA	1.47	0.00
AT5G06930	NA	-1.15	0.00	AT5G07380	NA	1.04	0.00
AT5G06940	NA	-1.10	0.00	AT5G07680	ANAC079	1.30	0.00
AT5G07240	IQD24	-1.03	0.00	AT5G07850	NA	1.21	0.00
AT5G07630	NA	-1.03	0.00	AT5G08240	NA	1.25	0.00
AT5G07990	CYP75B1	-1.06	0.00	AT5G08350	NA	1.48	0.00
AT5G08280	HEMC	-1.04	0.00	AT5G09620	NA	1.20	0.00
AT5G08330	AtTCP11	-1.36	0.00	AT5G10625	NA	2.26	0.00
AT5G08760	NA	-1.09	0.00	AT5G10650	NA	1.18	0.00
AT5G09650	AtPPa6	-1.39	0.00	AT5G11680	NA	1.02	0.00
AT5G10020	NA	-1.18	0.00	AT5G12930	NA	1.19	0.00
AT5G10150	NA	-1.60	0.00	AT5G13080	ATWRKY75	1.87	0.00
AT5G10250	DOT3	-1.00	0.00	AT5G13200	NA	1.59	0.00
AT5G10520	RBK1	-1.54	0.00	AT5G13210	NA	2.88	0.00
AT5G10720	AHK5	-1.81	0.02	AT5G13580	ABCG6	2.34	0.00
AT5G11370	NA	-1.64	0.04	AT5G13700	APAO	2.04	0.00
AT5G11550	NA	-1.42	0.00	AT5G14130	NA	1.04	0.00

SUPPLEMENTARY MATERIALS

AT5G11790	NDL2	-1.17	0.00	AT5G14995	NA	2.21	0.00
AT5G11810	NA	-1.04	0.00	AT5G15260	NA	1.34	0.00
AT5G12050	NA	-1.44	0.00	AT5G16360	NA	2.50	0.00
AT5G12060	NA	-1.17	0.04	AT5G16370	AAE5	1.24	0.00
AT5G12170	CLT3	-1.12	0.00	AT5G16380	NA	1.08	0.00
AT5G12250	TUB6	-1.10	0.00	AT5G17210	NA	1.13	0.00
AT5G12970	NA	-1.36	0.00	AT5G17460	NA	1.14	0.00
AT5G13000	ATGSL12	-1.01	0.00	AT5G17490	AtRGL3	1.20	0.00
AT5G13140	NA	-1.33	0.00	AT5G17860	CAX7	1.37	0.00
AT5G13510	EMB3136	-1.03	0.00	AT5G18130	NA	1.02	0.00
AT5G14090	NA	-1.30	0.00	AT5G18270	ANAC087	2.89	0.00
AT5G14230	NA	-1.04	0.00	AT5G18370	NA	1.03	0.00
AT5G14790	NA	-1.06	0.00	AT5G20010	ATRAN1	1.21	0.00
AT5G14920	NA	-1.78	0.00	AT5G20430	NA	1.27	0.00
AT5G14970	NA	-1.10	0.00	AT5G22380	NAC090	2.04	0.00
AT5G15050	NA	-1.17	0.00	AT5G22510	A/N-InvE	1.03	0.00
AT5G15310	ATMIXTA	-1.25	0.00	AT5G22545	NA	1.69	0.00
AT5G15320	NA	-1.06	0.00	AT5G22550	NA	1.06	0.00
AT5G15580	LNG1	-1.29	0.00	AT5G22850	NA	1.18	0.00
AT5G16000	NIK1	-1.08	0.00	AT5G23190	CYP86B1	2.00	0.00
AT5G16340	NA	-1.19	0.00	AT5G23750	NA	1.76	0.00
AT5G16530	PIN5	-1.07	0.00	AT5G23950	NA	1.61	0.00
AT5G16810	NA	-1.08	0.00	AT5G24030	SLAH3	1.05	0.00
AT5G17700	NA	-1.23	0.00	AT5G24080	NA	2.70	0.00
AT5G17870	PSRP6	-1.10	0.00	AT5G24352	NA	1.03	0.00
AT5G18010	SAUR19	-1.57	0.00	AT5G24590	ANAC091	1.16	0.00
AT5G18290	SIP1;2	-1.11	0.00	AT5G24860	ATFPF1	1.26	0.00
AT5G18590	NA	-1.20	0.00	AT5G24870	NA	1.27	0.00
AT5G18650	NA	-1.07	0.00	AT5G25770	NA	1.68	0.00
AT5G18660	PCB2	-1.05	0.00	AT5G26340	ATSTP13	1.08	0.00
AT5G18840	NA	-1.46	0.00	AT5G26673	NA	1.38	0.00
AT5G18970	NA	-1.02	0.00	AT5G26770	NA	1.27	0.00
AT5G19090	NA	-1.19	0.00	AT5G28237	NA	1.80	0.00
AT5G19120	NA	-1.38	0.00	AT5G29613	NA	1.70	0.00
AT5G19160	TBL11	-1.21	0.00	AT5G37170	NA	1.18	0.00
AT5G19170	NA	-1.02	0.00	AT5G37570	NA	1.08	0.00
AT5G19340	NA	-1.27	0.00	AT5G37720	ALY4	1.14	0.00
AT5G19810	NA	-1.36	0.01	AT5G38240	NA	1.56	0.00
AT5G20635	AGG3	-1.20	0.00	AT5G38850	NA	1.03	0.00
AT5G20710	BGAL7	-1.15	0.00	AT5G39050	PMAT1	1.12	0.00
AT5G20740	NA	-1.94	0.00	AT5G39610	ANAC092	3.27	0.00
AT5G20850	ATRAD51	-1.12	0.00	AT5G39660	CDF2	1.06	0.00
AT5G20950	NA	-1.13	0.00	AT5G40390	RS5	1.05	0.00
AT5G20970	NA	-1.07	0.00	AT5G40690	NA	1.38	0.00
AT5G21060	NA	-1.13	0.00	AT5G41040	NA	1.24	0.00
AT5G21430	CRRL	-1.10	0.00	AT5G41700	ATUBC8	1.03	0.00
AT5G21920	ATYLMG2	-1.16	0.00	AT5G41800	NA	1.33	0.00
AT5G21930	ATHMA8	-1.31	0.00	AT5G42010	NA	1.19	0.00
AT5G21960	NA	-1.94	0.03	AT5G42050	NA	1.85	0.00
AT5G22930	NA	-1.48	0.00	AT5G42380	CML37	1.29	0.00
AT5G23010	IMS3	-1.13	0.00	AT5G42510	NA	2.40	0.00
AT5G23060	CaS	-1.40	0.00	AT5G42930	NA	1.10	0.00
AT5G23280	NA	-1.10	0.00	AT5G43030	NA	1.01	0.00
AT5G23760	NA	-1.03	0.00	AT5G43180	NA	1.09	0.00
AT5G23940	DCR	-1.44	0.00	AT5G43450	NA	1.06	0.00
AT5G25810	tny	-1.33	0.00	AT5G43650	BHLH92	2.32	0.00
AT5G25880	ATNADP-ME3	-1.11	0.00	AT5G43770	NA	1.77	0.00
AT5G26630	NA	-1.21	0.00	AT5G43950	NA	1.00	0.00
AT5G27330	NA	-1.20	0.00	AT5G44540	NA	2.04	0.00
AT5G27390	NA	-1.06	0.00	AT5G44670	NA	1.33	0.00
AT5G27550	NA	-1.14	0.00	AT5G45240	NA	1.58	0.00
AT5G28030	DES1	-1.12	0.00	AT5G45340	CYP707A3	1.53	0.00

AT5G35480	NA	-1.01	0.00	AT5G45640	NA	1.53	0.00
AT5G35490	ATMRU1	-1.59	0.00	AT5G45810	CIPK19	2.87	0.00
AT5G35670	iqd33	-1.15	0.00	AT5G46180	DELTA-OAT	1.24	0.00
AT5G36920	NA	-1.28	0.00	AT5G46250	NA	1.04	0.00
AT5G37940	NA	-1.42	0.00	AT5G46295	NA	1.72	0.00
AT5G38010	NA	-1.67	0.00	AT5G46720	NA	1.01	0.00
AT5G38420	NA	-1.14	0.00	AT5G47180	NA	1.12	0.00
AT5G38530	TSBtype2	-1.05	0.00	AT5G47740	NA	1.24	0.00
AT5G39000	NA	-1.05	0.00	AT5G47810	PFK2	1.10	0.00
AT5G40010	AATP1	-1.13	0.04	AT5G47980	NA	2.68	0.00
AT5G40150	NA	-1.61	0.00	AT5G48180	NSP5	1.89	0.00
AT5G40460	NA	-1.20	0.00	AT5G48410	ATGLR1.3	1.32	0.00
AT5G40630	NA	-1.35	0.00	AT5G48510	NA	1.29	0.00
AT5G40820	ATATR	-1.24	0.00	AT5G49190	ATSUS2	1.15	0.00
AT5G40830	NA	-1.35	0.00	AT5G49270	COBL9	1.20	0.00
AT5G41050	NA	-1.25	0.00	AT5G49280	NA	1.59	0.00
AT5G41060	NA	-1.47	0.00	AT5G49520	ATWRKY48	1.32	0.00
AT5G41070	DRB5	-1.32	0.00	AT5G49525	NA	1.05	0.00
AT5G42100	ATBG_PPAP	-1.17	0.00	AT5G49600	NA	1.58	0.00
AT5G42110	NA	-1.40	0.00	AT5G49690	NA	1.86	0.00
AT5G42720	NA	-1.37	0.00	AT5G49780	NA	1.65	0.00
AT5G42760	NA	-1.38	0.00	AT5G50170	NA	1.16	0.00
AT5G42880	NA	-1.45	0.00	AT5G50720	ATHVA22E	1.26	0.00
AT5G43020	NA	-1.19	0.00	AT5G50780	NA	1.04	0.00
AT5G43700	ATAUX2-11	-1.12	0.00	AT5G51070	CLPD	1.60	0.00
AT5G43750	NDH18	-1.23	0.00	AT5G51760	AHG1	3.06	0.00
AT5G43970	ATTOM22-V	-1.16	0.00	AT5G51990	CBF4	2.25	0.00
AT5G44600	NA	-1.12	0.00	AT5G52290	SHOC1	1.01	0.00
AT5G45590	NA	-1.01	0.00	AT5G52730	NA	1.04	0.00
AT5G45650	NA	-1.69	0.00	AT5G53010	NA	1.08	0.00
AT5G45670	NA	-1.74	0.00	AT5G53130	ATCNGC1	1.09	0.00
AT5G45850	NA	-1.17	0.00	AT5G53220	NA	1.54	0.00
AT5G46110	APE2	-1.25	0.00	AT5G53360	NA	1.17	0.00
AT5G46220	NA	-1.27	0.00	AT5G53660	AtGRF7	1.02	0.00
AT5G46450	NA	-1.06	0.00	AT5G54225	LCR83	1.52	0.00
AT5G46710	NA	-1.25	0.00	AT5G54230	AtMYB49	1.21	0.00
AT5G46780	NA	-1.07	0.00	AT5G54510	DFL1	1.14	0.00
AT5G46790	PYL1	-1.69	0.00	AT5G54585	NA	1.66	0.00
AT5G46930	NA	-1.55	0.01	AT5G54650	ATFH5	2.20	0.00
AT5G47250	NA	-1.22	0.00	AT5G55410	NA	1.12	0.00
AT5G47500	PME5	-1.69	0.00	AT5G56420	NA	1.13	0.00
AT5G47770	FPS1	-1.13	0.00	AT5G57310	NA	1.20	0.00
AT5G48450	sks3	-1.01	0.00	AT5G57480	NA	2.39	0.00
AT5G48490	NA	-1.62	0.00	AT5G57610	NA	1.33	0.00
AT5G48545	HINT3	-1.05	0.00	AT5G57670	NA	1.19	0.00
AT5G48660	NA	-1.22	0.00	AT5G57810	TET15	1.13	0.00
AT5G48790	NA	-1.39	0.00	AT5G57840	NA	1.16	0.00
AT5G48910	LPA66	-1.01	0.00	AT5G58380	CIPK10	1.52	0.00
AT5G49030	OVA2	-1.10	0.00	AT5G58650	PSY1	1.73	0.00
AT5G49480	ATCP1	-1.41	0.00	AT5G59820	RHL41	1.14	0.00
AT5G49770	NA	-1.01	0.00	AT5G60530	NA	1.15	0.00
AT5G50375	CPI1	-1.41	0.00	AT5G60600	CLB4	1.10	0.00
AT5G50450	NA	-1.12	0.00	AT5G60945	NA	1.69	0.00
AT5G50880	NA	-1.04	0.03	AT5G61120	NA	2.71	0.00
AT5G51470	NA	-1.23	0.00	AT5G61430	ANAC100	1.08	0.00
AT5G51720	NA	-1.17	0.00	AT5G61560	NA	1.18	0.00
AT5G52320	CYP96A4	-1.02	0.00	AT5G61600	ERF104	1.64	0.00
AT5G52830	ATWRKY27	-1.52	0.00	AT5G62100	ATBAG2	1.17	0.00
AT5G52900	MAKR6	-1.26	0.00	AT5G62620	NA	1.62	0.00
AT5G52930	NA	-1.53	0.00	AT5G62627	NA	3.03	0.00
AT5G53160	PYL8	-1.19	0.00	AT5G63190	NA	1.13	0.00
AT5G53200	TRY	-1.43	0.00	AT5G63450	CYP94B1	2.31	0.00

SUPPLEMENTARY MATERIALS

AT5G53500	NA	-1.03	0.00	AT5G63640	NA	1.38	0.00
AT5G53980	ATHB52	-1.29	0.00	AT5G64190	NA	2.25	0.00
AT5G54200	NA	-1.12	0.00	AT5G64230	NA	1.39	0.00
AT5G54270	LHCB3	-1.45	0.00	AT5G64310	AGP1	2.86	0.00
AT5G54380	THE1	-1.30	0.00	AT5G64750	ABR1	1.80	0.00
AT5G55620	NA	-1.45	0.00	AT5G65110	ACX2	2.16	0.00
AT5G55730	FLA1	-1.49	0.00	AT5G65230	AtMYB53	1.24	0.00
AT5G56670	NA	-1.06	0.00	AT5G65280	GCL1	1.62	0.00
AT5G57440	GPP2	-1.27	0.00	AT5G65990	NA	1.52	0.00
AT5G57660	ATCOL5	-1.24	0.00	AT5G66631	NA	1.01	0.00
AT5G57700	NA	-1.46	0.00	AT5G66650	NA	1.04	0.00
AT5G58310	ATMES18	-1.64	0.00	AT5G66780	NA	6.15	0.00
AT5G58390	NA	-1.70	0.00	AT5G67080	MAPKKK19	2.62	0.00
AT5G58500	LSH5	-1.38	0.00	AT5G67090	NA	1.02	0.00
AT5G58550	EOL2	-1.49	0.00	AT5G67140	NA	1.10	0.00
AT5G59770	NA	-1.32	0.00	AT5G67340	NA	1.08	0.00
AT5G59850	NA	-1.04	0.00				

REFERENCE

- Alexandersson, E., Danielson, J.A., Råde, J., Moparthy, V.K., Fontes, M., Kjellbom, P., and Johanson, U. (2010). Transcriptional regulation of aquaporins in accessions of *Arabidopsis* in response to drought stress. *Plant J* **61**, 650-660.
- Alexandersson, E., Fraysse, L., Sjövall-Larsen, S., Gustavsson, S., Fellert, M., Karlsson, M., Johanson, U., and Kjellbom, P. (2005). Whole gene family expression and drought stress regulation of aquaporins. *Plant Mol Biol* **59**, 469-484.
- Alford, S.R., Rangarajan, P., Williams, P., and Gillaspay, G.E. (2012). myo-Inositol Oxygenase is Required for Responses to Low Energy Conditions in *Arabidopsis thaliana*. *Front Plant Sci* **3**, 69.
- Allakhverdiev, S.I., Kreslavski, V.D., Klimov, V.V., Los, D.A., Carpentier, R., and Mohanty, P. (2008). Heat stress: an overview of molecular responses in photosynthesis. *Photosynth Res* **98**, 541-550.
- Aprile, A., Mastrangelo, A.M., De Leonardis, A.M., Galiba, G., Roncaglia, E., Ferrari, F., De Bellis, L., Turchi, L., Giuliano, G., and Cattivelli, L. (2009). Transcriptional profiling in response to terminal drought stress reveals differential responses along the wheat genome. *BMC Genomics* **10**, 279.
- Baniwal, S.K., Bharti, K., Chan, K.Y., Fauth, M., Ganguli, A., Kotak, S., Mishra, S.K., Nover, L., Port, M., Scharf, K.D., Tripp, J., Weber, C., Zielinski, D., and von Koskull-Döring, P. (2004). Heat stress response in plants: a complex game with chaperones and more than twenty heat stress transcription factors. *J Biosci* **29**, 471-487.
- Bansal, A., and Sankararamakrishnan, R. (2007). Homology modeling of major intrinsic proteins in rice, maize and *Arabidopsis*: comparative analysis of transmembrane helix association and aromatic/arginine selectivity filters. *BMC Struct Biol* **7**, 27.
- Bates, B., Kundzewicz, Z.W., Wu, S., and Palutikof, J. (2008). Climate change and water. (Intergovernmental Panel on Climate Change (IPCC)).
- Baumberger, N., Doesseger, B., Guyot, R., Diet, A., Parsons, R.L., Clark, M.A., Simmons, M.P., Bedinger, P., Goff, S.A., Ringli, C., and Keller, B. (2003). Whole-genome comparison of leucine-rich repeat extensins in *Arabidopsis* and rice. A conserved family of cell wall proteins form a vegetative and a reproductive clade. *Plant Physiol* **131**, 1313-1326.
- Bienert, G.P., Møller, A.L., Kristiansen, K.A., Schulz, A., Møller, I.M., Schjoerring, J.K., and Jahn, T.P. (2007). Specific aquaporins facilitate the diffusion of hydrogen peroxide across membranes. *J Biol Chem* **282**, 1183-1192.
- Bokszczanin, K.L., and Fragkostefanakis, S. (2013). Perspectives on deciphering mechanisms underlying plant heat stress response and thermotolerance. *Front Plant Sci* **4**, 315.
- Boursiac, Y., Chen, S., Luu, D.T., Sorieul, M., van den Dries, N., and Maurel, C. (2005). Early effects of salinity on water transport in *Arabidopsis* roots. Molecular and cellular features of aquaporin expression. *Plant Physiol* **139**, 790-805.

- Boursiac, Y., Boudet, J., Postaire, O., Luu, D.T., Tournaire-Roux, C., and Maurel, C.** (2008). Stimulus-induced downregulation of root water transport involves reactive oxygen species-activated cell signalling and plasma membrane intrinsic protein internalization. *Plant J* **56**, 207-218.
- Bray, E.A.** (1997). Plant responses to water deficit. *Trends Plant Sci* **2**, 48-54.
- Buckley, T.N.** (2015). The contributions of apoplastic, symplastic and gas phase pathways for water transport outside the bundle sheath in leaves. *Plant Cell Environ* **38**, 7-22.
- Caldeira, C.F., Jeanguenin, L., Chaumont, F., and Tardieu, F.** (2014a). Circadian rhythms of hydraulic conductance and growth are enhanced by drought and improve plant performance. *Nat Commun* **5**, 5365.
- Caldeira, C.F., Bosio, M., Parent, B., Jeanguenin, L., Chaumont, F., and Tardieu, F.** (2014b). A hydraulic model is compatible with rapid changes in leaf elongation under fluctuating evaporative demand and soil water status. *Plant Physiol* **164**, 1718-1730.
- Campbell, P., and Braam, J.** (1999). Xyloglucan endotransglycosylases: diversity of genes, enzymes and potential wall-modifying functions. *Trends Plant Sci* **4**, 361-366.
- Caspar, T., Lin, T.P., Monroe, J., Bernhard, W., Spilatro, S., Preiss, J., and Somerville, C.** (1989). Altered regulation of beta-amylase activity in mutants of *Arabidopsis* with lesions in starch metabolism. *Proc Natl Acad Sci U S A* **86**, 5830-5833.
- Chaumont, F., Moshelion, M., and Daniels, M.J.** (2005b). Regulation of plant aquaporin activity. *Biology of the Cell* **97**, 749-764.
- Chaves, M.M., Pereira, J.S., Maroco, J., Rodrigues, M.L., Ricardo, C.P., Osório, M.L., Carvalho, I., Faria, T., and Pinheiro, C.** (2002). How plants cope with water stress in the field. Photosynthesis and growth. *Ann Bot* **89 Spec No**, 907-916.
- Claisse, G., Charrier, B., and Kreis, M.** (2007). The *Arabidopsis thaliana* GSK3/Shaggy like kinase AtSK3-2 modulates floral cell expansion. *Plant Mol Biol* **64**, 113-124.
- Crawford, A.J., McLachlan, D.H., Hetherington, A.M., and Franklin, K.A.** (2012). High temperature exposure increases plant cooling capacity. *Curr Biol* **22**, R396-397.
- Da Ines, O.** (2008). Functional analysis of PIP2 aquaporins in *Arabidopsis thaliana*. *Ludwig-Maximilians-Universität, München*.
- Da Ines, O., Graf, W., Franck, K.I., Albert, A., Winkler, J.B., Scherb, H., Stichler, W., and Schäffner, A.R.** (2010). Kinetic analyses of plant water relocation using deuterium as tracer - reduced water flux of *Arabidopsis pip2* aquaporin knockout mutants. *Plant Biol (Stuttg)* **12 Suppl 1**, 129-139.
- Daniels, M.J., Mirkov, T.E., and Chrispeels, M.J.** (1994). The plasma membrane of *Arabidopsis thaliana* contains a mercury-insensitive aquaporin that is a homolog of the tonoplast water channel protein TIP. *Plant Physiol* **106**, 1325-1333.
- Daniels, M.J., Chaumont, F., Mirkov, T.E., and Chrispeels, M.J.** (1996). Characterization of a new vacuolar membrane aquaporin sensitive to mercury at a unique site. *Plant Cell* **8**, 587-599.
- de Bianchi, S., Betterle, N., Kouril, R., Cazzaniga, S., Boekema, E., Bassi, R., and Dall'Osto, L.** (2011). *Arabidopsis* mutants deleted in the light-harvesting protein Lhcb4 have a disrupted photosystem II macrostructure and are defective in photoprotection. *Plant Cell* **23**, 2659-2679.

- di Pietro, M., Vialaret, J., Li, G.W., Hem, S., Prado, K., Rossignol, M., Maurel, C., and Santoni, V. (2013). Coordinated post-translational responses of aquaporins to abiotic and nutritional stimuli in *Arabidopsis* roots. *Mol Cell Proteomics* **12**, 3886-3897.
- Dynowski, M., Schaaf, G., Loque, D., Moran, O., and Ludewig, U. (2008). Plant plasma membrane water channels conduct the signalling molecule H₂O₂. *Biochem J* **414**, 53-61.
- Egert, A., Keller, F., and Peters, S. (2013). Abiotic stress-induced accumulation of raffinose in *Arabidopsis* leaves is mediated by a single raffinose synthase (*RS5*, At5g40390). *BMC Plant Biol* **13**, 218.
- Ehlert, C., Maurel, C., Tardieu, F., and Simonneau, T. (2009). Aquaporin-mediated reduction in maize root hydraulic conductivity impacts cell turgor and leaf elongation even without changing transpiration. *Plant Physiol* **150**, 1093-1104.
- Erban, A., Schauer, N., Fernie, A.R., and Kopka, J. (2007). Nonsupervised construction and application of mass spectral and retention time index libraries from time-of-flight gas chromatography-mass spectrometry metabolite profiles. In *Metabolomics* (Springer), pp. 19-38.
- Fricke, W., and Peters, W.S. (2002). The biophysics of leaf growth in salt-stressed barley. A study at the cell level. *Plant Physiol* **129**, 374-388.
- Fujiyoshi, Y., Mitsuoka, K., de Groot, B.L., Philippsen, A., Grubmüller, H., Agre, P., and Engel, A. (2002). Structure and function of water channels. *Curr Opin Struct Biol* **12**, 509-515.
- Gerbeau, P., Amodeo, G., Henzler, T., Santoni, V., Ripoche, P., and Maurel, C. (2002). The water permeability of *Arabidopsis* plasma membrane is regulated by divalent cations and pH. *Plant J* **30**, 71-81.
- Guyot, G., Scoffoni, C., and Sack, L. (2012). Combined impacts of irradiance and dehydration on leaf hydraulic conductance: insights into vulnerability and stomatal control. *Plant Cell Environ* **35**, 857-871.
- Hachez, C., Laloux, T., Reinhardt, H., Cavez, D., Degand, H., Grefen, C., De Rycke, R., Inzé, D., Blatt, M.R., Russinova, E., and Chaumont, F. (2014). *Arabidopsis* SNAREs SYP61 and SYP121 coordinate the trafficking of plasma membrane aquaporin PIP2;7 to modulate the cell membrane water permeability. *Plant Cell* **26**, 3132-3147.
- Heckwolf, M., Pater, D., Hanson, D.T., and Kaldenhoff, R. (2011). The *Arabidopsis thaliana* aquaporin AtPIP1;2 is a physiologically relevant CO₂ transport facilitator. *Plant J* **67**, 795-804.
- Hejazi, M., Fettke, J., Kötting, O., Zeeman, S.C., and Steup, M. (2010). The Laforin-like dual-specificity phosphatase SEX4 from *Arabidopsis* hydrolyzes both C6- and C3-phosphate esters introduced by starch-related dikinases and thereby affects phase transition of alpha-glucans. *Plant Physiol* **152**, 711-722.
- Holm, L.M., Jahn, T.P., Moller, A.L., Schjoerring, J.K., Ferri, D., Klaerke, D.A., and Zeuthen, T. (2005). NH₃ and NH₄⁺ permeability in aquaporin-expressing *Xenopus* oocytes. *Pflugers Arch* **450**, 415-428.
- Hongo, S., Sato, K., Yokoyama, R., and Nishitani, K. (2012). Demethylesterification of the primary wall by PECTIN METHYLESTERASE35 provides mechanical support to the *Arabidopsis* stem. *Plant Cell* **24**, 2624-2634.

- Hooijmaijers, C., Rhee, J.Y., Kwak, K.J., Chung, G.C., Horie, T., Katsuhara, M., and Kang, H. (2012). Hydrogen peroxide permeability of plasma membrane aquaporins of *Arabidopsis thaliana*. *J Plant Res* **125**, 147-153.
- Howarth, C. (2005). Genetic improvements of tolerance to high temperature. Abiotic stresses: plant resistance through breeding and molecular approaches. Howarth Press Inc., New York.
- Ishikawa, F., Suga, S., Uemura, T., Sato, M.H., and Maeshima, M. (2005). Novel type aquaporin SIPs are mainly localized to the ER membrane and show cell-specific expression in *Arabidopsis thaliana*. *FEBS Lett* **579**, 5814-5820.
- Jang, J.Y., Kim, D.G., Kim, Y.O., Kim, J.S., and Kang, H. (2004). An expression analysis of a gene family encoding plasma membrane aquaporins in response to abiotic stresses in *Arabidopsis thaliana*. *Plant Mol Biol* **54**, 713-725.
- Javot, H., Lauvergeat, V., Santoni, V., Martin-Laurent, F., Güclü, J., Vinh, J., Heyes, J., Franck, K.I., Schäffner, A.R., Bouchez, D., and Maurel, C. (2003). Role of a single aquaporin isoform in root water uptake. *Plant Cell* **15**, 509-522.
- Johanson, U., Karlsson, M., Johansson, I., Gustavsson, S., Sjövall, S., Fraysse, L., Weig, A.R., and Kjellbom, P. (2001). The complete set of genes encoding major intrinsic proteins in *Arabidopsis* provides a framework for a new nomenclature for major intrinsic proteins in plants. *Plant Physiol* **126**, 1358-1369.
- Joubès, J., Raffaele, S., Bourdenx, B., Garcia, C., Laroche-Traineau, J., Moreau, P., Domergue, F., and Lessire, R. (2008). The VLCFA elongase gene family in *Arabidopsis thaliana*: phylogenetic analysis, 3D modelling and expression profiling. *Plant Mol Biol* **67**, 547-566.
- Kaldenhoff, R., Grote, K., Zhu, J.J., and Zimmermann, U. (1998). Significance of plasmalemma aquaporins for water-transport in *Arabidopsis thaliana*. *The Plant Journal* **14**, 121-128.
- Kammerloher, W., Fischer, U., Piechottka, G.P., and Schäffner, A.R. (1994). Water channels in the plant plasma membrane cloned by immunoselection from a mammalian expression system. *Plant J* **6**, 187-199.
- Kaplan, F., Kopka, J., Haskell, D.W., Zhao, W., Schiller, K.C., Gatzke, N., Sung, D.Y., and Guy, C.L. (2004). Exploring the temperature-stress metabolome of *Arabidopsis*. *Plant Physiol* **136**, 4159-4168.
- Klebl, F., Wolf, M., and Sauer, N. (2003). A defect in the yeast plasma membrane urea transporter Dur3p is complemented by *CpNIP1*, a Nod26-like protein from zucchini (*Cucurbita pepo* L.), and by *Arabidopsis thaliana* delta-TIP or gamma-TIP. *FEBS Lett* **547**, 69-74.
- Kline, K.G., Barrett-Wilt, G.A., and Sussman, M.R. (2010). In planta changes in protein phosphorylation induced by the plant hormone abscisic acid. *Proc Natl Acad Sci U S A* **107**, 15986-15991.
- Kotak, S., Larkindale, J., Lee, U., von Koskull-Döring, P., Vierling, E., and Scharf, K.D. (2007). Complexity of the heat stress response in plants. *Curr Opin Plant Biol* **10**, 310-316.
- Kötting, O., Santelia, D., Edner, C., Eicke, S., Marthaler, T., Gentry, M.S., Comparot-Moss, S., Chen, J., Smith, A.M., Steup, M., Ritte, G., and Zeeman, S.C. (2009). STARCH-EXCESS4 is a laforin-like Phosphoglucan phosphatase required for starch degradation in *Arabidopsis thaliana*. *Plant Cell* **21**, 334-346.

- Koussevitzky, S., Suzuki, N., Huntington, S., Armijo, L., Sha, W., Cortes, D., Shulaev, V., and Mittler, R. (2008). Ascorbate peroxidase 1 plays a key role in the response of *Arabidopsis thaliana* to stress combination. *J Biol Chem* **283**, 34197-34203.
- Krasensky, J., and Jonak, C. (2012). Drought, salt, and temperature stress-induced metabolic rearrangements and regulatory networks. *J Exp Bot* **63**, 1593-1608.
- Krishnaswamy, S., Verma, S., Rahman, M.H., and Kav, N.N. (2011). Functional characterization of four APETALA2-family genes (*RAP2.6*, *RAP2.6L*, *DREB19* and *DREB26*) in *Arabidopsis*. *Plant Mol Biol* **75**, 107-127.
- Larkindale, J., and Vierling, E. (2008). Core genome responses involved in acclimation to high temperature. *Plant Physiol* **146**, 748-761.
- Le, D.T., Nishiyama, R., Watanabe, Y., Tanaka, M., Seki, M., Ham le, H., Yamaguchi-Shinozaki, K., Shinozaki, K., and Tran, L.S. (2012). Differential gene expression in soybean leaf tissues at late developmental stages under drought stress revealed by genome-wide transcriptome analysis. *PLoS One* **7**, e49522.
- Lee, H.K., Cho, S.K., Son, O., Xu, Z., Hwang, I., and Kim, W.T. (2009). Drought stress-induced Rma1H1, a RING membrane-anchor E3 ubiquitin ligase homolog, regulates aquaporin levels via ubiquitination in transgenic *Arabidopsis* plants. *Plant Cell* **21**, 622-641.
- Lee, S.H., Chung, G.C., Jang, J.Y., Ahn, S.J., and Zwiazek, J.J. (2012). Overexpression of PIP2;5 aquaporin alleviates effects of low root temperature on cell hydraulic conductivity and growth in *Arabidopsis*. *Plant Physiol* **159**, 479-488.
- Leegood, R.C. (2008). Roles of the bundle sheath cells in leaves of C3 plants. *J Exp Bot* **59**, 1663-1673.
- Levin, M., Lemcoff, J.H., Cohen, S., and Kapulnik, Y. (2007). Low air humidity increases leaf-specific hydraulic conductance of *Arabidopsis thaliana* (L.) Heynh (Brassicaceae). *J Exp Bot* **58**, 3711-3718.
- Li, L., Foster, C.M., Gan, Q., Nettleton, D., James, M.G., Myers, A.M., and Wurtele, E.S. (2009). Identification of the novel protein QQS as a component of the starch metabolic network in *Arabidopsis* leaves. *Plant J* **58**, 485-498.
- Li, X., Wang, X., Yang, Y., Li, R., He, Q., Fang, X., Luu, D.T., Maurel, C., and Lin, J. (2011). Single-molecule analysis of PIP2;1 dynamics and partitioning reveals multiple modes of *Arabidopsis* plasma membrane aquaporin regulation. *Plant Cell* **23**, 3780-3797.
- Liepman, A.H., Nairn, C.J., Willats, W.G., Sorensen, I., Roberts, A.W., and Keegstra, K. (2007). Functional genomic analysis supports conservation of function among cellulose synthase-like a gene family members and suggests diverse roles of mannans in plants. *Plant Physiol* **143**, 1881-1893.
- Lim, C.J., Yang, K.A., Hong, J.K., Choi, J.S., Yun, D.J., Hong, J.C., Chung, W.S., Lee, S.Y., Cho, M.J., and Lim, C.O. (2006). Gene expression profiles during heat acclimation in *Arabidopsis thaliana* suspension-culture cells. *J Plant Res* **119**, 373-383.
- Lisec, J., Schauer, N., Kopka, J., Willmitzer, L., and Fernie, A.R. (2006). Gas chromatography mass spectrometry-based metabolite profiling in plants. *Nat Protoc* **1**, 387-396.
- Liu, F., Vantoai, T., Moy, L.P., Bock, G., Linford, L.D., and Quackenbush, J. (2005). Global transcription profiling reveals comprehensive insights into hypoxic response in *Arabidopsis*. *Plant Physiol* **137**, 1115-1129.

- Liu, L.H., Ludewig, U., Gassert, B., Frommer, W.B., and von Wirén, N.** (2003). Urea transport by nitrogen-regulated tonoplast intrinsic proteins in *Arabidopsis*. *Plant Physiol* **133**, 1220-1228.
- Luu, D.T., and Maurel, C.** (2005). Aquaporins in a challenging environment: molecular gears for adjusting plant water status. *Plant Cell Environ* **28**, 85-96.
- Martínez-Ballesta, M.C., Aparicio, F., Pallás, V., Martínez, V., and Carvajal, M.** (2003). Influence of saline stress on root hydraulic conductance and *PIP* expression in *Arabidopsis*. *J Plant Physiol* **160**, 689-697.
- Martre, P., Morillon, R., Barrieu, F., North, G.B., Nobel, P.S., and Chrispeels, M.J.** (2002). Plasma membrane aquaporins play a significant role during recovery from water deficit. *Plant Physiol* **130**, 2101-2110.
- Matsuura, H., Ishibashi, Y., Shinmyo, A., Kanaya, S., and Kato, K.** (2010). Genome-wide analyses of early translational responses to elevated temperature and high salinity in *Arabidopsis thaliana*. *Plant Cell Physiol* **51**, 448-462.
- Maurel, C., Reizer, J., Schroeder, J.I., and Chrispeels, M.J.** (1993). The vacuolar membrane protein gamma-TIP creates water specific channels in *Xenopus* oocytes. *EMBO J* **12**, 2241-2247.
- Maurel, C., Verdoucq, L., Luu, D.T., and Santoni, V.** (2008). Plant aquaporins: membrane channels with multiple integrated functions. *Annu Rev Plant Biol* **59**, 595-624.
- Mittal, D., Madhyastha, D.A., and Grover, A.** (2012). Genome-wide transcriptional profiles during temperature and oxidative stress reveal coordinated expression patterns and overlapping regulons in rice. *PLoS One* **7**, e40899.
- Mittler, R.** (2006). Abiotic stress, the field environment and stress combination. *Trends Plant Sci* **11**, 15-19.
- Mittler, R., Finka, A., and Goloubinoff, P.** (2012). How do plants feel the heat? *Trends Biochem Sci* **37**, 118-125.
- Monneuse, J.M., Sugano, M., Becue, T., Santoni, V., Hem, S., and Rossignol, M.** (2011). Towards the profiling of the *Arabidopsis thaliana* plasma membrane transportome by targeted proteomics. *Proteomics* **11**, 1789-1797.
- Monroe, J.D., and Preiss, J.** (1990). Purification of a beta-Amylase that Accumulates in *Arabidopsis thaliana* Mutants Defective in Starch Metabolism. *Plant Physiol* **94**, 1033-1039.
- Monroe, J.D., Salminen, M.D., and Preiss, J.** (1991). Nucleotide Sequence of a cDNA Clone Encoding a beta-Amylase from *Arabidopsis thaliana*. *Plant Physiol* **97**, 1599-1601.
- Morgan, J.M.** (1984). Osmoregulation and water stress in higher plants. *Ann Rev Plant Physiol* **35**, 299-319.
- Nakashima, K., Ito, Y., and Yamaguchi-Shinozaki, K.** (2009). Transcriptional regulatory networks in response to abiotic stresses in *Arabidopsis* and grasses. *Plant Physiol* **149**, 88-95.
- Ndamukong, I., Chetram, A., Saleh, A., and Avramova, Z.** (2009). Wall-modifying genes regulated by the *Arabidopsis* homolog of trithorax, *ATX1*: repression of the *XTH33* gene as a test case. *Plant J* **58**, 541-553.
- Nonami, H., and Boyer, J.S.** (1993). Direct Demonstration of a Growth-Induced Water Potential Gradient. *Plant Physiol* **102**, 13-19.
- Osakabe, Y., Osakabe, K., Shinozaki, K., and Tran, L.S.** (2014). Response of plants to water stress. *Front Plant Sci* **5**, 86.

- Ottosen, C.-O., Mortensen, L., and Gislerød, H. (2002). Effect of relative air humidity on gas exchange, stomatal conductance and nutrient uptake in miniature potted roses. *Gartenbauwissenschaft* **67**, 143-147.
- Panikulangara, T.J., Eggers-Schumacher, G., Wunderlich, M., Stransky, H., and Schöffl, F. (2004). Galactinol synthase1. A novel heat shock factor target gene responsible for heat-induced synthesis of raffinose family oligosaccharides in *Arabidopsis*. *Plant Physiol* **136**, 3148-3158.
- Pantin, F., Simonneau, T., and Muller, B. (2012). Coming of leaf age: control of growth by hydraulics and metabolics during leaf ontogeny. *New Phytol* **196**, 349-366.
- Parent, B., Hachez, C., Redondo, E., Simonneau, T., Chaumont, F., and Tardieu, F. (2009). Drought and abscisic acid effects on aquaporin content translate into changes in hydraulic conductivity and leaf growth rate: a trans-scale approach. *Plant Physiol* **149**, 2000-2012.
- Péret, B., Li, G., Zhao, J., Band, L.R., Voß, U., Postaire, O., Luu, D.T., Da Ines, O., Casimiro, I., Lucas, M., Wells, D.M., Lazzerini, L., Nacry, P., King, J.R., Jensen, O.E., Schäffner, A.R., Maurel, C., and Bennett, M.J. (2012). Auxin regulates aquaporin function to facilitate lateral root emergence. *Nat Cell Biol* **14**, 991-998.
- Postaire, O., Tournaire-Roux, C., Grondin, A., Boursiac, Y., Morillon, R., Schäffner, A.R., and Maurel, C. (2010). A PIP1 aquaporin contributes to hydrostatic pressure-induced water transport in both the root and rosette of *Arabidopsis*. *Plant Physiol* **152**, 1418-1430.
- Prado, K., Boursiac, Y., Tournaire-Roux, C., Monneuse, J.M., Postaire, O., Da Ines, O., Schäffner, A.R., Hem, S., Santoni, V., and Maurel, C. (2013). Regulation of *Arabidopsis* leaf hydraulics involves light-dependent phosphorylation of aquaporins in veins. *Plant Cell* **25**, 1029-1039.
- Prak, S., Hem, S., Boudet, J., Viennois, G., Sommerer, N., Rossignol, M., Maurel, C., and Santoni, V. (2008). Multiple phosphorylations in the C-terminal tail of plant plasma membrane aquaporins: role in subcellular trafficking of AtPIP2;1 in response to salt stress. *Mol Cell Proteomics* **7**, 1019-1030.
- Prasch, C.M., and Sonnewald, U. (2013). Simultaneous application of heat, drought, and virus to *Arabidopsis* plants reveals significant shifts in signaling networks. *Plant Physiol* **162**, 1849-1866.
- Qu, A.L., Ding, Y.F., Jiang, Q., and Zhu, C. (2013). Molecular mechanisms of the plant heat stress response. *Biochem Biophys Res Commun* **432**, 203-207.
- Quigley, F., Rosenberg, J.M., Shachar-Hill, Y., and Bohnert, H.J. (2002). From genome to function: the *Arabidopsis* aquaporins. *Genome Biol* **3**, Research0001.
- Rae, L., Lao, N.T., and Kavanagh, T.A. (2011). Regulation of multiple aquaporin genes in *Arabidopsis* by a pair of recently duplicated DREB transcription factors. *Planta* **234**, 429-444.
- Reiter, W.D., Chapple, C.C., and Somerville, C.R. (1993). Altered growth and cell walls in a fucose-deficient mutant of *Arabidopsis*. *Science* **261**, 1032-1035.
- Richmond, T.A., and Somerville, C.R. (2000). The cellulose synthase superfamily. *Plant Physiol* **124**, 495-498.
- Rivers, R.L., Dean, R.M., Chandy, G., Hall, J.E., Roberts, D.M., and Zeidel, M.L. (1997). Functional analysis of nodulin 26, an aquaporin in soybean root nodule symbiosomes. *J Biol Chem* **272**, 16256-16261.

- Rizhsky, L., Liang, H., and Mittler, R.** (2002). The combined effect of drought stress and heat shock on gene expression in tobacco. *Plant Physiol* **130**, 1143-1151.
- Rizhsky, L., Liang, H., Shuman, J., Shulaev, V., Davletova, S., and Mittler, R.** (2004). When defense pathways collide. The response of *Arabidopsis* to a combination of drought and heat stress. *Plant Physiol* **134**, 1683-1696.
- Roessner, U., Luedemann, A., Brust, D., Fiehn, O., Linke, T., Willmitzer, L., and Fernie, A.R.** (2001). Metabolic profiling allows comprehensive phenotyping of genetically or environmentally modified plant systems. *Plant Cell* **13**, 11-29.
- Sack, L., and Holbrook, N.M.** (2006). Leaf hydraulics. *Annu. Rev. Plant Biol.* **57**, 361-381.
- Sade, N., Shatil-Cohen, A., Attia, Z., Maurel, C., Boursiac, Y., Kelly, G., Granot, D., Yaaran, A., Lerner, S., and Moshelion, M.** (2014). The role of plasma membrane aquaporins in regulating the bundle sheath-mesophyll continuum and leaf hydraulics. *Plant Physiol* **166**, 1609-1620.
- Sakuma, Y., Maruyama, K., Osakabe, Y., Qin, F., Seki, M., Shinozaki, K., and Yamaguchi-Shinozaki, K.** (2006). Functional analysis of an *Arabidopsis* transcription factor, DREB2A, involved in drought-responsive gene expression. *Plant Cell* **18**, 1292-1309.
- Salvucci, M.E., and Crafts-Brandner, S.J.** (2004). Inhibition of photosynthesis by heat stress: the activation state of Rubisco as a limiting factor in photosynthesis. *Physiol Plant* **120**, 179-186.
- Sampedro, J., and Cosgrove, D.J.** (2005). The expansin superfamily. *Genome Biol* **6**.
- Santoni, V., Vinh, J., Pflieger, D., Sommerer, N., and Maurel, C.** (2003). A proteomic study reveals novel insights into the diversity of aquaporin forms expressed in the plasma membrane of plant roots. *Biochem J* **373**, 289-296.
- Seibt, U., Rajabi, A., Griffiths, H., and Berry, J.A.** (2008). Carbon isotopes and water use efficiency: sense and sensitivity. *Oecologia* **155**, 441-454.
- Seki, M., Umezawa, T., Urano, K., and Shinozaki, K.** (2007). Regulatory metabolic networks in drought stress responses. *Curr Opin Plant Biol* **10**, 296-302.
- Seki, M., Narusaka, M., Abe, H., Kasuga, M., Yamaguchi-Shinozaki, K., Carninci, P., Hayashizaki, Y., and Shinozaki, K.** (2001). Monitoring the expression pattern of 1300 *Arabidopsis* genes under drought and cold stresses by using a full-length cDNA microarray. *Plant Cell* **13**, 61-72.
- Seki, M., Ishida, J., Narusaka, M., Fujita, M., Nanjo, T., Umezawa, T., Kamiya, A., Nakajima, M., Enju, A., Sakurai, T., Satou, M., Akiyama, K., Yamaguchi-Shinozaki, K., Carninci, P., Kawai, J., Hayashizaki, Y., and Shinozaki, K.** (2002). Monitoring the expression pattern of around 7,000 *Arabidopsis* genes under ABA treatments using a full-length cDNA microarray. *Funct Integr Genomics* **2**, 282-291.
- Sharkey, T.D.** (2005). Effects of moderate heat stress on photosynthesis: importance of thylakoid reactions, rubisco deactivation, reactive oxygen species, and thermotolerance provided by isoprene. *Plant Cell Environ* **28**, 269-277.
- Shatil-Cohen, A., Attia, Z., and Moshelion, M.** (2011). Bundle-sheath cell regulation of xylem-mesophyll water transport via aquaporins under drought stress: a target of xylem-borne ABA? *Plant J* **67**, 72-80.
- Shinozaki, K., and Yamaguchi-Shinozaki, K.** (2007). Gene networks involved in drought stress response and tolerance. *J Exp Bot* **58**, 221-227.

- Shinozaki, K., Yamaguchi-Shinozaki, K., and Seki, M.** (2003). Regulatory network of gene expression in the drought and cold stress responses. *Curr Opin Plant Biol* **6**, 410-417.
- Siefritz, F., Tyree, M.T., Lovisolo, C., Schubert, A., and Kaldenhoff, R.** (2002). PIP1 plasma membrane aquaporins in tobacco from cellular effects to function in plants. *Plant Cell* **14**, 869-876.
- Siefritz, F., Otto, B., Bienert, G.P., van der Krol, A., and Kaldenhoff, R.** (2004). The plasma membrane aquaporin *NtAQP1* is a key component of the leaf unfolding mechanism in tobacco. *Plant J* **37**, 147-155.
- Silver, D.M., Kötting, O., and Moorhead, G.B.** (2014). Phosphoglucan phosphatase function sheds light on starch degradation. *Trends Plant Sci* **19**, 471-478.
- Smyth, G.K., Michaud, J., and Scott, H.S.** (2005). Use of within-array replicate spots for assessing differential expression in microarray experiments. *Bioinformatics* **21**, 2067-2075.
- Steudle, E.** (1994). Water transport across roots. *Plant and Soil* **167**, 79-90.
- Steudle, E.** (2001). The Cohesion-Tension Mechanism and the Acquisition of Water by Plant Roots. *Annu Rev Plant Physiol Plant Mol Biol* **52**, 847-875.
- Steudle, E., and Peterson, C.A.** (1998). How does water get through roots? *J Exp Bot* **49**, 775-788.
- Stockinger, E.J., Gilmour, S.J., and Thomashow, M.F.** (1997). *Arabidopsis thaliana* *CBF1* encodes an AP2 domain-containing transcriptional activator that binds to the C-repeat/DRE, a cis-acting DNA regulatory element that stimulates transcription in response to low temperature and water deficit. *Proc Natl Acad Sci U S A* **94**, 1035-1040.
- Sutka, M., Li, G., Boudet, J., Boursiac, Y., Dumas, P., and Maurel, C.** (2011). Natural variation of root hydraulics in *Arabidopsis* grown in normal and salt-stressed conditions. *Plant Physiol* **155**, 1264-1276.
- Taiz, L., and Zeiger, E.** (2006). *Plant physiology* (2006). Sunderland, MA: Sinaur Associates Inc.
- Takano, J., Wada, M., Ludewig, U., Schaaf, G., von Wiren, N., and Fujiwara, T.** (2006). The *Arabidopsis* major intrinsic protein NIP5;1 is essential for efficient boron uptake and plant development under boron limitation. *Plant Cell* **18**, 1498-1509.
- Tournaire-Roux, C., Sutka, M., Javot, H., Gout, E., Gerbeau, P., Luu, D.T., Bligny, R., and Maurel, C.** (2003). Cytosolic pH regulates root water transport during anoxic stress through gating of aquaporins. *Nature* **425**, 393-397.
- Tryfona, T., Theys, T.E., Wagner, T., Stott, K., Keegstra, K., and Dupree, P.** (2014). Characterisation of FUT4 and FUT6 alpha-(1 --> 2)-fucosyltransferases reveals that absence of root arabinogalactan fucosylation increases *Arabidopsis* root growth salt sensitivity. *PLoS One* **9**, e93291.
- Tsukaguchi, T., Kawamitsu, Y., Takeda, H., Suzuki, K., and Egawa, Y.** (2003). Water Status of Flower Buds and Leaves as Affected by High Temperature in Heat-Tolerant and Heat-Sensitive Cultivars of Snap Bean (*Phaseolus vulgaris* L.). *Plant Prod Sci* **6**, 24-27.
- Uehlein, N., Sperling, H., Heckwolf, M., and Kaldenhoff, R.** (2012). The *Arabidopsis* aquaporin PIP1;2 rules cellular CO₂ uptake. *Plant Cell Environ* **35**, 1077-1083.
- Verdoucq, L., Grondin, A., and Maurel, C.** (2008). Structure-function analysis of plant aquaporin *AtPIP2;1* gating by divalent cations and protons. *Biochem J* **415**, 409-416.

- Vile, D., Pervent, M., Belluau, M., Vasseur, F., Bresson, J., Muller, B., Granier, C., and Simonneau, T.** (2012). *Arabidopsis* growth under prolonged high temperature and water deficit: independent or interactive effects? *Plant Cell Environ* **35**, 702-718.
- von Koskull-Döring, P., Scharf, K.D., and Nover, L.** (2007). The diversity of plant heat stress transcription factors. *Trends Plant Sci* **12**, 452-457.
- Wahid, A., Gelani, S., Ashraf, M., and Foolad, M.R.** (2007). Heat tolerance in plants: an overview. *Environmental and Experimental Botany* **61**, 199-223.
- Wallace, I.S., and Roberts, D.M.** (2004). Homology modeling of representative subfamilies of *Arabidopsis* major intrinsic proteins. Classification based on the aromatic/arginine selectivity filter. *Plant Physiol* **135**, 1059-1068.
- Wallace, I.S., Choi, W.G., and Roberts, D.M.** (2006). The structure, function and regulation of the nodulin 26-like intrinsic protein family of plant aquaglyceroporins. *Biochim Biophys Acta* **1758**, 1165-1175.
- Wang, Q., Monroe, J., and Sjölund, R.D.** (1995). Identification and characterization of a phloem-specific beta-amylase. *Plant Physiol* **109**, 743-750.
- Weig, A., Deswarte, C., and Chrispeels, M.J.** (1997). The major intrinsic protein family of *Arabidopsis* has 23 members that form three distinct groups with functional aquaporins in each group. *Plant Physiol* **114**, 1347-1357.
- Will, R.E., Wilson, S.M., Zou, C.B., and Hennessey, T.C.** (2013). Increased vapor pressure deficit due to higher temperature leads to greater transpiration and faster mortality during drought for tree seedlings common to the forest-grassland ecotone. *New Phytol* **200**, 366-374.
- Willats, W.G., and Knox, J.P.** (1996). A role for arabinogalactan-proteins in plant cell expansion: evidence from studies on the interaction of beta-glucosyl Yariv reagent with seedlings of *Arabidopsis thaliana*. *Plant J* **9**, 919-925.
- Wu, X.N., Sanchez Rodriguez, C., Pertl-Obermeyer, H., Obermeyer, G., and Schulze, W.X.** (2013). Sucrose-induced receptor kinase SIRK1 regulates a plasma membrane aquaporin in *Arabidopsis*. *Mol Cell Proteomics* **12**, 2856-2873.
- Yángüez, E., Castro-Sanz, A.B., Fernández-Bautista, N., Oliveros, J.C., and Castellano, M.M.** (2013). Analysis of genome-wide changes in the transcriptome of *Arabidopsis* seedlings subjected to heat stress. *PLoS One* **8**, e71425.
- Zhang, J., and Davies, W.** (1990). Changes in the concentration of ABA in xylem sap as a function of changing soil water status can account for changes in leaf conductance and growth. *Plant Cell Environ* **13**, 277-285.
- Zhang, W.H., and Tyerman, S.D.** (1999). Inhibition of water channels by HgCl₂ in intact wheat root cells. *Plant Physiol* **120**, 849-858.
- Zhang, X., Li, J., Liu, A., Zou, J., Zhou, X., Xiang, J., Rerksiri, W., Peng, Y., Xiong, X., and Chen, X.** (2012). Expression profile in rice panicle: insights into heat response mechanism at reproductive stage. *PLoS One* **7**, e49652.
- Zhao, J.** (2013). Roles of *PIP* aquaporins in lateral root development and stress responses in *Arabidopsis thaliana*. *Ludwig-Maximilians-Universität, München*.

CURRICULUM VITAE

Name: **Ming Jin**
Date of birth: Nov. 07, 1984
Place of birth: Huhehaote, Inner Mongolia, P.R. China
Nationality: Chinese
Gender: Female

EDUCATION & RESEARCH EXPERIENCE

Since 10/2010 Graduate student in Biochemistry at Ludwig-Maximilians Universität München, Germany

Research topic: The Role of PIP aquaporins in response to various environmental scenarios in *Arabidopsis thaliana*

Supervisor: PD Dr. Anton Schäffner, Institute of Biochemical Plant Pathology, Helmholtz Zentrum München, Germany

09/2007 - 07/2010 Master in Plant Molecular Biology at Lanzhou University, China

Research topic: Construction of the cold resistance genomic library for *Chorispora bungeana* and isolated the full length of a transcription Factor, *FZF*, which is up regulated under cold stress

Supervisor: Prof. Lizhe An, College of Life Science, Lanzhou University, China

09/2003 - 07/2007 Bachelor in Biology at Lanzhou University, China

FELLOWSHIP

09/2010 - 09/2014 Chinese Scholarship Council (CSC)

PROFESSIONAL TRAINING

28 - 29/02/2014 Statistische Datenanalyse mit R, Helmholtz Zentrum

17 - 21/03/2012 12th Spring School of Bioinformatics for Molecular Biologists, Helmholtz Zentrum

03 -07/10/2011 Thematic School on Transmembrane Water Transport in Plants, Montpellier, France

ACKNOWLEDGEMENT

Foremost, I would like to express my sincere gratitude to my supervisor PD Dr. Anton Schöffner for providing me the opportunity to pursue my scientific career abroad, for his patient and continuous encouragement of my Ph.D study, for his systematic guidance and valuable advices in my research, for his critical comments and careful correction of my thesis. His scientific enthusiasm and stringency to science have set a good example for me and will deeply influence my future work.

I would like to especially thank Prof. Dr. Jörg Durner for his good ideas, helpful advices during my thesis committee meetings, and for his willingness to review this work. My thanks are extended to the other committee members for reading and commenting this dissertation.

I would like to express my sincere thanks to Dr. Elisabeth Georgii for her smart ideas and great contributions on the statistical analysis of the microarray data, for her patient correction and valuable suggestions of my thesis writing. My thanks are also extended to Dr. Christine Gläßer of the Institute of Bioinformatics and Systems Biology and to Theresa Faus-Keßler of the Institute of Developmental Genetics for their strong support on the statistical analysis of the microarray data and kind introduction to statistics.

My sincere thanks also go to all the other collaborators of this project. I would like to thank Dr. J. Barbro Winkler of the Research Unit Environmental Simulation for her kind guidance with the gas exchange measurements and valuable advices for the data analysis. I wish to express my deep thanks to Dr. Andreas Albert, Peter Bader and Andreas Glaser of the Research Unit Environmental Simulation for their strong support on the climate simulation chambers during water stress treatments. I am so grateful to Franz Buegger of the Institute of Soil Ecology for his help with carbon isotope measurements and Dr. Martin Lehmann of the Faculty of Biology of the Ludwig-Maximilians-Universität for his kind help with the GC-MS measurements. My great thanks also go to Dr. Ruben Ispiryan for his help with photographic data collection.

I am also deeply thankful to my colleagues of the Institute of Biochemical Plant Pathology. My sincere thanks go to Dr. Günther Bahnweg for his kind help with correcting and proofreading the English writing of my thesis. I am grateful to Dr. Jin Zhao for her nice cooperation with this project and brilliant suggestions on structuring and correcting my thesis. My deep thanks also go to Chen Liu for her good advices during discussions and her kind encouragement all the time. I also would like to thank Birgit Geist and Susanne Stich for their excellent assistance and kind help with a variety of sophisticated techniques. My special thanks also go to the other members of Dr. Schäffner's group including Dr. Malay Das, Dr. Ruohe Yin, Dr. Veronica von Saint Paul, Dr. Stephan Dräxl, Dr. Wei Zhang, Kerstin Schuster, Rafal Maksym and Jessica Lutterbach, for their kind help with the material harvesting of this project and their insightful discussion. I also would like to give my thanks to all the other colleagues of BIOP.

I would like to sincerely thank the "Chinese Scholarship Council" (CSC) for their financial support.

Finally, I would like to offer my deep thanks to my parents for their selfless love and strong support during my Ph.D study. They are always there to cheer me up when I am down and stand by me through the bad times.